HETEROGENEITY OF HEPATOCELLULAR MALIGNANT PHENOTYPE

A THESIS SUBMITTED TO
THE DEPARTMENT OF MOLECULAR BIOLOGY AND GENETICS
AND THE INSTITUTE OF ENGINEERING AND SCIENCE OF
BILKENT UNIVERSITY
IN PARTIAL FULFILLMENT OF THE REQUIREMENTS
FOR THE DEGREE OF DOCTOR OF PHILOSOPHY

BY
NURİ ÖZTÜRK
AUGUST, 2006

TO MY FAMILY

I certify that I have read this thesis and that in my opinion it is fully adequate, in scope, and in quality, as a thesis for the degree of Doctor of Philosophy.

Prof. Dr. Mehmet Öztürk

I certify that I have read this thesis and that in my opinion it is fully adequate, in scope, and in quality, as a thesis for the degree of Doctor of Philosophy.

Prof. Dr. Hakan Bozkaya

I certify that I have read this thesis and that in my opinion it is fully adequate, in scope, and in quality, as a thesis for the degree of Doctor of Philosophy.

Prof. Dr. Ediz Demirpençe

I certify that I have read this thesis and that in my opinion it is fully adequate, in scope, and in quality, as a thesis for the degree of Doctor of Philosophy.

Assist. Prof. Dr. Uygar Tazebay

I certify that I have read this thesis and that in my opinion it is fully adequate, in scope, and in quality, as a thesis for the degree of Doctor of Philosophy.

Assist. Prof. Dr. Tamer Yağcı

Approved for the Institute of Engineering and Science

Prof. Dr. Mehmet Baray

Director of the Institute of Engineering and Science

ABSTRACT

Heterogeneity of Hepatocellular Malignant Phenotype

Nuri Öztürk
Ph.D. in Molecular Biology and Genetics
Supervisor: Prof. Dr. Mehmet Öztürk
August, 2006, 155 Pages

Hepatocellular carcinoma (HCC) is one of the most wide-spread carcinomas throughout the world - responsible for more than 600,000 deaths annually - and is strongly associated with several etiological factors; including aflatoxin B1, alcohol, and Hepatitis virus B and C. In HCC, many genes undergo somatic aberrations with a tendency to cluster at genes involved in cell cycle regulation, in the p53 and canonical Wnt signaling pathways, and in the TGF-β/IGF axis. Almost a third of HCCs display mutations affecting canonical Wnt signalling. However, the role of canonical Wnt signaling aberrations in HCC is not known in detail, since transgenic mice which express mutant β-catenin (an integral component of canonical Wnt signaling) do not develop liver tumours.

To study the heterogeneity of hepatocellular malignancies, we have concentrated on canonical Wnt signaling in HCC cell lines. We have found that canonical Wnt signaling was active in 80% of well-differentiated, and 14% of poorly-differentiated cell lines respectively. Furthermore, ectopic expression of a mutant β-catenin resulted in strong canonical Wnt activity in well-differentiated, but not in poorly-differentiated HCC cells. Our findings suggested that heterogeneity in HCC exists even in the same pathway as exemplified by differential canonical Wnt signaling activity in well- and poorly-differentiated HCC cell lines. During this study, we produced monoclonal antibodies against β-catenin to distinguish between the pools of nuclear/cytoplasmic and membrane-associated β-catenin in cells, since it is believed that the nuclear β-catenin pool is more potent in tumorigenesis. Monoclonal antibody (MAb), 4C9 recognised β-catenin out of adherens junctions, while another MAb, 9E10 recognised all β-catenin forms even though their epitopes were adjacent.

Differential Wnt signaling activity in HCC cell lines prompted us to investigate the interactions between β-catenin and other molecules, which have important functions in hepatocytes and may affect β-catenin/TCF transcriptional activity. C/EBPα is a potent inhibitor of cell proliferation in HCC cell lines and is involved in liver-specific gene expression, and some somatic alterations of it have been observed in AML and HCC. We investigated the effect of C/EBPα on β-catenin signalling. We have found that C/EBPα inhibits mutant β-catenin-TCF transcriptional activity, and physically interacts with β-catenin in HCC cells.

While we were analyzing some stably mock-transfected Huh7 clones to use as controls, we observed heterogeneity in their proliferation rates. Further analysis of these clones revealed that some clones ceased to proliferate when passaged extensively. One of these clones (C3) was not tumorigenic in immunodeficient mice. Based on these observations, we hypothesized that some cancer cells could produce senescencent progeny in cell culture. Indeed, we showed that breast- and liver-cancer-derived cells display senescencent phenotypes at variable ratios. By using our experimental system, we also showed that replicative senescence program may work independently of functional p53 and p16 pathways, and the SIP1 gene is partially responsible for replicative senescent phenotypes in our Huh7-derived senescent clone C3. Overexpression of mouse SIP1 in p53- and Rb-deficient Hep3B cells induced partial senescent phenotypes at early passages. However, stable Hep3B cells repressed mouse SIP1 expression by an unknown mechanism and escaped senescent arrest in late passages.

Our results suggest that Wnt pathway may have a dual role in hepatocellular malignancy, as it is active/easily inducible in well-differentiated HCC cells and inactive/repressed in poorly-differentiated ones. The further study of β-catenin in tumor samples by using our monoclonal antibodies may reveal new aspects in β-catenin signaling. However, the mechanism of these phenomena and the inhibition of β-catenin-TCF signaling by C/EBPα require more study to reach a more comprehensive conclusion. The study of reprogramming of replicative senescence in HCC-derived cells indicated that senescence program may work independent of p53 and p16 pathways and heterogeneity of hepatocellular malignancy exists even within the established HCC derived cell lines.

ÖZET

Hepatoselüler Malignansi Fenotipinin Heterojenliği

Nuri Öztürk
Moleküler Biyoloji ve Genetik Doktorası
Tez Yöneticisi: Prof. Dr. Mehmet Öztürk
Ağustos, 2006, 155 sayfa

Hepatoselüler karsinoma (HCC), en yaygın karsinomlardan olup dünya genelinde her yıl 600.000'den fazla ölüme sebep olmaktadır ve aflatoksin B1, alkol ve Hepatit B ve C gibi etiyolojik faktörlerle ilişkilendirilmektedir. HCC'de bir çok gen somatik değişime uğramakla birlikte hücre döngüsünde, p53 ve kanonik Wnt yolaklarında ve TGFβ/IGF ekseninde bulunan genler daha çok etkilenmektedir. HCC'lerin yaklaşık üçte birinde kanonik Wnt yolağını etkileyen mutasyonlara rastlanmaktadır. Bununla birlikte, mutant β-katenin (kanonik Wnt sinyalinin temel öğelerinden biri) anlatımı yapan transgenik fareler karaciğer tümörü geliştirmediği için, bu yolak değişimlerinin karaciğer tümörlerindeki etkileri ayrıntılı bilinmemektedir.

Karaciğer tümörlerindeki heterojenliği çalışmak amacıyla, HCC hücre hatlarında kanonik Wnt yolağı üzerine yoğunlaştık. Kanonik Wnt yolağının %80 oranında iyi farklılaşmış ve %14 oranında az farklılaşmış HCC hücre hatlarında etkin olduğunu tespit ettik. Bu bulguya ek olarak, mutant β-katenininin ektopik anlatımı iyi farklılaşmış HCC hücre hatlarında az farklılaşmış olanların aksine kuvvetli kanonik Wnt aktivitesine sebep oldu. Elde ettiğimiz sonuçlar HCC'deki heterojenliğin aynı sinyal yolağı içinde bile olabileceğine işaret etmektedir ve bu olgu, kanonik Wnt yolağının iyi ve az derecede farklılaşmış HCC hücrelerinde farklı olmasıyla örneklendirilmiştir. Bu çalışma sırasında, nükleer/sitoplazmik β-katenin havuzunun tümör gelişiminde daha önemli olduğu varsayıldığından, bu havuzu zardaki β-kateninden ayırt edebilmek amacıyla monoklonal β-katenin antikorları ürettik. 4C9 ve 9E10 epitopları birbirine yakın olmakla birlikte, 4C9 monoklonal antikoru (MAb) sadece yapışma kavşakları dışındaki β-katenini tanımaktayken diğer MAb, 9E10, tüm β-katenin formlarını tanımıştır.

Kanonik Wnt yolağının HCC hücrelerinde farklı aktivite göstermesi, bizi HCC'de önemli fonksiyonları olan ve β-katenin ile etkileşerek β-katenin/TCF yazılım aktivesini değiştirebilecek molekül adaylarını araştırmaya yöneltti. C/EBPα karaciğer hücrelerinde

hücre büyümesini durdurmakta ve karaciğere özgü genlerin anlatımını düzenlemektedir. Bu genin somatik değişimleri AML ve hepatoselüler karsinomada gözlenmiştir. Bu sebeple, C/EBPα'nın β-katenin sinyali üzerine etkisini araştırdık. Hepatoselüler karsinoma hücre hatlarında, C/EBPα'nın mutant β-katenin-TCF yazılım aktivitesini inhibe ettiğini ve β-katenin proteini ile fiziksel olarak etkileştiğini bulduk.

Kontrol olarak kullanmak amacıyla elde edilen kararlı eşdeğer Huh7 hücre hattı klonlarında büyüme hızlarının farklı olduğunu gözlemledik. Bu hücrelerin ayrıntılı analizlerinde, kültürde uzun dönem üretildiklerinde büyümeyi kestikleri gösterilmiştir. Bu klonlardan birisi (C3) yabancı dokuya cevap veremeyen farelerde tümör oluşturamamıştır. Bu gözlemlere dayanarak bazı kanser hücrelerinin kültür ortamında kendiliğinden yaşlanmış yavru hücreler verebilecekleri tezini oluşturduk. Gerçekten de, meme ve hepatoselüler kanser hücrelerinin değişen oranlarda yaşlanmış hücreler ürettiğini tespit ettik. Buna ek olarak, elimizdeki modeli kullarak replikatif yaşlanmanın fonksiyonel p53 ve p16 yolakları olmadan da gerçekleşebildiğini ve SIP1 geninin Huh7'den türetilmiş bir klonda (C3) gözlemlenen replikatif yaşlanmada kısmen sorumlu olduğunu gösterdik. Bunlara ek olarak, p53 ve Rb bakımından eksik Hep3B hücre hattında fare SIP1 geninin anlatımı kısmi yaşlanmaya yol açmıştır. Fakat, bu hücreler uzun süre kültürde tutulduğunda bilinmeyen bir mekanizma ile fare SIP1 geninin anlatımını baskıladılar ve yaşlanma bariyerinden kaçtılar.

Kanonik Wnt sinyalinin iyi derecede farklılaşmış hücrelerde aktif/kolayca indüklenebilir olması ve az derecede farklılaşmış hücrelerde inaktif/baskılanmış olması sebebiyle bu yolak karaciğer hücrelerinde çift yönlü rol oynamaktadır. Tümör örneklerinde β-kateninin bizim antikorlarımızla incelenmesi β-katenin sinyalinin yeni yönlerini açığa çıkarabilir. Bu bulguların mekanizmasının açıklanması ve β-katenin-TCF sinyalinin C/EBPα tarafından baskılanmasının net olarak yorumlanması için daha fazla çalışma yapılmalıdır. Hepatoselüler karsinomadan türetilmiş hücrelerde yaşlanmanın yeniden programlanabilmesi çalışması, replikatif yaşlanmanın p53 ve p16 yolaklarından bağımsız gerçekleşebileceğini ve hepatoselüler karsinomada heterejonliğin yıllardır kültürde tutulmuş HCC hücre hatlarının kendi içinde bile olduğuna işaret etmektedir.

ACKNOWLEDGMENTS

Thank you …

…Dr. Mehmet Öztürk, my supervisor, for all that I have learnt from you and for your patience.

…Dr. Rengül Çetin-Atalay, for the knowledge and experience you have shared, and the support you have given.

…Dr. Can Akçalı for the experience you have shared and for your patience.

…Dr. Tamer Yağcı, for the experience you have shared and for your patience.

…Ayça Arslan-Ergül, for the two-year-internship, the friendship and the knowledge you have shared.

…Haluk Yüzügüllü for the experience you have shared and for your friendship.

…Şerif Şentürk, for the experience you have shared and for your friendship.

…Dr. Esen Oktay, for your patience and friendship.

…Nilgün Taşdemir for your patience and friendship.

…Oğuz Kanca and Alper Tunga for your patience and friendship.

…Hani Al-Otaibi, for the friendship and the experience you have shared.

…Dr. Esra Erdal, for the friendship and the experience you have shared.

…Dr. Tolga Çağatay, Dr. Emre Sayan, Dr. Berna Sayan for the friendship and the experience you have shared.

…Molecular Oncology Group, Mine Mumcuoğlu, Sevgi Bağışlar, Özge and Guvanch for the friendship and the experience you have shared.

…MBG supervisors, Dr. Özlen Konu, Dr. Uygar Tazebay, Doç. Dr. Işık Yuluğ, Prof. Dr. Tayfun Özçelik, Dr. İhsan Gürsel, Dr. Cengiz Yakıcıer for the knowledge and experience you have shared.

… The department personnel for your cooperation and reciprocal friendship.

…My family.

This Ph.D. thesis research was supported by grants from TUBİTAK.

TABLE OF CONTENTS

LIST OF TABLES

LIST OF FIGURES

ABBREVIATIONS

AD	activation domain
AFB1	aflotoxinB1
AFP	alpha-feto protein
AI	allelic imbalance
Amp	ampicillin
ALT	alternative mechanism of telomere lengthening
AP	alkaline phosphatase
ARF	Alternative Reading Frame
BMP	bone morphogenetic protein
BRCA	breast cancer gene, early onset
BrdU	Bromodeoxyuridine
Brm	Brahma
bZIP	basic region leucine zipper
C/EBP	CCAAT enhancer binding protein
CaMK	calmodulin-dependent protein kinase
CDK	Cyclin Dependent Kinase
CDP	CAAT displacement protein
CFA	Freund's complete adjuvant
CK	Casein Kinase
CK19	Cytokeratin 19
Co-IP	Co-Immunoprecipitation
CO2	carbon dioxide
CRC	colorectal cancer
CRD	cysteine-rich domain
C-terminus	carboxy terminus
Dkk	Dickkopf
DNA	Deoxyribonucleic acid
Dsh	Dishevelled (in Drosophila)
Dvl	Dishevelled (in vertebrates)

ED	embriyonal day
EDTA	ethylenediaminetetraacetic acid
EtBr	ethidium bromide
FAP	familial adenomatous polyposis
FBS	fetal bovine serum
Fz	Frizzled
g	gram
g	gravity
GAPDH	glyceraldehyde-3-phosphate dehydrogenase
GSK3β	glycogen synthase kinase 3 beta
HAT	Hypoxanthine Aminopterin Thymidine
HB	Hepatoblastoma
HBV	Hepatitis B Virus
HbX	hepatitis B virus X protein
HBXAg	Hepatitis B virus X antigen
HCC	Hepatocellular Carcinoma
HCV	Hepatitis C Virus
HDAC	histone deacetylase
HH	hereditary hemochromatosis
HMG	high mobility group
hMSH2	Human Mut S homolog-2
HRP	horse radish peroxidase
HT	Hypoxanthine-Thymidine
hTERT	human Telomerase Reverse Transcriptase
hTR	human telomerase RNA
I	immortal
IFA	incomplete Freund's adjuvant
Ig	immunoglobulin
i.p	intraperitoneal
IP	immunoprecipitation
IGF2	insulin-like growth factor 2

IGF2R1	IGF2 Receptor
IGFBP	IGF-binding protein
JNK	Jun Kinase
Kan	kanamycin
Kb	Kilo base
kDa	kilo Dalton
LAP	Latent Associated Protein
LB	Luria-Bertani media
LCD	large cell-dysplasia
LEF	lymphocyte enhancer-binding factor
LOH	loss of heterozygosity
LRP5	LDL-receptor related protein 5
LRP6	LDL-receptor related protein 6
LTBP	Latent TGF- β Binding Protein
LTR	long terminal repeat
M6P/IGF2R	mannose-6-phosphate/insulin-like growth factor 2 receptor
MAb	monoclonal antibody
MAP/ERK	mitogen activated protein/extracellular signal-regulated kinase
MAPK	Mitogen Activated Protein Kinase
MDM2	Mouse Double Minute 2
mg	milligram
µg	microgram
$MgSO_4$	Magnesium Sulfate
$MHBS^t$	carboxyterminal truncated middle hepatitis B surface protein
ml	milliliter
µl	microliter
MMLV	Murine Maloney Leukemia Virus
MQ	MilliQ water
NaCl	Sodium Chloride
NaF	sodium fluoride
NaOH	Sodium Hydroxide

Na_3VO_4	sodium ortho-vanadate
NEAA	Non-essential Amino Acid
nm	nanometer ($1/10^9$ of a meter)
NS3	Nonstructural Protein 3
NS5A	Nonstructural Protein 5A
N-terminus	amino terminus
O/N	over night
OD	Optical Density
PAb	polyclonal antibody
PAGE	Polyacrylamide gel electrophoresis
PBS	Phosphate Buffered Saline
PBS-T	Phosphate Buffered Saline with Tween-20
PCP	planar cell polarity
PCR	Polymearase chain reaction
PD	poorly-differentiated
PD	Population doubling
PI-3 kinase	Phosphatidylinositol 3-kinase
PKR	double-stranded RNA protein kinase
PMSF	Phenylmethylsulphonylfluoride
PP2A	protein phosphatase 2A
PPARγ	peroxisome proliferators antigen receptor γ
pRb	Retinoblastoma protein
PS	presenescent
RD	regulatory domains
RNA	Ribonucleic acid
ROS	reactive oxygen species
rpm	revolutions per minute
RTK	receptor tyrosine kinases
S	senescent
s.c	subcutaneous
S/N	supernatant

SABG	senescence associated beta galactosidase
SAP	shrimp alkaline phosphatase
SCD	small cell-dysplasia
SDS	Sodium Dodecyl Sulfate
SDS-PAGE	SDS- Polyacrylamide Gel Electrophoresis
sFRPs	secreted Frizzled-related proteins
shRNA	short hairpin RNA
SIP1	Smad interacting protein 1
siRNA	Small interfering RNA
Smad	homolog of mothers against decapentaplegic (MAD)
SWI/SNF	switching-defective and sucrose nonfermenting
TBS	Tris Buffered Saline
TBS-T	Tris Buffered Saline with Tween-20
TCF	T-Cell Factor (T-cell specific, HMG-box)
TEMED	N, N, N, N-tetramethyl-1, 2 diaminoethane
TGFα	transforming growth factor alpha
TGF-β	Transforming growth factor
TNF	Tumor necrosis factor
Tris	Tris (hydroxymethyl)-methylamine
UV	Ultraviolet
WD	well-differentiated
WIF-1	Wnt-inhibitory factor-1
X-Gal	5-bromo-4-chloro-3-indolyl-b-D-galactoside
ZFHX1B	Zinc finger homeobox 1B

CHAPTER 1. INTRODUCTION

1.1 Hepatocellular malignancy

The liver is the largest internal organ in the body, filling the upper right side of the abdomen and protected by the rib cage. The physiological functions of the liver can be summarized as follows: 1) Bile production and excretion. 2) Excretion of bilirubin, cholesterol, hormones, and drugs. 3) Metabolism of fats, proteins, and carbohydrates. 4) Enzyme activation. 5) Storage of glycogen, vitamins, and minerals. 6) Synthesis of plasma proteins, such as albumin and globulin, and clotting factors 7) Blood detoxification and purification.

A malignancy is cancerous growth, in which a mass of cells grows in an uncontrolled fashion, with a tendency to create daughter cells that break away and grow elsewhere, invading and damaging surrounding tissue. Primary liver cancer is different from cancers that have spread from other places in the body to the liver (liver metastases). There are two main kinds of primary liver cancer, hepatoma and cholangiocarcinoma. Hepatoma originates from the hepatocytes, the main functioning liver cells, while cholangiocarcinoma originates in the bile ducts.

Hepatoblastoma (HB) is the most common pediatric liver malignancy, comprising approximately 1% of all pediatric cancers (Schnater JM. et al., 2003). Liver angiosarcoma is a very rare type of primary liver cancer developing from the cells of blood vessels within the liver.

Hepatocellular carcinoma (HCC), the most frequent primary liver cancer, is the fifth most common cancer world-wide and one of the most deadly cancers with approximately 600,000 yearly deaths (Llovet JM., 2003). Hepatocarcinogenesis nearly always develops in the setting of chronic hepatitis or cirrhosis; conditions in which many hepatocytes are killed, inflammatory cells invade the liver and connective tissue (Thorgeirsson SS. and Grisham GW., 2002). Infection with hepatitis B virus (HBV), hepatitis C virus (HCV) and chronic exposure to aflatoxin B1 (AFB1) are responsible for about 80% of all HCCs in humans (Bosch FX. et al., 1999). Development of HCC is slow process requiring 10-30 years from the initiation of to the fully malignant

phenotype. The preneoplastic liver is often the site of chronic hepatitis, cirrhosis, or both. Hepatocyte cycling leads to the production of monoclonal populations of aberrant and dysplastic hepatocytes that have telomere erosion and telomerase re-expression, sometimes microsatellite instability, and occasionally structural aberrations in genes and chromosomes. Development of dysplastic hepatocytes in foci and nodules and emergence of hepatocellular carcinoma are associated with the accumulation of irreversible structural alterations in genes and chromosomes, however the genomic basis of the malignant phenotype is heterogeneous (Thorgeirsson SS. and Grisham GW., 2002). The sequential events leading to HCC may be summarized in five steps: chronic liver injury that produces inflammation, cell death, cirrhosis and regeneration, DNA damage, dysplasia, and finally HCC (Figure 1.1) (Tannapfel A. and Wittekind C., 2002). More than 60–80% of HCC cases arise in cirrhotic liver.

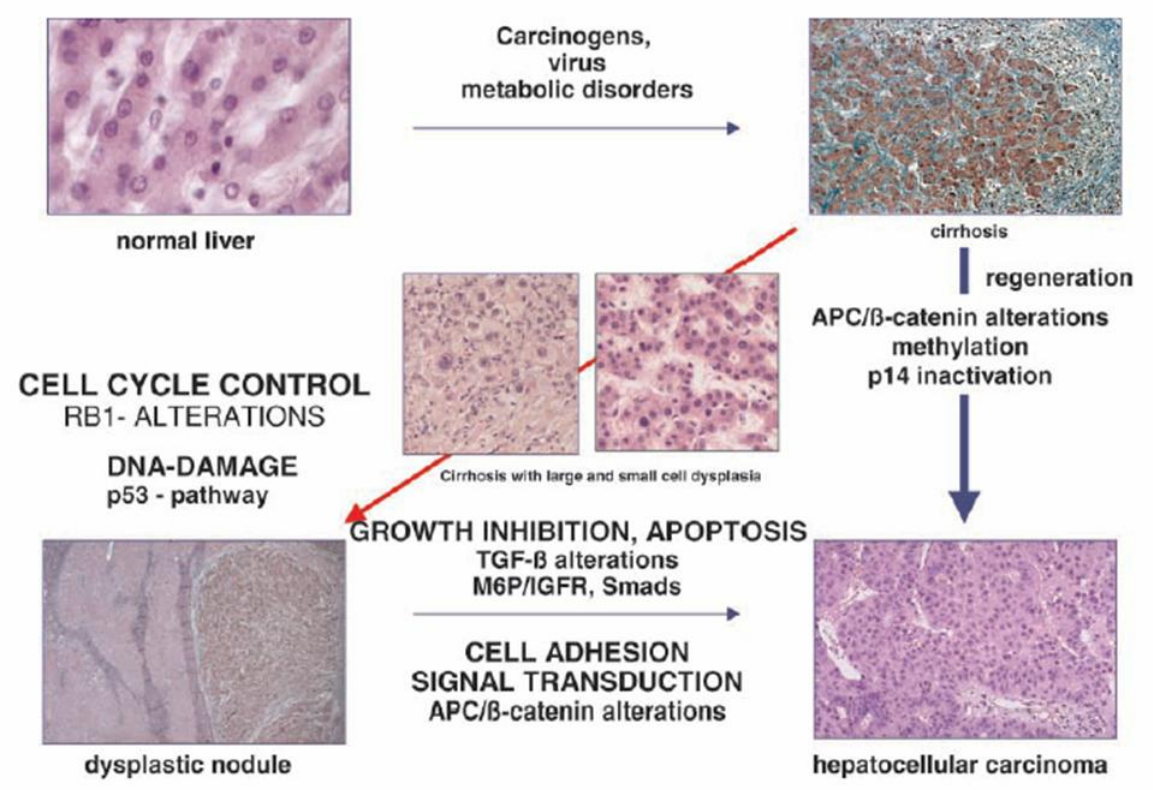

Figure 1.1: **Multistage process of hepatocarcinogenesis** (Tannapfel A. and Wittekind C., 2002) (See text for details).

1.2 Pathogenesis of hepatocellular carcinoma

1.2.1 Significance of viral hepatitis in hepatocellular carcinoma

The epidemiologic association of chronic HBV or HCV infection with HCC has been well established. The availability of cloned HBV and HCV genomes made it possible to detect hepatitis viruses in hepatocellular carcinomas, and their involvement in hepatocarcinogenesis. Oncogenic mechanism of HBV and HCV infection may be simply defined as releasing the growth control of hepatocytes by coding for a factor like the X protein of HBV (HbX) that activates otherwise dormant genes or activates proto-oncogenes or silences anti-oncogenes; by inserting its DNA sequences that can activate and influence the transcription of cellular genes; by causing chronic inflammation with cell death and hepatocyte regeneration and with fibrosis; and by activation of the immune system liberating cytokines at the wrong time at the wrong place. Following liver cell necrosis, inflammation, regeneration, and fibrosis, quiescent hepatocytes start to proliferate. During this physiological process, irregular regeneration of hepatocytes through clonal expansion may lead to loss of control over growth and development of HCC (Ueno Y. et al., 2001).

Regarding the contribution of HBV to hepatocarcinogenesis, the role of integration of HBV DNA into host chromosomes and the subsequent chromosomal instabilities is an interesting issue. Integration of HBV DNA into HepG2 cells or into transgenic mouse chromosomes has resulted in chromosomal instability that may lead to loss of heterozygosity (LOH) in many loci during chronic infection (Hino O. et al., 1991; Livezey KW. and Simon D., 1997). It has also been shown that HBV chronic carriers display a higher incidence of chromosomal instabilities than the corresponding the uninfected population (Simon D. et al., 1991; Laurent-Puig P. et al., 2001).

Transcriptional activation of a wide range of viral, as well as cellular genes such as *c-fos , c-myc, insulin-like growth factor 2* (IGF2), *insulin-like growth factor I receptor* (IGF_{R1}) and *β-interferon* , were shown to be induced by HBV encoded X antigen (HBxAg) (Twu JS. and Schloemer RH., 1987; Colgrove R. et al., 1989; d'Arville CN. et al., 1991; Caselmann WH., 1996; Kim SO. et al., 1996). In chronic HBV infection, it has been shown that HBxAg binds and functionally inactivates the tumor suppressor p53 (Ueda H. et al., 1995; Huo TI. et al., 2001) and the negative growth regulator $p55^{sen}$

(Feitelson MA., 1999), both of which are involved in senescence related pathways. Inactivation of the retinoblastoma (Rb) tumor suppressor by hyperphosphorylation resulting in the activation of E2F1 and the trigger of the cell cycle has been reported in HbxAg-positive HCC cells (Sirma H. et al., 1999). It has also been shown that HBxAg can down regulate the expression of translational factor sui1, and cyclin-dependent kinase inhibitor $p21^{WAF1/CIP1/SDI1}$ (Sirma H. et al., 1999). As with HbxAg, carboxyterminal truncated middle hepatitis B surface protein ($MHBS^t$) can activate various viral and cellular gene promoters (Caselmann WH. et al., 1990; Kekule AS. et al., 1990). Recent data suggests that HbxAg contributes to HCC development also by mechanisms other than transactivation. HBxAg binds to the X-associated protein 1 and possibly disturbs its function in nucleotide excision repair mechanism (Becker SA. et al., 1998). It has also been shown that HBxAg-stimulated cell growth is associated with constitutive activation of the ras/raf/MAPK and NFκ-B signal transduction pathways (Lucito R. and Schneider RJ., 1992; Benn J. and Schneider RJ., 1994; Shirota Y. et al., 2001).

Studies have recently begun to clarify the molecular mechanisms of HCV-induced carcinogenesis. Studies with HCV proteins showed that viral proteins interact with various cellular proteins, including 14-3-3 protein, apolipoprotein AII, tumor necrosis factor (TNF) receptor, lymphotoxin-ß receptor, DEAD domain of RNA helicase, nuclear ribonucleoprotein, double-stranded RNA protein kinase (PKR), p53 and SNARE-like protein (Ghosh AK. et al., 1999; Shimotohno K., 2000; Ray RB. and Ray R., 2001).

In chronic HCV infection, inactivation of p53 can be achieved either by HVC core protein which transcriptionally represses the *p53* promoter (Ray RB. et al., 1997; Pontisso P. et al., 1998), or by nonstructural protein 3 (NS3) and NS5A which bind and most likely inactivates p53 (Ishido S. and Hotta H., 1998; Majumder M. et al., 2001). Recently, stable expression of HCV core protein in HepG2 cells was shown to result in constitutive activation of the mitogen activated protein kinase/extracellular signal-regulated kinase (MAPK/ERK) pathway (Hayashi J. et al., 2000).

Chronic infection by HBV, HCV and chronic hepatitis lead to the activation of cytokines and growth factors such as transforming growth factor-α (TGF-α) and insulin-like growth factor-2 (IGF2), and the simultaneous decrease in IGF-binding proteins (IGFBPs), which increases the bioavailability of the insulin-like growth factors (IGFs).

IGF2 and TGFα in preneoplastic hepatocytes conbribute to the increase in the rate of proliferation (Grisham JW., 2001). Structural genomic alterations accumulate slowly during the preneoplastic phase (Thorgeirsson SS. and Grisham JW., 2002; Suriawinata A. and Xu R., 2004). However, once the hepatocytes acquire a dysplastic phenotype, characterized by small cell size, increased nuclear to cytoplasmic ratio, basophilia and abnormal nuclear morphology the rate at which these cells acquire additional disruptions to the genome increases dramatically (Hytiroglou P., 2004) (Figure 1.2).

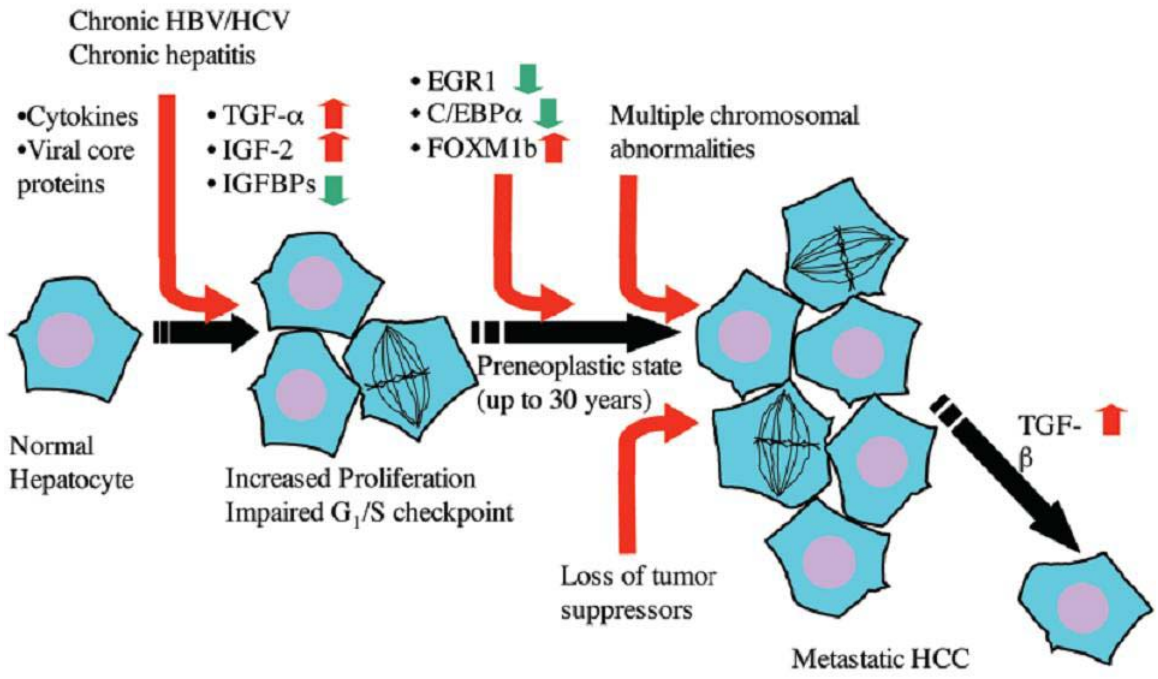

Figure 1.2: Simplified model of molecular changes during hepatocellular carcinogenesis. Normal hepatocytes proliferate at a very slow rate. Chronic infection by HBV, HCV and chronic hepatitis lead to the activation of cytokines and growth factors such as TGFα and IGF2, and the simultaneous decrease in IGFBPs, which increases the bioavailability of the IGFs. These changes lead to an increased rate of proliferation, which for many years is balanced by loss of hepatocytes through apoptosis. During the preneoplastic period, additional changes are acquired, including multiple chromosomal abnormalities, loss of tumor suppressors, decreased expression of EGR1 and C/EBPα, and increased expression of FOXM1b. At later stages, increased expression of TGF-β is thought to promote angiogenesis and metastasis (Greenbaum LE, 2004).

1.2.2 Alcohol and cirrhosis

Beside for the HBV and mostly HCV-associated cirrhosis, non-viral induced cirrhosis is also coupled with elevated risk of HCC (Furuya K. et al., 1988; Floreani A. et al., 1999).

It has been shown that alcoholic cirrhosis is associated with both HCC and cholangiocarcinoma. In the absence of cirrhosis, however, alcohol has not been shown to be carcinogenic in animal studies. It appears that, in large part, the relationship of alcoholic cirrhosis to liver cancer may be due to concomitant infection with HCV (Farber E., 1996). The effects of ethanol metabolism on DNA integrity and repair mechanisms are likely to play a significant role in the process of transformation. However, it is becoming increasingly apparent that ethanol, the metabolism of ethanol, or both also affect cell signaling pathways that regulate normal and abnormal hepatocyte function, proliferation, and apoptosis (McKillop IH. and Schrum LW., 2005).

1.2.3 Hepatotoxic chemicals

Aflatoxin B1 (AFB_1), benzo(a)pyrene and vinly chloride were shown to have a well-defined genotoxic effect in hepatocarcinogenesis. Consumption of food contaminated with aflatoxins, toxic metabolites of some species of Aspergillus fungi, has been allied with both human and animal HCCs. Aflatoxin metabolism produces aflatoxin B1-8,9-epoxide, a toxic product that induces a G to T mutation of the p53 gene at codon 249 up-regulating insulin-like growth factor II , which leads to a reduction of apoptosis (Bressac B. et al., 1991; Hsu IC. et al., 1991; Lee YI. et al., 2000).The genotoxic effects of benzo(a)pyrene and vinly chloride on *p53* gene has been supported by human and animal data (Puisieux A. et al., 1991; Barbin A. et al., 1997).

1.2.4 Hemochromatosis and iron

Alteration in iron absorption and deposition in the liver and other organs occurs in hereditary hemochromatosis (HH), which is an autosomic recessive disease (Bailey MA. et al., 2002). Iron overload has been associated with a high risk of HCC in patients with untreated hemochromatosis and dietary iron intake in patients without hereditary iron overload (Hann HW. et al., 1989; Fargion S. et al., 1992). Iron overload as a cofactor for

hepatocarcinogenesis is the iron deposition which occurs in hepatocytes, Kupffer cells and bile ducts. It results in increased production of oxygen free radicals, peroxidation of membrane lipids, and other reactive oxygen species (ROS)-mediated damages (Kicic A. et al., 2001).

1.2.5 Obesity and HCC

Recently, several epidimological observations have implicate obesity as a risk factor for certain malignancies such as endometrium cancer, breast cancer etc. Obesity and diabetes mellitus were suggested as important risk factors for cryptogenic chronic liver disease in patients with HCC is supported by the analysis of surgically treated patients (Regimbeau JM. et al., 2004).

1.3 Liver cirrhosis and senescence

Liver cirrhosis, the irreversible terminal stage of chronic liver disease, characterized by widespread fibrous scarring, is a major cause of morbidity and mortality worldwide, with no effective therapy. Independent of its cause, cirrhosis is considered a major clinical and histopathological risk factor for HCC development. A variety of factors induce liver cirrhosis, including viral hepatitis, alcohol abuse, prolonged biliary obstruction, genetically transmitted metabolic disorders, and others. Serious complications of liver cirrhosis includes those: accumulation of fluid in the abdomen (ascites), bleeding disorders (coagulopathy), increased pressure in the blood vessels (portal hypertension), and confusion or a change in the level of consciousness (hepatic encephalopathy). Regenerative nodules are characteristic lesions of the cirrhotic liver. They exhibit a lack of bile ducts and poorly organized hepatocytes surrounded by fibrosis and proliferating cholangiocytes. Dysplastic foci, which are smaller than 1 mm, can be found in regenerative nodules. There are two types of dysplastic foci in cirrhotic livers, small cell-dysplasia (SCD) and the large cell-dysplasia (LCD), according to the nuclear/cytoplasmic ratio. SCD are thought to be HCC precursor lesions that result from the proliferation of hepatocytes and oval cells. On the other hand, LCD apparently arise from persistent necroinflammation-induced senescent hepatocytes and are therefore not considered to be HCC precursor lesions (Libbrecht L. et al., 2005).

Hepatocyte telomere shortening and senescence are general markers of human liver cirrhosis, and correlates with progression of fibrosis in cirrhosis samples (Wiemann SU. et al., 2002). Additionally, Paradis V. et al. observed an increasing percentage of replicative senescent liver cells from normal liver to chronic hepatitis and HCC (Paradis V. et al., 2002).

1.3.1 Cellular senescence

In 1961, Leonard Hayflick and Paul Moorhead discovered that human cells derived from embryonic tissues can only divide a finite number of times when cultured (Hayflick and Moorhead, 1961). This phenomenon is now known as replicative senescence. Hayflick and Moorhead worked with fibroblasts, a cell type found in connective tissue, but replicative senescence has been found in other cell types: keratinocytes, endothelial cells, lymphocytes, adrenocortical cells, vascular smooth muscle cells, chondrocytes, etc.

Senescence is now understood to be the final phenotypic state adopted by a cell in response to several distinct cell physiological processes. A variety of cell physiological stimuli can provoke a cell to enter senescence, telomere uncapping, DNA damage, oxidative stress, oncogenic activation, improper cell contacts, and lack of growth stimulating factors (Figure 1.3).

Senescent cells have a large, flat morphology, senescence associated β-galactosidase (SABG) activity, cease to proliferate. Even though, different stimuli result similar phenotype in senescent cells, they use distinct but not mutually exclusive effectors of senescence. For example, the replicative senescence is accompanied by telomere shortening, but stress-induced senescence caused by ectopic expression of the Ras oncoprotein is not accompanied by telomere shortening.

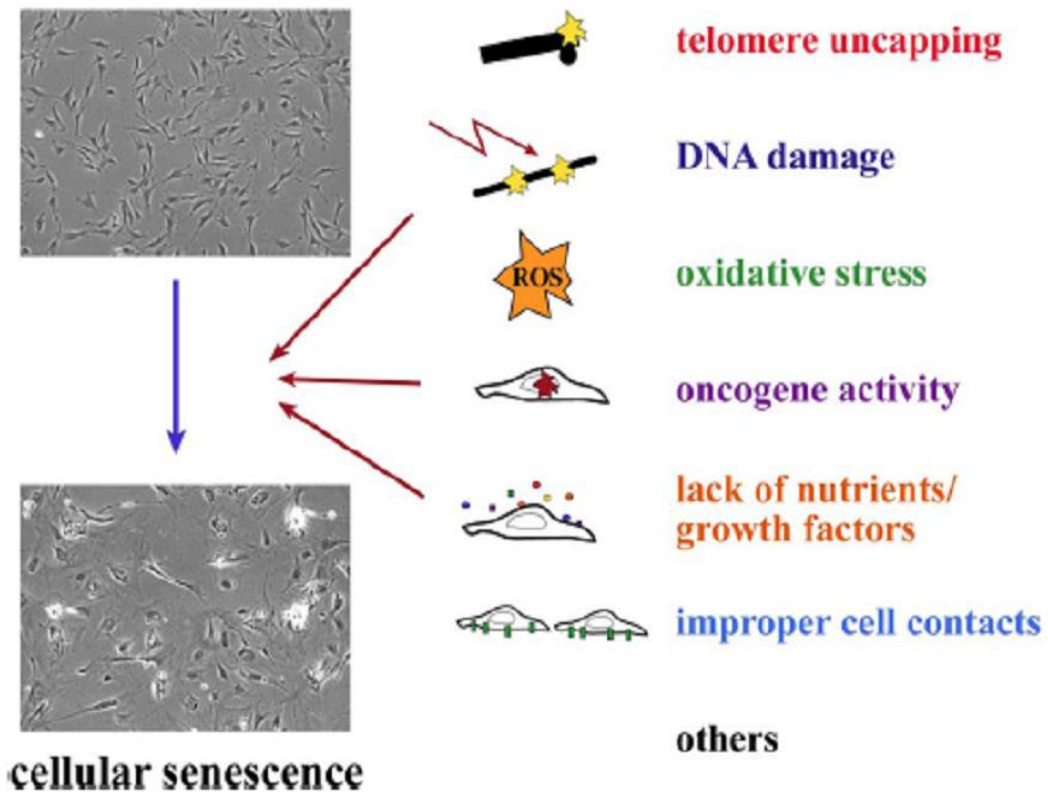

Figure 1.3: Cell physiological stimuli provoking a cell to enter senescence. (Ben-Porath I. and Weinberg RA., 2005)

1.3.2 Replicative senescence and telomere shortening

Telomeres are specialized nucleoprotein structures at the end of eukaryotic chromosomes (Blackburn EH., 1991). They serve as protective caps to distinguish the natural ends from random breaks, preventing the activation of DNA repair mechanisms and the resultant chromosome fusions (de Lange T., 2004). Expression of telomerase reverse transcriptase (TERT) is not detected in most human cell types (Ducrest AL. et al., 2002). This ensures that tumor suppression, by the telomere counting mechanism, is adequately enforced in the soma. However telomere erosion is counter-balanced by the de novo synthesis of telomeric repeats in germline cells, some stem cells, and most tumor cells. In other words, chromosome ends are stabilized by telomerase, a specialized reverse transcriptase that adds telomeric repeats (TTAGGG) to these ends in these cells. The main components of this telomerase complex are a reverse transcriptase (hTERT, human telomerase) and an integral RNA component (hTR). On the other had,

noncanonical functions of hTERT have also been described. To name a few, Sharma GG. et al. suggested that hTERT associates with human telomeres and enhances genomic stability and DNA repair (Sharma GG. et al., 2003). It has been recently shown that hTERT has a novel role in the modulation of cyclin D1 expression (Jagadeesh S. and Banerjee PP., 2006). Telomerase activity is not the sole means by which telomere maintenance may be achieved in human cells. An alternative to the telomerase-dependent lengthening of telomeres was discovered when it was observed that telomeres elongated in the absence of detectable telomerase (Bryan TM. et al., 1995). The mechanism of alternative lengthening of telomeres (ALT) resembles homologous recombination and requires many protein factors, such as Rad50, MRE11 and NBS1 (Bechter OE. et al., 2003; Jiang WQ. et al., 2005).

With each round of cell division and DNA replication, loss of telomeric DNA via the end replication problem limits the proliferative capacity of primary cells *in vitro* at the stage of cellular senescence (Harley CB. et al., 1990; Yu GL. et al., 1990; Wright WE. and Shay JW., 1992). Cells in culture display progressively shorter telomeres as the cells approach replicative senescence (Harley CB. et al., 1990), and cells collected from older organisms, which have presumably undergone more cell divisions *in vivo*, display both shorter replicative lifespans in culture and shorter telomeric DNA (Hastie ND. et al. 1990). Ectopic expression of hTERT, the catalytic subunit of telomerase, restores telomere length in fibroblasts and results in immortalization of primary human fibroblasts (Bodnar AG. et al., 1998). However, the ectopic expression of hTERT in keratinocytes, mammary epithelial cells, and other cell types restores telomerase enzymatic function and telomere lengths but still does not allow these cells to bypass senescence (Kiyono T. et al., 1998; Dickson MA. et al. 2000). These data suggest that in certain cell types, even when shortened telomeres are restored by the ectopic expression of hTERT, additional signals activate or enforce the senescence program (Lundberg AS. et al., 2000).

1.3.3 The p53 and p16 pathways in replicative senescence

Replicative senescence (permanent growth arrest also called M1 stage) is believed to be initiated by a DNA damage-type signal generated by critically shortened telomeres, or by the loss of telomere integrity, leading to the activation of cell cycle checkpoint

pathways involving p53, $p16^{INK4a}$ and/or retinoblastoma (pRb) proteins (Campisi J., 2005; Dimri GP., 2005). In the absence of functional p53 and/or $p16^{INK4a}$ /pRb pathway responses telomeres continue to shorten resulting in crisis (also called M2 stage). Cells that bypass the M2 stage by reactivating hTERT expression gain the ability for indefinite cell proliferation, also called immortality. (Ben-Porath, I. and Weinberg, RA., 2004; Campisi J., 2005; Shay JW. and Wright WE., 2005). There is accumulating evidence that cancer cells undergo a similar process during carcinogenesis to acquire immortality. Telomerase activity associated with hTERT re-expression is observed in ~80% of human tumors (Shay JW. and Bacchetti S., 1997), and senescence controlling p53 and $p16^{INK4a}$ genes are commonly inactivated in the majority of human cancers (Sherr CJ. and McCormick F., 2002). Moreover, experimental transformation of normal human cells to tumor cells requires hTERT-mediated immortalization, as well as inactivation of p53 and pRb genes (Boehm JS. and Hahn WC., 2005). Another signal implicated in replicative senescence is $p21^{cip1}$ (Noda A. et al., 1994). $p21^{cip1}$ has since been well characterized as a downstream effector of p53-mediated growth arrest following DNA damage. Although p53 mediates growth arrest in senescence, the involvement of its $p21^{cip1}$ effector remains unclear (Bond JA. et al., 1995; Pantoja C. and Serrano M., 1999).

The aberrant expression of hTERT, together with the loss of p53 and $p16^{INK4a}$/pRB control mechanisms suggests that the replicative immortality is a permanent and irreversible characteristics of cancer cells. Although some cancer cells may react to some extrinsic factors by a senescence-like stress response, this response is immediate, telomere-independent and can not be qualified as replicative senescence (Roninson IB. 2003). Experimental inactivation of telomerase activity in cancer cells mostly results in cell death (Shay JW. and Roninson IB., 2004), whereas ectopic expression of p53, $p16^{INK4a}$, or pRb provocate an immediate senescence-like growth arrest, rather than replicative senescence programming (Roninson IB., 2003). Thus, do date there is no experimental evidence for spontaneous reprogramming of replicative senescence in immortalized cancer cells.

1.3.4 SIP1 and telomerase

The *SIP1* gene (*Zinc finger homeobox 1B; ZFHX1B*) encodes a transcriptional repressor protein that interacts with SMAD proteins of the TGF-β signalling pathway and CtBP co-repressor (Verschueren K. et al., 1999; Postigo AA. et al., 2003). The *SIP1* gene is expressed at high levels in almost all human somatic tissues tested, including liver (Cacheux V. et al., 2001). Although the *SIP1*, as a repressor of E-cadherin promoter, has been suggested to be a promoter of invasion in malignant epithelial tumors (Comijn J. et al., 2001), this gene has recently been implicated in TGF-β-dependent regulation of hTERT expression in breast cancer cells (Lin SY. and Elledge SJ., 2003).

1.4 Genetics of HCC

Cancer proceeds through the accumulation of mutations in genes that govern cell proliferation and death. The long latency period of tumor development indicates at least five different genetic events may be required to reach the fully malignant phenotype (Fearon, ER. and Vogelstein B., 1990). It is believed that hepatocarcinogenesis also shares this common molecular pathogenesis as well as common biological features. The genetic (Table 1.1) and epigenetic alterations generally result in disruption of p53, Wnt or Rb-p16 pathways in HCC.

gene	mutation %	references
p53	28-50%	Oda T..et al., 1992; Puisieux A. and Ozturk M., 1997
M6P/IGF2R	25-55%	De Souza AT. et al., 1995; Yamada T. et al., 1997
β-catenin	18-41%	Nhieu JT. et al., 1999 ; Terris B. et al., 1999
p16	10%	Liew CT. et al., 1999
Axin1&Axin2	5-10%	Taniguchi K. et al., 2002
Smad2&Smad4	3-6%	Yakicier MC. et al., 1999
BRCA2	5%	Katagiri T. et al., 1996
Rb	rare	Zhang X. et al., 1994
Ras	rare	Shen HM. and Ong CN., 1996

Table 1.1: Mutations in tumor suppressor genes and oncogenes in HCC.

1.4.1 Allelic imbalance and microsatellite instability

Conventional cytogenetic methods were first used for genetic analysis of hepatoma cell lines and primary liver tumors, and they revealed that most HCCs are aneuploid and harbor multiple different chromosomal abnormalities, with recurrent deletions of the short arm of chromosome 1 (Simon D. et al., 1991). By comparative genomic hybridization, chromosomes 1q, 8q, and 17q show gene dose increase while chromosomes 1p, 4q, 8p, 9p, 13q, 16p, 16q, and 17p show gene dose loss. Frequent LOH, or more comprehensive, allelic imbalance (AI), is consistently observed on chromosomes 1p, 4q, 6p, 8p, 13q, 16q, and 17p by whole-genome allelotyping (Tannapfel A. and Wittekind C., 2002). The chromosome regions with gene dose increase may contain critical oncogenes while those with gene dose loss may contain tumor-suppressor genes. For chromosomes 17p, 13q, 9p, 6q, and 16p, LOH could be related to *p53*, *Retinoblastoma 1(RB1), p16, Insulin-like Growth Factor2 Receptor (IGF2R)* inactivation (Feitelson MA. et al., 2002). In dysplastic nodules LOH has been observed with a prevalence of about 50% and 80%, respectively (Thorgeirsson SS. and Grisham JW., 2002). Microsatellite instability is associated with a mutator phenotype at the nucleotide level; it is caused by defects in the DNA mismatch repair genes *MSH2* and *MLH1* located on chromosomes 2 and 3 (Lengauer C. et al., 1998). In HCC, however, these chromosomal regions are not frequently affected by allelic losses, and microsatellite instability has not been detected by microsatellite marker analysis. But mutations in a mismatch repair gene know as Human Mut S homolog-2 (hMSH2) has been reported at about 30% of HCCs examined (Yano M. et al., 1999). Furthermore, very few mutations have been detected in the mononucleotide repeats in *Bax, IGF-IIR*, or *MLH* genes in HCC (Kondo Y. et al., 1999; Salvucci M. et al., 1999).

1.4.2 Cell cycle regulation

Cells respond to proliferative or anti-proliferative signals through the cyclinD1-Rb-Cdk 4/6 pathway or the p53-p14^{ARF} pathway. As cells enter the cycle from quiescence (G0), one or more D-type induced in response to mitogenic signals. These cyclins associate with either Cdk 4 or Cdk 6 subunits and the complex becomes activated by phosphorylation. Active cyclin/CDK complexes drive the cell cycle forward via

phosphorylation of substrates such as Rb in late G1 phase (Weinberg RA., 1995). Rb is thereby inactivated, and its growth repressive functions abolished, resulting in release of a class of associated transcription factors known as E2Fs. Then "free" E2F transactivates cyclin E gene and promote DNA synthesis necessary cell cycle progression. According to this, loss of Rb or its aberrant phosphorylation leads to a loss of growth control at the G_1 phase. To maintain Rb protein in its active, anti-proliferative state, $p16^{INK4a}$ inhibit the activity of Cdk 4 by specifically binding thus preventing its association with cyclin D and/or blocking the catalytic activity of kinase (Hirai H. et al., 1995). The $p14^{ARF}$ tumor suppressor, encoded by an alternative reading frame of the INK4a-ARF locus (9q21), senses "mitogenic current" flowing through the Rb pathway and is induced by abnormal growth promoting signals. By antagonizing Mdm2, a negative regulator of the p53 tumor suppressor, ARF triggers a p53-dependent transcriptional response that diverts incipient cancer cells to undergo growth arrest or apoptosis. Although ARF is not directly activated by signals that damage DNA, its loss not only dampens the p53 response to abnormal mitogenic signals but also renders tumor cells resistant to treatment by cytotoxic drugs and irradiation.

Taken together, disturbances in the p16-cyclin D-Cdk 4-Rb and p14-Mdm2-p53 pathways could be a main axis of genetic events in HCC because all "players" in these pathways seem to be altered in HCC. The *Rb* gene, one of the main players, is localized to chromosome 13q, which is a common deletion site for HCC and Rb mutations are also observed at 15% of HCCs (Ozturk M., 1999). Moreover, Rb protein is a target for ubiquitin dependent degradation and the degradation mechanism was shown to be dysregulated in HCCs by overexpression of a pRb specific ubiquitin ligase, gankyrin (Higashitsuji H. et al., 2000). Additionally, overexpression of cyclin D has been observed in about 10-13% of HCC cases (Ozturk M., 1999). It has recently been shown in a transgene mouse model that overexpression of cyclin D_1 is sufficient to initiate hepatocellular carcinogenesis (Deane NG. et al., 2001). The transduction of antisense cyclin D_1 inhibits tumor growth in a xenograft hepatoma model. Correcting alterations that have occurred in the G_1 phase regulatory machinery may therefore provide a novel weapon to treat and prevent HCC (Deane NG. et al., 2001). Also, it was reported that about 50% of HCC display *de novo* methylation of INK4a-ARF locus that encodes

$p16^{INK4}$ and $p14^{ARF}$ and LOH at the same locus with 20 % (Ozturk M. 1999; Liew CT. et al., 1999).

1.4.3 Alterations of the TGF-β /IGF-axis

Transforming growth factor-β (TGF-β) is a cytokine with pleiotropic activity, and is released in an inactive form. To exhibit its biological activity, it requires binding to extracellular matrix proteins and, after that, proteolytic elimination of latent associated protein (LAP) and latent TGF- β Binding Protein (LTBP). Active TGF-β is a homodimeric 25kDa protein. TGF-β initiates signaling through heteromeric complexes of transmembrane type I and type II serine/threonine kinase receptors. Activated TGF-β receptors phosphorylate receptor-regulated Smads which induces both inhibition and apoptosis in hepatocytes. Genetic alterations of the TGF-β pathway are mediated by mutations of the Smad2 and Smad4 gene, which occur in about 10% of HCC cases (Yakicier CM. et al., 1999). Mutations of the TGF-β receptor (TGF-β1RII) gene itself are detected in patients with HCC and may also abrogate TGF-β signaling (Enomoto A. et al., 2001). It has been suggested that Smad7, expressed in tumor cells, is considered to be one of resistance mechanisms to increased TGF-β1 in late stage hepatocarcinogenesis, especially in advanced HCCs without reduced TGF-beta receptor II. Smad4, in stellate cells of HCCs, might be involved in the host resistance to hepatocarcinogenesis (Park YN. et al., 2004).

A potent activator of TGF-β is the mannose-6-phosphate/insulin-like growth factor 2 receptor (M6P/IGF2R) which suppresses cell growth through binding to the insulin-like growth factor (IGF) 2 and latent complex of TGF-β. The deregulation of the IGF axis, including the autocrine production of IGFs, IGF binding proteins (IGFBPs), IGFBP proteases, and the expression of the IGF receptors, has also been identified in the development of HCC. Also, both LOH and mutations of the M6P/IGF2R have been reported in about 30% HCC patients (Oka Y. et al., 2002; Piao Z. et al., 1997, De Souza AT. et al., 1995).

PTEN/MMAC1/TEP1 (PTEN) tumor suppressor gene was shown to block growth-stimulatory and survival signals mediated by PI-3 kinase and converging on the activation of protein kinase B/Akt. Alterations, mainly mutations but also LOH, of *PTEN*

have been reported in about 27% of HCC cases (Kawamura N. et al., 1999). Recently it has been shown that PTEN expression is down-regulated in HCC cell lines probably due to loss of activity of PTEN promoter (Ma DZ. et al., 2005).

1.4.4 Wnt signaling

Aberrant Wnt/β-catenin (canonical Wnt) signaling has been found in 30%–40% of human hepatocellular carcinomas (de La Coste A. et al., 1998; Giles RH. et al., 2003).

Axin, an important regulator of β-catenin, is mutated in about 10% of HCC cases, leading to an activation of the Wnt pathway. However, mutations in the *axin* gene have until now been identified only in HCC that lack mutations in the β-catenin gene It was shown that transduction of the wild-type *axin* gene (*AXIN1*) induces apoptosis in HCC cells, indicating that axin 1 may be an effective growth suppressor of hepatocytes (Satoh S. et al., 2000).

Somatic APC mutations are rare events in HCC, but it was reported that biallelic inactivation of the APC gene contributed to the development of HCC in a patient with familial adenomatous polyposis (FAP) and a known germline mutation of the APC gene at codon 208 (Su LK. et al., 2001). E-cadherin, a compenet of adherens junctions, which is essential both for maintenance of tissue structure and regulation of free cytoplasmic β-catenin level, is rarely mutated in HCC. However, loss of function of *E-cadherin* due to LOH or de novo methylation occurs in about 30% of HCC cases (Slagle BL. et al., 1993).

1.4.4.1 Wnt signaling pathways

Wnt proteins constitute a large family of cysteine rich secreted ligands that regulate cell growth, motility, and differentiation during embryonic development. Wnts act in a paracrine fashion by activating at least three diverse signaling cascades inside the target cells (Figure 1.4).

1) The canonical Wnt pathway (Wnt/β-catenin signaling): The ‘‘classical’’, also called canonical, Wnt pathway activates target genes through stabilization of β-catenin and relocalization in the nucleus. The function of this pathway during embryonic development has been originally elucidated by experimental analysis of axis development in the frog *Xenopus laevis* and of segment polarity and wing development in the fly

Drosophila melanogaster. The abnormalities of this pathway lead to several human diseases, including tumor formation and bone abnormalities.

2) The planar cell polarity pathway: This pathway involves RhoA and Jun Kinase (JNK) and controls cytoskeletal rearrangements. Its main role is the temporal and spatial control of embryonic development, as exemplified in the polar arrangement of cuticular hairs in *Drosophila* or the convergent-extension movements in *Xenopus* embryos. On a cellular level, this pathway regulates the polarity of cells through effects on their cytoskeletal organization. To date, there is no evidence for the involvement of the planar cell polarity pathway in tumor development (Veeman MT. et al., 2003; Nelson WJ. and Nusse R., 2004; Bejsovec A., 2005).

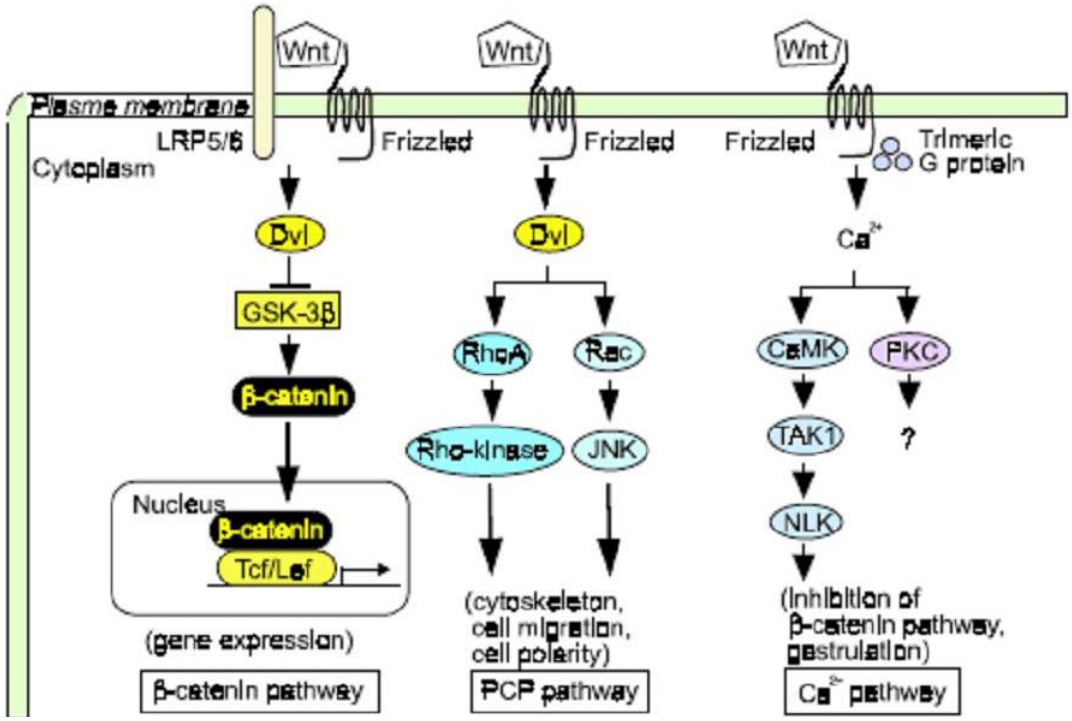

Figure 1.4: Wnt signaling pathways (Kikuchi A. et al., 2006). Wnts act in a paracrine fashion by activating at least the diverse signaling cascades inside the target cells. The Canonical Wnt signaling regulates gene expression through the stabilization and translocation of β-catenin into nucleus. The Planar cell polarity pathway activates Dvl, small G proteins (Rho or Rac), and Rho kinase or JNK, resulting in regulation of the cytoskeleton, cell migration, and cell polarity. Wnt/Ca^{2+} pathway activates CaMK, PKC, TAK, and NLK, resulting in the inhibition of the β-catenin pathway and regulates gastrulation. Dvl, Dishevelled; JNK, Jun N-terminal kinase; CaMK, calmodulin-dependent protein kinase.

3) Wnt/Ca^{2+} pathway: This pathway is stimulated by Wnt 5a and Wnt 11 and involves an increase in intracellular Ca^{2+} and activation of Ca^{2+}-sensitive signaling components, such

as calmodulin-dependent kinase, the phosphatase calcineurin, and the transcription factor NF-AT (Veeman MT. et al., 2003; Nelson WJ. and Nusse R., 2004; Bejsovec A., 2005). The Wnt/Ca2+ pathway can counteract the canonical Wnt pathway (Weidinger G. and Moon RT., 2003). It is not clear whether this pathway is conserved in mammals and whether it is implicated in tumorigenesis.

1.4.4.2 Canonical Wnt signaling pathway

Wnt/β-catenin signaling pathway, named also canonical Wnt pathway, refers to the molecular cascade initiated by a Wnt ligand and culminating in the stabilization and translocation of the β-catenin protein into nucleus. *Wnt-1* (originally named *int-1*, in *Drosophila* the homologous gene is called wingless, and the combination of both names led to the term) was the first identified as a gene activated by integration of the LTR of the mouse mammary tumor virus resulting in the development of mammary tumors in mice (Nusse R. and Varmus HE., 1982). β-catenin is the main executer of canonical Wnt signaling. In the absence of Wnts, β-catenin is phosphorylated by casein kinases 1α at serine residue 45; this in turn enables glycogen synthase kinase 3β to phosphorylate serine/threonine residues 41, 37, and 33. Phosphorylation of these amino acids triggers ubiquitination of β-catenin by β-transduction repeat containing protein (β-TrCP) and degradation in proteasomes. Phosphorylation of β-catenin occurs in a multiprotein complex containing the scaffold protein axin and/or its homologue axin2/conductin, the tumor suppressor gene product APC and GSK3β. In the presence of Wnts, β-catenin can be stabilized by two mechanisms. According to first model, Wnt signaling triggers CKIε-dependent phosphorylation of Dvl (Dsh in *Drosophila*) and enhances the binding of Dvl (Dsh) to Frat-1. Frat-1 binds to GSK-3β in the Axin complex, resulting in a reduction of the phosphorylation of β-catenin by GSK-3β. According to second model, Wnt triggers the phosphorylation of LRP6 by CK1γ and GSK-3β, which provides a docking site for Axin and recruits it to the plasma membrane. Wnt also enhances the binding of Dvl (Dsh) to Frizzled, and Dvl (Dsh) bound to Frizzled is necessary for the formation of a complex between Axin and LRP6, resulting in reduced phosphorylation of β-catenin and Axin by GSK-3β (Figure 1.5).

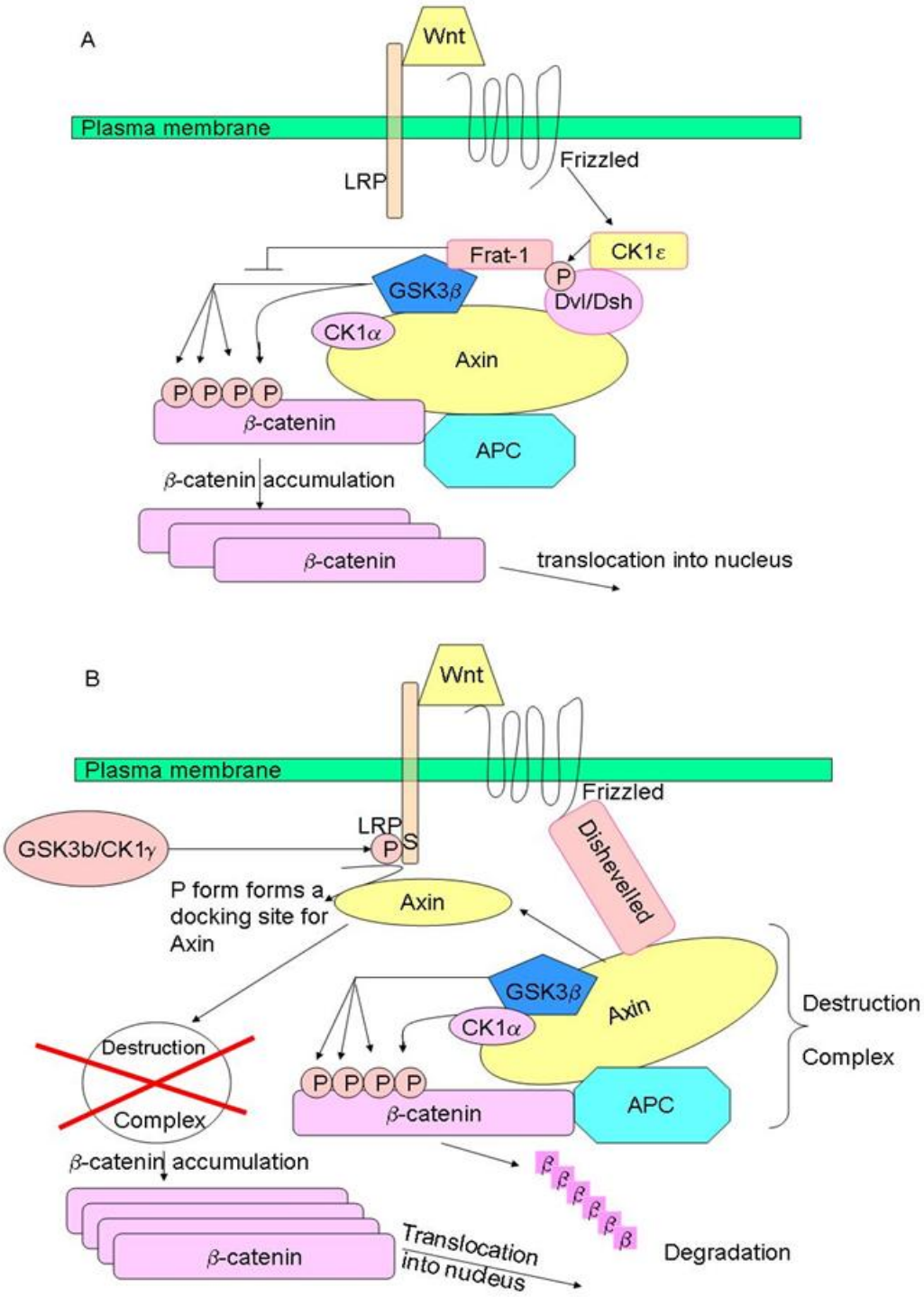

Figure 1.5: Wnt-dependent stabilization of β-catenin . **A)** Through the Dvl/Frat complex. Wnt signaling inhibits β-catenin phosphorylation by GKS3β through Dvl and Frat1.**B)** Through the Axin and LRP6 complex. Wnt triggers the phosphorylation of LRP6 by CKγ1 and GSK3β. Axin is recruited to the plasma membrane, which is a component of destruction complex, leading to the inhibition of β-catenin phosphorylation.

Stabilized β-catenin translocates into the nucleus and makes complexes with TCF transcription factors, leading to the transcription of Wnt target genes.

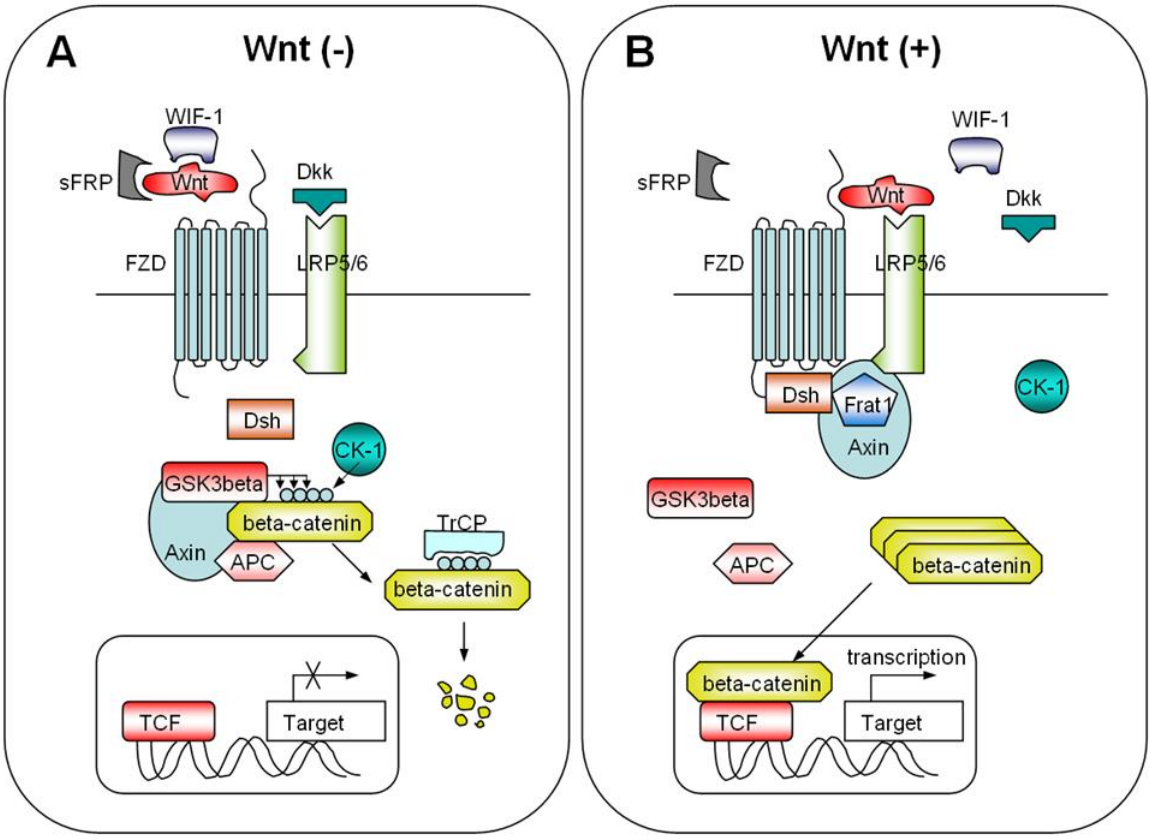

Figure 1.6: Overview of the canonical Wnt signaling pathway (Lee HC. et al, 2006). **A)** In the absence of Wnt, the cytoplasmic β-catenin is degraded in the destruction complex, consisting of APC, axin/conductin, and GSK-3β. First, β-catenin is phosphorylated on Ser 45 residue by CKIα (priming), primed β-catenin is further phosphorylated at Thr 41, Ser 37, and Ser 33 residues by GSK-3β. Phosphorylation of these amino acids triggers ubiquitination of β-catenin by β-TrCP and degradation in proteasomes. Therefore, the cytoplasmic level of β-catenin is kept low in the absence of Wnt. The LEF/TCFs cannot activate the target genes without β-catenin. The WIF-1, sFRP, and/or Dkk can inhibit the Wnt signaling by binding to Wnt ligands or LRP5/6. **B)** In the presence of Wnt, a) Wnt signaling triggers CKIε-dependent phosphorylation of Dvl (Dsh) and enhances the binding of Dvl (Dsh) to Frat-1. Frat-1 binds to GSK-3β in the Axin complex, resulting in a reduction of the phosphorylation of β-catenin by GSK-3β; or b) Wnt triggers the phosphorylation of LRP6 by CK1γ and GSK3β, which provides a docking site for Axin and recruits it to the plasma membrane. Wnt also enhances the binding of Dvl (Dsh) to Frizzled, and Dvl (Dsh) bound to Frizzled is necessary for the formation of a complex between Axin and LRP6, resulting in reduced phosphorylation of β-catenin and Axin by GSK3β. Therefore, β-catenin escapes from phosphorylation and subsequent ubiquitylation, and accumulates in the cytoplasm. The accumulated cytoplasmic β-catenin goes into the nucleus, where it binds to LEF/TCFs and activates the transcription of target genes.

Transcriptional activation is mediated by the interaction of TCF and β-catenin complexes with various activators, such as the histone acetyl transferase CBP and the chromatin remodeling SWI/SNF complex. Additionally, legless/bcl-9 recruits the nuclear protein pygopus to β-catenin thereby activating the TCF and β-catenin complex. A variety of Wnt/β-catenin target genes have been identified which include regulators of cell proliferation, developmental control genes, and genes implicated in tumor progression (Figure 1.6).

The canonical Wnt signaling is involved in a number of developmental processes, including establishment of the dorsoventral body axis (Parr BA. and McMahon AP., 1994). β-catenin accumulates in dorsal nuclei as one of the earliest indicators of dorsal development in Spemann organizer of *Xenopus* embryo (Schneider, S. et al. 1996). Wnt knock-out mice revealed different phenotypes. To name few, the expansion of the CNS fails in Wnt1 mutants (Megason SG. and McMahon AP., 2002). *Wnt3*$^{-/-}$ mice develop a normal egg cylinder but do not form a primitive streak, mesoderm or node (Liu P. et al., 1999). In adult organism it regulates tissue homeostasis, stem cells maintenance and if perturbed leads to several diseases including cancer. The best-known example of a disease involving a Wnt pathway mutation that produces tumors is familial adenomatous polyposis (FAP), an autosomal, dominantly inherited disease in which patients display hundreds or thousands of polyps in the colon and rectum. This disease is caused most frequently by truncations in APC (Kinzler KW. et al., 1991). To name a few more, Tetra-amelia, a rare human genetic disorder characterized by absence of limbs, has been proposed to result from WNT3 loss-of-function mutations (Niemann S. et al., 2004). An LRP mutation has been identified that causes increased bone density at defined locations such as the jaw and palate (Boyden LM. et al., 2002; Little RD. et al., 2002). Mutations in LRP5 were correlated with decreased bone mass (Gong Y. et al., 2001). A nonsense mutation in *Axin2* has been shown to produce severe tooth agenesis, or oligodontia, a condition in which multiple permanent teeth are missing (Lammi L. et al., 2004). Recently, mutations of Wnt10B have been linked to human obesity (Christodoulides C. et al., 2006). Canonical Wnt signaling has been linked to tumor development since the discovery of Int-1 integration site in viral carcinogenesis experiments in mice. To date, besides colorectal cancer and hepatocellular carcinoma which harbor the highest rate of

Wnt pathway gene mutations, canonical Wnt pathway abnormal reactivation has been linked to many other cancer types including those which do not harbor any activating mutation such as breast cancer.

1.4.4.3 Major components of the canonical Wnt signaling pathway

1.4.4.3.1 Wnts

19 Wnt genes were identified in human and mouse, seven in Drosophila and five in *C. elegans* (Nusse R., 2005).Wnt molecules are palmitoylated on a conserved cysteine and therefore much more hydrophobic than predicted from the primary amino acid sequence (Willert K. et al., 2003). Wnt proteins are secreted from cells and act on target cells through a complex pathway, and subject to extensive feed-back control. They are defined by characteristic primary amino acid sequences rather then functional properties. They contain a signal sequence followed by a highly conserved cysteine distribution. Although, heparan sulfate proteoglycans have been shown to have a role in stabilizing Wnt protein or aiding them to move between cells, the transport mechanism of Wnt proteins remains to be fully characterized molecularly. It is widely accepted that the Frizzled (Fz) molecules are primary receptors for Wnts (Bhanot P. et al., 1996). Wnt signaling requires not only a functional Fz, but also the presence of a long single pass transmembrane molecule of the LRP (LDL receptor related protein) class, identified as the gene arrow in Drosophila (Wehrli M. et al.,2000) and as LRP5 or 6 in vertebrates. Wnt molecules can also bind to LRP and form a trimeric complex with a Frizzled. The cytoplasmic tail of LRP may interact directly with Axin, one of the downstream components in Wnt signaling (Tolwinski NS. et al., 2003).

1.4.4.3.2 Frizzleds

Frizzleds, the primary receptors of the Wnt proteins, are seven-transmembrane receptors with a long N-terminal extension called a cysteine-rich domain (CRD). The human genome has ten different frizzleds genes: *Frizzled-1* to *-10*. All frizzled proteins contain a conserved extracellular CRD followed by seven transmembrane segments. Contrarily, their C-terminal cytoplasmic regions differ significantly in length and in sequence. As transmembrane receptor, frizzled proteins engage in multiple interactions

with different partners in the extracellular and intracellular milieu. Similarly to Wnt ligands, frizzled receptors have been shown to activate distinct Wnt signaling pathways and can be loosely classified accordingly. In *Xenopus*, *Frizzled-3, -4,* and *–7,* have been shown to activate Wnt/β-catenin pathway while human *Frizzled-6* and rat *Frizzled-2* have been shown to inhibit it (Umbhauer M. et al., 2000). The mechanism of action of frizzled signaling is not fully elucidated. However, heptahelical structure of frizzled molecules suggests that they are able to signal through heterotrimeric G proteins. Disheveled (Dsh, Dvl) is a candidate molecule that may directly interact with Frizzleds and, known to be required for Wnt signaling (Chen W. et al., 2003; Wong HC. et al., 2003). Wnt signaling leads to differential phosphorylation of Dsh. A conserved motif (Lys-Thr-X-X-X-Trp) located two amino acids after the seventh transmembrane domain of frizzleds was shown to be engaged in the frizzled/dishevelled interaction and required for Wnt/β-catenin activation via mediating Disheveled relocalization and phosphorylation (Umbhauer M. et al., 2000). The co-receptor, LRP, may also contact a cytoplasmic component of the pathway, as it has been reported that Axin can interact with the cytoplasmic tail of LRP (Tolwinski NS. et al., 2003). It has been suggested that Wnt signaling can lead to the formation of a complex including the two receptors, plus Axin and Dsh. Direct interactions between Axin and Dsh can be the first step in reconfiguring the destruction complex containing (Nusse R., 2005).

1.4.4.3.3 LRP/Arrow co-receptors

In addition to frizzleds, the canonical Wnt signaling pathway also requires single-span transmembrane proteins that belong to a subfamily of low-density-lipoprotein (LDL) receptor related proteins (LRPs): vertebrate Lrp5 and Lrp6, and their Drosophila ortholog Arrow. Human LRP5 was isolated through its homology to LDLR (Hey P. et al., 1998). Human LRP6 was identified by its homology to LRP5 (Brown SD. et al., 1998). LRP5 and LRP6 share 73% and 64% identity in extracellular and intracellular domains, respectively. The concrete evidence of LRP role for canonical Wnt signaling comes from several experiments. A mutant Lrp6 protein lacking the intracellular domain is completely inactive, and in fact blocks Wnt and Fz signaling in a dominant-negative fashion (Tamai K. et al., 2000). Additionally, mutant Lrp6 protein that lacks the

extracellular domain but is anchored on the membrane activates the canonical Wnt signaling constitutively in mammalian cells (Liu G. et al., 2003) and in *Xenopus* embryos (Tamai K. et al., 2004).

1.4.4.3.4 Extracellular inhibitors

In the extracellular milieu, Wnt signaling can be inhibited by two groups of inhibitory factors. The first group composed of secreted frizzled-related proteins (sFRPs), Wnt-inhibitory factor-1 (WIF-1), Cerberus and Coco can sequester Wnt ligand and prevent its interaction with the receptors. In human, sFRP family consists of five members. They contain a cysteine-rich domain (CRD), which shares 30-50 % sequence homology with the CRD of Frizzled receptors (Melkonyan HS. et al., 1997). WIF-1 contains a unique conserved WIF domain and five EGF–like repeats. Cerberus and Coco are related proteins interacting with a variety of growth factors including Wnt ligands and bone morphogenetic protein (BMP) to inhibit the signaling of the respective pathways in Xenopus. The inhibitory effect of Cerberus and Coco mammalian orthologs on Wnt signaling has not yet been proved. The second group inhibits Wnt signaling by binding to LRP5 and LRP6. In human three members of the Dickkopf (Dkk) family (Dkk-1, -2 and –4) were found. The inhibitory effect of Dkk-2 and Dkk-4 proteins requires the participation of Kremen2 to form a tertiary complex with LRP co-receptor that will lead to the internalization of LRP and make it unavailable for Wnt reception (Mao BY. et al., 2003).

1.4.4.3.5 Dishevelled

Dishevelled is an essential component for the canonical Wnt signaling as well as for the Drosophila PCP pathways. In mammals, there are three homologs of the *Drosophila* Dishevelled, named Dishevelled-1, -2 and –3. Dishevelled protein is composed of three conserved domains, an N-terminal DIX domain, a central PDZ domain and a C-terminal DEP domain. Mutations in the DEP domain affect the PCP pathway, whereas mutations in the DIX domain affect cell-fate signaling (Penton A. et al., 2002). Although the mechanism by which Dishevelled transduces the Wnt signal remains debatable, some mechanisms have been suggested. 1) Upon Wnt signaling, Dishevelled can interact with the C-terminal cytoplasmic tail of Frizzled and gets phosphorylated

most likely by the Wnt –regulated protein kinase Par-1 (Sun TQ. et. al., 2001). 2) Wnt stimulation of mammalian cells induces the Lrp5-Axin association within minutes (Mao J. et al., 2001), Importantly, Axin preferentially binds to the phosphorylated PPPSP motif of Lrp6, whose phosphorylation is rapidly induced by Wnt (Tamai K. et al., 2004). Therefore, it was proposed that Wnt activates Lrp6 signaling by inducing Lrp6 phosphorylation at the PPP(S/T)P motifs, which serve as inducible docking sites for Axin, thereby recruiting Axin to the plasma membrane (He X. et al, 2004). 3) It was proposed that Wnt binding to frizzled and LRP could promote a direct interaction between Axin and Dishevelled through their DIX domains to dissociate the protein complex that regulate β-catenin degradation (Logan CY. and Nusse R., 2004).

1.4.4.3.6 Axin

Axin-1 is an inhibitor of the canonical Wnt signaling pathway acting as a scaffolding protein. Axin has specific binding sites for β-catenin, GSK3β, CKIα, APC, Dvl, LRP, and protein phosphatase 2A (PP2A). Its main function is to bring together β-catenin and the protein kinases CKIα and GSK3β, thus promoting the phosphorylation and consequent destruction of β-catenin. Upon Wnt signaling, this function is overcome, allowing β-catenin to accumulate and enter the nucleus. The major product of the Axin gene is a protein of 832 or 868 amino acids (depending on alternative splicing) containing two highly conserved domains: 1) RGS domain, encompasses the binding site for APC. 2) DIX domain, a region of homology with Dvl proteins that is implicated in the binding of Axin to Dvl as well as in homodimerization.

Axin-2 (also known as Conductin) is 44% identical to Axin and shares the RGS and DIX domains as well as the binding sites for β-catenin, GSK3β, Diversin, and Smad3. While Axin2 has been studied less extensively than Axin, most data suggest that they are similar in function.

The function of Axin as an inhibitor of canonical Wnt signaling has been confirmed through different approaches. Axin mRNA injection into frog embryos inhibited dorsal axis formation (Zeng L. et al., 1997). Furthermore, truncating mutations of Axin-1 leads to the nuclear accumulation of β-catenin in hepatocellular carcinomas and the adenoviral transfer of wild-type Axin-1 into these cell or HepG2 cells decreased

the nuclear accumulation of β-catenin and lowered TCF/LEF mediated transcriptional activity (Satoh S. et al., 2000). Additionally, Axin-1 loss of function has been found in 8-10% of HCCs (Satoh S. et al., 2000; Taniguchi K. et al., 2002), in 7% of hepatoblastomas. Axin-2 mutations are rare in human cancer and have been found only in 3% of HCC (Taniguchi K. et al., 2002).

1.4.4.3.7 APC

Activating mutations of the Wnt pathway are the only known genetic alterations present in early pre-malignant lesions in the intestine (Powell SM. et al., 1992). APC is a negative regulator of the canonical Wnt signaling and mutated up to 85% of all sporadic CRCs. The vast majority of these mutations, which are insertions, deletions or non-sense mutations, lead to frame-shifts or premature stop codons in the APC transcript and non-functional APC protein (Giles RH. et al., 2003). APC bind to β-catenin and promotes its degradation. Three different structural motifs in APC are responsible for its β-catenin-regulating function: three 15-amino acid repeats binding β-catenin and plakoglobin, seven 20-amino acid repeats involved with both binding and down-regulating these proteins, and three so-called SAMP repeats facilitating axin and conductin binding. Additionally, APC can capture and escort nuclear β-catenin to the cytoplasmic destruction machinery (Neufeld KL. et al., 2000). A paralogue of APC termed APC2 or APCL was identified in humans and mouse. APC2 can bind h-catenin and regulate its concentrations as efficiently as APC (van Es JH. et al., 1999; Nakagawa H. et al., 1998).

1.4.4.3.8 GSK3β

The serine/threonine kinase GSK3β is an integral component and negative regulator of Wnt signaling. An alternative spliced form has been described (Mukai F. et al., 2002). GSK3β activity is significantly reduced by phosphorylation of Ser9, and facilitated by phosphorylation of Tyr216. In the absence of Wnt signaling, the GSK3β phosphorylates primed β-catenin (phosphorylated β-catenin at Ser45 by Casein Kinase I) at Thr41 and, subsequently, at Ser37 and Ser33, which triggers the degradation of β-

catenin). The down-regulatory nature of *GSK-3β* is qualified as putative tumor suppressor. However, *GSK-3β* mutations were not found in cancers.

1.4.4.3.9 Protein phosphatase 2A

Protein phosphatase 2A (PP2A) is a serine-threonine phosphatase. Its catalytic subunit binds to the C terminal domain of axin which suggested that PP2A interacts with the APC-β-catenin-axin-GSK3β complex. PP2A antagonize the phosphorylation of β-catenin from GSK3β by dephosphorylation of β-catenin (Hsu W. et al., 1999). However, overexpressing a regulatory subunit of PP2A (B56), which binds to the amino-terminal third of APC, reduces the amount and signaling of β-catenin. This suggests that PP2A may dephosphorylate GSK3β thereby increasing its activity, which in turn increases the phosphorylation of β- catenin and its subsequent degradation (Seeling JM. et al., 1999).

1.4.4.3.10 β–catenin

The β-catenin is 92 kDa multifunctional protein, and initially identified as a component of adherens junctions (AJs) (Ozawa M. et al., 1989; McCrea PD. et al., 1991). There, β-catenin links cadherin adhesion receptors to α-catenin, which in turn links to the cytoskeleton. This adhesion function is based on a membrane associated and stable form of β-catenin (Figure 1.7).

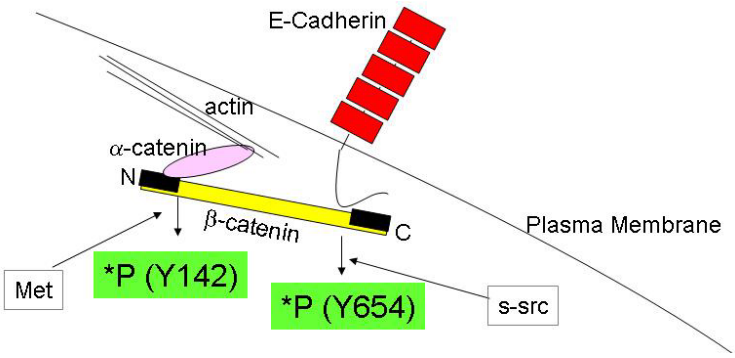

Figure 1.7: β-catenin in adherens junctions. E-cadherin dimers interact in a zipper-like fashion in adherens junctions. E-cadherin cytoplasmic tail interacts with β-catenin armadillo repeats, α-catenin interacts with the amino-terminal domain of β-catenin and with actin cytoskeleton. Phosphorylation of tyrosine-654, for instance by c-src, leads to loss of E-cadherin-binding. The tyrosine kinases Fer, Fyn or Met can induce phosphorylation of tyrosine-142 of β-catenin. This induces loss of binding to α-catenin and promotes the interaction with the nuclear co-factor BCL9-2

Variable level of free β-catenin is found in the cytoplasm and occasionally in the nuclei depending on the cell type indicating the presence of a second function of β-catenin related with gene transcriptional regulation. Contrarily to the stable membrane bound form, the cytoplasmic β-catenin is unstable and continuously degraded by the proteasomal machinery in most of the normal cells of an adult organism. Free β-catenin functions as an essential component of the canonical Wnt signaling pathway. The primary structure of the β-catenin protein reveals that it contains a 130 amino acid amino-terminal domain, an armadillo domain composed of 12 imperfect repeats of 42 amino acids (arm repeats), and a carboxy-terminal domain of 100 amino acids. Several proteins bind to β-catenin through the central region (arm repeats) and this positively-charged groove may serve as a binding motif including TCF/LEF, APC and adherent junction protein E-cadherin.

Even though, β-catenin has no DNA−binding domain or activity was identified, the carboxyl terminal domain functions as a transcriptional activator when fused to the GAL4 DNA-binding domain (van de Wetering M. et al., 1997). It uses the DNA binding propriety of the LEF/TCF family of transcription factors to transactivate its target genes expression. The amino terminus of β-catenin is known to be important for regulating the stability of β-catenin. This region of β-catenin, also called destruction box, contains a series of serine and threonine residues, which may be phosphorylated. Phosphorylation of serine/threonine residues at positions 29, 33, 37, 41 and 45 by CKIα and GSK-3β in complex with Axin and APC appears to be a prerequisite for ubiquitination. Phosphorylated β-catenin is then recognized by the β-transduction repeat containing protein (β-TrCP) of the E3 ubiquitin ligase complex and led to the proteasomal degradation system (Ilyas, M. 2005). Although, GSK-3β-mediated degradation of β-catenin is the main mechanism that controls its cytoplasmic low level, another GSK-3β-independent mechanism has been shown to promote β-catenin degradation. In the Siah-1-dependent pathway, Siah-1 interacts with the carboxyl terminus of APC, recruits the ubiquitination complex, and promotes the degradation of β-catenin through a pathway independent of both GSK-3β and β-TrCP, an F-box protein in the E3 ubiquitin ligase complex (Liu J. et al., 2001) (Figure 1.8).

The *β-catenin* is frequently mutated in many types of cancer. Most of these mutations affects in the destruction box, encoded by the exon3 of the *CTNNB1* gene, on the GSK-3β phosphorylation target residues. In frame-deletions covering this region are seen as well in hepatoblastomas. These mutations renders β-catenin resistant to proteasomal degradation. Stabilized β-catenin translocates to the nucleus, cooperate with the LEF/TCF family of transcription factors to exercise transcriptional activation of target genes depending on the cell type and context.

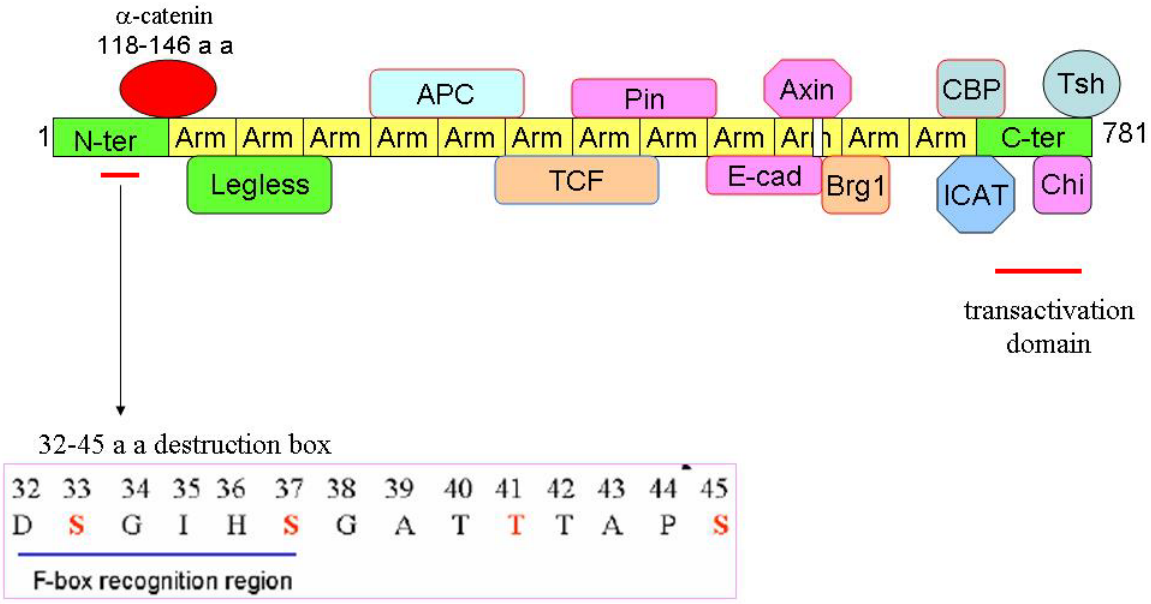

Figure 1.8: Primary β-catenin structure and protein interactions. CBP (P300), Histone acetylase. Brg-1, a component of mammalian SWI/SNF and Rsc chromatin-remodelling complexes. E-cad, E-cadherin. ICAT, inhibitor of b-catenin and T cell factor. Tsh, Teashirt. Chi, Chibby. Arm, armadillo repeat.

1.4.4.3.11 T-Cell Factor/Lymphocyte enhancer binding factor (TCF/LEF) family of transcriptional factors and other components in nucleus

Although LEF/TCFs bind directly to DNA through their HMG-domains, they are incapable of activating gene transcription (Roose J. and Clevers H. 1999). HMG-domain proteins appear to have intrinsic ability to either activate or repress transcription of target gene, a decision that may be regulated by interaction with β-catenin (Brannon M. et al.,

1997). So far, TCF-1, LEF-1, TCF3 and TCF4 were identified as family members involved in Wnt signaling. All members of the TCF family can bind β-catenin through a conserved N-terminal stretch of 55 amino acids. β-catenin thus functions as a classical co-activator of transcription (Molenaar M. et al., 1996; Korinek V. et al., 1998; Duval A. et al., 2000). TCF/LEF mRNAs undergo extensive alternative splicing. Alternative promoter usage in the *TCF*-and *LEF-1* gene generates protein isoforms that either carry or lack the N-terminal β-catenin interaction domain. The *TCF*s mutations do not directly contribute to cancer progression but can act in additive manner. Regarding this suggestion, it has been shown that *TCF-4* was mutated in a subset of colorectal tumors (Brannon M. et al., 1997), and also transgenic mice homozygous for mutations in *TCF-1* developed adenomatous intestinal polyps (Roose J. et al., 1999).

In the absence of the Wnt signal, TCF acts as a repressor of the canonical Wnt signaling target genes (Brannon M. et al., 1997) by forming a complex with Groucho (Cavallo R. et al., 1998). The repressing effect of Groucho is mediated by interactions with histone deacetylases (HDAC), which are thought to make DNA refractive to transcriptional activation (Chen G. et al., 1999). In the nucleus, β-catenin converts the TCF repressor complex into a transcriptional activator complex by displacing Groucho from TCF/LEF and recruiting the histone acetylase CBP/p300 (cyclic AMP response element-binding protein). CBP may bind to the β-catenin/TCF complex as a coactivator (Hecht A. et al., 2000; Takemaru KI. and Moon RT., 2000). Another activator, Brg-1, is a component of the SWI/SNF (switching-defective and sucrose nonfermenting) chromatin remodeling complex which, with CBP, may induce chromatin remodeling that favors target gene transcription (Barker N. et al., 2001). Further interactions between the TCF-β-catenin complex and chromatin could be mediated by Legless (Bcl9) and Pygopos (Kramps T. et al., 2002; Parker DS. et al., 2002, Thompson B. et al., 2002). Mutations in either of these genes result in wingless-like phenotypes in Drosophila, and both genes promote Wnt signaling in mammalian cell culture experiments (Thompson B. et al., 2002). Wnt signaling in the nucleus are controlled by a number of protein partners. For example, the protein Chibby is a nuclear antagonist that binds to the C terminus of β-catenin (Takemaru K. et al., 2003). Another β-catenin-binding protein, ICAT (Tago K. et al., 2000), not only blocks the binding of β-catenin to TCF (Tago K. et al., 2000) but also

leads to dissociation of complexes between β-catenin, LEF, and CBP/p300 (Daniels DL. and Weis WI., 2002; Graham TA. et al., 2002). Additionally, it was shown that β-catenin can interact with other binding partners in the nucleus, such as Pitx2. β-catenin can convert Pitx2 from a transcriptional repressor into an activator (Kioussi C. et al., 2002), similar to its interaction with LEF1/TCF.

1.4.4.4 On/Off states of the canonical Wnt signaling pathway

1.4.4.4.1 Off state

When there is no canonical Wnt signaling, the inhibitory mechanisms act to ensure that β-catenin protein membrane unbound β-catenin levels stay below the threshold. β-catenin is constitutively produced and degraded to keep low level monomeric protein pool in the cytoplasm. The main mechanism for controlling cytoplasmic β-catenin level is through ubiqitin dependent proteolysis in a large multi-protein complex. Axin1, the central scaffold of this complex, provides binding sites for β-catenin, APC, GSK3β, CKIα, and PP2A. The complex is stabilized by GSK3β-mediated phosphorylation of Axin and APC (Seeling JM. et al., 1999). β-catenin is phosphorylated at serine 45 by CKIα (primed). Thereafter, GSK3β phosphorylates primed β-catenin at threonine-41, serine-37, and serine-33 sequentially. Phosphorylated, β-catenin is recognized by β-transducin repeat containing protein (β-TrCP) as a protein which is to be ubiquitinated (Latres E. et al., 1999; Hart M. et al., 1999). β-TrCP is an F-box containing protein which, together with Skp1, Cullen, and Rbx-1, constitutes the enzyme ubiquitin ligase (E3). Ubiquitin activation enzyme (E1), ubiquitin conjugating enzyme (E2) and E3 cause ubiquitination of β-catenin, which is then destroyed by the proteasome system (Ciechanover A., 1998).

In off state, β-catenin cannot accumulate since it is kept below the threshold. . In the absence of nuclear β-catenin, the LEF/TCF proteins are found in complex with the transcriptional repressor Groucho (Roose J. et al., 1998). Other transcriptional repressors, suchas histone deacetylases, are also recruited to the complex, thereby ensuring that the target genes are not activated. If β-catenin inappropriately enters the nucleus, Chibby can compete with β-catenin for the LEF/TCF proteins (Takemaru KI. et al., 2003).

1.4.4.4.2 On state

Canonical Wnt signaling is initiated when Wnt ligands interact with frizzled receptors in the presence of LRP-5 or -6 (Mao JH. et al., 2001; Pinson KI. et al., 2000). The formation of the trimolecular complex (Wnt–Frizzled–LRP5/6) has two consequences. Firstly, Dishevelled is recruited to the cell surface and phosphorylated by casein kinase Iε (CK Iε) (Kishida M. et al., 2001). The phosphorylated Dishevelled protein can form a complex with Frat1 and GSK3β which serves to inhibit the activity of GSK3β (Lee E. et al., 2001). Secondly, LRP can interact with Axin. This will result in the accumulation of β-catenin. Additionally, all four serine/ threonine residues in the GSK3β recognition motif of β-catenin must be phosphorylated in order to be recognized by β-TrCP. Any mutations causing the failure to phosphorylate even one of the residues will result in failure to ubiquitinate and degrade β-catenin. The net effect is stabilization of β-catenin and accumulated β-catenin translocates into the nucleus. The mechanism by which β-catenin translocates into the nucleus is not completely clear, as it does not contain a nuclear localization signal and thus may be transported by other proteins. APC protein has been shown to shuttle in and out of the nucleus and it has been suggested that this may be another method of transporting β- catenin to the nucleus (Rosin-Arbesfeld R. et al., 2000; Neufeld KL. et al., 2000). More recently, it has been shown that the proteins pygopus and Bcl9/legless can form a complex with β-catenin in the cytoplasm and, due to the inherent nuclear localization activity of pygopus, the complex can translocate into the nucleus (Townsley FM. et al., 2004). Once within the nucleus, β-catenin can compete with Groucho for binding with the LEF/TCF proteins. The LEF/TCF family consists of four proteins (LEF1, TCF1, TCF3, and TCF4) which complex with DNA at the heptameric consensus motif (A/T)(A/T)CAA(A/T)G (Brantjes H. et. al., 2002). These proteins serve to provide a DNA binding domain for β-catenin. The complex includes the essential co-factors pygopus and Bcl9/legless (Kramps T. et. al., 2002). Together with a large array of other proteins [such as p300/Creb binding protein (CBP)], which allow specific target genes to be transcribed (Brantjes H. et. al., 2002; Roose J. and Clevers H., 1999). The amount of available β-catenin for target gene activation can also be increased by shifting protein from E-cadherin-bound pool to the cytoplasmic pool. A number of

receptor tyrosine kinases (RTK), on binding of their cognate ligand, are able to phosphorylate β-catenin at tyrosine residues, which causes dissociation of β-catenin from E-cadherin–catenin complex. The β-catenin protein thus liberated can be recycled to the cytoplasmic pool, which is then followed by increased expression of β-catenin target genes. Thus, surface receptors, such as c-RON, epidermal growth factor receptor (EGFR) and c-ErbB2, can stimulate canonical Wnt signaling (Graham NA. and Asthagiri AR., 2004; Bonvini P. et al., 2001) as well as activating the signaling pathways with which they are more usually associated.

Just as other signaling pathways can inhibit Wnt signaling, they are also able to activate Wnt signaling or facilitate the effects of Wnt signaling (Eger A. et. al., 2004). Integrin signaling, through integrin-linked kinase, can cause nuclear localization of β-catenin. The mechanisms by which the other signaling pathways achieve their effects are uncertain, although it will most likely be through the manipulation of the various 'On' and 'Off' switches. For example, GSK3β is integral to the insulin-like growth factor (IGF) signaling pathway, and IGF-1 and -2 can activate Wnt signaling through inhibition of GSK3β (Morali OG. et. al., 2001; Desbois-Mouthon C. et. al., 2001; Playford MP. et. al., 2000; D'Amico M. et. al., 2000; Novak A. et al., 1998).

Finally, certain oncogenic viruses are associated with the development of malignancy. The Epstein–Barr virus (EBV) is associated with both epithelial and lymphoid malignancies. It has been shown that EBV can activate canonical Wnt signaling through GSK3β inhibition (Morrison JA. et. al., 2003), HBV-X protein (HBX) upregulates β-catenin (Ding Q. et. al., 2005). HCV core protein stimulates HCC cell proliferation at least partly through up-regulation of Wnt-1 at the transcriptional level (Fukutomi T. et. al., 2005).

1.4.4.5 Canonical Wnt signaling in HCC

Studies in recent years clearly established that the deregulation of Wnt signaling pathway via oncogenic activation of β-catenin plays a key role in hepatocellular carcinomas. Activating mutations in *β-catenin* are quite prevalent in human hepatocellular cancers (de La Coste A. et al., 1998; Miyoshi Y. et al., 1998). Succeeding studies have demonstrated that prevalence of aberrant accumulation of β-catenin is

between 33-69%, while only 8-13% of studied HCCs display β-catenin mutations (Hsu HC. et al., 2000; Wong CM. et al., 2001). The second most likely component of Wnt pathway for oncogenic β-catenin activation is Axin 1, a putative tumor suppressor gene. The overall mutational and/or LOH screening studies in HCC samples have shown that only a small fraction of screened samples (7-9%) were subject to Axin 1 mutations (Satoh S. et al., 2000; Laurent-Puig P. et al., 2001; Taniguchi K. et al., 2002).The molecular etiology for accumulation of β-catenin in HCC is not completely understood. Studies in transgenic mice and chemical carcinogenesis have shown that both the pattern and frequency of β-catenin mutations are heterogeneous (Tsujiuchi T. et al., 1999; Calvisi DF. et al., 2001; Devereux TR. et al., 2001). Almost half of the β-catenin aberrations in human hepatoblastoma are interstitial deletions covering the third exon of the gene (Koch A. et al., 1999; Wei Y. et al., 2000). However, the role of β-catenin in cancer formation and/or progression in cholangiocarcinoma has not been well-studied. There are only two reports which showed that β-catenin mutations were present in 8 of 107 (7.5%) studied biliary tract cancer form China, and only 15% of cholangiocarcinoma displayed aberrant nuclear accumulation of β-catenin without genetic mutation (Sugimachi K. et al., 2001). The finding of mutated β-catenin in early stages of human HCC (de La Coste A. et al., 1998; Miyoshi Y. et al., 1998; Hsu HC. et al., 2000), in adenomas in c-myc transgenic mice, and rapid development of hepatomegaly in mutated β-catenin expressing transgenic mice suggest (Cadoret A. et al., 2001; Calvisi DF. et al., 2001) that aberrations in Wnt pathway can be considered as an early event in hepatocarcinogenesis. An unexpected feature of HCC is the high frequency of β-catenin accumulation despite the presence of rather low levels of β–catenin and Axin1 mutations. This suggests that β-catenin accumulation can be caused by additional mechanisms.

1.4.4.6 β-catenin mutations in well-differentiated and poorly-differentiated HCC

Several years ago, two independent studies showed that β-*catenin* mutations are associated with distinct subsets of HCCs (Hsu HC. et al., 2000; Laurent-Puig P. et al., 2001). According to Hsu et al., β-*catenin* mutations are associated with a subset of well differentiated and low-stage HCCs with a favorable prognosis (Hsu HC. et al., 2000). On

the other hand, Laurent-Puig P. et al. determined that HCCs form two distinct groups according to the chromosome stability status. One group demonstrates chromosome stability, β-catenin mutation and chromosome 8p losses. The other group demonstrates chromosome instability and frequent *Axin1* and *p53* mutations (Laurent-Puig P. et al., 2001). These observations have now been confirmed and extended by many other studies based on mutation analysis or nuclear β-catenin staining. High frequencies of β-*catenin* mutation and nuclear β-catenin staining were detected in early stage well differentiated HCCs, but both aberrations were declining in late stage less differentiated HCCs (Wong CM. et al., 2001; Mao TL. et al., 2001; Inagawa S. et al., 2002; Fujito T. et al., 2004). Although a few studies did not agree with some of the findings (Suzuki T. et al., 2002; Tien LT. et al., 2005), these observations are consistent with the hypothesis that β-catenin aberrations in HCC occur during the initial step of neoplastic transformation at the time when the well-differentiated HCC lesions emerge from dysplastic nodules. Indeed, dysplastic nodules display no β-*catenin* mutation (Prange W. et al., 2003; Park JL. et al., 2005). As *APC* mutations (leading to aberrant activation of β-catenin) are the earliest changes detected in colorectal cancers (Gregorieff A. and Clevers H., 2005), a similar finding in HCC does not come as a surprise. However, the progressive decline of β-catenin aberrations in less differentiated and more aggressive HCCs is unexpected. As stated earlier, constitutive activation of the canonical Wnt signaling as a result of aberrant β-catenin accumulation is considered to play a key role in colorectal cancers.

1.5 C/EBPα

CAAT/enhancer binding proteins (C/EBPs) are members of basic region leucine zipper (bZIP) protein family. First members of C/EBPs was discovered as a heat-stable DNA-binding protein found in rat liver nuclei and was shown to be capable to bind selectively to the CCAAT motif of several viral promoters, as well as to the "core homology" sequence of several viral enhancers (Landschulz WH. et al., 1988). Several C/EBPs (C/EBPα, C/EBPβ, C/EBPγ, C/EBPδ, C/EBPε, and C/EBPζ) were discovered and characterized and designated according the proposal by Cao et al, who suggested a systematic nomenclature in which C/EBP name is followed by a Greek letter, indicating the chronological order of their discovery (Cao Z. et al., 1991). C/EBP subfamily

members consist of three structural components in a modular fashion that include a C-terminal leucine-zipper, a basic DNA-binding region, and an N-terminal transactivating region (Ramji DP. and Foka P., 2002) (Figure 1.9).

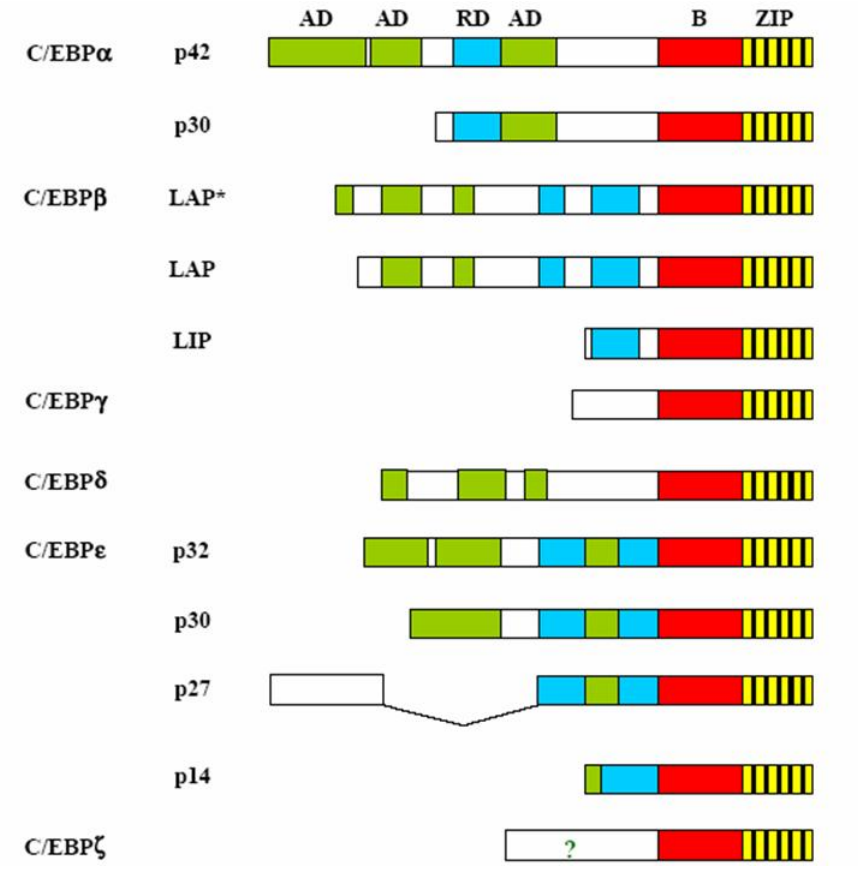

Figure 1.9: Schematic representation of the C/EBP family members (Ramji DP. and Foka P., 2002).The leucine zipper is shown in yellow, with black vertical lines indicating the leucine residues, and the basic region is coloured red. The position of the activation domains (AD) and negative regulatory domains (RD) are shown in green and blue respectively. ? indicates that the N-terminus of C/EBPζ contains an activation domain, although its exact position remains to be determined. C/EBPβ mRNA can produce at least three isoforms, 38 kDa (LAP*), 35 kDa (LAP) and 20 kDa (LIP), with the LAP and the LIP forms being the major polypeptides produced in cells. Although C/EBPε and C/EBPζ are members of the C/EBP subfamily, both do not belong to the exclusive group of liver-enriched transcription factors.

C/EBPα gene has one exon that encodes a 2.7kb mRNA translated into two isoforms; 42kDa and 30kDa due to leaky ribosome scanning. The human C/EBPα is expressed in a tissue restricted manner with high expression in placenta, liver, lung, skeletal muscle, pancreas, small intestine, colon and peripheral blood leukocytes but no or low expression is detected in brain, kidney, thymus, testis and ovary (Antonson P. and

Xanthopoulos KG., 1995). C/EBPs bind to CCAAT box motif found in the promoter regions of several genes through DNA binding domain and leucine zipper domains at the C terminus. The consensus binding site, RTTGCGYAAY (R = A or G, and Y = C or T), are similar with small variations within the C/EBP family members (Osada S. et al., 1999). C/EBPα activates the transcription of several genes in hepatocytes, adipocytes and hematopoietic cells. The C/EBPα gene is conserved among species, especially in its DNA binding region. It has 90% homology to the rat C/EBPα, 100% identity in DNA binding region (Hendricks-Taylor LR. and Darlington GJ., 1995). The gene C/EBPα gene is autoregulated by C/EBPα, but other C/EBP-related proteins may also be involved in its regulation (Legraverend C. et al., 1993). Activation of the murine C/EBPα promoter by direct binding of C/EBPα to a site within 200 bp of the transcriptional start was shown to elevate activity by approximately 3-fold (Legraverend C. et al., 1993; Timchenko N. et al., 1995). However, the human C/EBPα gene promoter does not contain a cis element where C/EBPα protein. However, cotransfection studies in human hepatoma derived Hep3B2 cells show that C/EBPα stimulates transcription of a reporter gene driven by 437 bp of the C/EBPα promoter. The human C/EBPα protein stimulates upstream stimulating factor (USF) to bind to a USF consensus element within the C/EBPα promoter and activates it by 2- to 3-fold (Timchenko N. et al., 1995).

1.5.1 C/EBPα isoforms

C/EBPα mRNA is translated into two major isoforms (42 kDa and 30 kDa) differing in their content of N-terminus by differential use of translation initiation codons (Lin FT. et al., 1993) The C/EBPα mRNA has four AUG start codons. When the conditions are favorable, the activity of the translation initiation factors, elF2α and elF4E, increases and translation start from first AUG (suboptimal initiation site). Translation from this site generates small upstream open reading frame and translation is reinitiated from fourth AUG that generates p30 isoform. When the activity of these translation initiation factors are low, translation is initiated from second AUG (optimal initiation site) which generates p42 isoform (Calkhoven CF. et al., 2000). The full-length p42 form acts as a

transactivator in the liver, whereas the N-terminally truncated p30 form lacks transcription activation potential (Ossipow V. et al., 1993; Calkhoven CF. et al., 1994).

p42 isoform has three activation domains. Activation domains, TEI and TEII interact with components of the basal transcription machinery TBP/TFIIB and histone acetyltransferases CBP/p300, respectively (Nerlov C. et al., 1995; Kovacs KA. et al., 2003). TEI and TEII are not present in p30 form, which lacks the N terminal 117 amino acids. The third activation domain (TEIII) which recruits chromatin remodeling complex SWI/SNF (Pedersen TA. et al., 2001) and DNA binding domain are present in both isoforms (Figure 1.10).

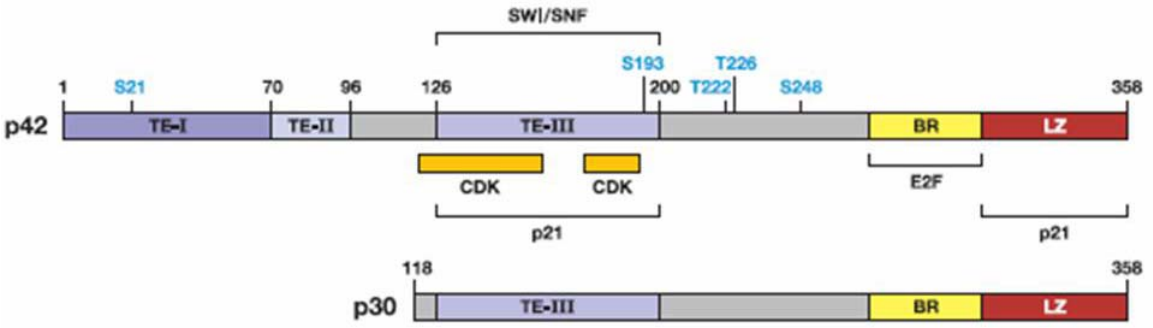

Figure 1.10: Functional domains of C/EBPα isoforms (Johnson PF., 2005). p42 isoform has the all three transactivation elements, TE-I, TE-II, TE-III while the p30 isoform lacks the TE-I and TE-II. Basic region and leucine zipper domain are present in both isoforms. The interacting protein domains are indicated.

Generation of C/EBPα isoforms is tightly regulated by PKR and mTOR signaling pathways and the ratio of these isoforms determine the cell fate (Calkhoven CF. et al., 2000). p42 to p30 ratio regulates the proliferation and differentiation control (Figure 1.11). p42 isoform has the ability to block proliferation and induces adipogenic and granulocytic differentiation unlike p30 isoform, which is not antimitotic and although it induces early adipocyte differentiation, it inhibits terminal differentiation (Lin FT. et al., 1993). p30 isoform binds DNA less efficiently comparing to p42 and acts as dominant negative mutant (Figure 1.10).

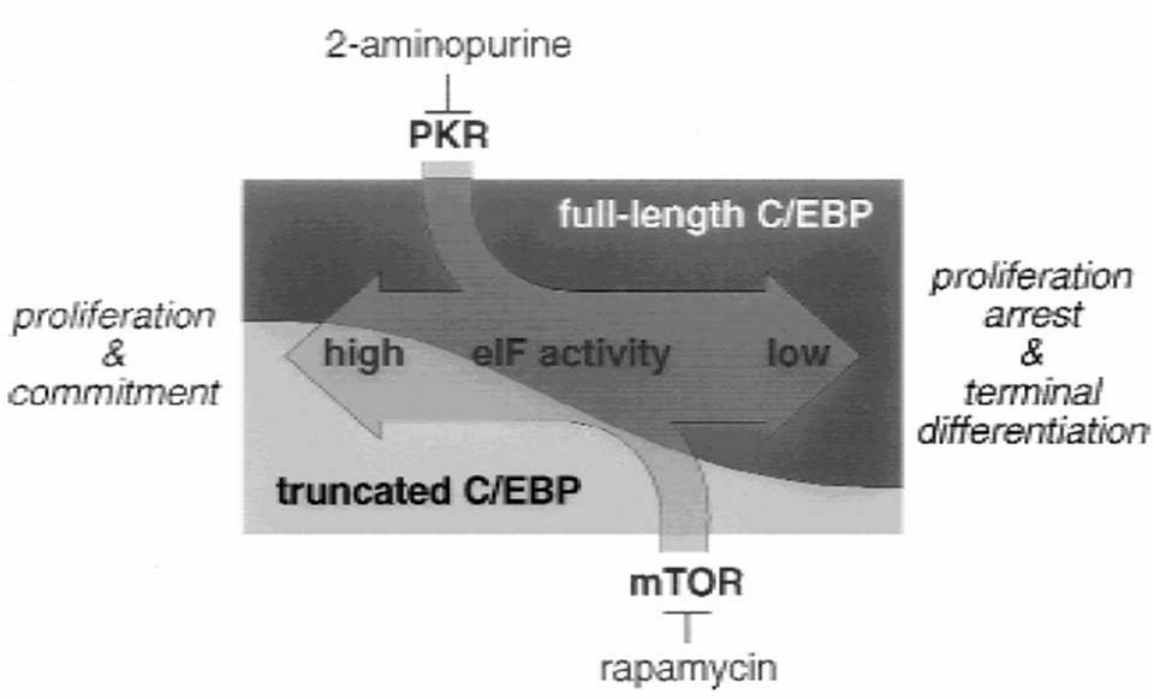

Figure 1.11: Translation initiation factor activity determines cell fate through modulation of the C/EBP isoform ratio. (Calkhoven CF. et al., 2000). Two C/EBP isoforms are formed by alternative use of translation initiation codons, which is regulated by mTOR and PKR pathways. p42 to p30 ratio regulates the proliferation and differentiation control.

The nuclear matrix protein CAAT displacement protein (CDP) is a competitive repressor for CCAAT binding factors in experiments on gene regulation of the sperm histone H2B-1 of the sea urchin *Psammechinus miliaris* (Barberis A. et al., 1987). The repression of the human cholesterol 7α-hydroxylase CYP7A1 gene is mediated by the matrix attachment site-bound repressor CDP, involves displacement of two hepatic transcriptional activators, HNF-1α and C/EBPα, from their binding sites within intron 1 of the CYP7A1 gene, and thus represses transactivation mediated by these two activators (Antes TJ. et al., 2000). CDP is abundant in undifferentiated cells and is down-regulated in differentiated epithelial cells (Ai W. et al., 1999). This might indicate that the availability of CDP for its sites within intron 1 of the *CYP7A1* gene is high early in liver development and thus binding of the liver-specific transcription factors may be blocked (Antes TJ. et al., 2000) Calreticulin interacts with the GC-rich regions of the C/EBPα and C/EBPβ mRNAs and inhibits translation of full-length C/EBP proteins (Timchenko LT. et al., 2002).

1.5.2 Physiological roles of C/EBPα

C/EBPα plays a central regulatory role in energy metabolism in the liver (Crosson SM. et al., 1997). High levels of C/EBPα mRNA were observed in tissues known to metabolize lipid and cholesterol related compounds at uncommonly high rates and included liver, fat, intestine, lung, adrenal gland, and placenta. C/EBPα is essential for adipogenesis and neonatal gluconeogenesis (Arizmendi C. et al., 1999).The involvement of C/EBPα in diverse physiological contexts highlights the important roles of these transcription factors in liver biology (Figure 1.12).

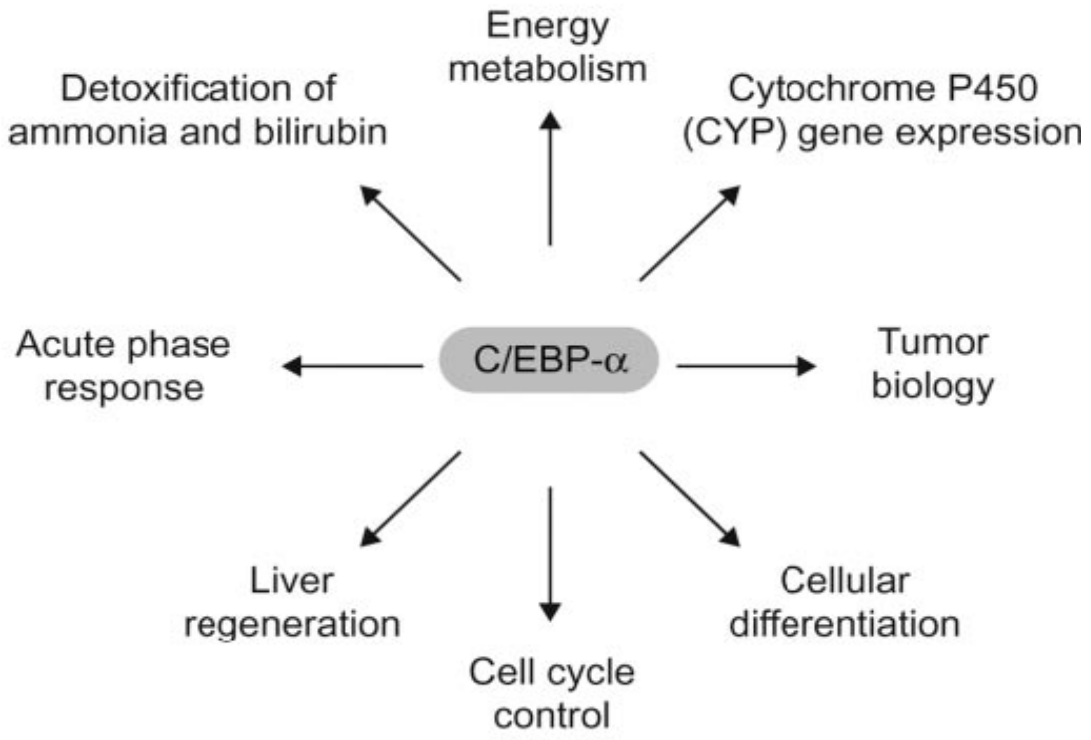

Figure 1.12: The involvement of C/EBPα in diverse physiological contexts. (Schrem H. et al., 2004)

1.5.3 C/EBPα knock-out and knock-in mice

C/EBPα knockout mice die soon after birth due to hypoglycemia and impaired energy homeostasis in liver and adipose tissue (Wang ND. et al., 1995). C/EBPα -/- mice have reduced expression of genes involved in glycogenesis such as glycogen synthase, phosphoenolpyruvate carboxykinase and glucose-6-phosphatase (Wang ND et al., 1995;

Lee YH. et al., 1997). C/EBPα -/- mice also have abnormality in control of hepatic growth and lung development. The liver architecture of the mice lacking C/EBPα is impaired, resembling regenerating liver after partial hepatoectomy or pseudoglandular hepatocellular carcinoma. C/EBPα -/- mice show induced hepatic proliferation and expression of c-myc, c-jun, β-actin and α-fetoprotein are increased several folds. In addition, induced levels of PCNA/cyclin is observed showing that the hepatocytes are in the G1/S phase of the cell cycle (Flodby P. et al., 1996). Blood ammonia concentrations in mutant mice are several-fold higher than wild-type mice, thus C/EBPα is crucial for ammonia detoxification by ornithine cycle enzymes (Kimura T. et al., 1998).

Targeted disruption of C/EBPα prevents neutrophil differentiation. C/EBPα -/- mice do not have mature neutrophils and eosinophils in the blood or fetal liver; however, the other blood cells are not affected. The defect in the differentiation of neutrophils is due to reduced expression of granulocyte colony-stimulating factor receptor (Zhang DE. et al., 1997). Tan EH. et al. investigated the potential of reactivating C/EBPα expression during hepatic carcinogenesis to prevent tumor cell growth by investigated the potential of reactivating C/EBPα expression during hepatic carcinogenesis to prevent tumor cell growth. Diethylnitrosamine produced half the number of hepatocellular nodules in knock-in mice as in WT mice. Nuclear p21 was absent in WT nodules whereas cytoplasmic p21 was abundant; knock-in nodules were positive for nuclear p21. Results suggested that controlled C/EBP production can inhibit liver tumor growth in vivo (Tan EH. et al., 2005).

1.5.4 The role of C/EBPα in adipocyte differentiation

C/EBPα is expressed at high levels in terminally differentiated adipocytes and it has role in the differentiation of adipocytes together with peroxisome proliferators-activated receptor γ (PPARγ) (Rosen ED. et al., 2002).When the expression of C/EBPα is inhibited by antisense RNA in 3T3-L1 preadipocyte cell line, adipocyte specific genes are not expressed and differentiation is blocked (Lin FT. and Lane MD., 1994). Adipocyte differentiation is induced by the rapid and transient increase in the expression of C/EBPβ and C/EBPδ upon treatment with the differentiation inducers. C/EBPβ and C/EBPδ induce the expression of C/EBPα, which leads to cell cycle arrest and

transcriptional activation of many genes involved in adipocyte differentiation such as GLUT4, SCD1, leptin and 422/aP2. PPARγ and C/EBPα induce each other's expression and promotes and maintains differentiated state (Rosen ED. et al., 2002).

1.5.5 The role of C/EBPα in lung development and lung cancer

C/EBPα is expressed in bronchial cells and type II pneumocytes in the lung and regulates expression of several genes involved in lung differentiation. C/EBPα knockout mouse shows abnormal proliferation of type II pneumocytes (Flodby P. et al., 1996). C/EBPα is proposed to be a candidate tumor suppressor gene in lung cancer since its expression is downregulated in large proportion of lung cancers (Halmos B. et al., 2002). Berg T. et al. generated transgenic mice ectopically expressing C/EBPα in the lung epithelium using the human surfactant protein-C promoter. Lungs from these mice were of normal size but exhibited a phenotype characterized by fewer and larger developing epithelial tubules, indicating that the branching process was affected. The results suggested a role for C/EBPα in lung development and suggest a function in the later stages of lung branching morphogenesis (Berg T. et al., 2006).

1.5.6 The role of C/EBPα in granulopoiesis and in acute myeloid leukemia

Granulopoiesis is the formation of mature neutrophil granulocytes from immature myeloblasts. C/EBPα expressed in the stem and myeloid progenitor cells but not in other cells in the hematopoietic system. C/EBPα expression is initiated during the commitment of multipotential precursors to the myeloid lineage and its expression is up regulated during granulocytic differentiation, and is rapidly downregulated during the monocytic pathway (Scott LM. et al., 1992; Radomska HS. et al., 1998). C/EBPα activates the transcription of granulocyte specific genes; receptors for the growth factors, macrophage colony-stimulating factor, granulocyte colony stimulating factor (G-CSF) (Smith LT. et al., 1996; Zhang DE. et al., 1996).

The importance of C/EBPα in granulocytic differentiation comes from the evidences from knockout mice studies and mutations of C/EBPα in acute myeloid leukemia (AML). C/EBPα knockout mice have disruption in granulopoiesis and do not

have any mature neutrophils while the other blood cells are not affected (Zhang DE. et al., 1997).

C/EBPα is mutated approximately 9% of the AML patients, especially M2 subtype where the C/EBPα mutation is 20%. Mutations in C/EBPα have not been found in patients with the t(8;21), inv 16 (Timchenko NA. et al., 1998) and t(15;17) translocations in which the function or expression of C/EBPα is repressed by other mechanisms (Nerlov C., 2004). AML1-ETO, the fusion product of t(8;21) translocation, repress the C/EBPα expression by inhibiting positive autoregulation of the C/EBPα promoter (Pabst T. et al., 2001). PML-RARα fusion protein of acute promyelocytic leukemia is reported to repress C/EBPα activity by trapping it in the cytoplasm (Truong BT. et al., 2003). Therefore, inactivation of C/EBPα by either mutation or other mechanisms is common in AML and thought to be important in malignant transformation.

1.5.7 The role of C/EBPα in hepatocyte proliferation and differentiation

The liver enriched transcription factors (C/EBP, HNF1, HNF3, HNF4 and HNF6) accomplish the transcription of hepatocyte specific genes through interacting promoter/enhancer sites. Distinct classes of transcription factors regulate the liver development, differentiation and regeneration. C/EBPα has role in liver differentiation regulating transcription of genes involved in hepatic glycogen synthesis, gluconeogenesis and lipid homeostasis and it negatively regulates hepatocyte proliferation (Costa RH. et al, 2003).

C/EBPα plays a role in maintaining the quiescent state of hepatocytes and other cells. Furthermore, it appears that the effects of C/EBP are not mediated through p53 or Rb and are not altered by T-antigen (Hendricks-Taylor LR. and Darlington G.J., 1995). C/EBPα functions as a growth arrest gene in hepatocytes (Diehl AM. et al., 1996). The expression of C/EBPα is reduced during hepatocyte proliferation in regenerating liver and in hepatocellular carcinoma (Mischoulon D. et al., 1992). It was proposed that the growth inhibition function of C/EBPα in liver is not to be due to reduced transcriptional activity but due to protein-protein interactions (Wang H. et al., 2001).

C/EBPα inhibits cell proliferation by increasing p21 gene expression and by post-translational stabilization of p21 protein. Since transcription of antisense p21 mRNA eliminates growth inhibition by C/EBPα, induction of p21 is responsible for the C/EBPα-dependent inhibition of cell proliferation Additionally, C/EBPα mediated growth inhibition can be through the stabilization of p21 protein by C/EBPα (Timchenko NA. et al., 1996). C/EBPα directly interacts with p21 and protects it from proteolytic degradation (Timchenko NA. et al., 1997), and cooperates with p21 to inhibit cyclin-dependent kinase-2 activity and induces growth arrest independent of DNA binding (Harris TE. et al., 2001). However, other studies suggest that the p21 is not important for C/EBPα mediated growth inhibition since p21 knockout mice do not show any alteration in hepatocyte proliferation (Deng C. et al., 1995), and p21 is not the critical target of C/EBP-mediated growth inhibition in murine fibroblasts (Muller C. et al., 1999).

In addition to p21, C/EBPα interacts with several other proteins, which have role in the cell cycle progression and transcription. One of these proteins is cyclin-dependent kinases, which regulate the cell cycle progression through association with cyclins. Cdk2-cyclin E, A and cdk4-cyclinD mediate the S phase transition of cell cycle through Rb-dependent repression of E2F. C/EBPα directly interacts with cdk2 and cdk4 and arrests cell proliferation by inhibiting these kinases. A short-growth inhibitory region of C/EBPα has been mapped between amino acids 175 and 187. This portion of C/EBPα is responsible for direct inhibition of cyclin-dependent kinases and causes growth arrest in cultured cells. C/EBPα inhibits cdk2 activity by blocking the association of cdk2 with cyclins. C/EBPα knockout liver has the increased activities of the cdk2 and cdk4 consistent with increased rate of proliferation. These data demonstrate that C/EBPα brings about growth arrest through direct inhibition of cdk2 and cdk4 (Wang H. et al., 2001). C/EBPα also reduces the protein level of cdk4 by mediating proteasome-dependent degradation of cdk4 (Wang H. et al., 2002). C/EBPα also interacts with the SWI/SNF chromatin-remodeling complex during the regulation of genes involved in differentiation. C/EBPα cannot inhibit the proliferation in cells, which are defective in SWI/SNF (Muller C. et al., 2004).

C/EBPα- mediated repression of E2F is believed to be important for proliferation arrest. E2F regulates the transcription of genes, which are involved in DNA synthesis and

mitosis and E2F-dependent transcription is regulated by Rb-mediated phosphorylation. A region of C/EBPα that has sequence similarity to E2F is sufficient for the disruption of the E2F/p107 complexes. Despite its role as a DNA binding protein, C/EBPα brings about a change in E2F complex composition through a protein/protein interaction. The disruption of E2F-p107 complexes correlates with C/EBPα-mediated growth arrest of hepatocytes in newborn mice. E2F interacts with Rb and Rb-like proteins, p107 and p130, at different stages of cell cycle. In quiescent cells, p130-E2F complex is seen and p107-E2F complex is seen in dividing cells. C/EBPα disrupts the p107-E2F complex through interacting with p107 (Timchenko NA. et al., 1999).

In liver extracts of the young mice, C/EBPα interacts with cdk2, and this interaction represses the E2F and c-myc expression. Ageing leads to increase in the Brahma protein (Brm), which replaces the cdk2 and binds to C/EBPα, leading to formation of C/EBPα-Rb-E2F complex. This complex represses the E2F dependent expression of c-myc and it is not disrupted after partial hepatoectomy. This explains the reduced proliferative capacity of liver by aging (Iakova P. et al., 2003). However, this complex involves the Rb and it has been previously shown that the growth-inhibitory function of the C/EBPα is independent of Rb (Hendricks-Taylor LR. and Darlington GJ., 1995).

The CDK2/CDK4 inhibitory domain of C/EBPα was pinpointed to a 15-amino-acid sequence (QPPPPPPPPHPHASP; 180 to 194 of the rat C/EBPα protein) containing S193 (Wang HP. et al., 2001). This serine was later shown to be dephosphorylated in liver tumors as well as in hepatoma cell lines through a PI3K/Akt-mediated dephosphorylation, and mutation of S193A disabled the growth-inhibitory effect of C/EBP (Wang GL. et al., 2004). However, homozygous C/EBPα PHR/PHR mice, carrying a modified cebpa allele lacking amino acids 180 to 194, were born at the Mendelian ratio, reached adulthood, and displayed no apparent adverse phenotypes. Additionally, Porse BT. et al. failed to detect any CDK2 in the precipitates when nuclear extracts from cells transfected with FLAG-tagged wild-type C/EBP Additionally, C/EBPα knockout fetal livers did not express increased levels of either PCNA or of cyclin A, and did not displayed any overall increase of BrdU incorporation. As a result, Porse BT. et al. concluded that The Proline-Histidine-Rich (PHR) CDK2/CDK4 Interaction

Region of C/EBPα is dispensable for C/EBPα-mediated growth regulation *in vivo* (Porse BT. et al., 2006).

CHAPTER 2. OBJECTIVES AND RATIONALE

Hepatocellular carcinoma (HCC) is a heterogeneous disease, and originates from hepatocytes as a well differentiated tumor and progresses with a stepwise process of dedifferentiation (Kojiro M. et al., 2005). HCC derived from different stages of cellular differentiation may have different clinical and pathobiological behavior. Early well-differentiated tumors are highly proliferative and become less differentiated when they reach 1-1.5 cm. At this stage, HCC cells start to acquire the abilities of angiogenesis, tissue invasion and metastasis. Later on, they become undifferentiated and are able to invade vessels and form extra-hepatic metastases (Bruix J. et al., 2004). This dedifferentiation process is associated with a progressive accumulation of genomic changes including chromosomal gains and losses, as well as *p53* mutations (Thorgeirsson, SS. and J. W. Grisham., 2002). Laurent-Puig P. et al. suggested that HCCs could be classified into two distinct groups according to the chromosome stability status. One group demonstrates chromosome stability, *β- catenin* mutation and chromosome 8p losses. The other group demonstrates chromosome instability and frequent *Axin1* and *p53* mutations (Laurent-Puig P. et al., 2001). Almost a third of HCCs displays constitutive activity of canonical Wnt signaling caused by mutations in *CTNNB1* or *Axin1* genes (Reya T. and Clevers H., 2005). Indeed, in HCC, β-*catenin* mutations have been found in 22% of cases in average, and an additional 7% display *Axin1* mutations (Buendia MA., 2002). Interestingly, the status of the *CTNNB1* gene makes the exception for the general picture. Unlike the other genomic changes accumulating during HCC evolution such as chromosomal instability, *p53* and *Axin1* mutations; high frequencies of *CTNNB1* mutation and nuclear β-catenin protein staining were detected in early-stage well differentiated HCCs, but both aberrations were declining in late-stage less differentiated HCCs (Wong CM. et al., 2001; Mao J. et al., 2001; Inagawa S. et al., 2002; Fujito T. et al., 2004). This data prompted us to analyze canonical Wnt signaling in HCC cell lines, and classify them according to differentiation status and TCF/LEF activity.

β-catenin is tightly regulated at protein and localization levels, and the β-catenin pool out of adherens junctions is likely to be more important for tumor development. Therefore, it is important to have molecular tools distinguishing the pools of β-catenin.

For this aim, we decided to produce our own monoclonal antibodies against a recombinant human β-catenin protein in order to distinguish between different cellular β-catenin pools.

C/EBPα is a potent inhibitor of cell cycle in hepatocytes, and its mutations are observed also in AML patients. Additionally, genetic alterations of C/EBPα in HCC cell lines and samples were found (Yuva Y. et al., unpublished data). Moreover, it has been shown that overexpressed β-catenin and C/EBPα co-immunoprecipitated from Hek293 cells (Kennell JA. et al., 2003). Therefore, we hypothesized that C/EBPα and β-catenin may interact in HCC cell lines. For this aim, we focused on the effect of C/EBPα on mutant β-catenin/TCF dependent transcriptional activity and β-catenin protein level.

While we were analyzing stably transfected Huh7 clones related our Wnt signaling study, we noticed that some mock-transfected clones ceased proliferation when cultured extensively. Additionally, we knew that differentiated cells had stem-like properties based on their heterogeneous staining for AFP, CK19 (Erdal E. et al., unpublished data), Therefore, we hypothesized that some HCC cell lines could produce progeny programmed to terminal differentiation, as manifested by replicative senescent phenotype. We decided to investigate the mechanism of spontaneous senescence in HCC-derived cells. We also hypothesized that the replicative senescent phenotype is a reflection of cirrhosis in liver, and senescent cells should exist in cirrhotic tissues and primary tumors. Therefore, we decided to screen cirrhotic liver samples, non-tumor, and tumor samples from different tissues for senescent phenotype.

CHAPTER 3. MATERIALS AND METHODS

3.1 MATERIALS

3.1.1 Reagents

All laboratory chemicals were analytical grade from Sigma (St. Louis, MO, U.S.A), Farmitalia Carlo Erba (Milano, Italy) and Merck (Schucdarf, Germany) with the following exceptions: Ethanol was from Delta Kim Sanayi ve Ticaret A.S (Turkey). Midi-prep kit and Qiaex kit kit (for recovery and extraction of DNA from agarose gel) were from Qiagen (Chatsworth, CA, U.S.A). Agar, tryptone and yeast extract were obtained from Gibco, BRL Life Technology Inc. (Gaithersburgs, MD, U.S.A). Tetralcycline was purchased from Appligene (France).

3.1.2 Bacterial Strains

The bacterial strains used in this work were DH5α and M15 (*E. coli* strains).

3.1.3 Enzymes

Restriction endonucleases used for gene cloning were purchased from MBI Fermentas GmbH (Germany). Shrimp Alkaline Phosphatase was purchased from Invtrogen (Carlsbad, CA, USA). T4 DNA ligase was purchased from Promega (Madison, WI, USA).

3.1.4 Nucleic Acids

DNA molecular weight standard and ultrapure deoxyribonucleotides were purchased from MBI Fermentas GmbH (Germany). pEGFP-N2 (Clontech, Palo Alto, CA), pcDNA3 (Invitrogen), pCI-Neo (Promega), pSuper, pSuperior.puro, pSuper.retro.gfp.neo (Oligoengine), and pGEX-4T1 (Amersham/Pharmacia, NJ, USA) were commercially obtained. pCI-Neo-S33Y, pGL3-OT and pGL3-OF constructs were a gift from Bert Vogelstein (John Hopkins Oncology Center, Baltimore, MD, USA). pCDNA3-S33Y were prepared by inserting of S33Y cDNA from pCI-Neo-S33Y into

pcDNA3. pAUCT-ΔN-β-catenin were prepared by inserting Xho I/Not I fragment of pCI-Neo-S33Y into pAUCT/CCW vector. pcDNA3.C/EBPα was kindly provided by Gokhan S. Hotamisligil, (Harvard University). pAUCT-C/EBPα was prepared by inserting BamHI-XhoI from pCDNA3.C/EBPα into pAUCT/CCW. pSuper.puro was prepared by EcoRI/Hind III fragment from pSuper into EcoRI/Hind III into pSuperior.puro.

3.1.5 Oligonucleotides

The sequencing-primer used for cycle sequencing reactions oligonucleotides used in polymerase chain reactions (PCR), and 60 bp. HPLC grade oligos used for gene knock-down experiments were synthesized by İONTEK (Istanbul, Turkey).

3.1.6 Electrophoresis and photography, luciferase assay, ELISA readings and spectrophotometry

Electrophoresis grade agarose was obtained from Sigma Biosciences Chemical Company Ltd. (St. Louis, MO, USA). Horizontal electrophoresis apparatuses were from Stratagene (Heidelberg, Germany) and E-C Apparatus Corporation (Florida, USA). The power supply Power-PAC300 and Power-PAC200 was from Bio Rad Laboratories (CA, USA). The Molecular Analyst software used in agarose gel profile visualizing was from BioRad Laboratories (CA, USA). The Reporter Microplate Luminometer Reader was from Turner BioSystems Inc (Sunnyvale, CA, USA). ELISA reader and Spectrophotometer were from Backman.

3.1.7 Tissue culture reagents and cell lines

Dulbecco's modified Eagle's medium (DMEM), fetal calf serum was obtained from BIOCHROM AG (Berlin, Germany). L-glutamine, calcium and magnesium-free phosphate buffered saline (PBS), Penicillin/Streptomycin mixture was from Biological Industries (Haemel, Israel). Tissue culture flasks, petri dishes, 15 ml polycarbonate centrifuge tubes with lids and cryotubes were purchased from Costar Corp. (Cambridge, England). Geneticin-G418 sulfate was purchased from GibcoBRL, Life tech. (USA), Puromycin was purchased from Sigma (St. Louis, MO, USA)

3.1.8 Antibodies and chemiluminescence

The antibodies used in immunoblotting (western blotting) were obtained from different sources, and their working dilutions are given in Table 3.1.

ECL Western Blotting detection kit was purchased from Amersham Pharmacia Biotech Ltd. (Buckinghamshire, UK).

3.1.9 TRAP and Telomere Length Assays Kits

Telo*TAGGG* Telomerase PCR ELISAPLUS and Telo*TAGGG* Telomere Length Assay were purchased from Roche Diagnostics (Mannheim, Germany).

3.2 SOLUTIONS AND MEDIA

3.2.1 General Solutions

50X Tris-acetic acid-EDTA (TAE):	2 M Tris-acetate, 50 mM EDTA pH 8.5 Diluted to 1X for working solution.
Ethidium bromide:	10 mg/ml in water (stock solution), 30 ng/ml (working solution)
1X Gel loading buffer:	0.25% bromophenol blue, 0.25% xylene cyanol**,** 50% glycerol, 1mM EDTA

3.2.2 Solutions for plasmid DNA isolation

Solution I	50 mM Glucose, 25 mM Tris.Cl, pH 8.0, 10 M EDTA. Sterilized in autoclave.
Solution II	0.2 N NaOH, 1% (wt/vol) SDS
Solution III	3 M Potassium acetate, pH 4.8

Bradford Stock Solution	4.75 ml of 95 % ethanol, 10 ml of 85% phosphoric acid , 17.5 mg Coomassie Brilliant Blue. Stored in dark at 4°C.
Bradford Working Solution	21.25 ml double distilled water, 0.75 ml of 95% ethanol, 1.5 ml of 85% phosphoric acid, 1.5 ml of Bradford stock solution. Filtered through Whatman No.1 paper and prepared freshly.

3.2.3 Microbiological media, reagents and antibiotics

Luria-Bertani medium (LB)	*Per liter:* 10 g bacto-tryptone, 5 g bacto-yeast extract, 10 g NaCl. For LB agar plates, add 15 g/L bacto agar.
Glycerol stock solution	65% glycerol, 0.1 M $MgSO_4$, 0.025 M Tris.Cl, pH 8.0
Ampicillin	100 mg/ml solution in double-distilled water, sterilized by filtration and stored at -20°C (stock solution).100 μg/ml (working solution)
Kanamycin	300 mg/ml solution in double-distilled water sterilized by filtration and stored at -20°C (stock solution). Working solution was 30 μg/ml.
0.1 M IPTG	1.41 g IPTG in 50 ml double-distilled water, sterilized by filtration and stored at -20^{o}C.

Luria-Bertani medium (LB)	*Per liter:* 10 g bacto-tryptone, 5 g bacto-yeast extract, 10 g NaCl. For LB agar plates, 15 g/L bacto agar was added.
SOB medium:	*Per liter:* 20 g tryptone (2%), 5 g yeast extract (0.5%), 0.584 gr NaCl (10 mM), 0.1864 g KCl (2.5 mM) autotclaved to sterilize. Then, 2.46 g MgSO4 and 2.03 g MgCl2 (10 mM) are added.
SOC medium:	SOB + 20 mM glucose from filter sterilized 1 M glucose stock solution in ddH2 O.
Transformation Buffer (TB):	10 mM K.PIPES, 55 mM MnCl2, 15 mM CaCl2, 250 mM KCl. Filter sterilized and stored at 4 oC.
Glycerol stock solution	65% glycerol, 0.1 M $MgSO_4$, 0.025 M Tris.Cl, pH 8.0. were mixed with 50% bacteria culture. Alternatively, 25% glycerol were added into bacteria culture.

3.2.4 Tissue culture solutions

DMEM/RPMI working medium	10% FBS, 1% penicillin/streptomycin, 1% Non-Essential Amino Acid were added and stored at 4^oC.
10X Phosphate-buffered saline (PBS)	*Per liter:* 80 g NaCl, 2 g KCl, 14.4 g Na_2HPO_4, 2.4 g KH_2PO_4, pH 7.4

BES Transfection solutions

2.5 M $CaCl_2$	3.675 g $CaCl_2$ in 10 ml double-distilled water. Sterilized by filtration through 0,2µm filter. Stored at -20°C
100 mM BES, pH 6.95	0.2132 g BES (N,N-bis(2-hydroxyethly) in double-distilled water. pH was adjusted to 6.95 with NaOH at room temperature. Stored at -20°C
2X BBS (BES buffer saline)	50 mM BES, pH 6.95, 280 mM NaCl, 1.5 mM Na_2HPO_4 in double-distilled water. Sterilized by filtration through 0,2µm filter. Stored at -20°C.

Antibiotics

Geneticin-G418 Sulfate)	500 mg/ml solution in double-distilled water. Sterilized by filtration and stored at -20°C (stock solution). 500 µg/ml (working solution for stable cell line selection), and 250 µg/ml (working solution for maintenance of stable cell lines).
Puromycin	2 mg/ml solution in double-distilled water, sterilized by filtration (0.2 um pores) and stored at -20°C (stock solution). 2 µg/ml (working solution for stable cell line selection), and 1 µg/ml (working solution for maintenance of stable cell lines).
Tetracycline	1 mg/ml solution in 70% Ethanol, sterilized by filtration (0.2 um pores) and stored at -

	20°C (stock solution). 5 µg/ml (working solution).

3.2.5 SDS (Sodium Deodecyl Sulfate)-PAGE (Polyacrylamide Gel Electrophoresis) solutions

30% Acrylamide mix (1:29)	*Per 100 ml*: 29 g acrylamide, 1 g bis-acrylamide in double-distilled water, filtered, degassed, and stored at 4°C (stock solution).
5X SDS gel-loading buffer	3.8 ml double-distilled water, 1 ml of 0.5 M Tris-HCl, 0.8 ml glycerol, 1.6 ml of 10% SDS, o.4 ml of 0.05% bromophenol-blue. Before use, β-mercaptoethanol was added to 5% to reach 1% when mixed with samples.
5X SDS-electrophoresis buffer	*Per liter:* 15.1 g Tris base, 95 g Glycine, 5 g SDS. Diluted to 1 X for working solution. Stored up to 1 month at 4°C.
10% Ammonium persulfate (APS)	0.1 g/ml solution in double distilled water (Prepared freshly).
1.5 M Tris-HCl, pH 8.8	54.45 g Tris base (18.15 g/100 ml) ~150 ml distilled water Adjust to pH 8.8 with 1 N HCl. Completed to 300 ml with distilled water and stored at 4° C.
1 M Tris-HCl, pH 6.8	12.14 g Tris base ~ 60 ml distilled water Adjust to pH 6.8 with 1 N HCl. Completed to 100 ml with distilled water and store at 4° C.

3.2.6 Immunoblotting solutions

Semi-dry transfer buffer	*Per liter*: 48 mM Tris-base, 39 mM glycine, 0.037% SDS, 20% methanol.
10X Tris-buffer saline (TBS)	*Per liter:* 100 mM Tris-base, 1.5 M NaCl, pH 7.6 in double distilled water.
TBS-Tween (TBS-T)	0.1-0.5% Tween-20 solution in TBS. (Prepared freshly)
Blocking solution	3-5% (w/v) non-fat milk, 0.1-0.5% Tween-20 in TBS. (Prepared freshly).

3.2.7 RNA Study Solutions

DEPC-treated water	0.1% Diethylpyrocarbonate (DEPC) (v/v) in double-distilled water was stirred in loosely plugged bottle. Then autoclaved and stored at room temperature.
5X Formaldehyde gel running buffer	*Per liter:* 20 ml of 2M Sodium Acetate, 20.6 g MOPS, 780 ml of DEPC treated distilled water. pH was adjusted to 7.0 with 5M NaOH. Then 10 ml of 0.5 M EDTA pH 8.0 and volume was completed to 1 liter with DEPC-treated water. Stored at room temperature.

RNA loading buffer	50% formamide, 20% formaldehyde, 15% 5X running buffer, and 15% glycerol-dye. Stored at -20 °C.

3.2.8 Immunofluorescence solutions

H33258 fluorochrome dye	1 mg/ml solution in double-distilled water and stored at -20 °C. Working solution was 1 μg/ml.
DAPI (4', 6-diamidino-2-phenylindole)	0.1-1 μg/ml (working solution in PBS).
4% paraformaldehyde	4 g paraformaldehyde, 5 mM NaOH in 100 ml. PBS, pH 7.4. Stable at 4°C for a week.
PBS-TritonX-100 (PBS-T)	0.1 TritonX-100 in PBS.

3.2.9 ELISA solutions

10X Phosphate-buffered saline (PBS)	*Per liter:* 80 g NaCl, 2 g KCl, 14.4 g Na_2HPO_4, 2.4 g KH_2PO_4, pH 7.4.
Blocking solution	3-5% (w/v) non-fat milk, 0.1% Tween-20 in 1X PBS. (Prepared freshly).
AP reagent:	Sigma Fast p-Nitrophenyl Phosphate (Product No. N2770). Tablets were dissolved in 20 ml water. 150 μl is used per well.
AP-Stop Solution:	3 N NaOH

3.3 METHODS

3.3.1 General Methods

3.3.1.1 Transformation of *E .coli*

Transformation of plasmid DNA into *E. coli* was achieved by using calcium chloride method. Competent *E. Coli* was prepared by two different methods as described below.

3.3.1.2 Preparation of competent cells

3.3.1.2.1 Conventional "Calcium Chloride" method

5 ml LB was inoculated with a single colony from a freshly grown plate of *E. coli* strain (*DH5*α) and incubated for approximately 2.5 hours at 37^{o}C, shaking at 200 rpm to an optical density 0.6 at 590 nm (OD $_{590}$). Then, 1.5 ml of growing cells was centrifuged at 13,000 rpm for 1 minute in a bench-top centrifuge. Excess LB was removed away. The cells were resuspended in 0.5 ml of 50 mM $CaCl_2$ by gently vortexing, before being placed on ice for 30 minutes. The cells were harvested by centrifugation for 1 minute at 13,000 rpm and the supernatant was discarded. The pellet was resuspended in 0.1 ml of 50 mM $CaCl_2$ by gently vortexing. At this stage, bacterial cells were competent, and transformed as described in 3.3.1.3.1.

3.3.1.2.2 Super competent *E. Coli* preparation

This method is based on a report by Inoue *et al*. 1990 (Inoue H. et al., 1990).

DH5α cells were grown in SOB medium at 30^{o}C to an A_{600} of 0.5-0.6 with vigorous shaking at 200 rpm and cooled down on ice for 10 minutes. Cells were transferred to 500 ml centrifuge bottles and centrifuged at 300 rpm (Beckman JA10 rotor, pre-cooled to 4^{o}C). The pellet was resuspended in ice-cold transformation buffer (1/3 of initial culture volume) by gently swirling and kept on ice for 10 minutes. The suspension was then centrifuged at 3,000 rpm for 10 minutes. The pellet was gently resuspended in ice-cold transformation buffer (1/12.5 of initial culture volume), DMSO was added with gently swirling to a final concentration of 7 %, and incubated on ice for 10 minutes.

Tubes were immersed in liquid nitrogen to freeze rapidly and stored at –80°C. Supercompetent bacteria were transformed as described in 3.3.1.3.2.

3.3.1.3.1 Conventional "Calcium Chloride" transformation

This method was used for transformation of plasmids.20 ng plasmid was added to competent cells in 0.1 ml of 50 mM $CaCl_2$ and incubated on ice for 30 minutes. Then, cells were incubated for 60-90 seconds at 42°C (heat-shock), and placed on ice for 2 minutes. 800 µl of pre-warmed LB was added onto cells. Cells were cultured for 1hour at 37°C with vigorous shaking (200 rpm). After 1 hour incubation, samples were centrifuged at 13,000 rpm for 30 seconds, and excess LB was discarded but leaving approximately 100 µl of LB. The pellet was resuspended in the remaining LB. Resuspended bacteria cells were plated out on LB-agars with selection agents ampicillin, kanamycin or ampicillin/kanamycin) and incubated overnight at 37°C without shaking to allow the growth of the transformants.

3.3.1.3.2 Super Competent *E.coli* Transformation

This method was used for transformation of ligation products. Competent cells from –80°C stock were thawed on ice. 50-100 µl of cells was dispensed into plastic tubes. 150 ng of ligation product was added onto supercompetent cells. Then cells were incubated on ice for 30 minutes. After heat-shock for 30 seconds at 42°C, the tubes were put on ice and 800 µl SOC was added. Following incubation for 1 hour at 37°C with vigorous shaking, cells were plated out on LB-agar with selective agent(s).

3.3.1.3 Long term storage of bacterial strains

To keep bacterial cells including plasmid in it or as empty for future experiments and to have a stock of strain in a laboratory is necessary. The most frequently used method is "Glycerol-Stock" method. A single colony picked from either an agar plate or a loop-full of bacterial stock was inoculated into 5 ml LB (with a selective agent if necessary) in 15 ml screw capped tubes. Tubes were incubated overnight at 37°C and at 200 rpm. For glycerol stock, 700 µl of saturated culture was added into 700 ml of 65%

glycerol v/v (32.5 ml glycerol, 5 ml $MgSO_4$, 1.25 ml Tris-Cl pH 8.0 completed to 50 ml with sterile water). This mix was frozen/stored at –70 or -80^oC

3.3.1.4 Purification of plasmids

3.3.1.4.1 Small scale preparation of plasmids (miniprep)

This method was preferred for isolation of plasmids to assess the existence of inserts in plasmids. This protocol is based on the alkaline lysis method of Birnboim and Doly (Birnboim HC. and Doly J., 1979) and modified in some parts. The transformed bacterial strain containing the plasmid of interest was grown in 5 ml LB+ selective agent overnight at 37^oC with vigorous shaking at 200 rpm. 1.5 ml of the saturated bacterial culture was centrifuged for 1 minute at 13,000 rpm in a bench-top micro centrifuge. After removal of supernatant, the pellet was resuspended in 100 µl ice-cold Solution I and stored at room temperature for 5 minutes. Freshly prepared 200 µl of Solution II was added and mixed by inverting the tube very gently and then tube was placed on ice for 5 minutes. Bacterial chromosomal DNA and proteins (cell debris) were precipitated by addition of 150 µl of ice-cold Solution III. This mixture was left on ice for 5 minutes, and then centrifuged for 5 minutes at 13,000 rpm to pellet the host DNA and cell debris. The supernatant was mixed very well with an equal volume of phenol-chloroform (1:1) and centrifuged in a microcentrifuge for 3 minutes to separate the two phases. The top-phase was transferred to another 1.5 ml tube. The plasmid DNA was precipitated by adding 800 µl ice-cold absolute ethanol and mixture was incubated for 15 minutes to 1 hour at –20^oC. The plasmid was pelleted by centrifugation at 13,000 rpm, room temperature for 15 minutes. The supernatant was discarded and the pellet was washed with 300 µl of 70% room temperature ethanol and centrifuged at 13,000 rpm for 15 minutes. The supernatant was discarded and the pellet was left at room temperature for 15-20 minutes to dry and then resuspended in 20 µl of sterile distilled H2O containing 20 µg/ml RNaseA and incubated for 30 minutes to 1 hour at 37^oC. Samples were stored at 4^oC for short term or at –20oC for long term. This procedure yields approximately 1-3 µg of DNA. The quality of mini-prep was checked by loading 1-2 µl of 20 µl final yields on agarose gel and visualizing under U.V.

3.3.1.4.2 Purification of plasmid DNA using MN (Macherey-Nagel) miniprep kit

This method was preferred for isolation of plasmids in order to use in sequencing or cloning procedures. 5 ml of saturated culture was used for isolation of plasmid DNA by using "MN miniprep plasmid DNA purification kit" (MN Macherey-Nagel, Duren, Germany) following manufacture's instructions.

3.3.1.4.3 Large-scale plasmid DNA purification

This method was used for isolation of plasmids in order to use in sequencing or mammalian cell transfection procedures by using "Qiagen large-scale plasmid DNA purification kit" following manufacture's instructions.

3.3.1.5 Preparation of genomic DNA from cultured Cells for "Telo*TAGGG* Telomere Length Assay"

Cultured cells were grown in 15mm tissue culture dishes to 70-80% confluency, trypsinized, and washed with 1X PBS. Genomic DNA was isolated by using "MN Genomic DNA isolation kit" following manufacturer's instructions.

3.3.1.6 Quantification and qualification of nucleic acids

Concentration and purity of the double stranded nucleic acids (plasmid and genomic DNAs), oligonucleotides and total RNAs were determined by using the Beckman Instruments Du Series 600 Spectrophotometer software programs (ds DNA, Oligo DNA Short and RNA methods) on the Beckman Spectrophotometer Du640 (Beckman Instruments Inc. CA. USA).

3.3.1.7 Restriction enzyme digestion of DNA

Restriction enzyme digestions were routinely performed in 20 μl reaction volumes and typically 0.5-5 μg DNA was used. Reactions were carried out with the appropriate reaction buffer and conditions according to the manufacturer's recommendations.

Digestion of DNA with two different restriction enzymes was performed in the same reaction buffer to provide the optimal condition for both restriction enzymes. If no single reaction buffer could be found to satisfy the buffer requirements of both enzymes, the reactions were carried out sequentially.

3.3.1.8 Gel electrophoresis of nucleic acids

3.3.1.8.1 Horizontal agarose gels of DNA samples

DNA fragments were fractionated by horizontal electrophoresis by using standard buffers and solutions. DNA fragments less than 1 kb were generally separated on 1.0% or 20 % agarose gel, those greater than 1 kb (up to 11 kb) were separated on 0.8 % agarose gels.

Agarose gels were completely dissolved in 1x TAE electrophoresis buffer to required percentage in microwave and ethidium bromide was added to final concentration of 30 μg/ml. The DNA samples were mixed with one volume loading buffer and loaded onto gels. The gel was run in 1x TAE at different voltage and time depending on the size of the fragments at room temperature.

3.3.1.8.2 Gel electrophoresis of total RNA

RNA was fractionated through 1% (w/v) agarose gels containing formaldehyde which disrupts hydrogen bonds. 0.5 g agarose was melted in 1X formaldehyde gel running buffer, allowed to cool, and 10 ml of 37% formaldehyde was added. The gel was immediately poured in a laminar hood. 5μl of RNA sample was mixed with 15 μl of RNA loading buffer and heated at 70 °C for 5 minutes. Samples were quenched on ice and loaded onto gel. Electrophoresis was performed at a constant voltage (85 V) for 4 hr at 4 °C in 1X formaldehyde gel running buffer. Following electrophoresis, gel was soaked for 5 min in 5 volumes water to remove formaldehyde. This step was repeated for 3 times. The gel was stained in 30ug/ml ethidium bromide solution for 5 min, and destained overnight in double-distilled water.

Nucleic acids were visualized under ultraviolet light (long wave, 340 nm) and GeneRuler (MBI Fermentas) DNA size markers was used to estimate the fragment sizes.1 kb DNA ladder for horizontal agarose gels and 100 bp ladder for vertical agarose gels.

3.3.2 Computer analyses

Restriction endonuclease maps of the plasmid DNAs were analyzed by using the WebCutter program (Max Heiman, 1995, maxwell@minerva.cis.yale.edu) available for free and public use at http://rna.lundberg.gu.se/cutter2/. Primers were designed by using web software provided by Steve Rozen and Whitehead Institute for Biomedical Research at http://frodo.wi.mit.edu/cgi-bin/primer3/primer3_www.cgi. Alignments of nucleic acids or protein sequence were performed by using web page at http://www.ncbi.nlm.nih.gov/BLAST/.

3.3.3 Production and characterization of anti-β-catenin monoclonal antibodies

3.3.3.1 Immunization of mice with recombinant β-catenin protein

Production and isolation of 6x His-tagged recombinant 90-781 human β-catenin were performed as described previously (Ozturk N., 2000). BALB/c mice were primed with complete Freund's adjuvant (CFA) plus 25 mg recombinant protein subcutaneously (s.c), and boosted with 25 mg recombinant protein plus incomplete Freund's adjuvant (IFA) s.c at days 14, 28, 42. 50 µl of blood was taken from the tail of immunized mouse 7 days after each boost. Serum obtained from tail blood was used to screen immunoreactivity by using ELISA. The spleen of immunized mouse was harvested at day 50, and used for fusion with SP-2 myeloma cell line.

3.3.3.2 Fusion

Harvested spleen was rinsed in the 100 mm petri dish containing 10 ml of serum-free high-glucose DMEM, then placed in the second 100 mm petri dish containing 3 ml of serum-free high-glucose DMEM. With a medium-filled syringe (5 ml) in each hand, the spleen was poked at 30-50 holes. Then, the spleen was minced with sterile small 26 gauge needles. Dissociated cells were centrifuged at 1000 rpm

for 5 minutes. When the spleen cells pellet is free of red blood cells, the cells were combined with SP-2 BALB/c myeloma cells by resuspending the cells in 15 ml of complete high-glucose medium at room temperature. Combined cells were centrifuged at 800 g for 5 minutes; supernatant was aspirated and washed for a second time. Then, supernatant was aspirated off all. Cell pellet was quickly resuspended in 1 ml of 50% PEG-4000. Then, 10 ml of complete medium was added into tube in about 5 minutes. Cells were carefully inverted to mix thus diluting the PEG. Cells were centrifuge at 400 g for 3 minutes and supernatant was aspirated off. 10 ml of HAT medium was added at a rate sufficient to dislodge the pellet without dispersing the cells. The fused cells were allowed to "rest" for 10 minutes then drew into a pipette and expelled with just enough force to disperse the cells. The cells were taken into a 75cm² tissue culture flask in a total of 150 ml of HAT medium, then plated evenly into eight 96-well microtiter plates. The cultures were feed with one drop per well (approx. 60 μl) of fresh medium every 3-5 days. When cells were grown until their medium color got yellowish, supernatant samples were taken to test immunoreactivity with ELISA. Antibody producing hybridoma clones were selected for recloning.

3.3.3.3 Recloning (Subcloning)

96 well culture plates were coated with spleen cells from non-immunized mice. Next day, hybridoma clones were serially diluted into these wells. Clones growing in the most diluted wells were taken and tested for immunoreactivity. Subclones were cultured in HAT medium for one month and then in HT medium for another month.

3.3.3.4 Maintenance of hybridomas and collection of hybridoma supernatant

Hybridoma cells were maintained in completed high-glucose medium and supernatant were collected when cells reach the confluency. Medium was centrifuged at 800 g to rid off cell debris. Collected hybridoma supernatants were tested for immunoreactivity with ELISA, and stored at -20^{o}C or 4^{o}C.

3.3.3.5 Characterization of Ig subtypes of the anti-β-catenin antibodies

Subtypes of anti-β-catenin antibodies were identified by using "ImmmunoPure Monoclonal Antibody Isotyping Kit II" (Pierce) following kit instructions.

3.3.3.6 Production of anti-β-catenin ascites in BALB/c mice

The BALB/c mice was primed by injecting 200 µl incomplete Freund's adjuvant into peritoneal cavity. $10x10^6$ cells were washed twice in sterile PBS and centrifuged at 1500 rpm for 5 minutes. The cell pellet was resuspended in 500 µl PBS and injected to the intraperitoneal region of the mice after 7-14 days of priming. After 7-14 days the ascitic fluid was aspirated from the animal by using an injector and was incubated at 37°C for 1 hour. The ascitic fluid was then incubated at 4°C overnight and centrifuged at 800 g for 10 minutes. The oil layer was discarded and the supernatant was stored at –70°C or -20°C.

3.3.4 Epitope mapping of home-made monoclonal anti β-catenin antibodies

Epitopes of home-made monoclonal β-catenin antibodies were identified by using β-catenin fragments fused to GST protein.

3.3.4.1 Bacterial expression constructs

Short β-catenin fragment coding sequences were amplified from pCI-Neo-S33Y with Pfu Polymerase. Bam HI site and stop codon plus Sal I sites were added into 5' of forward and reverse primers respectively. PCR products were cut with Bam HI and Sal I, and inserted into Bam HI and Sal I sites of pGEX4T1. Fidelity of constructs was verified by sequencing with pGEX4T1 sequencing primers.

Primer ID	Sequence (5' → 3')
DTDL deletion (Reverse)	AGGTCGAC*TTA*AAACCAGGCCAGCTGATTG
S Later deletion (Reverse)	GCGTCGAC*TTA*ATCACCTGGGGGCAGCC
BCAT-341-F (Forward)	GGAGGATCCAGCAGAGTGCTGAAGGTGCT
BCAT-535-F (Reverse)	CAAGTCGAC*TTA*TCGTGGAATGGCACCCT
BCAT-652 (Reverse)	AGCGTCGAC*TTA*CGCCACACCTTCATTCCT
BCAT-654-F (Forward)	TGGGATCCTACGCAGCTGCTGTCCTATT
BCAT-644-F (Forward)	ACAGGATCCCTCCACTCCAGGAATGAAGG
BCAT-725-F (Forward)	TCTGGATCCTACGGCCAGGATGCCTT
BCAT -739-R (Reverse)	ATGGTCGAC*TCA*CATCTCATGCTCCATCATAGG
BCAT-749 (Reverse)	CAGGTCGAC*TTA*TGGATAGTCAGCACCAGG

Table 3.1: The sequences of primers used for cloning and sequencing. Underlined sequences represent restriction enzymes sites, italic sequences represent stop codons.

3.3.4.2 Induction and batch purification of GST fusion proteins.

DH5α strain transformed with expression constructs were grown in LB until cultures reached 0.6 at OD_{600}. Expression of recombinant proteins was induced by adding 0.5 mM IPTG into cultures and incubating for 2 hours at 37^{o}C. 10 ml of induced cultures were centrifuged for 10 minutes at 5500 rpm. The pellet was resuspended in 5 ml 1x ice-cold PBS, and sonicated. 1 ml of Glutathione Sepharose 4B equilibrated with PBS was added onto the sonicated bacteria, and incubated with gentle agitation at room temperature for 30 minutes. The mixture were loaded into column, and washed with 20 ml of 1x PBS at room temperature. Recombinant proteins were eluted with 2 ml of 50 mM Tris-HCl, 10 mM reduced glutathione, and 50 µl aliquots were kept -20^{o}C.

3.3.5 Tissue culture techniques

3.3.5.1 Cell Lines and stable clones

14 HCC derived cell lines (Huh7, FOCUS, Mahlavu, Hep40, Hep3B, HepG2, PLC/PRF/5, SK-Hep1, Snu182, Snu387, Snu398, Snu423, Snu449 and Snu475) were

used in this study, and cultured as described in previously (Cagatay T. and Ozturk M., 2002).

Breast cancer cell lines T-47D (ATCC) and BT-474 (ATCC) were cultivated in DMEM. hTERT-HME cells (Clontech) were cultivated in DMEM/Ham's F-12 (Biochrom) containing insulin (3.5 mg/ml), EGF (0.1 ng/ml), hydrocortisone (0.5 μg/ml), and 10% FBS (Biochrom). Huh7- and Hep3B-derived isogenic clones were obtained by either G-418 selection after transfection with neomycin- resistance pcDNA3.1 (Invitrogen) or pEGFP-N2 (Clontech) plasmids, or by low-density cloning. Huh7-derived isogenic clones C1 and C3 were obtained with pCDNA3.1 and G12 with pEGFP-N2. Huh7-derived C11, and Hep3B-derived 3B-C6, 3B-C11 and 3B-C13 were obtained by low-density cloning. Cells transfected with calcium phosphate DNA-precipitation method were cultivated in the presence of geneticin G-418 sulfate (500 μg/ml; GIBCO), and isolated single cell-derived colonies were picked up by using cloning cylinders and expanded in the presence of 200 μg/ml geneticin G-418 sulfate. For low-density cloning, cells were plated at 30 cells per cm^2 and single-cell derived colonies were expanded. Initial cell stocks were prepared when total number of cells became 1–3 $x10^7$, and the number of accumulated population doubling (PD) at this stage was estimated to be 24, assuming that the progeny of the initial colony-forming cells performed at least 24 successive cell divisions until that step. Subsequent passages were performed every 4–7 days, and the number of additional PD was determined by using a described protocol (Masutomi K. et al., 2003). Briefly, $5x10^4$ cells were seeded in six-well plates in triplicates and cultured for 48 hr. Following trypsinization, cells were resuspended in culture medium and counted manually with a hemocytometer. PD were determined by the formula: PD = Log(Nf/Ni)/Log2, where Nf =the number of cells counted and Ni = the number of cells seeded.

3.3.5.2 Thawing cell lines

One vial of the frozen cell line from the liquid nitrogen tank was taken and immediately put into ice. The vial was left 1 minute on the bench to allow excess nitrogen to evaporate and then placed into 37°C water bath until the external part of the cell solution was thawed (takes approximately 1-2 minutes). The cells were

resuspended gently using a pipette and transferred immediately into a 15 ml. sterile tube containing 10 ml cold fresh medium. The cells were centrifuged at 1500 rpm at 4^{o}C for 5 minutes. Supernatant was discarded and the pellet was resuspended in 10 ml 37^{o}C culture medium to be plated into 100 mm dish. After overnight incubation in a humidified incubator at 37°supplied with 5% CO_2, culture mediums were replenished.

3.3.5.3 Growth conditions of cells

Dulbecco's modified Eagle's medium (DMEM) or RPMI 1640 supplemented with 10% FCS, 1 mM glutamine and penicillin and streptomycin (50 mg/ml), and 1% NEAA was used to culture the HCC cell lines. The cells were incubated in at 37°C in an incubator with an atmosphere of 5% CO_2 in air. hTERT-HME cells (Clontech) were cultivated in DMEM/Ham's F-12 (Biochrom) containing insulin (3.5 mg/ml), EGF (0.1 ng/ml), hydrocortisone (0.5 μg/ml), and 10% FBS (Biochrom). Empty vector transfected stable clones were cultured in parental cell line's culture medium + 200 μg/ml geneticin G-418 sulfate, or 1 μg/ml puromycin. Tetracycline inducible cells were cultured in parental cell line's culture medium + 200 μg/ml geneticin G-418 sulfate + 5 μg/ml tetracycline.

The cells were passaged before reaching confluence. The growth medium was aspirated and the cells were washed once with calcium and phosphate-free PBS. Trypsin was added to the flask to remove the monolayer cells from the surface. The fresh medium was added and the suspension was pipetted gently to disperse the cells. The cells were transferred to either fresh petri dishes or fresh flasks using different dilutions (from 1:2 to 1:10) depending on requirements.

All media and solutions used for culture were kept at 4°C (except stock solutions) and warmed to 37°C before use.

3.3.5.4 Cryopreservation of cell lines

Exponentially growing cells were harvested by trypsinization and neutralized with growth medium. The cells were counted and precipitated at 1500 rpm for 5 min. The pellet was suspended in a freezing solution (10% DMSO, 20% FCS and 70% DMEM for

adherent cells; 10% DMSO, 90% FCS for hybridoma cells) at a concentration of $4x10^6$cells/ml. 1 ml of this solution was placed into 1 ml screw capped-cryotubes. The tubes were left at -70°C overnight. The next day, the tubes were transferred into the liquid nitrogen storage tank.

3.3.5.5 Transient transfection of eukaryotic cells using BES method

Certain amount of cells was plated tissue culture dishes the day before the transfection to obtain 50-60% confluency on the day of transfection. 1 hour before transfection, growth medium was aspirated and replaced with 9 ml growth medium without antibiotics. Appropriate amount of supercoiled eukaryotic expression/reporter were mixed with double-distilled water. Certain amount of 2.5 mM $CaCl_2$ was added in dropwise manner while vortexing the DNA solution. After incubation at room temperature for 10 min, certain amount of 2X BBS was added to DNA-$CaCl_2$ solution in dropwise fashion, and incubated at room temperature for 40 min until calcium phosphate-DNA precipitates. Calcium phosphate-DNA solution was added dropwise to the plate of cells, and the mixture was stirred gently and incubated for 18 hr at 37°C in an incubator with an atmosphere of 5% CO_2 in air. The medium was aspirated and rinsed twice with fresh growth medium, re-fed and placed back to the incubator for a further 24 hr. The appropriate amounts of DNA and reagents used for transfection in different culture plates were given in Table 3.2.

Reagent	100 mm petri dishes	6 well plates	24 well plates
DNA	Up to 24 μg	Up to 4 μg	Up to 0.8 μg
2.5 mM	50 μl	15 μl	5 μl
ddH_2O	450 μl- DNA volume	135 μl –DNA volume	45 μl – DNA volume
2xBBS	500 μl	150 μl	50 μl
Culture medium	9 ml	2.7 ml	1 ml

Table 3.2: The amounts of reagents and media used in BES- transfection method.

3.3.5.6 Transient transfection of eukaryotic cells using "Lipofectamine Reagent"

Transfection was performed with Lipofectamin 2000 reagent (Invitrogen) following manufacturer's instructions.

3.3.6 Extraction of total RNA from tissue culture cells and tissue samples

Total RNAs were isolated from cultured cells using the NucleoSpin RNA II Kit (MN Macherey-Nagel, Duren, Germany) according to the manufacturer's protocol.

3.3.7 First strand cDNA synthesis

First strand cDNA synthesis from total RNA was performed using RevertAid First Strand cDNA synthesis kit (MBI Fermantas, Germany). The RevertAid kit relies on genetically engineered version of Moloney Murine Leukemia Virus reverse transcriptase (RevertAid M-MuLV RT) with low RNase H activity. This allows the synthesis of full-length cDNA from long templates. The first strand reactions were primed with oligo(dT)18 primer to specifically amplified mRNA population with 3'-poly(A) tails. As the reaction conditions and components of this kit and those of conventional PCR are compatible, first strand synthesized with this system can be used as a template for PCR.

1 to 5 µg total RNA was used to synthesize the first stand cDNA following the manufacturer's instruction. After 1:1 dilution of total reaction products in DEPC-treated water, 2 µl of diluted first strand cDNA was used for PCR.

3.3.8 Primer design for expression analysis by semi-quantitative PCR

The primer pairs that have been used in expression profile analyses were designed carefully. Forward and reverse primer were positioned on different exons of the gene of interest, so that the primer pair was either be able to produce a longer amplicon from genomic DNA or not be able to amplify from the covered genomic DNA region in a given PCR condition (critical parameter was extension time). Therefore the amplicon, which was amplified from cDNA, was not be longer than 1500 bp. Primers used for expression analysis have been designed strictly considering these criteria, and listed in Table 3.3.

3.3.9 Fidelity and DNA contamination control in first strand cDNAs

The fidelity and genomic DNA contamination of first strand cDNAs were checked before performing expression analyses. 2µl of diluted first strand cDNA was used for cold-PCR amplification of the *glyceraldehyde-3-phosphate dehydrogenase (GAPDH)* transcript. *GAPDH* primer pair for this analysis was designed to produce a 151 bp fragment from cDNA and 250 bp fragment from genomic DNA.

3.3.10 Expression analysis of a gene by semi-quantitative PCR

Determination of optimal cycle of a gene for semi-quantitative PCR

Using equal amount of templates for PCR amplifications of a gene of interest give comparable results at a certain number of PCR cycles. The number of optimal PCR cycle was determined by an initial study for each gene by performing 35-cycle PCR during which PCR amplicon samples were collected by 2-cycle intervals. Agarose gel analysis of samples from 20^{th}, 23^{rd}, 26^{th}, 29^{th}, 32^{nd}, 35^{th}, 36^{th} 39^{th}, 41^{st}, 43^{rd}, 45^{th} cycles of PCR with an equal load defined the minimum number of cycle to visualize the product on agarose gel and the saturation cycle. Agarose gels were analyzed by Densitometric Fluorescence-Chemiluminescence image analyzer and The Molecular Analyst software (BioRad). The determined cycle number was used for amplification of the gene of interest.

GAPDH normalization

Equal volume (2µl) of all first strand cDNA samples was used for cold-PCR amplification of *GAPDH* transcript using the pre-determined optimal cycle number for GAPDH. Then an equal volume of each sample was loaded onto agarose gel and intensity of each band was analyzed by Densitometric Fluorescence-Chemiluminescence image analyzer and The Molecular Analyst software. After intensities were determined, intensity of sample with the highest densitometric reading and 2 µl loading volume were used as reference points for normalization of input loading volume of other samples for expression analysis of both *GAPDH* and gene of interest by cold PCR amplification. Amplification products were analyzed in computer.

Target	Oligos (5'→ 3')	Tm=^{o}C
hTERT-F	CGGAAGAGTGTCTGGAGCAA	58
hTERT-R	GGATGAAGCGGAGTCTGGA	
hSIP1-F	GGAAGACAAGCTTCATATTGC	60
hSIP1-R	ATGGCTGTGTCACTGCGCTGA	
GAPDH-F	GGCTGAGAACGGGAAGCTTGTCAT	62
GAPDH-R	CAGCCTTCTCCATGGTGGTGAAGA	
mSIP1-F	GGCTTACCTGCAGAGCATC	58
mSIP1-R	CCTCTGAACTGTCGTCCATC	
Cyclin E-F	TTGACCGGTATATGGCGACACAAG	62
Cyclin E-R	ATGATACAAGGCCGAAGCAGCAAG	
Mad1-F	ACCAAATCGACCAGCTTCAG	60
Mad1-R	AGTTGTGGGCAGGTCCAATA	
Menin-F	GACCTGTCCCTCTATCCTCG	55
Menin-R	TGACCTCAGCTGTCTGCTCC	
Rak-F	CCGATGTATGGTCATTTGGA	58
Rak-R	CTGATTGTGCAGTTGGTTGA	
BRIT1-F	CGAAGTGAGTGCCACTTGTC	59
BRIT1-R	ACGCCAGTTCCTTCTCTTCA	
Cyclin D1-F	GAGAAGCTGTGCATCTACACCGAC	62
Cyclin D1-R	CACATCTGTGGCACAAGAGGCAAC	
$p16^{INKa}$ -F	CGGAGAGGGGGAGAACAGAC	60
$p16^{INKa}$ -R	GGCAGTTGTGGCCCTGTAGG	
$p14^{ARF}$ -F	TCACCTCTGGTGCCAAAGG	60
$p14^{ARF}$ -R	GGCAGTTGTGGCCCTGTAGG	
c-Myc-F	GGAACTATGACCTCGACTACGACTC	62
c-Myc-R	GCGGCGGCCGAGAAGCCGCTCCACAT	
hSIR2-F	GGTACCGAGATAACCTTCTGTTC	58
hSIR2-R	GGACCTATCCGTGGCCTT	
$p21^{Cip1}$-F	CAGGGGACAGCAGAGGAAGA	
$p21^{Cip1}$-R	TTAGGGCTTCCTCTTGGAGAA	
E-Cadherin-F	TCCCATCAGCTGCCCAGAAA	60
E-Cadherin-R	TGACTCCTGTGTTCCTGTTA	
TGF-β1-F	TGCGGCAGCTGTACATTGA	60
TGF-β1-R	TGGTTGTACAGGGCCAGGA	

Table 3.3: RT-PCR primer list.

3.3.11 Crude total protein extraction

Adherent monolayer cells (both stable and parental cells) were grown to 70% confluency in growth medium lacking selective antibiotic. After removal of growth medium, cells were washed twice with ice-cold PBS to remove any serum residue. 400 µl of RIPA lysis-buffer (150 mM NaCl, 50 mM Tris-HCl pH 8.0, 0.5% sodium deoxycholate, 1 % NP-40, 0.1% SDS and 1X Complete Protein Inhibitor mix (Roche)) was added into 10 cm tissue culture petri dish, and cells were scraped with rubber scrapper. Complete lysis was achieved by pipetting of crude cell lysates several times and by incubating the lysates on ice for 30 min, and then centrifuged at 13.000 g for 30 minutes. Total cell protein was collected as supernatant.

3.3.12 Western blotting

The conventional Bradford protein assay was employed to quantity the protein in the lysates obtained from either Crude total. After protein quantification, protein lysates were aliquoted into fresh tubes and, stored at –70°C.

8%, 10%, 12%, or 15% resolving gel and 5% stacking gel was used in SDS-PAGE analysis of protein lysates.

EC-120 (E-C Apparatus Corp., Holbrook, NY, USA) and ProteanII-xi (BioRad) vertical gel system was set up according to manufacturer's instructions. The standard SDS-electrophoresis buffer system was used.

Equal amounts of cell lysates were solubilized in 1X SDS gel-loading buffer, denatured at 100°C for 7 min and incubated on ice for 2 min. After a quick spin, samples were loaded onto SDS-polyacrylamide gel. After electrophoresis at 80 V for 20 minutes followed by 120 V for 1-2 hours, proteins were transferred onto PVDF western blotting membrane (Roche) by using Transblot-Semi Dry (BioRad) elektroblotting apparatus according to the manufacturer's instructions at 12V for 45 min for EC-120 gel.

Membrane was immediately treated for an hour in blocking solution at room temperature and probed with primary antibody either for an hour at room temperature or overnight at 4°C. After washing 4 times for (5 min, 15 min, 5 min, 5 min) in TBS-T solution at room temperature, the membrane was incubated with appropriate HRP-

conjugated secondary antibody for 1 hr. The membrane was washed 3 times for 5 min in TBS-T solution at room temperature. After final wash, the blot was exposed to ECL western blot detection kit (Amersham) according to manufacturer's instructions. The chemiluminescence emitted was captured on X-ray film within 30 sec. to 5 min. exposure times.

Antibody	Working Dilution (WB)	Source
β-catenin (MAb)	1:5000	Transduction Labs.
β-catenin (MAb)	1:5000	AbCam
β-catenin (Rab. PAb)	1:2000	AbCam
C/EBPα (Rabbit PAb)	1:500	Santa Cruz
C/EBPα (Goat. GAb)	1:500	Santa Cruz
p53 (MAb)	1:1	Clone 6B10; Yolcu E. et al., 2001
Cyclin D1	1:500	Santa Cruz
p16	1:500	Abcam
Rb	1:1000	Santa Cruz
Calnexin (Rabbit PAb)	1:10000	Sigma
Cyclin E	1:500	Transduction
Cyclin A	1:500	AbCam
$p21^{Cip1}$	1:500	Santa Cruz
CDK4	1:500	Santa Cruz
CDK2	1:500	Santa Cruz
E-cadherin	1:2000	Santa Cruz

Table 3.4: Antibodies used for immunoblot assays and their working dilutions. MAb: Mouse monoclonal antibody; Pab; PAb: Rabbit polyclonal antibody; Goat PAb: Goat Polyclonal antibody

3.3.13 Immunofluorescence

Autoclaved-sterilized coverslips were placed into the well of 6-multiwell plates. $6x10^4$ cells were seeded onto each coverslip and grown overnight in 1 ml growth medium. Cells were washed with PBS and fixed in 1 ml of 3% formaldehyde for 3 min. After fixation cells were permeabilized with 0.5% TritonX-100 in PBS for 3 min and blocked in 1 ml blocking solution (3% bovine serum albumin-Fraction V, 0.1% TritonX-100 in 1X PBS) for 30 min at room temperature. Coverslips were probed with primary antibody in appropriate dilution for 1 hr at room temperature. After 3 times washing for 5 min each with PBS-T, appropriate FITC-conjugated secondary antibody was applied for 45 min at room temperature. Cells were washed 3 times for 5 min with PBS-T and DNA counter staining was performed by with Hoechst 33258 for 3 min. Hoechst 33258 was aspirated and destaining was done in double-distilled water for 15 min. Immediately after

coverslips were taken out from the well and excess water removed by tissue paper, coverslips were mounted onto slides containing 10 µl 80% glycerol. All steps after the addition of FITC-conjugated secondary antibody were performed in the dark.

Stained cells were examined under fluorescence microscope (ZEISS) and pictures were captured in a digital Kodak Camera (DC290, Eastman Kodak Co., Rochester, NY), using Adobe Photo Deluxe (Adobe Systems Inc.) software. The pictures were edited using Adobe Photoshop 5.0 (Adobe Systems Inc.) software. Digital images were magnified when needed during picture editing.

3.3.14 Immunoprecipitation and SAP treatment

Huh7 cells were cultured to confluency in 100 mm petri dishes. Cells were lysed in NP40 buffer (50 mM Tris pH 8.0, 150 mM NaCl, 1X protease inhibitor cocktail (Roche), 1.0% NP-40, 0.5% Sodium Deoxycholate, 1 mM Na3VO4, 1 mM NaF, and1 mM PMSF). Lysate was pre cleared by centrifuging at 13,000 rpm, at 4°C for1 5 minutes. Supernatant was transferred into a new tube, 4 µg of polyclonal anti-β-catenin antibody or E-cadherin antibody (for co-immunoprecipitation of E-cadherin associated β-catenin pool) was added. However, for E-cadherin immunoprecipitation NP-40 lysis buffer included 1 mM EDTA, pH 8.0. The tubes were rotated overnight at 4^{o}C to allow formation of immune complexes. 60 ml of 50% slurry Protein G equilibrated with NP-40 buffer was added into the mixture, and rotated for 1 hour at 4^{o}C. Immune complexes were washed three times with NP-40 lysis buffer. The bead-bound immune complexes were additionally washed with 50 mM Tris-HCl, pH 8.5 twice. Then immune complexes were resuspended and equal amounts were dispersed into two tubes. Mock or SAP treated tubes were incubated for 30 minutes at 37^{o}C. The reaction was stopped by adding 1x SDS-loading dye. Samples were subjected to Immunoblotting with 4C9, 9E10 or commercial antibodies.

For co-IP of β-catenin with C/EBPα, the same protocol was followed until washing step of immune complexes with NP-40 buffer. In this case, NP-40 lysis buffer did not include Na3VO4 and PMSF. Immune complexes were washed 5 times in this case, and then dissolved in 1x SDS-loading dye.

3.3.15 BrdU incorporation assay.

Subconfluent cells were labeled with BrdU for 24 h in freshly added culture medium and tested as described (Erdal E. et al., 2005), using anti-BrdUrd antibody (Dako) followed by tetramethylrhodamine B isothiocyanate-labeled secondary antibody (Sigma). DAPI (Sigma) was used for counterstaining.

3.3.16 Low-density clonogenic assay

Cells (30–50 per cm2) were plated in six-well plates and grown 1–3 weeks to obtain isolated colonies formed with 100–1,000 cells. The medium was changed every 4 days, and colonies were subjected to SABG staining.

3.3.17 In vivo studies

Cells were injected s.c. into CD-1 *nude* mice (Charles River Breeding Laboratory). Tumors and nontumorigenic cells at the injection sites were collected at day 35 and analyzed directly or after *in vitro* culture by SABG assay. These experiments have been approved by the Bilkent University Animal Ethics Committee.

3.3.18 SABG assay

SABG activity was detected by using a described protocol (Dimri GP. et al., 1995). After DAPI or eosin counterstaining, SABG positive and negative cells were identified and counted.

3.3.19 TRAP and telomere length assays

Telomerase activity and telomere length assays were performed by using Telo*TAGGG* Telomerase PCR ELISAPLUS and Telo*TAGGG* Telomere Length Assay (Roche Diagnostics), following kit instructions.

3.3.17 shRNA

SIP1-directed shRNA was designed according to a previously described effective siRNA sequence using the pSUPER RNAi system instructions (Oligoengine) and cloned

into pSuper.retro.neo_GFP and pSUPER.puro (Oligoengine), respectively. SIP1 shRNA-encoding sequence was inserted by using oligonucleotides described below.

(sense, 5' → 3')

GATCCCCCTGCCATCTGATCCGCTCTTTCAAGAGAAGAGCGGATCAGATGCAGTTTTTA

(antisense, 5'→3')

AGCTTAAAAACTGCCATCTGATCCGCTCTTCTCTTGAAAGAGCGGATCAGATGGCAGGGG

The integrity of the inserted shRNA-coding sequence has been confirmed by nucleic acid sequencing of recombinant plasmids. Cells were transfected with calcium phosphate precipitation method, using either pSuper.retro.neo_GFP-based or pSUPER.puro-based SIP1 shRNA expression plasmid, and cells were maintained in the presence of 500 μg/ml geneticin G-418 sulfate and 2 μg/ml puromycin (Sigma), respectively. Empty vectors were used as control. Media changed every 3 days, and cells were tested at days 5 and 30.

3.3.21 ELISA (Enzyme-linked immunosorbant assay)

This method combines the specificity of antibodies with the sensitivity of simple spectrophotometric enzyme assay by using antibodies or antigens coupled to an easily assayed enzyme having also a high turnover number. *Indirect ELISA* method may be used to measure the presence and/or levels of antibody in a liquid such as sera. The antiserum reacts with specific antigen attached to a solid phase. Specific antibody will bind to the antigen and all other material is washed away. A second antibody conjugated to an enzyme recognizes common parts of antibodies bound to the antigen. The complex is washed and substrate for enzyme is added. Color change rate will indicate the amount of specific antibody against the antigen. The color changes are read by a plate reader.

50-100 ng of antigen, which had been optimized by using increasing concentrations, was put in each well and incubated overnight at $4^{o}C$ to coat the wells. Unbound regions were saturated with 5% nonfat dry milk in PBST. Wells were washed four times with PBST and incubated with primary antibody for 45 minutes at $37^{o}C$ temperature. Again washed and incubated with secondary antibody coupled to AP for 1hour at room temperature. Following washing AP reagent (Sigma Fast) was added to wells and incubated for 1 hour. From 30^{th} minute of the incubation, plates were read by a plate reader.

3.3.22 Luciferase assay

The pGL3-OT and pGL3-OF reporter plasmids (gift from Bert Vogelstein) were used to test β-catenin-TCF/LEF-dependent transcriptional activity as described previously (Erdal E. et al., 2005) with minor modifications. Cells were transfected using Lipofectamin 2000 reagent (Invitrogen), following instructions provided by the supplier. Mutant β-catenin-induced TCF/LEF-dependent transcriptional activity was tested after co-transfection of cells with constructs and reporters as indicated in Chapter results. At total, 800 ng and 20 μg of DNA were transfected into 24 well-plates and into 100 mM plates, respectively. 200 ng of reporter vectors was used 200 ng/well for 24 well-plates. pEGFP-N2 construct was used at 1:16 ratio of total DNA for co-transfection experiments. At 48 hours following transfection, the luciferase assay was performed by using the Luciferase Reporter Gene Assay, constant light signal kit (Roche Diagnostics GmbH., Mannheim, Germany). Luciferase activity was read with The Reporter® Microplate Luminometer (Turner BioSystems Inc., Sunnyvale, CA) and data was normalized according to transfection efficiency as estimated by counting the GFP expressing cells obtained with each transfection. This method was used for experiments shown in "C/EBPα inhibits mutant β-catenin/TCF transcriptional activity in hepatocellular carcinoma cells" section (Results 4.2). The experiments shown in "Dual Role of canonical Wnt (Wnt/β-Catenin) signaling in hepatocellular carcinoma**"** section (Results 4.1) were performed with Dual-luciferase assay kit (Promega) following instructions provided by the supplier. All experiments were performed in triplicate and TCF activity was reported as the ratio of normalized luciferase activities obtained with pGL-OT and pGL-OF plasmids, respectively.

CHAPTER 4. RESULTS

4.1 Dual Role of canonical Wnt (Wnt/β-Catenin) signaling in hepatocellular carcinoma

4.1.1 Differential activity of canonical Wnt signaling in well- and poorly-differentiated hepatocellular carcinoma cells

According to most accepted hypothesis, HCC arises as a well differentiated tumor and progresses with a stepwise process of dedifferentiation (Kojiro M., 2005). HNF-4α and HNF-1α are necessary for hepatocyte-specific expression of genes encoding proteins involved in liver functions (Kaestner KH., 2000; Duncan SA., 2000). On the basis of HNF expression, our liver cancer cell lines formed two groups (Erdal E. unpublished data). The first group, well-differentiated (WD), included Huh7, Hep3B, Hep40, HepG2 cell lines. The second group, poorly-differentiated (PD), formed by the remaining cell lines displayed an incomplete expression pattern. AFP and cytokeratin (CK19) are liver stem cell markers. α-foetoprotein (AFP), the earliest known marker for hepatic lineage competency, marks specifically hepatoblasts and "oval" cells, whereas CK19 is a marker for late hepatoblasts and "oval" cells, but also bile duct cells (Fausto N., 1994; Shafritz DA. and Dabeva MD., 2002). Well-differentiated cell lines, but not poorly differentiated cells also expressed albumin and AFP, as additional markers for hepatocyte-like differentiation (Erdal E. et al., unpublished data). These observations suggested that a subset of liver cancer cell lines (WD) have in common to specifically express the factors needed for hepatic lineage competency, as well as liver differentiation. The differentiation properties of the cell lines and the list of Wnt pathway mutations are given in Table 4.1.

	Cell Line	Differentiation Markers		Liver Stem Cell Markers		Mutation in Wnt pathway components		
		HNF4α	HNF1α	AFP	CK19	*CTNNB1*	*Axin-1*	*APC*
Well Differentiated	HepG2	+	+	+	+	Δ25-140/ WT	WT	WT
	Huh7	+	+	+	+	WT	WT	WT
	Hep3B	+	+	+	+	WT	WT	WT
	Hep40	+	+	+	+	WT	WT	WT
Poorly Differentiated	Snu398	-	-	-	ND	S33C/ WT	WT	WT
	Snu475	-	very weak	-	-	WT	Δexon 1-2	WT
	Snu449	weak	very weak	-	-	WT	WT	WT
	Snu387	-	-	-	-	WT	WT	WT
	Focus	-	-	-	-	WT	WT	WT
	Mahlavu	-	-	-	-	WT	WT	WT
	Snu182	-	weak	-	ND	WT	WT	WT

Table 4.1: The differentiation properties and the mutations of Wnt signaling components in HCC cell lines: Well-differentiated ones; HepG2, Huh7, Hep3B, Hep40. Poorly differentiated; Snu398, Snu475, Snu449, Snu387, Focus, Mahlavu, Snu182. AFP and CK19 expressions were determined with immunoblotting. HNF4α and HNF1α expression were determined with RT-PCR. WT: wild-type, ND: not determined. Modified from (Cagatay T. and Ozturk M., 2002; Erdal E. et al., unpublished data).

4.1.2 Canonical Wnt signaling activity in hepatocellular carcinoma cells

Canonical Wnt signaling activates TCF/LEF-dependent transcription, which can be monitored by reporters containing TCF-responsive elements (Morin PJ. et al., 1997). We surveyed canonical Wnt signaling activity in well-differentiated and poorly-differentiated cell line groups, using TCF/LEF reporter pGL3-OT and pGL3-OF plasmids, as described previously (Erdal E. et al., 2005; see also Material and Methods). First, we compared TCF/LEF activity in three cell lines with known mutations in canonical Wnt signaling pathway. The well-differentiated and hepatoblastoma-derived cell line HepG2 displays β-catenin mutation (Δ25-140). Poorly differentiated Snu398 cell line displays β-catenin missense mutation (S37C), and Snu475 cell line harbor *Axin1*

mutation (Satoh S. et al., 2000; Cagatay T. and Ozturk M., 2002) (Table 4.1). Normalized TCF/LEF activity was the highest in HepG2 cells. Snu398 cells displayed 50% less activity compared to HepG2. More interestingly, despite a homozygous deletion leading to a loss of Axin1 expression (Satoh S. et al., 2000; Cagatay T. and Ozturk M., 2002), there was no detectable TCF/LEF activity (pGL3-OT/pGL3-OF ratio equals 1.07) in Snu475 cells (Figure 4.1). In contrast, another *Axin-1*-mutant, but well differentiated HCC cell line, namely PLC/PRF/5 (Alexander) (Satoh S. et al., 2000) displayed high TCF/LEF activity (Ozturk N. et al., unpublished data). Next, we compared TCF/LEF activity of eight other cell lines that display wild type β-catenin and Axin1 expression. Hep40 cells harbor a missense Axin1 polymorphism (R454H), but its functional significance is unknown (Erdal E. et al., 2005). In contrast to Cha et al. (Cha MY. et al., 2004), we detected weak but significant TCF/LEF activity (more than 3 folds) in well differentiated Huh7 and Hep3B cell lines. On the other hand, all five poorly differentiated cell lines as well as the well-differentiated Hep40 cells displayed no detectable activity (Figure 4.1). Taken together, we collected TCF/LEF activity data from 12 hepatoma cell lines. Independent of β-catenin or Axin1 status, TCF/LEF activity was detected in four out of five (80%) well-differentiated cell lines, whereas only one out of seven (14%) poorly-differentiated cell lines had constitutive TCF/LEF activity. These findings clearly indicate that canonical Wnt signaling in HCC is closely dependent on the differentiation status. Well-differentiated HCC cells usually express constitutive canonical Wnt signaling, whereas poorly-differentiated HCC cells do not. Taken as a whole, this data suggested that canonical Wnt signaling is mostly active in well-differentiated cells, and inactive in poorly-differentiated cells.

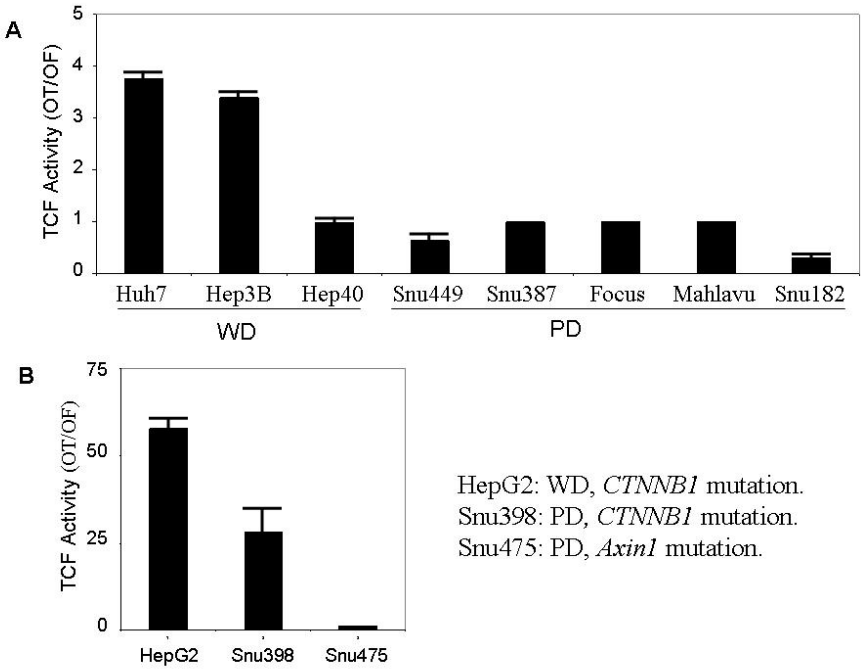

Figure 4.1.1: TCF/LEF activity in WD and PD HCC cell lines. A) TCF activity in well-differentiated (WD) and poorly differentiated (PD) HCC cell lines without any mutations in *CTNNB1 or Axin1*. Huh7 and Hep3B cells had low but significant TCF/LEF activity. **B)** TCF/LEF activity was higher in WD cell line HepG2 than in PD cell line Snu398, both with *CTNNB1* mutations. PD cell line Snu475 did not have any detectable activity. TCF activity denotes the ratio of signals detected with pGL3-OT (OT) and pGL3-OF (OF) plasmids, respectively. Assays in triplicate, error bars; SD.

4.1.3 Canonical Wnt signaling is repressed in poorly-differentiated hepatocellular carcinoma cells

The presence of canonical Wnt signaling in well-differentiated hepatoma cells was apparently due to *β-catenin* or *Axin-1* mutation, as well as other unknown factors. On the other hand, lack of canonical Wnt activity in poorly-differentiated cells could be due to either a lack of significant signaling activity, or alternatively to an active repression. To test these possibilities, we compared TCF/LEF activity in Huh7, Snu449 and Snu182 cell lines following transient expression of a mutant (S33Y)-β-catenin. Transfection with S33Y-β-catenin resulted in an increase in total β-catenin protein levels in all three cell lines. Changes in β-catenin levels in Huh7 and Snu449 cells were comparable, though Snu182 behaved slightly differently (Figure 4.1.2A) Well-differentiated Huh7 cells responded to S33Y-β-catenin expression by a strong activation of TCF/LEF reporter activity (pGL3-OT/pGL3-OF ratio >120). Under the same experimental conditions, the response of Snu449 cells was minimal (pGL3-OT/pGL3-OF ratio equals 5). More

importantly, Snu182 cells were totally unresponsive (pGL3-OT/pGL3-OF ratio <1) (Figure 4.1.2B).

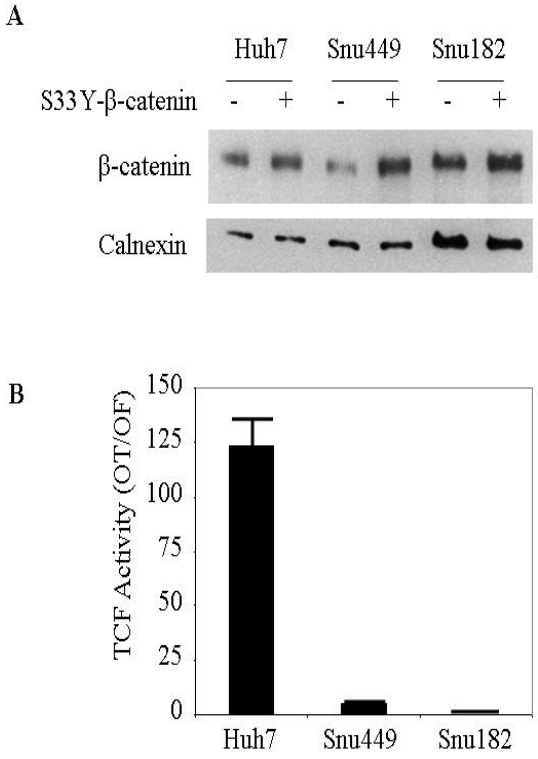

Figure 4.1.2: Ectopic expression of a mutant β-catenin (S33Y) results in high canonical Wnt activity in well-differentiated, but not in poorly-differentiated hepatocellular carcinoma cell lines. A) Well-differentiated Huh7, and poorly-differentiated Snu449 and Snu182 cell lines have been co-transfected with either pCI-neo-mutant –S33Y-β-catenin plasmid (S33Y-β-catenin +) or empty pCI-neo plasmid (S33Y-β-catenin -), and cellular β-catenin levels at post-transfection 48 h were tested by immunoblotting. Calnexin was used as a loading control. **B)** Cell lines were treated as described in (A), then pCI-neo-mutant-S33Y-β-catenin (S33Y)-transfected cells were subjected to TCF reporter assay. TCF activity denotes the ratio of signals detected with pGL3-OT (OT) and pGL3-OF (OF) plasmids, respectively. Assays in triplicate, error bars; SD. Co-transfections included pGL3-OT or pGL3-OF, in addition to pCI-neo plasmids in both (A) and (B).

These drastic differences between well-differentiated Huh7 and two different poorly-differentiated cell lines, Snu449 and Snu182, could not be explained by experimental differences, as the measured activities have been corrected for transfection efficiencies (see material and methods). Since β-catenin was already accumulated in these cell lines, we also transfected these cell lines with a truncated β-catenin encoding vector (pAUCT.ΔN-β-catenin) to distinguish transfected β-catenin from endogenous one (Figure 4.1.3)

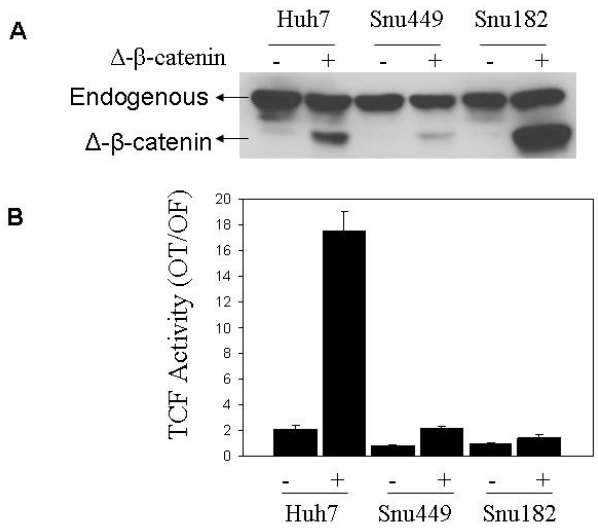

Figure 4.1.3: Ectopic expression of mutant β-catenin (ΔN-β-catenin) results in high canonical Wnt activity in well-differentiated, but not in poorly-differentiated hepatocellular carcinoma cell lines. A) Well differentiated Huh7, and poorly differentiated Snu449 and Snu182 cell lines have been co-transfected with either pAUCT-ΔN-β-catenin plasmid (+) or empty pAUCT plasmid (-), and cellular β-catenin levels at post-transfection 48 h were tested by immunoblotting. **B)** Cell lines were treated as described in (A) plus reporter plasmids, and then cells were subjected to TCF reporter assay. TCF activity denotes the ratio of signals detected with pGL3-OT (OT) and pGL3-OF (OF) plasmids, respectively. Assays in triplicate, error bars; SD. Co-transfections included pGL3-OT or pGL3-OF, in addition to pAUCT plasmids in both (A) and (B).

Since ΔN-β-catenin accumulation was lower in Snu449, we performed TCF reporter assay with Snu449.8 stable clones. This clone expressed ΔN-β-catenin in the absence of tetracycline. Snu449.8 cells were transfected with reporter assay, then cultured in the presence and absence of tetracycline. Even though, truncated β-catenin accumulated as much as endogenous β-catenin, TCF activity remained less than 4 folds (Figure 4.1.4).

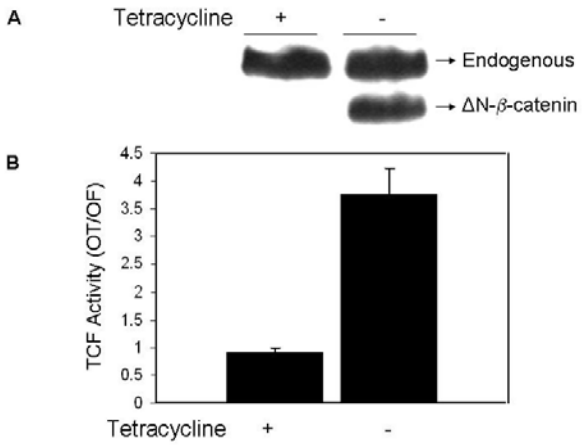

Figure 4.1.4: Ectopic expression of mutant β-catenin (ΔN-β-catenin) results in low canonical Wnt activity in PD Snu449 derived stable clone. A) Snu449.8 was cultured in the presence of tetracycline to repress the expression of the truncated β-catenin and in the absence of tetracycline to induce the expression of truncated β-catenin expression. **B)** Even though truncated β-catenin accumulated comparable to endogenous β-catenin, it produced only 4 fold TCF activity. TCF activity denotes the ratio of signals detected with pGL3-OT (OT) and pGL3-OF (OF) plasmids, respectively. Assays in triplicate, error bars; SD.

In transient transfection experiments, truncated β-catenin protein accumulated more in Snu182 than in Huh7. However, TCF/LEF activity was not detected in Snu182 while TCF/LEF activity (>16 folds) was detected in Huh7 cells. Therefore, our findings strongly support the hypothesis that canonical Wnt signaling is actively repressed in poorly-differentiated HCC cells. This repression appears to occur downstream to β-catenin accumulation (at β-catenin localization or chemical modification), at least in Snu449 and Snu182 cells tested here. These unexpected findings led us to conclude that the regulation of canonical Wnt signaling in well-differentiated and poorly-differentiated hepatocellular carcinoma cell lines is complex. This complexity could arise from the cellular context, including epigenetic differences in the expression of multiple Wnt signaling components. Since, the expression of non-canonical Wnt5A and Wnt5B ligands is restricted to poorly-differentiated hepatocellular carcinoma cell lines, Wnt5A and Wnt5B may be responsible for the repression of canonical Wnt signaling in poorly-differentiated HCC cell lines (Benhaj K. et al., unpublished data).

4.2 C/EBPα inhibits mutant β-catenin/TCF transcriptional activity in hepatocellular carcinoma cells

Oncogenic mutations of β-catenin are observed in hepatomas (de La Coste A. et al., 1998). The activation of canonical Wnt signaling by oncogenic form of β-catenin is not sufficient for tumorigenesis since transgenic mice expressing an oncogenic form of β-catenin in their hepatocytes developed only hepatomegaly (Cadoret A. et al, 2001).

C/EBPα functions as a potent inhibitor of cell division in hepatocytes (Iakova P. et al., 2003; Kurumiya Y. et al., 2000). The role of C/EBPα and β-catenin in liver prompted us to test if C/EBPα affects mutant β-catenin mediated TCF/LEF activity in hepatoma cells.

4.2.1 C/EBPα inhibits transfected mutant β-catenin/TCF transcriptional activity in Huh7 cells

Initially, we screened our HCC cell line collection for β-catenin/TCF activity by using luciferase reporters (Figure 4.1.1). We detected weak but significant TCF/LEF activity (more than 3 folds) in well differentiated Huh7 cell line, which may be due to the expression of a mutant p53 in this cell line causing β-catenin accumulation, as reported previously (Cagatay T. and Ozturk M., 2002). When a mutant β-catenin vector (S33Y) was overexpressed in Huh7, the protein accumulation was mild, since this oncoprotein is already accumulated in Huh7 (Figure 4.1.2A). However, this mild increase in β-catenin caused TCF fold activity (OT/OF) more than 120 times (Figure 4.1.2B). Transfection efficiency was normalized according to renilla luciferase signal.

Next, we confirmed the overexpression of transfected p42 form of C/EBPα in transfected Huh7 by immunoblotting (Figure 4.2.1A). When C/EBPα was co-transfected in increased amounts (0, 200 and 400 ng) with 300 ng of S33Y, TCF activity was decreased to less than basal level (Figure 4.2.1B). Transfected vector amount were kept equal in each transfection by adding empty vector up to 700 ng of total amount. Transfection efficiencies were normalized according to GFP signal.

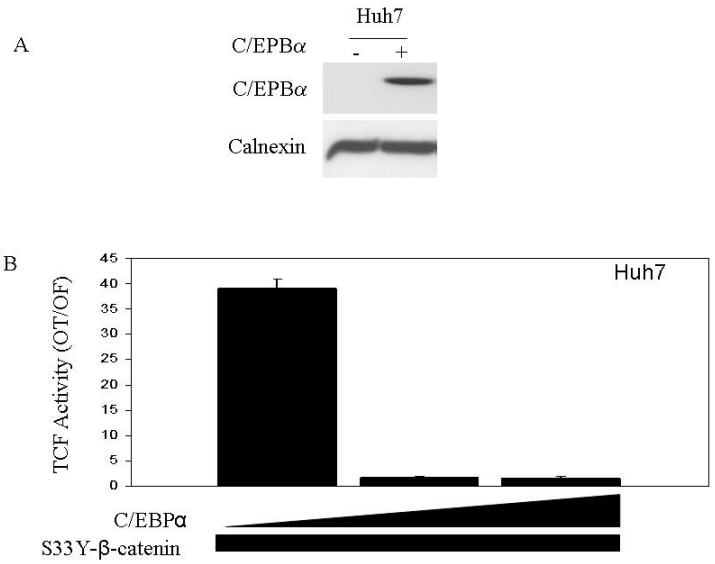

Figure 4.2.1: C/EBPα inhibits mutant S33Y-β-catenin driven TCF/LEF activity in Huh7 cell line. A) The overexpression of C/EBPα was confirmed with immunoblotting. **B)** Huh7 cells were co-transfected with pCDNA3-S33Y, pcDNA3 or pcDNA3-C/EBPα. To keep the equal amount of plasmid , each well was transfected with 1) 200 ng of pCDNA3-S33Y, 400 ng pcDNA3; 2) 200 ng S33Y, 200 ng pcDNA3, 200 ng C/EBPα; 3) 200 ng pCDNA3-S33Y, 400 ng pcDNA3.C/EBPα; and pGL3-OT or pGL3-OF. C/EBPα inhibited pcDNA3-S33Y driven TCF activity in Huh7 cells. Fold luciferase activity is the mean ±SD from 3 independent experiments.

4.2.2 C/EBPα inhibits endogenous mutant β-catenin/TCF transcriptional activity in HepG2 cells

To demonstrate that C/EBPα inhibits endogenous β-catenin/TCF activity, we selected HepG2 cell line for transfection. This hepatoblastoma cell line harbors a wild-type and a truncated β-catenin. Truncated β-catenin (Δ25-140) are resistant to proteasome-mediated degradation and accumulates compared to wild-type form. C/EBPα was transfected in increasing amounts (0, 200 and 400 ng) by adding empty vector in each transfection in order to keep equal amount of vector transfected. Transfection efficiencies were normalized according to GFP signal. 200 ng and 400 ng of C/EBPα decreased TCF/LEF activity from 55 times to ~8 and ~3 times respectively (Figure 4.2.2). The differences at inhibition between Huh7 and HepG2 systems may come from the following reason. In HepG2, overexpressed C/EBPα protein is not enough to repress reporter expression in 48 hours since there is already active endogenous β-catenin.

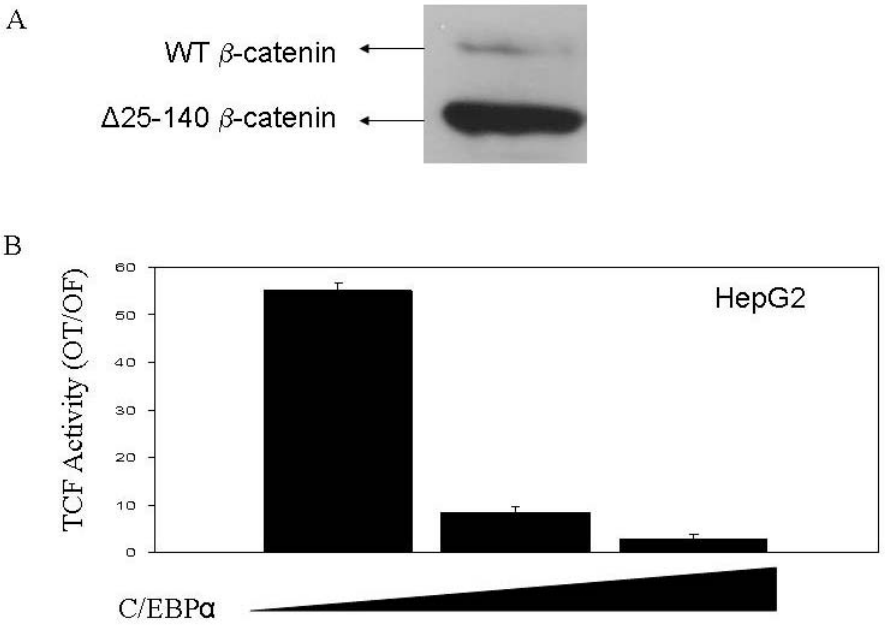

Figure 4.2.2: C/EBPα inhibits endogenous mutant β-catenin driven TCF/LEG activity in HepG2 cells. A) HepG2 has a Δ25-140 deleted β-catenin allele**.** This mutation renders β-catenin resistant to ubiqitin degradation, and truncated form of β-catenin accumulates. **B)** This cell line were transfected with 1) 600 ng pCDNA3; 2) 300 ng pCDNA3, 300 ng C/EBPα; 3) 600 ng C/EBPα and pGL3-OT or pGL3-OF. C/EBPα inhibited endogenous mutant β-catenin driven TCF/LEF activity in HepG2 cells. Fold luciferase activity is the mean ±SD from 3 independent experiments.

4.2.3 C/EBPα inhibits an inducible truncated β-catenin driven TCF/LEF activity

To show that the inhibition in Huh7 system is not an experimental artifact, we used an inducible system. Snu499 hepatoma cell line does not have any detectable TCF/LEF activity. We prepared an inducible Snu449 stable cell line expressing a truncated β-catenin (a.a. 98-781) in the absence of tetracycline (Snu449.8). The expression of truncated β-catenin was confirmed by immunoblotting (Figure 4.2.3A). This cell line was transfected with empty vector or pcDNA3.C/EBPα in the presence of tetracycline. After 12 hours of incubation, media was replaced with tetracycline plus or minus media. Transfection efficiencies were normalized according to GFP signal. C/EBPα. inhibited β-catenin driven TCF/LEF activity when cells were incubated in tetracycline-free medium for 36 hours following medium replacement (Figure 4.2.3B).

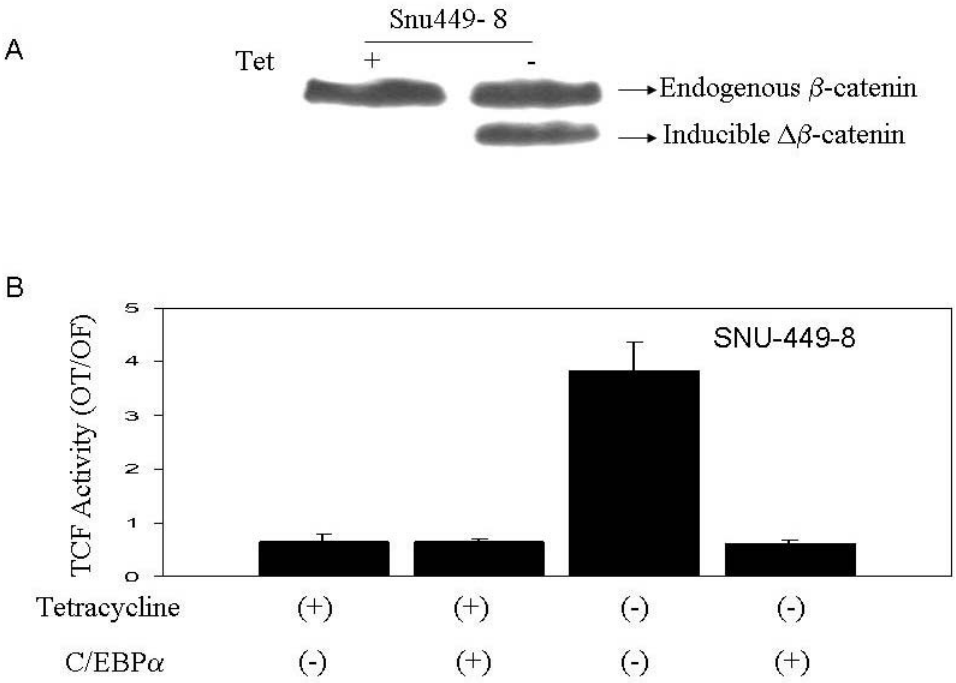

Figure 4.2.3: C/EBPα inhibits truncated β-catenin driven TCF/LEF activity in tetracycline regulated Snu449.8 stable clone. A) This stable cell line expresses N-terminal-deleted (Δ1-97) β-catenin form when cultured in the absence of tetracycline. The expression of mutant β-catenin was confirmed by immunoblotting. **B)** Snu449.8 cell does not have any detectable TCF/LEF activity in the presence of tetracycline. It has low but significant TCF/LEF activity in the absence of tetracycline, and this activity is inhibited when transfected with C/EBPα. Fold luciferase activity is the mean ±SD from 3 independent experiments.

4.2.4 Overexpressed C/EBPα and mutant β-catenin proteins interact in Huh7 cells

To get a clue about the mechanism of this inhibition, we tested if C/EBPα and mutant β-catenin physically interact. Since C/EBPα protein level was low, and β-catenin was wild type in Huh7 cells, we co-transfected p42 form of C/EBPα and mutant S33Y-β-catenin vectors. Then, C/EBPα and interacting proteins were immunoprecipitated with a goat polyclonal anti-C/EBPα antibody. Immune-complexes were subjected to immunoblotting with anti β-catenin antibody. C/EBPα immunoblotting was performed to check the equal loading of immune complexes. Additionally, we also checked the specifity of this interaction by immunoprecipitating with unrelated goat polyclonal antibody (anti-connexin32 antibody) and showing the absence of β-catenin in these complexes (Figure 4.2.4).

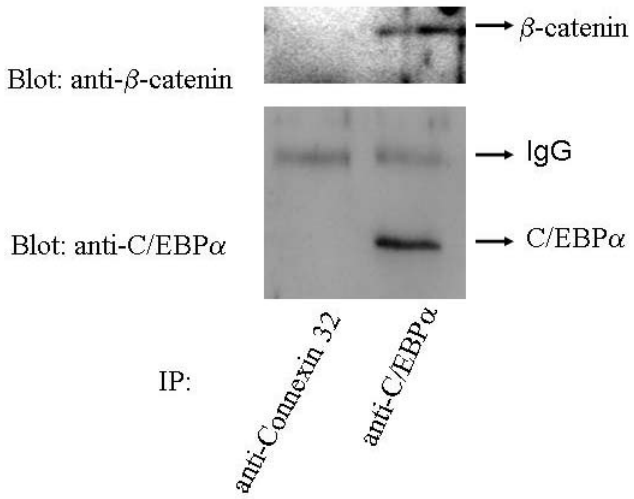

Figure 4.2.4: The overexpressed C/EBPα and β-catenin interacts in Huh7 cells: Huh7 cells were transfected with mutant S33Y-β-catenin and C/EBPα. Proteins were immunoprecipitated with anti connexin 32, and anti C/EBPα. Immune-complexes were subjected to immunoblotting with anti β-catenin and anti C/EBPα antibodies. β-catenin was detected in complexes which interacted with p42 of C/EBPα.

To study the long term effect of C/EBPα expression on β-catenin, we obtained tetracycline inducible Huh7-pAUCT-C/EBPα stable clones. We selected 6 Huh7 clones expressing C/EBPα for future experiments (Figure 4.2.5).

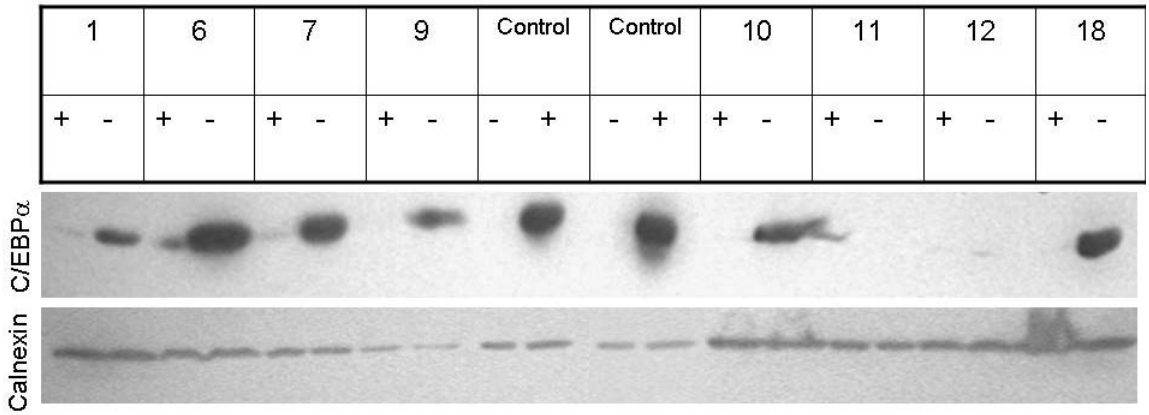

Figure 4.2.5: Screening of Huh7-pAUCT-C/EBPα clones for inducible C/EBPα expression. Clones 1, 6, 7, 9, 10, and 18 expressed C/EBPα in the absence of tetracycline. For clones, + indicates that cells were grown in tetracycline including medium. Control: Transient pcDNA3 (-) or pcDNA3-C/EBPα (+) transfected Huh7 cells were used as controls. Clones 11 and 12 did not overexpressed C/EBPα at all.

In this study, we showed that C/EBPα inhibits β-catenin driven TCF/LEF reporter activity in hepatoma cells. Since C/EBPα physically interacted with β-catenin, it is

possible that C/EBPα inhibits β-catenin driven TCF/LEF transcriptional activity by binding to β-catenin and altering its function.

4.3 Monoclonal anti-β-catenin antibodies as a novel tool to distinguish cellular pools of β-catenin

4.3.1 Production of home-made anti-β-catenin antibodies

β-catenin is found in different pools in cells. It is reasonable to believe that E-cadherin unbound β-catenin is more available for target gene activation. Therefore, it was important to obtain molecular tools distinguishing these cellular pools. For this purpose, we produced our monoclonal antibodies. N-terminal (Δ1-89) deleted form of human β-catenin protein fused to 6xHis tag at its N-terminus was produced in M15, and purified with affinity chromatography (Ozturk N., 2000). BALB/c mouse was immunized with the recombinant protein. Spleen was fused with SP2 cell line to obtain hybridomas. Immunoreactive clones were selected by using ELISA assay. 53 hybridoma clones were tested with immunofluorescence assay. From these clones, 12 hybridomas were selected for further study since they reacted with wild-type and/or truncated β-catenin proteins in HepG2 cell lysates (Figure 4.3.1).

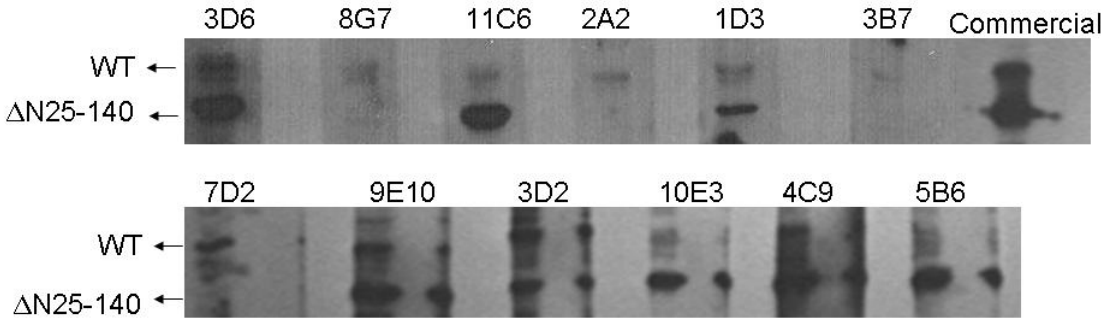

Figure 4.3.1: Home-made monoclonal anti-β-catenin antibodies recognize wild-type and mutant β-catenin forms differentially. HepG2 cell line harbors one wild-type and a deleted (Δ25-140) β-catenin. In this cell line, truncated β-catenin is accumulated compared to wild-type protein. However, our antibodies have different affinities for two forms. Commercial: Anti-β-catenin antibody purchased from Transductions Labs.

Since the antigen used for immunization has a 6 tag, some antibodies might cross-reacted with tag. For this reason, we produced human β-catenin fragment (Δ1-89) fused to GST protein. By using GST fused β-catenin as antigen, we selected two monoclonal antibodies for further study (9E10, and 4C9).

4.3.2 Epitope mapping and immunoglobulin subtyping for monoclonal antibodies 9E10 and 4C9

We produced human β-catenin fragment fused to GST protein for epitope mapping. First, we restricted binding sites of 9E10, and 4C9 to C-terminus of β-catenin (Figure 4.3.2). Both antibodies were IgG1 with kappa light chain.

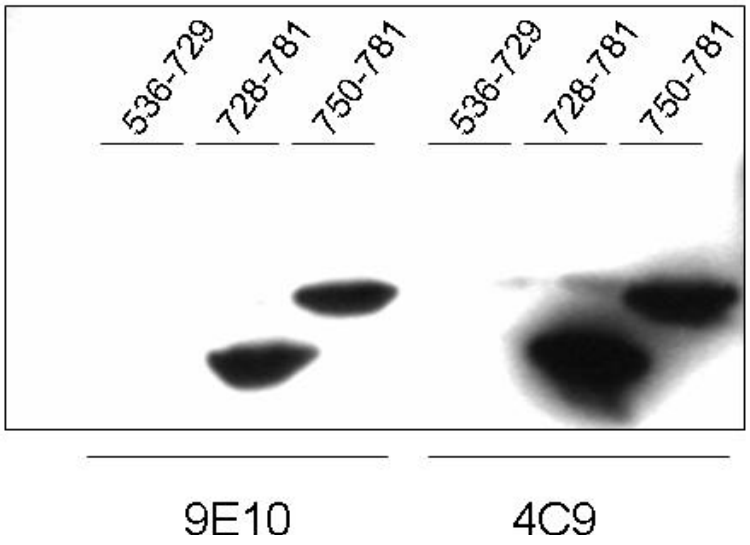

Figure 4.3.2: Restriction of 9E10 and 4C9 binding sites. Mouse β-catenin fragments fused to GST protein were blotted with hybridoma supernatants. 9E10 and 4C9 binds to epitopes between 728-781.

Since β-catenin C-terminus has a DTDL motif and possible phosphorylation of serine residue at codon 771, we decided to delete these sites to see if our antibodies require two sites for immunoreactivity. 9E10 and 4C9 immunoreactivity were lost when codons 771-781, and 778-781 were deleted, respectively (Figure 4.2.3).

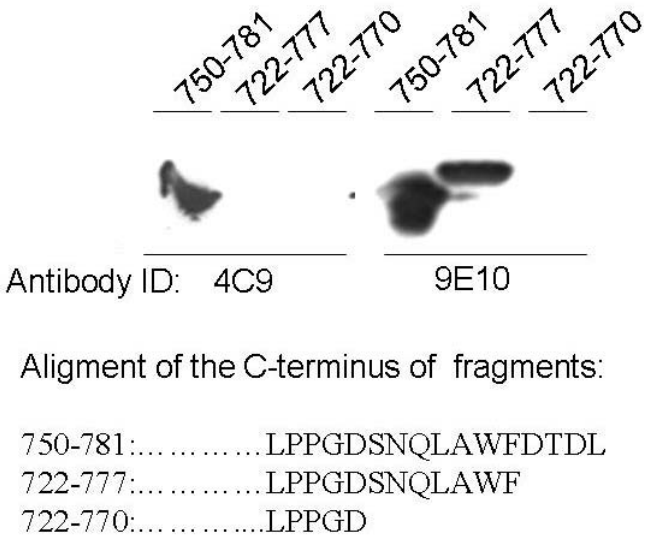

Figure 4.3.3: Epitopes of 4C9 and 9E10. DTDL and 771-781 a.a (which include a S residue) were deleted from GST-β-catenin fragment fusion proteins. 4C9 epitope was restricted to 778-781(DTDL), and 9E10 epitope was restricted to 771-777(SNQLAWF).

4.3.3 9E10 and 4C9 recognize different pools of β-catenin

We performed immunoperoxidase staining by using different cell lines. Characteristically, 9E10 recognize both membrane-associated and cytoplasmic/nuclear forms. However, 4C9 could not recognize membrane-associated β-catenin in HCC cells with immunoperoxidase assay (Figure 4.3.4).

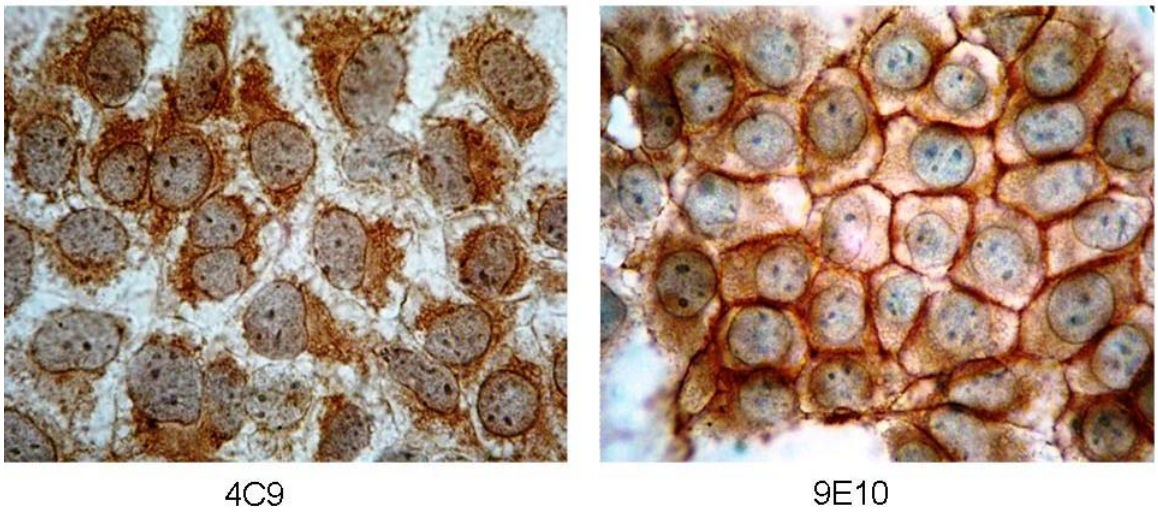

Figure 4.3.4: 4C9 and 9E10 can differentiate β-catenin forms in HCC cells. Huh7 cell line was stained with 4C9 and 9E10 hybridoma supernatants by using immunoperoxidase assay. 4C9 could not recognize membrane-associated β-catenin, while 9E10 can recognize.

Since 4C9 can not recognize membrane-associated β-catenin, we suspected that a chemical modification at this motif in membrane-associated β-catenin prevents immunoreactivity. T residue in DTDL motif was a good candidate for phosphorylation. We assumed that this residue is phosphorylated in membrane-associated but not in cytoplasmic or nuclear β-catenin. We immunoprecipitated β-catenin from confluent Huh7 cells by using a polyclonal antibody raised against the full length human β-catenin. Precipitated immune complexes were divided into two equal aliquots. The aliquots were SAP- or mock-treated at 37^{o}C for 30 minutes. When equal amount of these aliquots were immunoblotted, 9E10 immunoreactivity slightly increased in SAP treated samples but 4C9 immunoreactivity did not change on contrary to our expectation. Additionally, we failed to detect 4C9 immunoreactivity difference in E-cadherin co-immunoprecipitated and SAP treated β-catenin (Figure 4.3.5). However, we did not check if we properly removed phosphate groups from the precipitated β-catenin in our system.

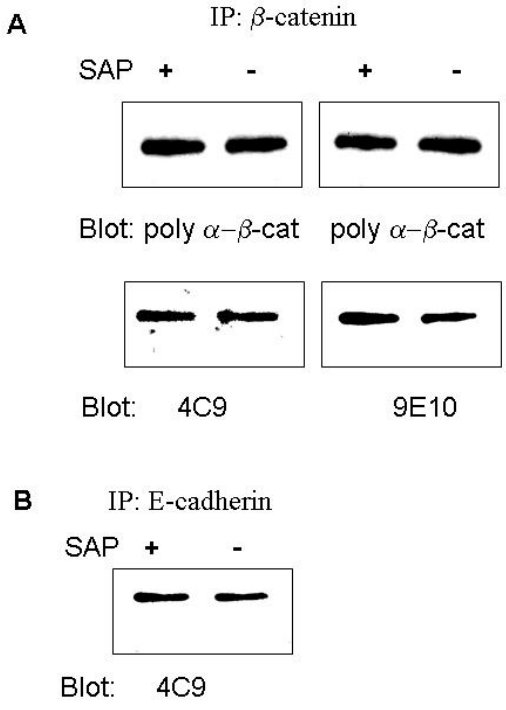

Figure 4.3.5: 4C9 immunoreactivity did not change when β-catenin is treated with SAP to remove phosphorylation. A) Huh7 cell line was grown to confluency to increase E-cadherin bound β-catenin pool. β-catenin was immunoprecipitated with a rabbit polyclonal antibody. When immunoprecipitated samples unphosphorylated with SAP treatment, 9E10 immunoreactivity was slightly increased. Membranes were striped and blotted with polyclonal anti-β-catenin antibody to check equal loading. **B)** Huh7 cells were grown to confluency, and membrane-associated β-catenin was co-immunoprecipitated with E-cadherin. Then, aliquots were mock- or SAP-treated. 4C9 immunoreactivity did not change.

4.4 Reprogramming of replicative senescence in hepatocellular carcinoma derived cells.

4.4.1 Senescent phenotype in cancer cell lines

While analyzing mock- transfected clones from established cancer cell lines related to our Wnt/β-catenin study, we observed that some clones change morphology and cease proliferation at late passages with features reminiscent of cellular senescence (Figure 4.4.1).

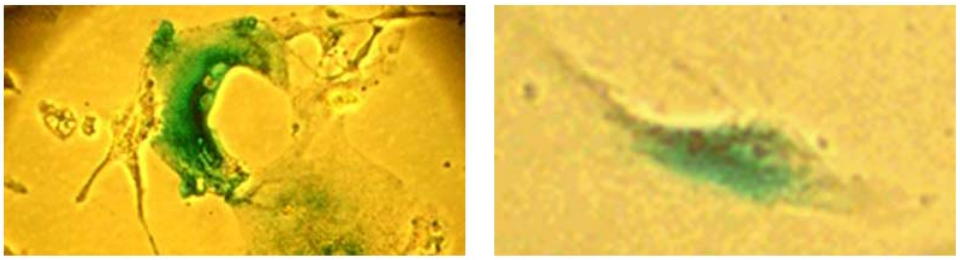

Figure 4.4.1: Huh7 derived clone C3 displays senescent phenotype when cultured extensively. MRC5 is a normal fibroblast, which enter senescent at passage 40. MRC5 was used as a positive control for SABG assay. C3 is a single cell derived clone of Huh7 cell line. When this clone and MRC5 were tested with SABG assay at late passages, both cease proliferation and display flattened morphology and SABG positive staining (blue color). SABG assay: Senescence associated β-galactosidase assay.

We reasoned that this could be an indication for generation of progeny programmed for replicative senescence. We surveyed a panel of HCC and breast carcinoma cell lines, and hTERT-immortalized human mammary epithelial cells (hTERT-HME). Plated at low clonogenic density, cells were maintained in culture until they performed 6-10 population doublings (PD), and tested for senescence-associated β-galactosidase (SABG) activity as described previously (Dimri GP. et al., 1995). Different cancer cell lines generated progeny with greatly contrasting SABG staining patterns. The first group, represented here by HCC-derived Huh7 and breast cancer-derived T-47D and BT-474 cell lines, generated heterogeneously staining colonies. Cells of some colonies were mostly positive for SABG, but others displayed significantly diminished or complete lack of staining (Figure 4.4.2A). The second group, represented by HCC-derived Hep3B and Mahlavu, and hTERT-HME generated only SABG-negative colonies (Figure 4.4.2B). Manual counting of randomly selected colonies demonstrated that mean

SABG-labelling indexes for Huh7, T-47D and BT-474 progenies were 45±23%, 40±29% and 33 ±7%, respectively (Figure 4.4.2C, lanes 1-3). In contrast, Hep3B, Mahlavu and hTERT-HME progenies displayed less than 3±3 % mean SABG-labelling indexes (Figure 4.4.2C, lanes 4-6). Clones from representative cell lines were expanded and subjected to the same analysis. SABG-staining patterns of all clones tested were closely similar to the patterns of their respective parental cell lines. For example, mean SABG staining indexes of Huh7-derived clones were 14±15%, 47±27% and 17±11% (Figure 4.4.2C, lanes 7-9), whereas Hep3B-derived clones generated less than 2±3% SABG-positive progenies (Figure 4.4.2C, lanes 10-12). We speculated that the first group of cell lines comprised progenies in different stages of replicative senescence process at the time of analysis, whereas second group of cell lines were composed mostly of immortal cells. The results obtained with the first group were unexpected. These cell lines have been established more than 20 years ago (Lasfargues ET. et al., 1978; Keydar I. et al., 1979; Nakabayashi H. et al., 1982) and expanded in culture over many years, with PD well beyond the known senescence barriers for normal human cells (Shay JW. and Wright WE., 2005), but they were still capable of generating presumably senescent progeny.

Tumor Origin of Cell Lines	Senescence-reversible Phenotype*	Immortal Phenotype	Senescence-reversible/ Total (%)
Hepatocellular Carcinoma	1	13	1/14 (7.1%)
Breast Cancer	2	4	2/6 (33.3%)
Colorectal Cancer	0	13	0/ 13 (0.0%)
Total	3	30	3/33 (10.0%)

Table 4.2: **Spontaneous senescence in epithelial cancer cell lines:** *At least 50 % of colonies showing SA-βGal positive cells, as compared to HME1-hTERT cells.

We expanded our study to other epithelial cancer cell lines in our laboratory for their senescence phenotype (Table 4.2).

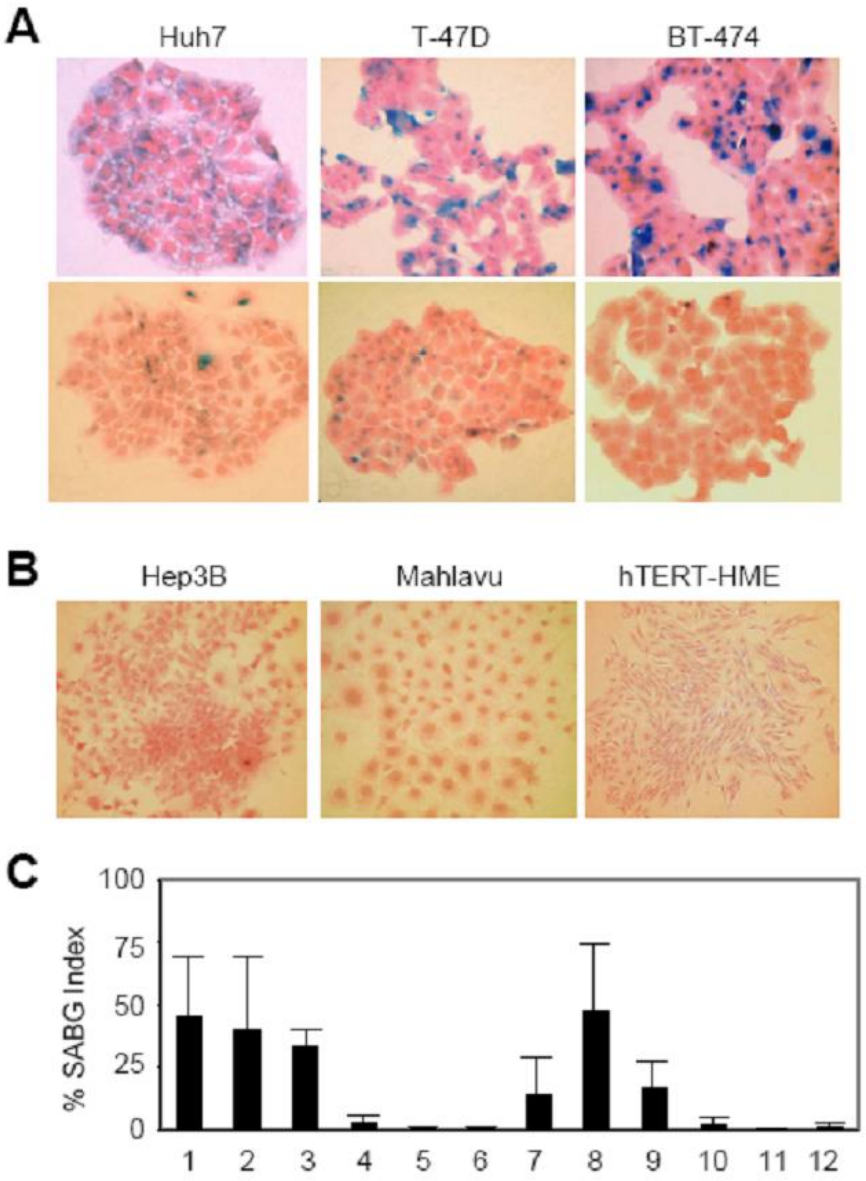

Figure 4.4.2: Established human cancer cell lines generate senescence-associated β-galactosidase (SABG)-expressing progeny. **A**) Representative pictures of HCC (Huh7) and breast cancer (T-47D and BT-474) cell lines that generates both SABG-positive (top) and SABG-negative (bottom) colonies. **B**) Representative pictures of HCC (Hep3B and Mahlavu) and telomerase-immortalized mammary epithelial (hTERT-HME) cell lines that generate only SABG-negative colonies. Cells were plated at clonogenic density to generate colonies with 6-10 population doublings, and stained for SABG activity (blue), followed by eosin counter-staining (red). **C**) Quantification of SABG-positive cells in colonies. Randomly selected colonies ($n \geq 10$) obtained from parental (lanes 1-6) cell lines and expanded clones (lanes 7-12) were counted to calculate the average % SABG positive cells per colony (% SABG index). Lanes 1-6 designate Huh7, T-47D, BT-474, Hep3B, Mahlavu, and hTERT-HME, respectively. Lanes 7-9 are Huh7-derived C1, C3 and C11 clones, and lanes 10-12 are Hep3B-derived 3B-C6, 3B-C11 and 3B-C13 clones. Error bars; S.D.

4.4.2 A model for cancer cell derived replicative senescent progeny: C3 clone

The study of a potentially active replicative senescence program in the progeny of immortal cancer cell lines requires the long-term follow up of single cell-derived clones. To this end, we chose to focus our investigations on Huh7 cell line. We expanded different Huh7-derived clones in long-term culture and examined their potential to undergo replicative senescence. Some clones performed more than 100 PD in culture with stable proliferation rates and heterogeneous SABG staining, while others sustained a limited number of PD, then entered a growth arrest phase with full SABG staining patterns. For example, Huh7 derived C3 clone performed only 80 PD, whereas Huh7 derived C1 clone replicated over 150 PD. Permanently arrested C3 cells (PD 80) displayed enlarged size, flattened shape, and fully positive SABG staining, whereas early passage C3 (PD 57) and C1 (PD 179) cells displayed normal morphology with heterogeneous SABG staining (Figure 4.4.4A-top). Normal human cells at replicative senescence (M1) are refractory to mitotic stimulation and display <5% BrdU index (Wei W. and Sedivy JM., 1999). Growth-arrested C3 cells displayed very low BrdU staining (2±2%), in contrast to early passage C3 and late passage C1 cells which exhibited 89±6%, and 96±3% BrdU indexes, respectively (Figure 4.4.4A-bottom). Senescent C3 cells remained growth-arrested, but alive when maintained in culture for at least 3 months, with no emergence of immortal clones. The cell proliferation rate were decreased in C3 clonal cells as telomeres lengths were decreased (Figure 4.4.3).

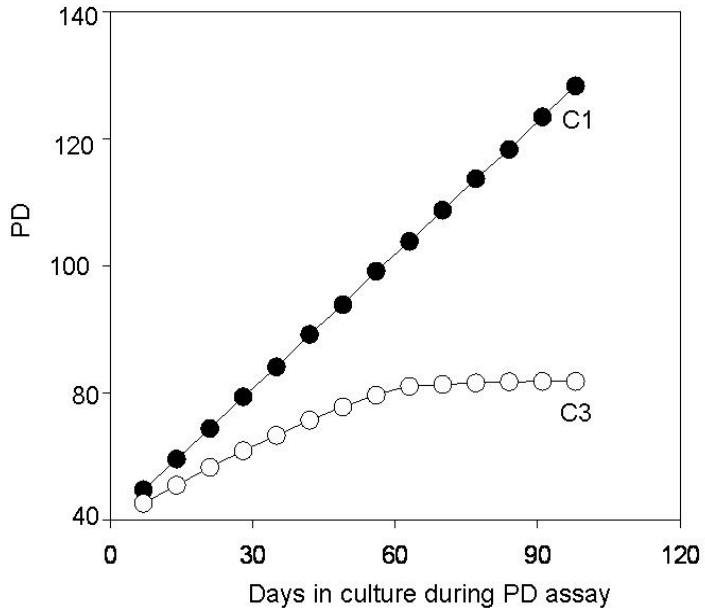

Figure 4.4.3: Proliferation rates of C1 and C3 clonal cells at different passages. C1 cells grow exponentially when supplied with mitosis stimuli. However, C3 cells cease proliferation at late passages. Initial PD (40) was calculated by considering the time passed from isolation of C3 clonal cell until the initial PD assay. Black circles, C1; white circles, C3.

Biological mechanisms of replicative senescence observed here are of particular interest, since senescence-regulatory p53 is inactivated (Bressac B. et al., 1990; Volkmann M. et al., 1994; Kubica S. et al., 1997) and $p16^{INK4a}$ promoter is hypermethylated (Roncalli M. et al., 2002) in Huh7 cells. Accordingly, there was no change in p53 levels, whereas low level $p16^{INK4a}$ expression further decreased in senescent C3 (PD 80) cells, when compared to presenescent C3 (PD 57) or immortal C1 (PD 179) cells. Retinoblastoma protein (pRb) displayed partial hypophosphorylation in senescent C3 cells, apparently in a p53- and $p16^{INK4a}$–independent manner (Figure 4.4.4B). Cyclin E and cyclin A levels were also decreased, but $p21^{cip1}$ levels were elevated in both presenescent and senescent C3 cells Cyclin D1, CDK4 and CDK2 protein levels (Figure 4.4.5A), and $p14^{ARF}$ transcript levels (Figure 4.4.5B) did not change.

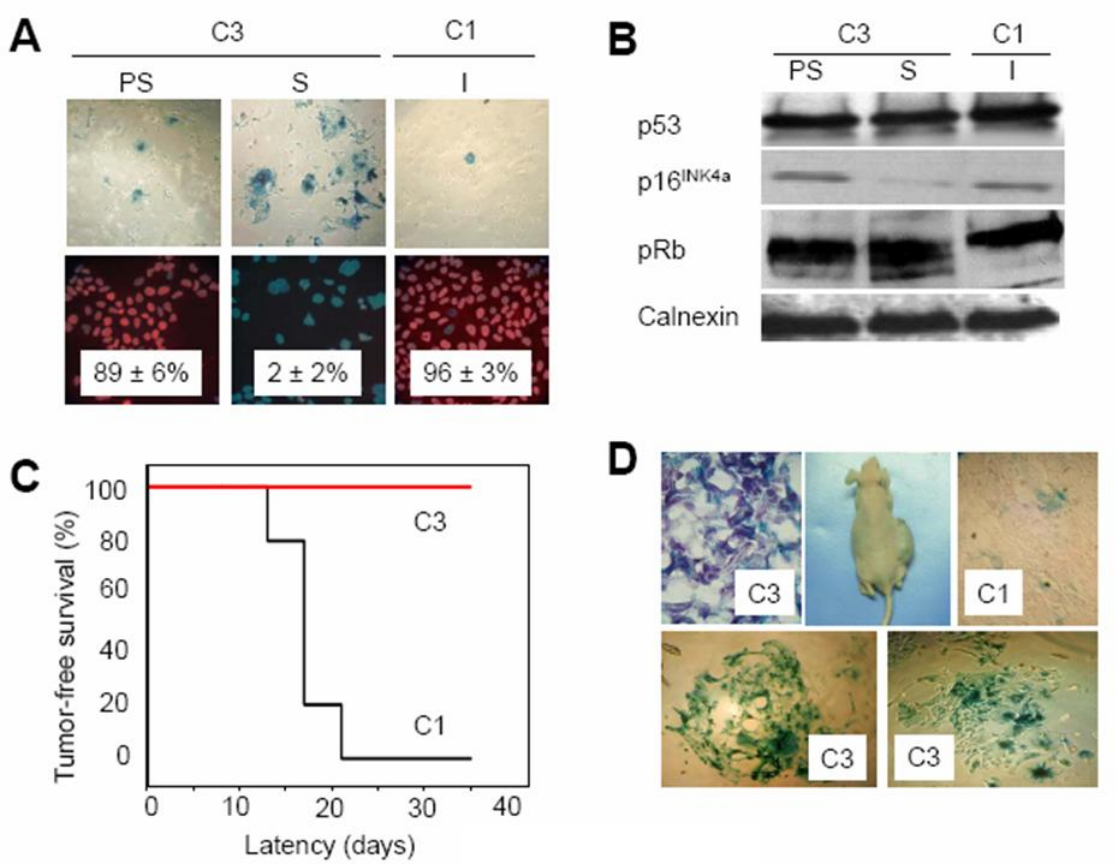

Figure 4.4.4: p53-and p16^{INK4a}-deficient Huh7 cells generate progeny that undergo *in vitro* and *in vivo* replicative senescence resulting in loss of tumorigenicity. A) Huh7-derived clones C3 and C1 were tested for replicative senescence arrest by SABG and BrdU staining at different passages. Presenescent C3 and immortal C1 cells display low SABG staining (top) and high BrdU incorporation (bottom), whereas senescent C3 cells are fully positive for SABG (top) and fail to incorporate BrdU into DNA following mitogenic stimuli (bottom). **B**) p53 and p16^{INK4a} protein levels show no increase in senescent C3 cells, compared to presenescent C3 and immortal C1 cells, but senescent C3 cells display partial hypophosphorylation of pRb. Calnexin was used as a loading control. Proteins were tested by immunoblotting. PS; presenescent (PD 57), S; senescent (PD 80), I; immortal (PD 179). **C and D)** C1 cells form tumors, but C3 cells undergo senescence in *nude* mice. **C**) C1 cells (black line) were fully tumorigenic, but C3 cells (red line) were not. **D**) C1 tumors displayed low SABG staining (top-right), whereas implanted C3 cells remaining at the injection site are fully positive for SABG *in situ* (top-left), as well as after short-term *in vitro* selection (bottom). Animals were injected with presenescent C3 (PD 59) and immortal C1 (PD 119) cells, tumors and non-tumorigenic cell samples were collected at day 35, and analyzed.

Cancer cell senescence that we characterized here shared many features with normal cell replicative senescence (Shay JW. and Wright WE., 2005), except that it was not accompanied with wild-type p53 or p16^{INK4a} induction. However, *in vivo* relevance of the replicative senescence observed in cell culture is debated (Ben-Porath I. and Weinberg RA., 2004). Therefore, we compared *in vivo* replicative potentials of C3 (PD 59) and C1

(PD 119) cells in CD-1 *nude* mice. C3 cells did not form visible tumors, whereas C1 cells were fully tumorigenic in the same set of animals (Figure 4.4.4C), like parental Huh7 cells (data not shown; Kaneko S. et al., 1995). C1 tumors collected at day 35 displayed scattered but low-rate SABG-positive staining, but remnant C3 cell masses collected from their injection sites were fully SABG-positive (Figure 4.4.4D-top). For confirmation, these remnants were removed from two different animals, passaged twice in cell culture for selection, and examined. Nearly all cells displayed senescence features including enlarged size, flattened shape and highly positive SABG staining (Figure 4.4.4D-bottom). We concluded that loss of C3 tumorigenicity was due to replicative senescence *in vivo*.

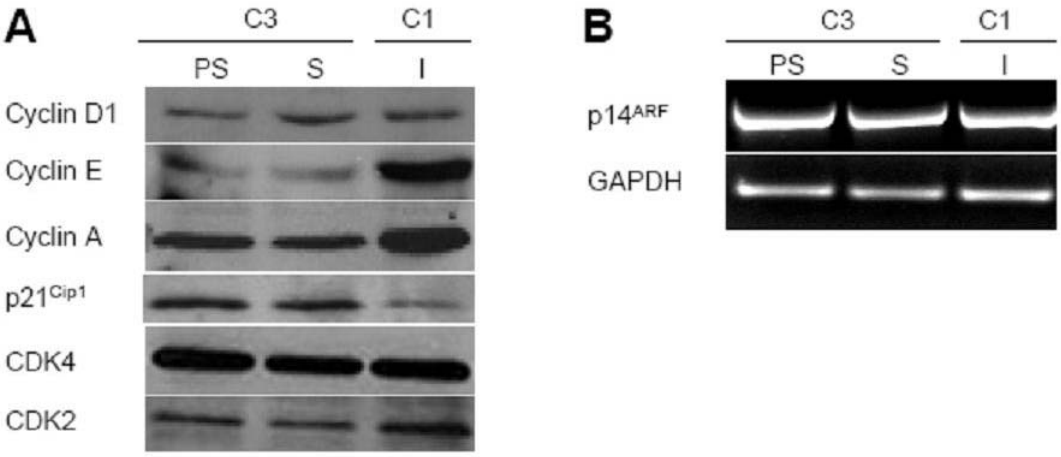

Figure 4.4.5: Complementary information on presenescent and senescent C3 cells, as compared to immortal C1 cells. A) Immunoblot data shows decreased levels of cyclin E and cyclin A, but not cyclin D1, CDK4 or CDK2. $p21^{Cip1}$ levels were slightly augmented in presenescent and senescent C3 cells (see Discussion for an explanation). **B**) RT-PCR data shows that $p14^{ARF}$ expression is similar between C1 and C3 clones. GAPDH was used as a control. PS; presenescent (PD 57), S: senescent (PD 80), I; immortal (PD 179).

Replicative senescence, also called telomere-dependent senescence is associated with progressive telomere shortening due to inefficient telomerase activity (Shay JW. and Wright WE., 2005). When compared to parental Huh7 cells, presenescent C3 cells at PD 57 had telomeres which have already been shortened to ~7 kbp from ~12 kbp. These cells eroded their telomeres to less than 5 kbp at the onset of senescence. In contrast, immortal C1 clone (PD 179) telomeres did not shorten (Figure 4.4.6A). These observations showed a perfect correlation with telomerase activity and hTERT expression. Immortal C1 cells

displayed robust telomerase activity, whereas both presenescent and senescent C3 cells had no detectable telomerase activity (Figure 4.5.6B). Accordingly, the expression of hTERT gene was high in C1, but barely detectable in Huh-C3 cells (Figure 4.4.6C). Thus, senescence observed with C3 cells was characterized with the loss of hTERT expression and telomerase activity, associated with telomere shortening.

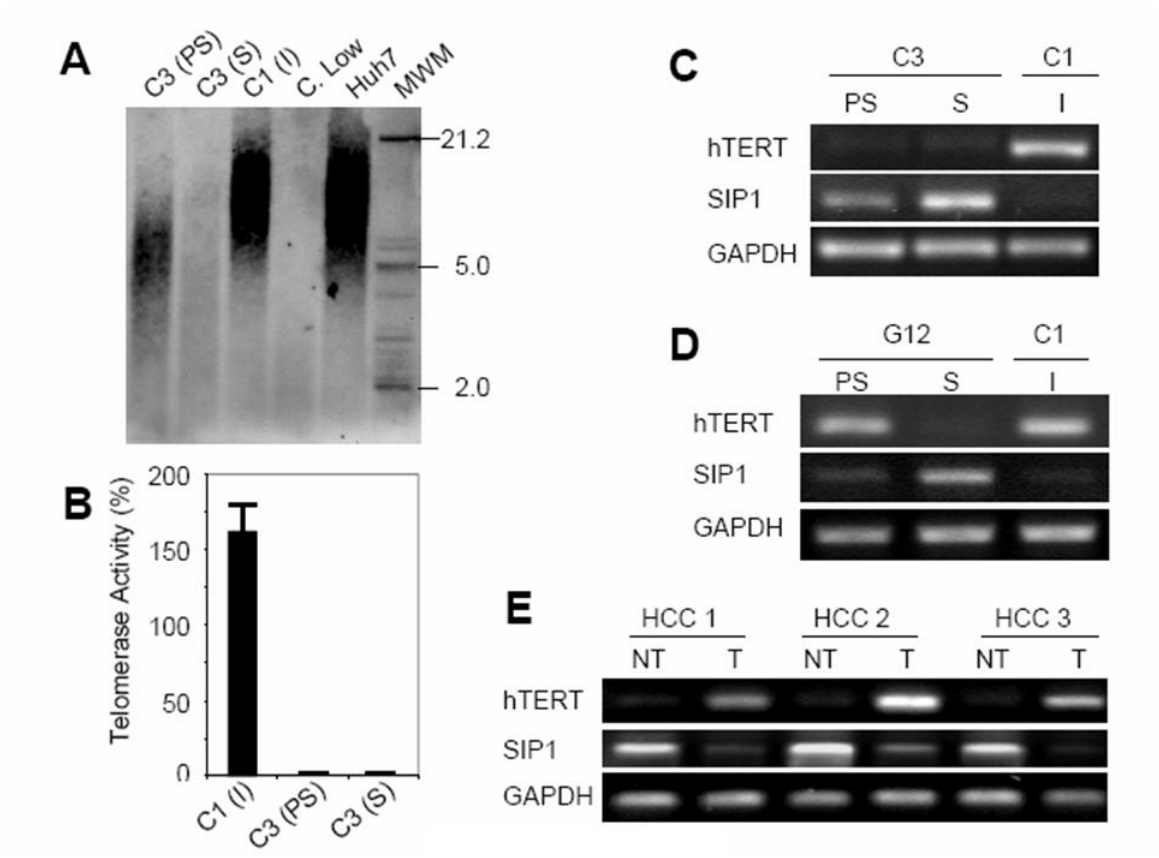

Figure 4.4.6: C3 clonal cells undergo telomere-dependent replicative senescence associated with SIP1 expression and hTERT repression. SIP1 expression is lost, while hTERT is repressed in primary HCC tumors. A) Genomic DNAs from parental Huh7 and immortal C1 cells display long telomeres, whereas C3 telomeres are progressively shortened in presenescent and senescent stages, respectively. Equal amounts of genomic DNAs were blotted with a telomere repeat probe. C. Low; short telomere control DNA. **B**) Presenescent and senescent C3 cells have lost telomerase activity, as measured by TRAP assay. Telomerase activity was shown as % value of test samples (±SD) compared to "high positive" control sample. **C**) hTERT expression as tested by RT-PCR was high in immortal C1, but decreased to weakly detectable levels in C3 cells. Inversely, SIP1 expression tested by RT-PCR was undetectable in C1 cells, but showed a progressive increase in presenescent and senescent C3 cells. **D**) Inverse relationship between SIP1 and hTERT expression was confirmed with another senescence-programmed Huh7 clone named G12 (see Figure S3 for SABG and BrdU assays). hTERT expression in G12 showed a slight decrease in presenescent stage, followed by a loss at the onset of senescence. Inversely, the expression of SIP1 gene was weakly positive in presenescent G12, but highly positive in senescent G12 cells. C1 was used as control. PS; presenescent, S; senescent, I; immortal. **E**) Negative correlation between hTERT and SIP1 expression in primary tumors (T) and non-tumor liver tissues (NT).

Mechanisms of hTERT expression are presently unclear, but several genes including SIP1, hSIR2, c-myc, Mad1, Menin, Rak and Brit1 have been implicated (Wang J. et al., 1998; Lin SY. and Elledge SJ., 2003). We analyzed their expression in C1 and C3 clones. All tested genes, except SIP1, were expressed at similar levels in both C1 and C3 clones, independent of hTERT expression (Figure 4.4.7).

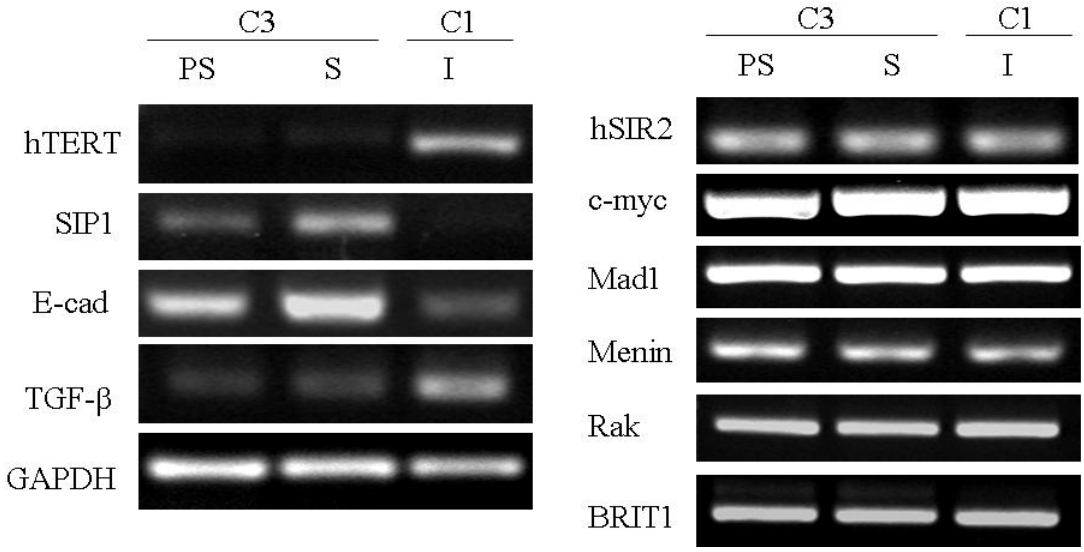

Figure 4.4.7: Complementary information on the expression of hTERT regulatory genes. RT-PCR data shows that the expression of hTERT regulators hSIR2, c-myc, Mad1, Menin, Rak and BRIT1 is similar in C1 and C3 clonal cells.

SIP1 transcripts were undetectable in C1 cells, but elevated in C3 cells, moderately in presenescent, but strongly in senescent stages (Figure 4.4.7). We verified these findings with another Huh7-derived clone (G12) that displayed replicative senescence resulting in permanent cell proliferation arrest. Like C3, presenescent G12 cells that displayed low SABG staining with high BrdU index (98±1%), and became fully positive for SABG, and nearly negative for BrdU (3±2%) at the onset of senescence (Figure 4.4.8). Presenescent G12 cells displayed only a weak hTERT repression associated with a slight increase in SIP1 expression, whereas SIP1 was strongly elevated in hTERT-negative senescent cells (Figure 4.4.6D). Thus, there was a close correlation between SIP1 expression and hTERT repression in all Huh7 clones tested. The analysis of SIP1 and hTERT expression in primary HCCs and their corresponding non-tumor liver tissues confirmed this relationship. SIP1 transcript levels were high, but hTERT expression was low in non-

tumor liver tissues, whereas respective HCC tumors displayed diminished SIP1 expression associated with upregulated hTERT expression (Figure 4.4.6E).

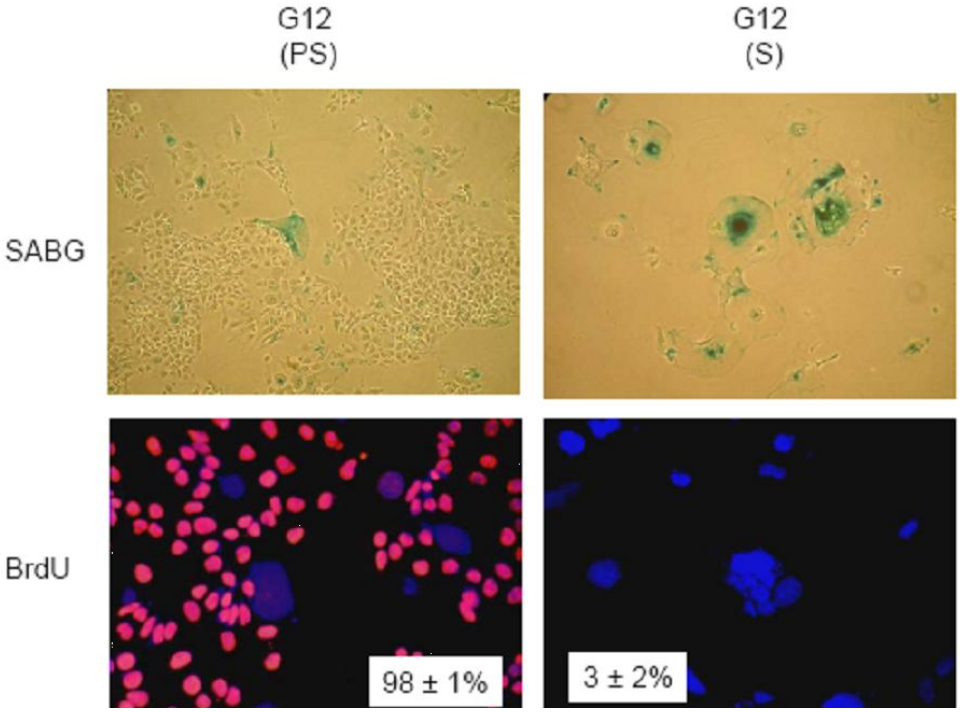

Figure 4.4.8: Data showing replicative senescence in Huh7-derived G12 clone. Presenescent G12 cells display low SABG staining (top) and high BrdU incorporation (bottom), whereas senescent G12 cells are fully positive for SABG (top) and fail to incorporate BrdU into DNA following mitotic stimulus (bottom). PS; presenescent, S; senescent.

The *SIP1* gene (*Zinc finger homeobox 1B*; *ZFHX1B*) encodes a transcriptional repressor protein that interacts with SMAD proteins of the TGF-β signalling pathway and CtBP co-repressor (Verschueren K. et al., 1999; Postigo A. et al., 2003). This gene has recently been implicated in TGF-β-dependent regulation of hTERT expression in breast cancer cells (Lin SY. and Elledge SJ., 2003). Our observations implicated SIP1 gene as a candidate regulator of replicative senescence in HCC cells. To investigate whether SIP1 expression constitutes a protective barrier against hTERT expression and senescence bypass, we constructed SIP1 shRNA-expressing plasmids, based on a previously reported effective SIP1 siRNA sequence (Lin SY. and Elledge SJ., 2003). SIP1 shRNA suppressed the accumulation in SIP1 in presenescent C3 (PD 75) cells, when expressed transiently (Figure 4.4.9A-day 5). This resulted in a weak increase in hTERT expression.

Transfected cells were maintained in culture and observed for 30 days. At this period, C3 cells transfected with a control plasmid reached senescence-arrested stage with further upregulation of SIP1 expression (Figure 4.4.9A-day 30) and resistance to BrdU incorporation after mitogenic stimuli (BrdU index=3±1%; Fig 4B-top-left). In sharp contrast, SIP1 shRNA-transfected cells lost SIP1 expression and upregulated hTERT transcripts (Figure 4.4.9A-day 30). Furthermore, SIP1-inactivated cells escaped senescence, as evidenced with 70±9% BrdU index (Figure 4.4.9B-top-right). Morphologically, SIP1 shRNA-transfected cells formed proliferating clusters, whereas cells transfected with control plasmid displayed hallmarks of senescence such as scattering, enlargement and multiple nuclei (Figure 4.4.9B-bottom). Twelve independent clones were selected from SIP1 shRNA-transfected C3 cells. All but one of these clones have performed so far more than 12 PD beyond the expected senescence barrier (data not shown). As an additional confirmatory assay, C3 cells were transfected with a puromycin-selectable SIP1 shRNA vector and subjected to puromycin selection. SIP1 shRNA-transfected cells survived and formed a large number of colonies after 30 days of puromycin selection. In contrast, no surviving colony was obtained from cells transfected with the control plasmid, as expected (Figure 4.4.9C).

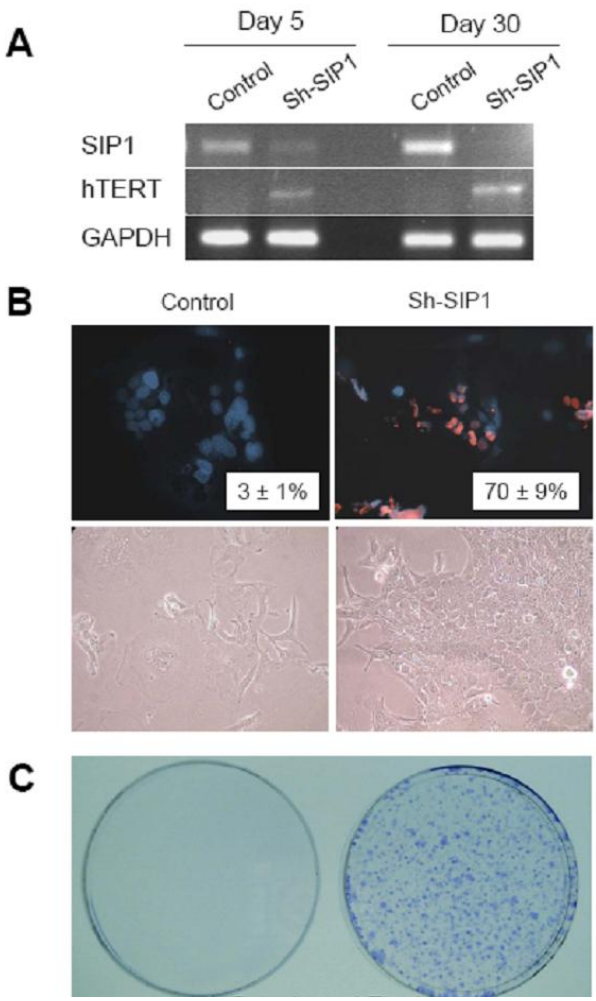

Figure 4.4.9: ShRNA-mediated downregulation of endogenous SIP1 transcripts releases hTERT repression and rescues C3 cells from senescence arrest. A) At day 5 following transfection, SIP1 shRNA-transfected cells (Sh-SIP1) show decreased expression of SIP1 and weak upregulation of hTERT expression. At day 30, the expression of SIP1 is lost completely, and hTERT expression is stronger. **B**) Cells transfected with empty vector (Control) are senescence-arrested as evidenced by resistance to BrdU incorporation (top-left) and morphological changes (bottom-left), but cells transfected with SIP1 shRNA vector (Sh-SIP1) escaped senescence arrest as indicated by high BrdU index (top-right) and proliferating cell clusters (bottom-right).**C**) Colony forming assay shows that C3 cells formed large number of colonies following puromycin selection after transfection with a puromycin-resistant SIP1-shRNA-expressing plasmid (right), whereas cells transfected with empty vector did not survive (left). Presenescent C3 cells at PD 75 were transfected with either SIP1 shRNA-expressing or empty plasmid vectors and tested at days 5 (**A**) and 30 (**A, B** and **C**).

4.4.3 Senescence in human tissues

We have analyzed human liver tissues and breast tissues for their senescence phenotype by using SABG staining (Figures 4.4.10, Figure 4.4.11, and Figure 4.4.12; Table 4.3). We have found that colorectal cancer, stomach cancer, and breast cancer samples had SABG positive cells. This indicated that tumors are composed of both

mortal and immortal cells. Additionally, we detected SABG positive cells in cirrhotic samples which was expected since telomere shortening and senescence are general markers of liver cirrhosis. In parallel to this view, we could not find SABG positive cells in liver samples with hepatitis.

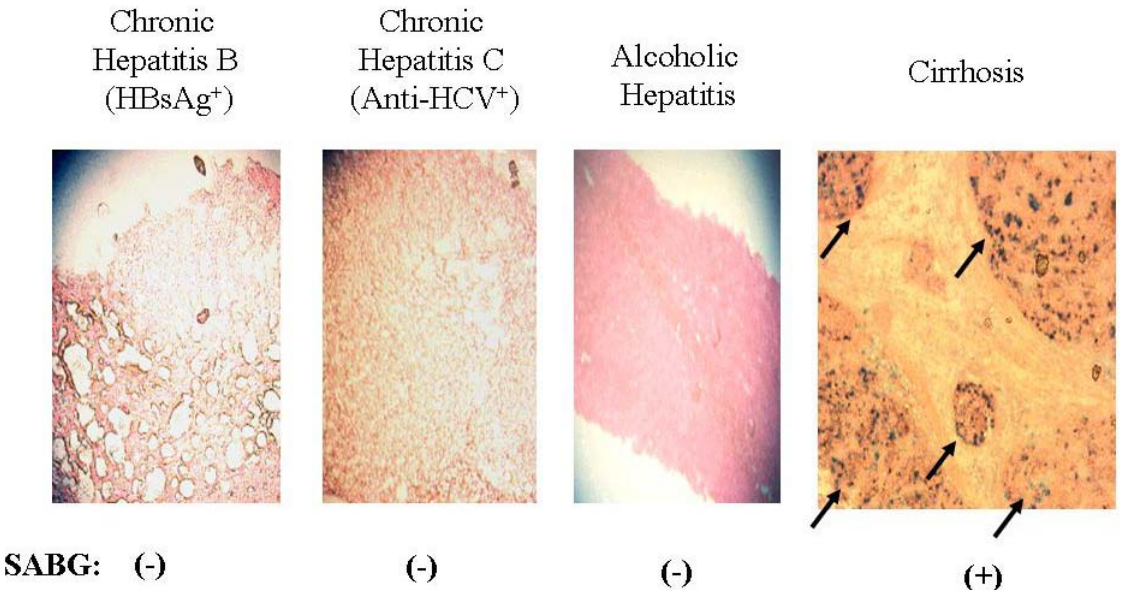

Figure 4.4.10: SABG staining in pathological liver tissues: Only cirrhotic liver had SABG positive areas. Arrows indicates SABG positive cells.

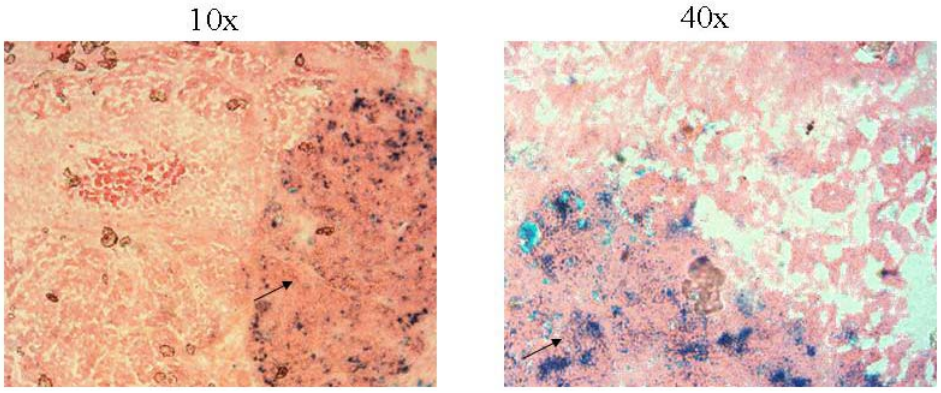

Figure 4.4.11: SABG staining in primary liver tissues. A primary liver tissue was SBAG- stained. Tumor tissue had some SABG positive cells. Picture was taken at 10X magnification (left) and 40 X magnification (right). Arrows indicates SABG positive cells.

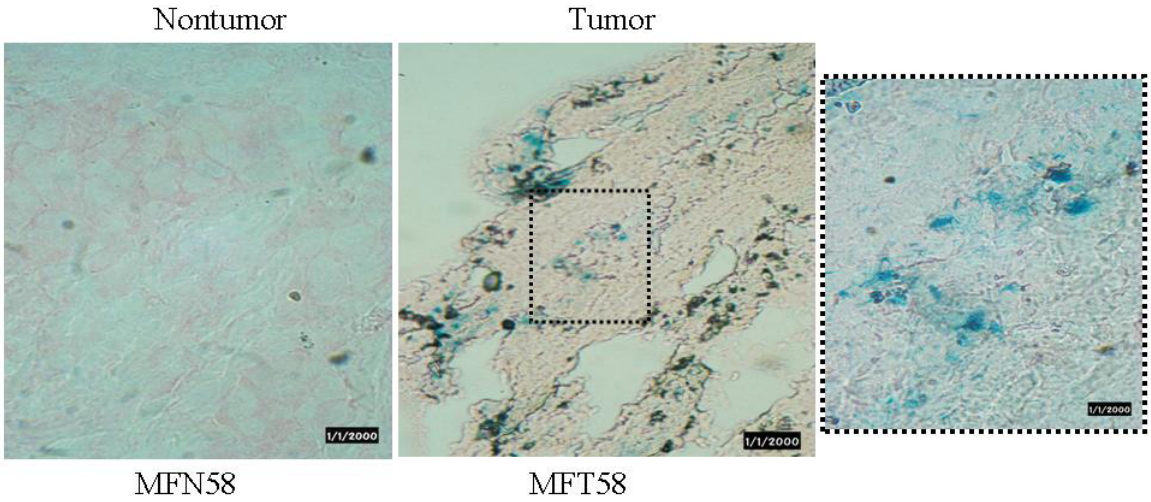

Figure 4.4.12: SABG staining in human breast tissues. Human breast cancer samples had some SABG positive areas. Non tumor breast tissue did not have any SABG positive areas. On the right, SABG positive area of tumor tissue (insert) was shown at higher magnification. MFN58, non tumor breast tissue; MFT58, adjacent breast tumor.

Tissues	Tested	Positive	% Positive
Chronic Hepatitis	7	0	0
Liver Cirrhosis	2	2	100
Hepatocellular Carcinoma	6	3	50
Breast Cancer	20	2	10
Colorectal Cancer	5	1	20
Stomach Cancer	11	1	9
Total Tumor	42	7	17

Table 4.3: Senescence in primary tumors and pathologic liver tissues. We tested pathological liver tissues and some primary cancer tissues. Interestingly, colorectal cancer samples had SABG staining, even though our colorectal cancer cell lines did not produce spontaneous senescent cells.

4.4.4 Analysis of HCC cells for SIP1, TGF-β1, hTERT and E-cadherin expressions

We have analyzed hTERT, SIP1, E-cadherin, TGF-β1 expression in HCC cell lines. TGF-β1 was expressed in all HCC at variable levels, hTERT was expressed in all HCC cells independent of SIP1 expression. Since SIP1 is suggested as a negative regulator of E-cadherin in HCC cells, we included expression analysis of E-cadherin in

our HCC cells. SIP1 and E-cadherin displayed inverted correlation. However, we could not see this inverted correlation in C3 and C1 clonal cells, this indicated that there are others factors regulating E-cadherin expression in these cells (Figure 4.4.7).

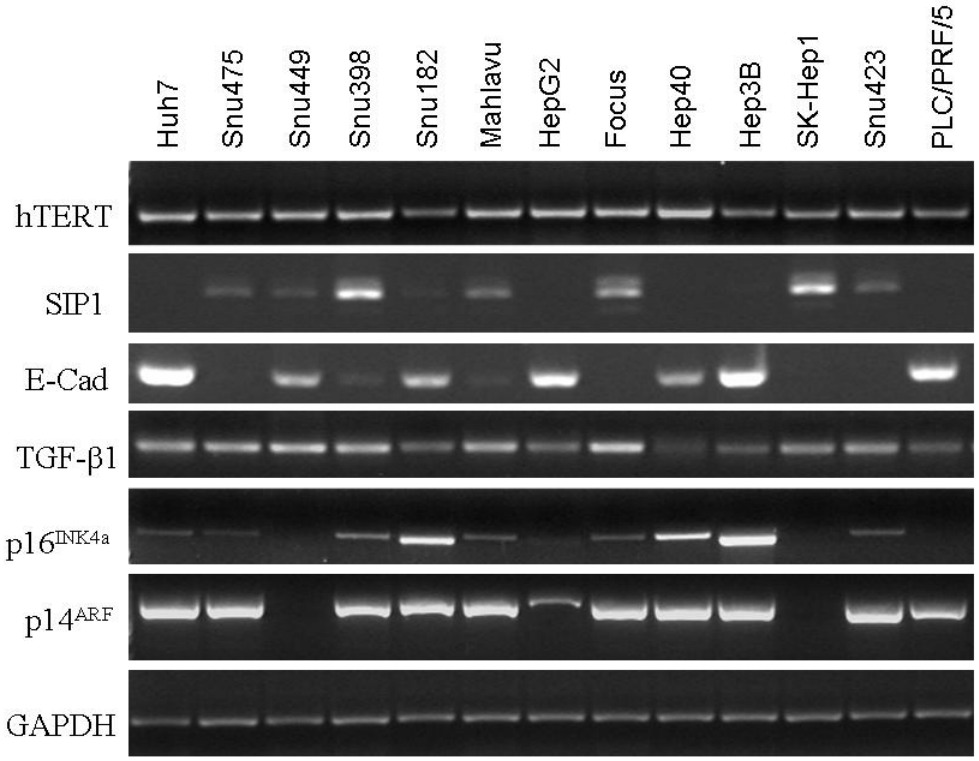

Figure 4.4.13: Sip1 and E-cadherin expression is conversely correlated. TGF-β1 is expressed in our HCC collection at variable degrees. Our HCC cell lines expressed hTERT. GAPDH was used for equal loading.

4.4.5 Overexpression of SIP1 in Hep3B cells

To confirm our findings that SIP1 knock-down release hTERT repression in our clones independent of p53 status, we decided to overexpress SIP1 in p53-null Hep3B cells. Stable transfectants were established following transfection of Hep3B cells with mouse SIP1-expressing or empty plasmids. Three SIP1-expressing (3B-S1, 3B-S3, 3B-S4) clones and one negative control (3B-C1) clone were selected for further study. Since parental Hep3B cells are deficient in p53 and pRb expression, Hep3B clones did not express p53 and pRb proteins as expected (Figure 4.4.14A). The expression of SIP1 in these clones resulted in partial repression of hTERT expression (Figure 4.4.14B). Hep3B clones were then subjected to SABG staining. Morphologically senescent cells were frequently identified in SIP1-expressing clones, but not in 3B-C1 clone (Figure 4.4.14C-

left). Next, the ability to generate senescent progeny was tested by plating cells at clonogenic density and maintaining in culture for 6-10 PD. Colonies derived from the 3B-C1 clone were usually SABG-negative, similar to parental Hep3B cells, whereas SIP1-expressing clones were able to generate colonies with highly SABG-positive progeny (Figure 4.4.14C -right). To test the significance of these findings, we calculated SABG-labelling indexes of randomly selected colonies (n=30) from each clone. The average SABG-labelling index was 2±2% for 3B-C1 cells. A statistically significant increase ($P<0.0001$) in the ability to generate SABG-positive progeny was observed with 3B-S1, -S2, and -S3 clones which respectively displayed 6±4%, 9±7%, and 10±6% SABG-labelling indexes (Figure 4.4.14D). We also performed SABG/BrdU double staining and calculated BrdU index for SABG-positive and SABG-negative cells. SABG-negative cells from all four isogenic clones displayed high labelling indexes (84±4% to 89±2%), as expected. SABG-positive cells of the 3B-C1 clone displayed a high BrdU index (61±6%), suggesting that they are not truly senescent. In contrast, BrdU-labelling indexes for SABG-positive 3B-S1, 3B-S3 and 3B-S4 cells were 16±3%, 14±7%, and 21±4%, respectively 1 (Figure 4.4.14E). Thus, ~80% of SABG-positive progeny in SIP1-expressing clones displayed permanent proliferation arrest, suggesting that they entered a senescent state. These observations provide plausible evidence that SIP1 expression in p53- and pRb-negative HCC cells can generate progeny with a fate change from immortality to replicative senescence.

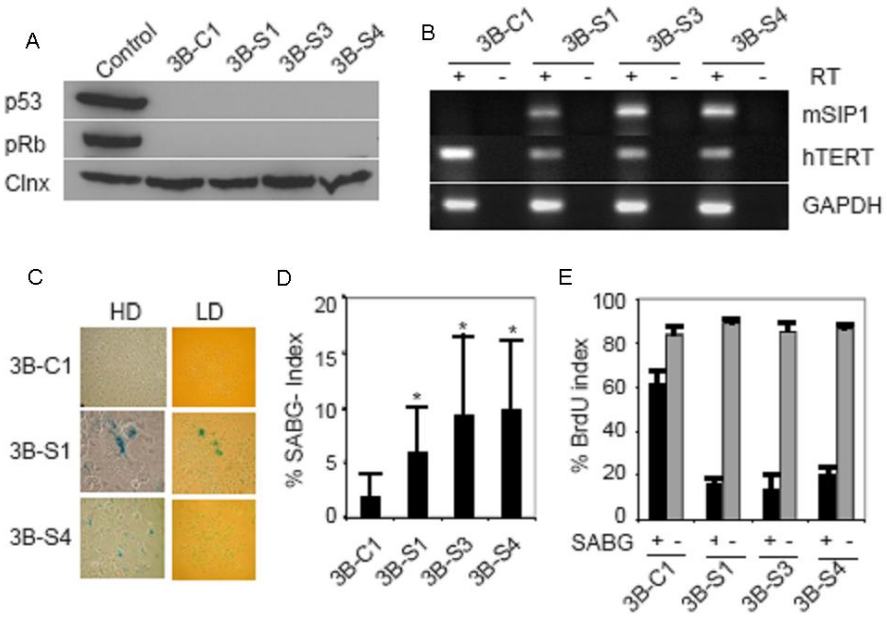

Figure 4.4.14: Ectopic expression of SIP1 in p53- and pRb-negative Hep3B hepatocellular carcinoma cells results in the repression of hTERT expression, and confers the ability to generate senescent progeny. **A)** Immunoblot analysis of proteins from Hep3B-derived clones demonstrate lack of pRb and p53 expression. Control: Huh7. **B)** RT-PCR analyses indicate that hTERT transcript levels are decreased in clones stably expressing mouse SIP1 (3B-S1, 3B-S3, 3B-S4), but not in control clone (3B-C1) transfected with empty vector. **C)** When tested at high cell density (HD), SIP1 expressing clones, but not control clone displayed frequently SABG-positive (blue) cells. SABG-staining of colonies generated after low density (LD) plating show that SIP1-expressing 3B-S1, 3B-S3 and 3B-S4, but not control (3B-C1) clones are able to generate senescent progeny. **D)** Ratios of senescence marker-positive progeny in randomly selected colonies (n=30) from control and SIP1-expressing clones were shown. * denotes that the increases observed SIP1-expressing clones were statistically significant ($P < 0.0001$). **E)** BrdU incorporation index of SABG-positive and SABG-negative cells (assays in triplicate) are shown. SABG-negative cells from all four clones displayed high (>80%) index. SABG-positive cells from 3B-C1 clones displayed relatively high BrDU incorporation index (>60%), whereas SIP1-expressing clones had consistently low index (<20%). Studies were performed with the following passage numbers: 3B-C1, passages 13-17; 3B-S1 and 3B-S3, passage 9; 3B-S4, passage 6.

When compared to parental mock transfected Hep3B clone, SIP1-expressing clones (3B-S1, 3B-S3 and 3B-S4) had telomeres which have already been shortened (Figure 4.4.15).

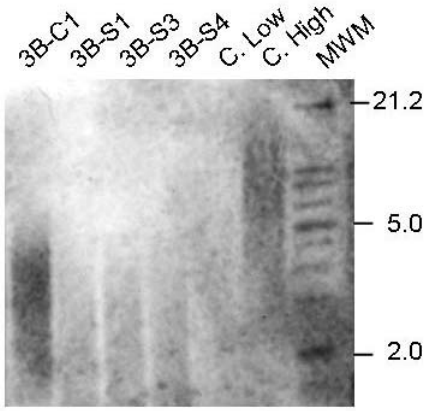

Figure 4.4.15: Ectopic expression of SIP1 in p53- and pRb-negative Hep3B hepatocellular carcinoma cells results in telomere shortening. Studies were performed with the following passage numbers: 3B-C1, passages 13-17; 3B-S1 and 3B-S3, passage 9; 3B-S4, passage 6. Equal amounts of genomic DNAs were blotted with a telomere repeat probe. C. Low; short telomere control DNA. H. Low; short telomere control DNA.

We cultured Hep3B stables long-term, and noticed that senescence markers were lost in late passages. Telomere lengths were longer in late passages than in early passages (Figure 4.4.16). Late passage clones reconstituted telomerase activity comparable to control clone (Figure 4.4.17). This phenomenon contrasted with our expectations. Then we analyzed the expression levels of mouse SIP1 and the functionality of it by analyzing E-cadherin expression. Mouse SIP1 expression was repressed in late passages by an unknown mechanism (Figure 4.4.18A). This resulted in the release of E-cadherin repression (Figure 4.4.18B). This data indicated that cells escaped SIP1 induced replicative senescence by repressing exogenous SIP1 expression.

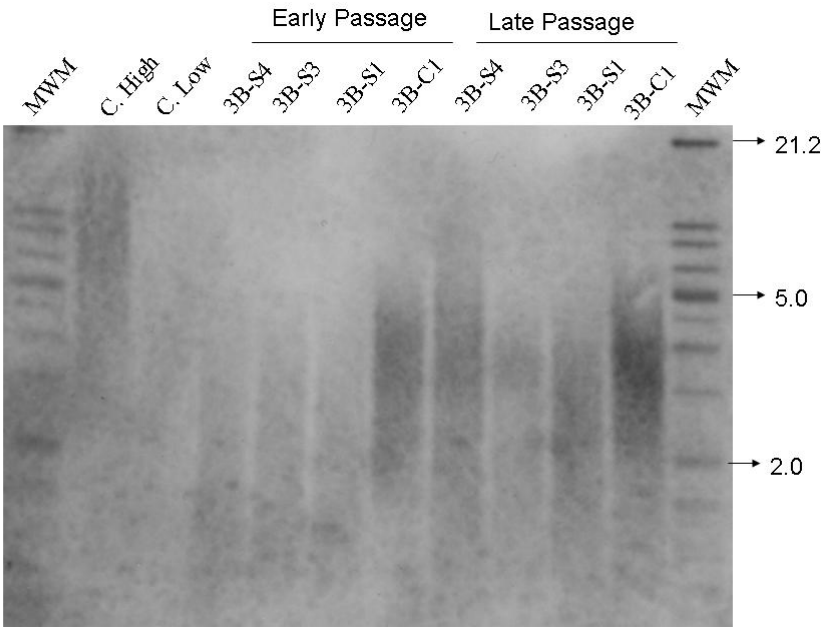

Figure 4.4.16: Telomere lengths in Hep3B clones at early and late passages. When SIP1 overexpressing Hep3B clones were cultured long term, the length of telomeres was restored since SIP1 expression was repressed in late passages. Equal amounts of genomic DNAs were blotted with a telomere repeat probe. C. Low; short telomere control DNA. H. Low; short telomere control DNA. . Early passages: 3B-S4, p3; 3B-S3, p2; 3B-S1, p5; 3B-C1, p3. Late passages: 3B-S4, p16; 3B-S3, p17; 3B-S1, p17; 3B-C1.

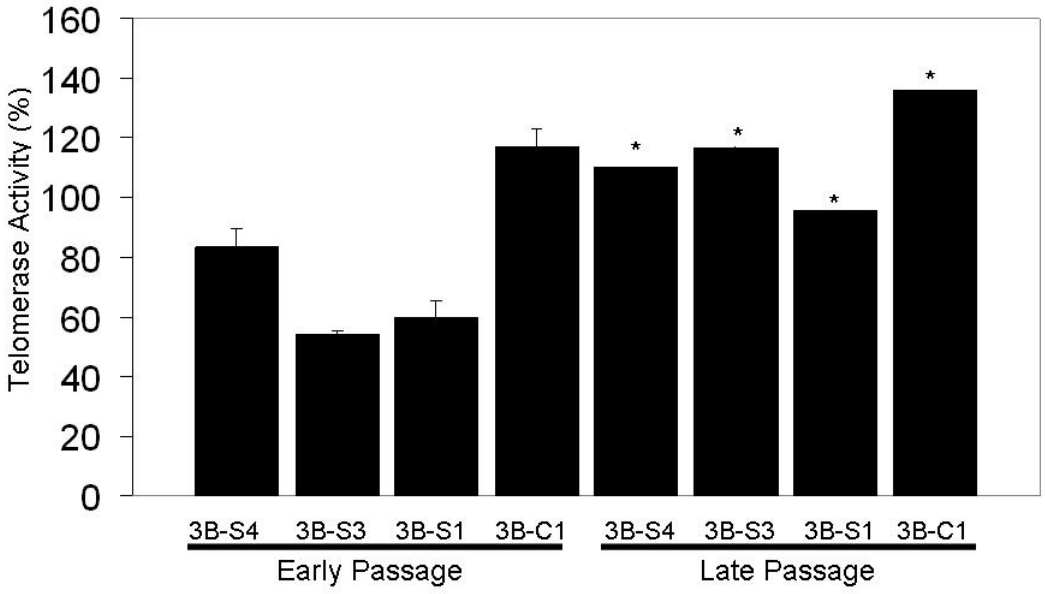

Figure 4.4.17: Telomerase activity in Hep3B clones at early and late passages. Hep3B-SIP1 clones have partially lost telomerase activity at early passages; however they reconstituted telomerase activity at late passages. Early passages: 3B-S4, p3; 3B-S3, p2; 3B-S1, p5; 3B-C1, p3. Late passages: 3B-S4, p16; 3B-S3, p17; 3B-S1, p17; 3B-C1. For early passages, telomerase activity was shown as % value of test samples (±SD) compared to "low positive" control sample. * donates that telomerase activity of duplicate assays and the average values were shown as % value of test samples compared to "low positive" control sample.

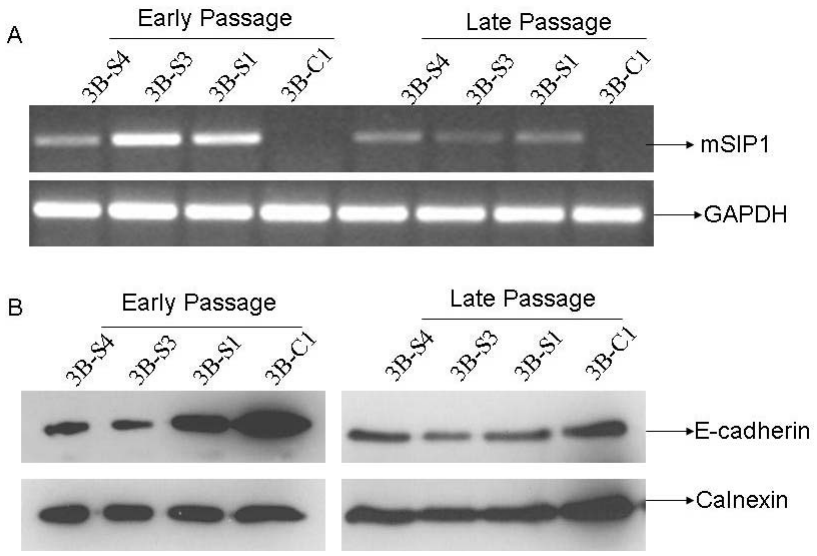

Figure 4.4.18: Exogenous SIP1 expression and repression of E-cadherin in early and late passages. **A)** SIP1 expression was repressed in late passages by an unknown mechanism. **B)** E-cadherin repression was released as a result of SIP1 repression in late passages. Early passages: 3B-S4, p3; 3B-S3, p2; 3B-S1, p5; 3B-C1, p3. Late passages: 3B-S4, p16; 3B-S3, p17; 3B-S1, p17; 3B-C1, p20. mSIP1: mouse SIP1. In this study, E-cadherin and calnexin immunoblottings for early and late passages were not performed using the same membrane. Therefore, the signal ratio of E-cadherin to calnexin has been considered to interpret the results.

Overall, our data indicated cells mouse SIP1 expression induced senescence program in Hep3B cells. However, mouse SIP1 induced senescence was escaped in these clones by repression of mouse SIP1 with an unknown mechanism.

CHAPTER 5. DISCUSSION

5.1 Canonical Wnt signaling in well- and poorly-differentiated HCC cell lines

5.1.1 Canonical Wnt signaling is active in well-differentiated and inactive in poorly-differentiated HCC cell lines

Our results provide evidence for the dual involvement of canonical Wnt signaling in HCC cells. We detected constitutive canonical Wnt signaling in 80% of well differentiated HCC cell lines, including two cell lines (Huh7 and Hep3B) with wild-type *β-catenin* and *Axin-1* genes (Figure 4.1.1) This strongly supports the hypothesis that canonical Wnt signaling is active in most well-differentiated HCC cells. This can occur by an autocrine mechanism, as shown recently in breast and ovarian cancer cell lines (Bafico A. et al., 2005). Additionally, the activity of canonical Wnt signaling in Huh7 can be explained by the existence of mutant p53 as suggested by Cagatay T. and Ozturk M. (Cagatay T. and Ozturk M., 2002). New components and the cross-talk of canonical Wnt signaling with other signaling pathways are being discovered continuously. Therefore, there is possibility that somatic alterations cause the constitutive canonical Wnt signaling in Huh7 and Hep3B cells. Constitutive canonical Wnt signaling has been linked to both stem cell and cancer cell self-renewal in certain cancer types. It was proposed that some adult cancers derive from stem/progenitor cells and canonical Wnt signaling in stem and progenitor cells can be subverted in cancer cells to allow malignant proliferation (Reya T. and Clevers H., 2005). Thus, our observations raise the interesting possibility that well differentiated HCCs represent a group of liver tumors originating from liver stem cells. In accordance with this hypothesis, our group showed that well-differentiated cell lines studied here display liver stem cell-like features, such as generation of differentiated progeny (Erdal E. et al., unpublished data). Additionally, we obtained two subpopulations from Huh7 cells, one with immortal and the other with mortal phenotype (see "Reprogramming of replicative senescence in hepatocellular carcinoma derived cells" section). Moreover, we have recently noticed that the overexpression of a mutant β-catenin in Huh7 cells altered the expression of liver differentiation markers (Ozturk N. et al., unpublished data). Overall, these findings support the hypothesis that well-

differentiated HCC cells display liver stem cell-like features, and canonical Wnt signaling is involved in this process.

5.1.2 Canonical Wnt signaling is easily activated in well-differentiated HCC cells and repressed in poorly-differentiated HCC cell lines

In sharp contrast with well differentiated HCC cell lines, most poorly differentiated HCC cell lines display no detectable canonical Wnt activity (Figure 4.1.1). More interestingly, we failed to detect TCF/LEF reporter activity in Snu475 cells with homozygous Axin-1 deletion (Figure 4.1.2B). On the other hand, well-differentiated PLC/PRF/5 with *Axin-1* (Δ Exon 4, 13 bp) mutation had significant TCF/LEF reporter activity (Ozturk N. et al., unpublished data). This data indicated that canonical Wnt signaling is not only inactive in poorly-differentiated cells but also repressed. Additionally, well-differentiated HepG2 cells (β-catenin; WT/ΔN25-140) had more TCF/LEF reporter activity than poorly-differentiated Snu398 cells (β-catenin; WT/S37C) (Figure 4.1.1B). However, one can suggest the possibility that difference at mutation type and at the origins of these cell lines (HepG2, Hepatoblastoma; Snu398, HCC) might affect the level TCF/LEF reporter activity in these cells. Therefore, we transfected Huh7 (WD), Snu499 (PD), and Snu182 (PD) cell lines with full length mutant β-catenin (S33Y) encoding vector. S33Y resulted in strong TCF/LEF reporter activity in Huh7 cell lines, while it resulted in weak and no TCF/LEF reporter activity in Snu449 (PD), and Snu182 (PD) respectively. Even though, the accumulation of β-catenin was highest in Snu182 cell line (Figure 4.1.2). This data supported the hypothesis that canonical Wnt signaling is repressed in poorly-differentiated HCC cell lines. All these cell lines already had accumulated β-catenin; therefore it was hard to differentiate the overexpressed β-catenin from endogenous one. For this reason, we repeated this experiment with an N-terminally truncated β-catenin, and obtained similar results (Figure 4.1.3). Finally, we obtained an inducible Snu449 clone (Snu449.8) overexpressing truncated β-catenin in the absence of tetracycline. The truncated β-catenin accumulated as much as the endogenous β-catenin in this clone, but resulted in a weak TCF/LEF reporter activity (less than 4 fold), which confirmed the results obtained with transient transfection (Figure 4.1.4).

The high accumulation of β-catenin in poorly-differentiated Snu182, and Snu449 derived Snu449.8 cells, and the absence of significant TCF/LEF activity provide evidence for that the signal generated by mutant protein is blocked at β-catenin level or downstream. As all poorly differentiated cell lines express both TCF1 and TCF4, a deficit at TCF/LEF family of transcription factors is unlikely (Benhaj K. et al., unpublished data). However, we did not explored if dominant negative TCF4 forms exist in poorly-differentiated cells. Moreover, we did not check the levels of negative regulators of canonical Wnt signaling in HCC cell lines. Therefore, the possibility that canonical Wnt signaling is repressed by Groucho, ICAT, CtBP, or Chibby remains unexplored. Moreover, in some contexts Wnt5A and Wnt5B inhibit the canonical pathway, at the level of β-catenin function (Topol L. et al., 2003; Ishitani T. et al., 2003; Kanazawa A. et al., 2005). Interestingly, both Wnt5A and Wnt5B are expressed in all poorly differentiated HCC cell lines, but not in well differentiated cell lines with the exception of Hep40 which also lacks canonical Wnt activity (Benhaj K. et. al., unpublished data). Although, it is not known at this time how the canonical Wnt signaling is repressed in poorly differentiated HCC cell lines, it is clear that this type of HCC cells do not need canonical Wnt signaling for survival and self-renewal. Pathological analyzes, and "nodule-in-nodule" HCC lesions strongly support the hypothesis that the progression of HCC is a stepwise process of dedifferentiation (Kojiro M., 2005). However, primary tumor data showing a gradual decrease in β-catenin mutation and nuclear accumulation frequencies in less differentiated HCCs (Hsu HC. et al., 2001; Wong CM. et al., 2001; Mao J. et al., 2001; Inagawa S. et al., 2002; Fujito T. et al., 2004) is in apparent contradiction with this prediction.

Our results provide evidence that canonical Wnt signaling is not active in most poorly differentiated cells. Taken together, these observations raise the possibility that poorly differentiated HCCs form a distinct type of tumor not directly related to well-differentiated HCCs with β-catenin mutation and constitutively active canonical Wnt signaling. It has been recently shown that activated β-catenin is localized in the perivenular area and the negative regulator APC is localized in periportal hepatocytes (Benhamouche S. et al., 2006). This may raise the possibility that well-differentiated HCC cells originated from perivenular area while poorly-differentiated HCC cells

originated from periportal hepatocytes. Another possibility is that well differentiated HCCs with activated canonical Wnt signaling rarely progress by a dedifferentiation process. Otherwise, the hypothesized dedifferentiation process would have to take into account a mechanism for selective elimination of mutant β-catenin, or active repression of the canonical Wnt signaling in the progeny of well differentiated HCC cells during tumor progression. Repression of canonical Wnt signaling, as shown here experimentally with Snu449 and Snu182 cell lines seems possible in less-differentiated HCC.. Alternatively, elimination of mutant *β-catenin* gene, although highly unlikely, is possible theoretically, since *β-catenin* mutations in HCC are heterozygous, leaving one allele in the wild-type form (de La Coste A. et al., 1998). To our knowledge, mutant β-catenin can not activate TCF/LEF reporter in certain cell lines (personal communications). Therefore, it seems possible that cell lines can be classified as "open" and "closed" cell lines according to the activation status of canonical Wnt signaling by mutant β-catenin. It would be interesting to confirm our results by activating endogenous β-catenin and comparing TCF/LEF reporter activity in well- and poorly-differentiated cells. This can be achieved by measuring TCF/LEF activity after cells are treated with lithium (which activates canonical Wnt signaling by inhibiting GSK3β) or Wnt-conditioned medium.

5.2 C/EBPα inhibits mutant β-catenin/TCF transcriptional activity in hepatocellular carcinoma cells

C/EBPα functions as a potent inhibitor of cell proliferation in hepatocytes (Kurumiya Y. et al., 2000; Iakova P. et al., 2003). Additionally, the somatic alterations of *CEBPA* gene were observed in HCC cell lines and samples; however their biological functions are not known yet (Yuva Y. et al., unpublished data). Even though, *β-catenin* mutations have been found in 22% of HCC cases in average, the activation of canonical Wnt signaling by oncogenic form of β-catenin is not sufficient for tumorigenesis since transgenic mice expressing an oncogenic form of β-catenin in their hepatocytes develop only hepatomegaly. Moreover, it has been recently shown that C/EBPα knock-in mouse are more resistant to diethylnitrosamine-induced liver tumorigenesis (Tan EH. et al., 2005). Additionally, it has been shown that overexpressed β-catenin and C/EBPα co-

immunoprecipitated from Hek293 cells (Kennell JA. et al., 2003). These observations prompted us to investigate the effect of C/EBPα on mutant β-catenin-TCF transcriptional activity in HCC cells. We have shown that the overexpression of C/EBPα inhibited both endogenous and transfected mutant β-catenin driven TCF/LEF reporter activity in HCC cell lines (Figures 4.2.1, 4.2.2., 4.2.3 and 4.2.4). Moreover, we have shown that β-catenin co-immunoprecipitated with the overexpressed C/EBPα from Huh7 cells (Figure 4.2.5). This data propose that C/EBPα regulate β-catenin in HCC. Therefore, the regulation of C/EBPα and β-catenin should be investigated from this point during liver regeneration following partial hepatectomy. Additionally, our preliminary studies indicated that β-catenin alter C/EBPα reporter activity (Tasdemir N. et al., unpublished data). Therefore, the interactions between C/EBPα and canonical Wnt signaling remain as an unexplored area.

5.3 Monoclonal anti-β-catenin antibodies as novel tools to differentiate cellular pools of β-catenin

β-catenin is tightly regulated at protein and localization levels, and the β-catenin pool out of adherens junctions is likely to be more important for tumor development. We decided to use monoclonal antibodies (MAb) in order to distinguish the cellular β-catenin pools. For this aim, we produced monoclonal antibodies against a truncated human β-catenin protein. We selected two MAbs (9E10 and 4C9) for further study since they differentially reacted with β-catenin pools in HCC cells. Their epitopes (located at the last 11 aa of C-terminus of β-catenin) were adjacent, however 4C9 did not recognized the membrane-associated β-catenin pool (Figure 4.3.4). Therefore, 4C9 is a good candidate to screen tumor samples in order to investigate aberrantly accumulated β-catenin. Although the carboxyl domain possesses important functions for Wnt signaling, details of the underlying molecular mechanisms are obscure. Using C-terminal residues in a sequence-specific manner (Hung AY. and Sheng M., 2002) several PDZ domain-containing proteins localize to sites of cell-cell contacts. β-catenin is one of the targets of at least two PDZ proteins, LIN-7 and MAGI-1 (Dobrosotskaya IY. et al., 2000). The β-catenin carboxyl terminal sequence (DTDL) 777-781, which is necessary for 4C9

immunoreactivity, is matching to a consensus PDZ-binding sequence, S/T-X-L/V (X: any amino acid). These PDZ proteins may recognize covalently modified forms of β-catenin by discriminating other forms of the molecule and translocates it to the cell-cell contracts. Since 4C9 (of which epitope includes DTDL motif) do not recognize β-catenin at the cell membrane, it is plausible that this motif can be covalently modified at adherens junctions. When β-catenin was immunoprecipitated or co-immunoprecipitated with E-cadherin and treated with SAP enzyme to remove any possible phosphorylation at this motif, we could not detect any difference in the immunoreactivity of 4C9 (Figure 4.3.6). However, in our experimental system, we could/did not confirm if we properly removed putative phosphorylation(s) at 4C9 epitope. It is also possible that this motif is hindered by a PDZ motif binding protein, which prevented 4C9 immunoreactivity in our staining assays. In summary, we could not conclude about the differential staining patterns of our MAbs.

5.4 Reprogramming of replicative senescence in hepatocellular carcinoma derived cells.

While analyzing clones from established cancer cell lines, we observed that some clones change morphology and cease proliferation at late passages with features reminiscent of cellular senescence (Figure 4.4.1). We reasoned that this could be an indication for generation of progeny programmed for replicative senescence. Our observations provide experimental evidence for generation of senescence-arrested clones from immortal HCC and breast cancer cell lines (Figure 4.4.2). Detailed analysis of clones from Huh7 cell line further indicated that what we observed is a replicative senescence, but not a stress-induced premature senescence-like arrest. Clonal C3 cells displayed telomerase repression (Figures 4.4.6B, 4.4.6C), progressive telomere shortening (Figure 4.4.6A), and permanent growth arrest after ~80 PD with senescence-associated morphological changes and SABG-positive staining (Figures 4.4.4A, 4.4.4D). Similar changes have also been observed with another independently derived clone, namely G12 (Figure 4.4.6D, Figure 4.4.8). Thus, we demonstrated that immortal cancer cells have the intrinsic ability to reprogram the replicative senescence. As expected, this shift in cell fate resulted in a complete loss of tumorigenicity (Figure 4.4.4C). It is of great interest that senescence-programmed Huh7 cells express a mutant p53 protein

(Bressac B. et al., 1990; Volkmann M. et al., 1994; Kubica S. et al., 1997) and they are deficient in $p16^{INK4a}$ expression (Roncalli M. et al., 2002). More importantly, the replicative senescence arrest that we identified with clonal C3 cells was not accompanied with the induction of p53, $p16^{INK4a}$, $p14^{ARF}$ or $p21^{Cip1}$ gene (Figure 4.4.4B, Figure 4.4.5). Although, the levels of $p21^{Cip1}$ protein displayed a slight increase in C3 cells, this was not related to senescence arrest, as early passage proliferating C3 cells also displayed this slight increase (Figure 4.4.5A). The early loss of hTERT expression in this clone could contribute to early $p21^{Cip1}$ up-regulation, since hTERT is known to down regulate $p21^{Cip1}$ promoter activity (Young JI. et al., 2003). p53, $p16^{INK4a}$, $p14^{ARF}$ and $p21^{Cip1}$ form a group of replicative senescence-related cell cycle checkpoint genes. The lack of induction of these genes in senescence-arrested C3 cells clearly indicated that, there were additional genes involved in senescence arrest in these tumor-derived cells.

The loss of hTERT expression in senescence programmed clones prompted us to analyze the expression of genes that have been implicated in hTERT regulation. Among seven candidate genes studied, only one, the SIP1 gene displayed a differential expression between immortal and senescence-programmed clones. This gene has been identified by Lin and Elledge (Lin SY. and Elledge SJ., 2003) as a mediator of TGF-β-regulated repression of hTERT expression in a breast cancer cell line, although it was not effective in an osteosarcoma cell line. In our studies, SIP1 was not expressed in immortal hTERT-expressing C1 clone, but expressed in senescence-programmed hTERT-repressed C3 and G12 clones (Figures 4.4.6C, 4.4.6D). Experimental depletion of SIP1 transcripts in senescence-programmed C3 cells resulted in hTERT upregulation (Figure 4.4.9A). Thus, SIP1 gene acts as an hTERT repressor in HCC cells. More importantly, we also showed the bypass of senescence arrest, following functional inactivation of SIP expression by shRNA in senescence-programmed C3 clonal cells. In contrast to C3 cells transfected with a control plasmid, SIP1 shRNA-treated cells displayed continued proliferation beyond PD ~80 as evidenced by 70% BrdU incorporation index (Figure 4.4.9B), and formation of a large number of colonies (Figure 4.4.9C). Selected shRNA-transfected clones from these experiments have already performed more than 15 PD beyond the senescence barrier. Thus, our findings indicate, for the first time that the

functional inactivation of SIP1 in senescence-programmed cancer cells is sufficient to bypass senescent arrest.

When we overexpressed mouse SIP1 in Hep3B cell line (with *p53* gene deleted), telomerase activity was partially repressed, and telomere lengths was shortened as a result of hTERT expression down-regulation (Figures 4.14, 4.15, 4.16) However, when these Hep3B clones were passaged extensively, they started to repress the expression of mouse SIP1, which is accompanied by restoration of both telomerase activity and telomere lengths (Figures 4.4.16, 4.4.17 and 4.4.18A). We checked the expression of E-cadherin in Hep3B cells as SIP1 reporter as suggested by others (Comijn J. et al., 2001). And found that repression of E-cadherin was released at late passages (Figure 4.18B). This data indicated that Hep3B cells escaped mouse SIP1 induced senescence program by repressing exogenous SIP1 expression.

SIP1 is a zinc finger and homeodomain containing transcription factor that exerts a repressive activity by binding to CACCT sequences in regulatory elements of target genes (Remacle JE. et al., 1999; Verschueren K. et al., 1999). The SIP1 gene is expressed at high levels in almost all human somatic tissues tested, including liver (Cacheux V. et al., 2001). Therefore, we also performed comparative analysis of hTERT and SIP1 expression in non tumor liver and primary HCC tissues. SIP1 was strongly positive in non-tumor liver samples, but its expression was significantly decreased in corresponding HCC samples. Inversely, hTERT expression was negative or low in non tumor liver samples, but highly positive in HCC tumors (Figure 4.4.6E). We also detected complete loss of SIP1 expression in 5/14 (36%) of HCC cell lines (Figure 4.4.13). Although there was no mutation in SIP1 gene, it is highly likely that SIP1 expression is altered in these cell lines by alternative mechanisms such as promoter methylation (Acun T., Yakicier C, and Ozturk M., unpublished data). Taken together with in vitro studies, these observations strongly suggest that SIP1 acts as a tumor suppressor gene in HCC. Although the SIP1, as a repressor of E-cadherin promoter, has been suggested to be a promoter of invasion in malignant epithelial tumors (Comijn J. et al., 2001), a tumor suppressive activity by the repression of hTERT and inhibition of senescence arrest can not be precluded.

Telomere shortening and senescence play a major role in liver cirrhosis which eventually gives rise to HCC associated with high rate of telomerase reactivation (Satyanarayana A. et al., 2004). Furthermore, p53 and $p16^{INK4a}$ are the most frequently inactivated genes in HCC, one of the most common cancers worldwide, with limited therapeutic options (Thorgeirsson SS. and Grisham JW., 2002; Bruix J. et al., 2004). This enhances the importance of our findings for potential therapeutic applications of replicative senescence programming in HCC. Additionally, isolation of two sub-populations from well-differentiated Huh7 cells, and the constitutive activity of canonical Wnt signaling in well-differentiated cells indicates that well-differentiated HCC cells may have a stem-like cell properties, as suggested by Erdal E. et al. (Erdal E. et al. unpublished data; see sections 5.1.1 and 4.1).

Overall, our study showed that heterogeneity exists even in established HCC cell lines.

CHAPTER 6. FUTURE PERSPECTIVES

Our work has opened new avenues to explain the heterogeneity of HCC. The follow-up experimental strategy will be explained for each item separately.

1) Dual role of canonical Wnt signaling in HCC: Mutant β-catenin has significant activity in well-differentiated HCC cells while does not have or have little activity in poorly-differentiated HCC cells. Since the accumulation of mutant β-catenin was higher in poorly-differentiated cells compared to well-differentiated ones, the difference at the activity should be explained at β-catenin itself or the down-stream of β-catenin. It is possible that mutant β-catenin is subjected to different chemical modification in poorly-differentiated cells, rendering overexpressed β-catenin transcriptionally inactive. APC is a nuclear–cytoplasmic shuttling protein that can export nuclear β-catenin to the cytoplasm for degradation. It has been shown that Pin1 regulates β-catenin turnover and subcellular localization by interfering with its interaction with APC (Ryo A. et al., 2001). This indicates that Pin1 should be considered to see if they contribute to differentiation-dependent canonical Wnt activity in HCC cells.

Even though, β-catenin can translocates into nucleus, it may still be transcriptionally inactive since inhibitory factors such as Groucho, ICAT, Chibby, CtBP, might be overexpressed in poorly-differentiated HCC cells. Expression analysis of these negative regulators in HCC cell should be performed. We could not explain the differential TCF/LEF reporter activity with TCF/LEF family of transcription factors since they were expressed in all HCC cells (Benhaj K. et al., unpublished data). However, this analysis did not include the dominant negative TCF forms. Since dominant negative TCF forms prevent β-catenin-TCF transcriptional activity, these forms should be analyzed in further studies. As we have shown that C/EBPα inhibits β-catenin-TCF reporter activity in HCC cells, the basal C/EBPα activity should be measured in HCC cells in order to see if C/EBPα functions as a negative regulator of canonical Wnt signaling in poorly-

differentiated HCC cells. On the other hand, Wnt5a and Wnt5b (functioning in non-canonical Wnt signaling) are overexpressed in poorly-differentiated HCC cells, and noncanonical Wnt signaling can inhibit canonical Wnt signaling. Therefore, Wnt5a and Wnt5b are good candidates to explain this phenomenon. Knock-down of these ligands in poorly-differentiated cells by siRNA technology, or treatments of well-differentiated cells with Wnt5a- or Wnt5b-conditioned medium are alternative strategies to follow. There is still possibility that all partners of β-catenin in nucleus do not affect the activity but an unidentified molecular alteration of β-catenin may render it inactive. Co-immunoprecipitation of tagged β-catenin with TCF from poorly-differentiated HCC cells may reveal if they are making complexes. Additionally, β-catenin can convert Pitx2 from a transcriptional repressor into an activator (Kioussi C. et al., 2002), similar to its interaction with LEF1/TCF. Therefore, Pitx2 should be considered for further study.

2) Monoclonal anti-β-catenin antibody study: We have characterized the epitopes of our two monoclonal antibodies (9E10 and 4C9), and have shown that 4C9 do not react with membrane-associated β-catenin. These antibodies should be tested with confocal microscopy to confirm our preliminary results. Any chemical modification at corresponding epitopes may change immunoreactivity. Therefore, all possible chemical modifications should be addressed. Tissue samples should be screened to find out if these antibodies differentiate aberrantly accumulated β-catenin pools.

3) Inhibition of mutant β-catenin-TCF transcriptional activity by C/EBPα: Since C/EBPα is a potent inhibitor of cell proliferation, it is necessary to work with inducible stable cell lines over expressing C/EBPα. The use of inducible of C/EBPα in a mutant β-catenin expression cell lines, such as HepG2, and analysis of canonical Wnt signaling target genes are necessary for confirmation of our findings in vivo. Immunohistochemical analysis for β-catenin localization or immunoblot analysis for β-catenin protein levels in C/EBPα expressing cells would be the first step to explain the mechanism of C/EBPα mediated canonical Wnt signaling inhibition in HCC cells. Additionally, our inducible C/EBPα overexpressing Huh7 (*CEBPA* gene is WT in this cell line) cells could be used

to study the target genes of C/EBPα by microarray technology. This inducible system should be analyzed for C/EBPα effects on HCC cell phenotype for properties such as cell proliferation rate, soft-agar growth assay, and tumorigenicity in nude mice.

4) Replicative senescence in HCC-derived cell lines: Microarray analysis for differentially expressed genes in our immortal, early and late senescent clones is immediate work to be done. Differentially expressed genes between immortal and early mortal clones can be used to extract the regulatory networks involved in the reversal of immortality and the initiation of replicative senescence program. On the other hand, differentially expressed genes between early and late mortal clones may be used to extract the regulatory networks functioning in the execution of senescence program. In order to identify the genes responsible for tissue-specific senescence, our gene list should be compared to the one involved in replicative senescence of fibroblasts. Since telomere shortening and senescence are proposed as general markers of human liver cirrhosis, microarray data should be explored in order to find candidate genes involved in liver cirrhosis program. Further genetic and functional analysis of selected genes may identify the regulatory networks and genes involved in replicative senescence and human liver cirrhosis.

REFERENCES

Ai W, Toussaint E, Roman A. 1999. CCAAT displacement protein binds to and negatively regulates human papillomavirus type 6 E6, E7, and E1 promoters. *Journal of virology* 73:4220-9

Antes TJ, Chen J, Cooper AD, Levy-Wilson B. 2000. The nuclear matrix protein CDP represses hepatic transcription of the human cholesterol-7alpha hydroxylase gene. *The Journal of biological chemistry* 275:26649-60

Antonson P, Xanthopoulos KG. 1995. Molecular cloning, sequence, and expression patterns of the human gene encoding CCAAT/enhancer binding protein alpha (C/EBP alpha). *Biochemical and biophysical research communications* 215:106-13

Arizmendi C, Liu S, Croniger C, Poli V, Friedman JE. 1999. The transcription factor CCAAT/enhancer-binding protein beta regulates gluconeogenesis and phosphoenolpyruvate carboxykinase (GTP) gene transcription during diabetes. *The Journal of biological chemistry* 274:13033-40

Bafico A, Liu G, Goldin L, Harris V, Aaronson SA. 2004. An autocrine mechanism for constitutive Wnt pathway activation in human cancer cells. *Cancer cell* 6:497-506

Bailey MA, Brunt EM. 2002. Hepatocellular carcinoma: predisposing conditions and precursor lesions. *Gastroenterology clinics of North America* 31:641-62

Barberis A, Superti-Furga G, Busslinger M. 1987. Mutually exclusive interaction of the CCAAT-binding factor and of a displacement protein with overlapping sequences of a histone gene promoter. *Cell* 50:347-59

Barbin A, Froment O, Boivin S, Marion MJ, Belpoggi F, et al. 1997. p53 gene mutation pattern in rat liver tumors induced by vinyl chloride. *Cancer research* 57:1695-8

Barker N, Hurlstone A, Musisi H, Miles A, Bienz M, Clevers H. 2001. The chromatin remodelling factor Brg-1 interacts with beta-catenin to promote target gene activation. *The EMBO journal* 20:4935-43

Bechter OE, Zou Y, Shay JW, Wright WE. 2003. Homologous recombination in human telomerase-positive and ALT cells occurs with the same frequency. *EMBO reports* 4:1138-43

Becker SA, Lee TH, Butel JS, Slagle BL. 1998. Hepatitis B virus X protein interferes with cellular DNA repair. *Journal of virology* 72:266-72

Bejsovec A. 2005. Wnt pathway activation: new relations and locations. *Cell* 120:11-4

Benhaj K. 2006. *Wnt/β-Catenin signaling pathway activation in epithelial cancers*. PhD. Thesis. Bilkent University, Ankara

Benhamouche S, Decaens T, Godard C, Chambrey R, Rickman DS, et al. 2006. Apc tumor suppressor gene is the "zonation-keeper" of mouse liver. *Developmental cell* 10:759-70

Benn J, Schneider RJ. 1994. Hepatitis B virus HBx protein activates Ras-GTP complex formation

and establishes a Ras, Raf, MAP kinase signaling cascade. *Proceedings of the National Academy of Sciences of the United States of America* 91:10350-4

Ben-Porath I, Weinberg RA. 2004. When cells get stressed: an integrative view of cellular senescence. *The Journal of clinical investigation* 113:8-13

Ben-Porath I, Weinberg RA. 2005. The signals and pathways activating cellular senescence. *The international journal of biochemistry & cell biology* 37:961-76

Berg T, Didon L, Nord M. 2006. Ectopic expression of C/EBP{alpha} in the lung epithelium disrupts late lung development. *Am J Physiol Lung Cell Mol Physiol*

Bhanot P, Brink M, Samos CH, Hsieh JC, Wang Y, et al. 1996. A new member of the frizzled family from Drosophila functions as a Wingless receptor. *Nature* 382:225-30

Birnboim HC, Doly J. 1979. A rapid alkaline extraction procedure for screening recombinant plasmid DNA. *Nucleic acids research* 7:1513-23

Blackburn EH. 1991. Structure and function of telomeres. *Nature* 350:569-73

Bodnar AG, Ouellette M, Frolkis M, Holt SE, Chiu CP, et al. 1998. Extension of life-span by introduction of telomerase into normal human cells. *Science* 279:349-52

Boehm JS, Hahn WC. 2005. Understanding transformation: progress and gaps. *Current opinion in genetics & development* 15:13-7

Bond JA, Blaydes JP, Rowson J, Haughton MF, Smith JR, et al. 1995. Mutant p53 rescues human diploid cells from senescence without inhibiting the induction of SDI1/WAF1. *Cancer research* 55:2404-9

Bonvini P, An WG, Rosolen A, Nguyen P, Trepel J, et al. 2001. Geldanamycin abrogates ErbB2 association with proteasome-resistant beta-catenin in melanoma cells, increases beta-catenin-E-cadherin association, and decreases beta-catenin-sensitive transcription. *Cancer research* 61:1671-7

Bosch FX, Ribes J, Borras J. 1999. Epidemiology of primary liver cancer. *Seminars in liver disease* 19:271-85

Bosch FX, Ribes J, Cleries R, Diaz M. 2005. Epidemiology of hepatocellular carcinoma. *Clinics in liver disease* 9:191-211, v

Boyden LM, Mao J, Belsky J, Mitzner L, Farhi A, et al. 2002. High bone density due to a mutation in LDL-receptor-related protein 5. *The New England journal of medicine* 346:1513-21

Brannon M, Gomperts M, Sumoy L, Moon RT, Kimelman D. 1997. A beta-catenin/XTcf-3 complex binds to the siamois promoter to regulate dorsal axis specification in Xenopus. *Genes & development* 11:2359-70

Brantjes H, Barker N, van Es J, Clevers H. 2002. TCF: Lady Justice casting the final verdict on the outcome of Wnt signalling. *Biological chemistry* 383:255-61

Bressac B, Galvin KM, Liang TJ, Isselbacher KJ, Wands JR, Ozturk M. 1990. Abnormal structure and expression of p53 gene in human hepatocellular carcinoma. *Proceedings of the*

National Academy of Sciences of the United States of America 87:1973-7

Bressac B, Kew M, Wands J, Ozturk M. 1991. Selective G to T mutations of p53 gene in hepatocellular carcinoma from southern Africa. *Nature* 350:429-31

Brown SD, Twells RC, Hey PJ, Cox RD, Levy ER, et al. 1998. Isolation and characterization of LRP6, a novel member of the low density lipoprotein receptor gene family. *Biochemical and biophysical research communications* 248:879-88

Bruix J, Boix L, Sala M, Llovet JM. 2004. Focus on hepatocellular carcinoma. *Cancer cell* 5:215-9

Bryan TM, Englezou A, Gupta J, Bacchetti S, Reddel RR. 1995. Telomere elongation in immortal human cells without detectable telomerase activity. *The EMBO journal* 14:4240-8

Buendia MA. 2000. Genetics of hepatocellular carcinoma. *Seminars in cancer biology* 10:185-200

Cacheux V, Dastot-Le Moal F, Kaariainen H, Bondurand N, Rintala R, et al. 2001. Loss-of-function mutations in SIP1 Smad interacting protein 1 result in a syndromic Hirschsprung disease. *Human molecular genetics* 10:1503-10

Cadoret A, Ovejero C, Saadi-Kheddouci S, Souil E, Fabre M, et al. 2001. Hepatomegaly in transgenic mice expressing an oncogenic form of beta-catenin. *Cancer research* 61:3245-9

Cagatay T, Ozturk M. 2002. P53 mutation as a source of aberrant beta-catenin accumulation in cancer cells. *Oncogene* 21:7971-80

Calkhoven CF, Bouwman PR, Snippe L, Ab G. 1994. Translation start site multiplicity of the CCAAT/enhancer binding protein alpha mRNA is dictated by a small 5' open reading frame. *Nucleic acids research* 22:5540-7

Calkhoven CF, Muller C, Leutz A. 2000. Translational control of C/EBPalpha and C/EBPbeta isoform expression. *Genes & development* 14:1920-32

Calvisi DF, Factor VM, Loi R, Thorgeirsson SS. 2001. Activation of beta-catenin during hepatocarcinogenesis in transgenic mouse models: relationship to phenotype and tumor grade. *Cancer research* 61:2085-91

Campisi J. 2005. Senescent cells, tumor suppression, and organismal aging: good citizens, bad neighbors. *Cell* 120:513-22

Cao Z, Umek RM, McKnight SL. 1991. Regulated expression of three C/EBP isoforms during adipose conversion of 3T3-L1 cells. *Genes & development* 5:1538-52

Caselmann WH. 1996. Trans-activation of cellular genes by hepatitis B virus proteins: a possible mechanism of hepatocarcinogenesis. *Advances in virus research* 47:253-302

Caselmann WH, Meyer M, Kekule AS, Lauer U, Hofschneider PH, Koshy R. 1990. A trans-activator function is generated by integration of hepatitis B virus preS/S sequences in human hepatocellular carcinoma DNA. *Proceedings of the National Academy of Sciences of the United States of America* 87:2970-4

Cavallo RA, Cox RT, Moline MM, Roose J, Polevoy GA, et al. 1998. Drosophila Tcf and Groucho

interact to repress Wingless signalling activity. *Nature* 395:604-8

Cha MY, Kim CM, Park YM, Ryu WS. 2004. Hepatitis B virus X protein is essential for the activation of Wnt/beta-catenin signaling in hepatoma cells. *Hepatology (Baltimore, Md* 39:1683-93

Chen G, Fernandez J, Mische S, Courey AJ. 1999. A functional interaction between the histone deacetylase Rpd3 and the corepressor groucho in Drosophila development. *Genes & development* 13:2218-30

Chen W, ten Berge D, Brown J, Ahn S, Hu LA, et al. 2003. Dishevelled 2 recruits beta-arrestin 2 to mediate Wnt5A-stimulated endocytosis of Frizzled 4. *Science* 301:1391-4

Christodoulides C, Scarda A, Granzotto M, Milan G, Dalla Nora E, et al. 2006. WNT10B mutations in human obesity. *Diabetologia* 49:678-84

Ciechanover A. 1998. The ubiquitin-proteasome pathway: on protein death and cell life. *The EMBO journal* 17:7151-60

Colgrove R, Simon G, Ganem D. 1989. Transcriptional activation of homologous and heterologous genes by the hepatitis B virus X gene product in cells permissive for viral replication. *Journal of virology* 63:4019-26

Comijn J, Berx G, Vermassen P, Verschueren K, van Grunsven L, et al. 2001. The two-handed E box binding zinc finger protein SIP1 downregulates E-cadherin and induces invasion. *Molecular cell* 7:1267-78

Costa RH, Kalinichenko VV, Holterman AX, Wang X. 2003. Transcription factors in liver development, differentiation, and regeneration. *Hepatology (Baltimore, Md* 38:1331-47

Crosson SM, Davies GF, Roesler WJ. 1997. Hepatic expression of CCAAT/enhancer binding protein alpha: hormonal and metabolic regulation in rats. *Diabetologia* 40:1117-24

D'Amico M, Hulit J, Amanatullah DF, Zafonte BT, Albanese C, et al. 2000. The integrin-linked kinase regulates the cyclin D1 gene through glycogen synthase kinase 3beta and cAMP-responsive element-binding protein-dependent pathways. *The Journal of biological chemistry* 275:32649-57

Daniels DL, Weis WI. 2002. ICAT inhibits beta-catenin binding to Tcf/Lef-family transcription factors and the general coactivator p300 using independent structural modules. *Molecular cell* 10:573-84

d'Arville CN, Nouri-Aria KT, Johnson P, Williams R. 1991. Regulation of insulin-like growth factor II gene expression by hepatitis B virus in hepatocellular carcinoma. *Hepatology (Baltimore, Md* 13:310-5

de La Coste A, Romagnolo B, Billuart P, Renard CA, Buendia MA, et al. 1998. Somatic mutations of the beta-catenin gene are frequent in mouse and human hepatocellular carcinomas. *Proceedings of the National Academy of Sciences of the United States of America* 95:8847-51

de Lange T. 2004. T-loops and the origin of telomeres. *Nat Rev Mol Cell Biol* 5:323-9

De Souza AT, Hankins GR, Washington MK, Fine RL, Orton TC, Jirtle RL. 1995. Frequent loss of heterozygosity on 6q at the mannose 6-phosphate/insulin-like growth factor II receptor locus in human hepatocellular tumors. *Oncogene* 10:1725-9

De Souza AT, Hankins GR, Washington MK, Orton TC, Jirtle RL. 1995. M6P/IGF2R gene is mutated in human hepatocellular carcinomas with loss of heterozygosity. *Nature genetics* 11:447-9

Deane NG, Parker MA, Aramandla R, Diehl L, Lee WJ, et al. 2001. Hepatocellular carcinoma results from chronic cyclin D1 overexpression in transgenic mice. *Cancer research* 61:5389-95

Deng C, Zhang P, Harper JW, Elledge SJ, Leder P. 1995. Mice lacking p21CIP1/WAF1 undergo normal development, but are defective in G1 checkpoint control. *Cell* 82:675-84

Desbois-Mouthon C, Cadoret A, Blivet-Van Eggelpoel MJ, Bertrand F, Cherqui G, et al. 2001. Insulin and IGF-1 stimulate the beta-catenin pathway through two signalling cascades involving GSK-3beta inhibition and Ras activation. *Oncogene* 20:252-9

Devereux TR, Stern MC, Flake GP, Yu MC, Zhang ZQ, et al. 2001. CTNNB1 mutations and beta-catenin protein accumulation in human hepatocellular carcinomas associated with high exposure to aflatoxin B1. *Molecular carcinogenesis* 31:68-73

Dickson MA, Hahn WC, Ino Y, Ronfard V, Wu JY, et al. 2000. Human keratinocytes that express hTERT and also bypass a p16(INK4a)-enforced mechanism that limits life span become immortal yet retain normal growth and differentiation characteristics. *Molecular and cellular biology* 20:1436-47

Diehl AM, Johns DC, Yang S, Lin H, Yin M, et al. 1996. Adenovirus-mediated transfer of CCAAT/enhancer-binding protein-alpha identifies a dominant antiproliferative role for this isoform in hepatocytes. *The Journal of biological chemistry* 271:7343-50

Dimri GP. 2005. What has senescence got to do with cancer? *Cancer cell* 7:505-12

Dimri GP, Lee X, Basile G, Acosta M, Scott G, et al. 1995. A biomarker that identifies senescent human cells in culture and in aging skin in vivo. *Proceedings of the National Academy of Sciences of the United States of America* 92:9363-7

Ding Q, Xia W, Liu JC, Yang JY, Lee DF, et al. 2005. Erk associates with and primes GSK-3beta for its inactivation resulting in upregulation of beta-catenin. *Molecular cell* 19:159-70

Dobrosotskaya IY, James GL. 2000. MAGI-1 interacts with beta-catenin and is associated with cell-cell adhesion structures. *Biochemical and biophysical research communications* 270:903-9

Ducrest AL, Szutorisz H, Lingner J, Nabholz M. 2002. Regulation of the human telomerase reverse transcriptase gene. *Oncogene* 21:541-52

Duncan SA. 2000. Transcriptional regulation of liver development. *Dev Dyn* 219:131-42

Duval A, Rolland S, Tubacher E, Bui H, Thomas G, Hamelin R. 2000. The human T-cell transcription factor-4 gene: structure, extensive characterization of alternative splicings, and mutational analysis in colorectal cancer cell lines. *Cancer research* 60:3872-9

Eger A, Stockinger A, Park J, Langkopf E, Mikula M, et al. 2004. beta-Catenin and TGFbeta signalling cooperate to maintain a mesenchymal phenotype after FosER-induced epithelial to mesenchymal transition. *Oncogene* 23:2672-80

Enomoto A, Esumi M, Yamashita K, Takagi K, Takano S, Iwai S. 2001. Abnormal nucleotide repeat sequence in the TGF-betaRII gene in hepatocellular carcinoma and in uninvolved liver tissue. *The Journal of pathology* 195:349-54

Erdal E, Ozturk N, Cagatay T, Eksioglu-Demiralp E, Ozturk M. 2005. Lithium-mediated downregulation of PKB/Akt and cyclin E with growth inhibition in hepatocellular carcinoma cells. *International journal of cancer* 115:903-10

Farber E. 1996. Alcohol and other chemicals in the development of hepatocellular carcinoma. *Clinics in laboratory medicine* 16:377-94

Fargion S, Mandelli C, Piperno A, Cesana B, Fracanzani AL, et al. 1992. Survival and prognostic factors in 212 Italian patients with genetic hemochromatosis. *Hepatology (Baltimore, Md* 15:655-9

Fausto N. 1994. Liver stem cells in the liver biology and pathobiology. ed. Iea Arias, pp. 1501-18 New York: Raven Press

Fearon ER, Vogelstein B. 1990. A genetic model for colorectal tumorigenesis. *Cell* 61:759-67

Feitelson MA. 1999. Hepatitis B virus in hepatocarcinogenesis. *Journal of cellular physiology* 181:188-202

Feitelson MA, Sun B, Satiroglu Tufan NL, Liu J, Pan J, Lian Z. 2002. Genetic mechanisms of hepatocarcinogenesis. *Oncogene* 21:2593-604

Flodby P, Barlow C, Kylefjord H, Ahrlund-Richter L, Xanthopoulos KG. 1996. Increased hepatic cell proliferation and lung abnormalities in mice deficient in CCAAT/enhancer binding protein alpha. *The Journal of biological chemistry* 271:24753-60

Floreani A, Baragiotta A, Baldo V, Menegon T, Farinati F, Naccarato R. 1999. Hepatic and extrahepatic malignancies in primary biliary cirrhosis. *Hepatology (Baltimore, Md* 29:1425-8

Fujito T, Sasaki Y, Iwao K, Miyoshi Y, Yamada T, et al. 2004. Prognostic significance of beta-catenin nuclear expression in hepatocellular carcinoma. *Hepato-gastroenterology* 51:921-4

Fukutomi T, Zhou Y, Kawai S, Eguchi H, Wands JR, Li J. 2005. Hepatitis C virus core protein stimulates hepatocyte growth: correlation with upregulation of wnt-1 expression. *Hepatology (Baltimore, Md* 41:1096-105

Furuya K, Nakamura M, Yamamoto Y, Togei K, Otsuka H. 1988. Macroregenerative nodule of the

liver. A clinicopathologic study of 345 autopsy cases of chronic liver disease. *Cancer* 61:99-105

Ghosh AK, Steele R, Meyer K, Ray R, Ray RB. 1999. Hepatitis C virus NS5A protein modulates cell cycle regulatory genes and promotes cell growth. *The Journal of general virology* 80 (Pt 5):1179-83

Giles RH, van Es JH, Clevers H. 2003. Caught up in a Wnt storm: Wnt signaling in cancer. *Biochimica et biophysica acta* 1653:1-24

Gong Y, Slee RB, Fukai N, Rawadi G, Roman-Roman S, et al. 2001. LDL receptor-related protein 5 (LRP5) affects bone accrual and eye development. *Cell* 107:513-23

Graham NA, Asthagiri AR. 2004. Epidermal growth factor-mediated T-cell factor/lymphoid enhancer factor transcriptional activity is essential but not sufficient for cell cycle progression in nontransformed mammary epithelial cells. *The Journal of biological chemistry* 279:23517-24

Graham TA, Clements WK, Kimelman D, Xu W. 2002. The crystal structure of the beta-catenin/ICAT complex reveals the inhibitory mechanism of ICAT. *Molecular cell* 10:563-71

Greenbaum LE. 2004. Cell cycle regulation and hepatocarcinogenesis. *Cancer biology & therapy* 3:1200-7

Gregorieff A, Clevers H. 2005. Wnt signaling in the intestinal epithelium: from endoderm to cancer. *Genes & development* 19:877-90

Grisham J, ed. 2001. *Molecular Basis of Human Cancer*. Totawa, New Jersey: Humana Press. 269-346 pp.

Halmos B, Huettner CS, Kocher O, Ferenczi K, Karp DD, Tenen DG. 2002. Down-regulation and antiproliferative role of C/EBPalpha in lung cancer. *Cancer research* 62:528-34

Hann HW, Kim CY, London WT, Blumberg BS. 1989. Increased serum ferritin in chronic liver disease: a risk factor for primary hepatocellular carcinoma. *International journal of cancer* 43:376-9

Harley CB, Futcher AB, Greider CW. 1990. Telomeres shorten during ageing of human fibroblasts. *Nature* 345:458-60

Harris TE, Albrecht JH, Nakanishi M, Darlington GJ. 2001. CCAAT/enhancer-binding protein-alpha cooperates with p21 to inhibit cyclin-dependent kinase-2 activity and induces growth arrest independent of DNA binding. *The Journal of biological chemistry* 276:29200-9

Hart M, Concordet JP, Lassot I, Albert I, del los Santos R, et al. 1999. The F-box protein beta-TrCP associates with phosphorylated beta-catenin and regulates its activity in the cell. *Curr Biol* 9:207-10

Hastie ND, Dempster M, Dunlop MG, Thompson AM, Green DK, Allshire RC. 1990. Telomere

reduction in human colorectal carcinoma and with ageing. *Nature* 346:866-8

Hayashi J, Aoki H, Kajino K, Moriyama M, Arakawa Y, Hino O. 2000. Hepatitis C virus core protein activates the MAPK/ERK cascade synergistically with tumor promoter TPA, but not with epidermal growth factor or transforming growth factor alpha. *Hepatology (Baltimore, Md* 32:958-61

Hayflick L, Moorhead PS. 1961. The serial cultivation of human diploid cell strains. *Experimental cell research* 25:585-621

He X, Semenov M, Tamai K, Zeng X. 2004. LDL receptor-related proteins 5 and 6 in Wnt/beta-catenin signaling: arrows point the way. *Development (Cambridge, England)* 131:1663-77

Hecht A, Vleminckx K, Stemmler MP, van Roy F, Kemler R. 2000. The p300/CBP acetyltransferases function as transcriptional coactivators of beta-catenin in vertebrates. *The EMBO journal* 19:1839-50

Hendricks-Taylor LR, Darlington GJ. 1995. Inhibition of cell proliferation by C/EBP alpha occurs in many cell types, does not require the presence of p53 or Rb, and is not affected by large T-antigen. *Nucleic acids research* 23:4726-33

Hey PJ, Twells RC, Phillips MS, Yusuke N, Brown SD, et al. 1998. Cloning of a novel member of the low-density lipoprotein receptor family. *Gene* 216:103-11

Higashitsuji H, Itoh K, Nagao T, Dawson S, Nonoguchi K, et al. 2000. Reduced stability of retinoblastoma protein by gankyrin, an oncogenic ankyrin-repeat protein overexpressed in hepatomas. *Nature medicine* 6:96-9

Hino O, Tabata S, Hotta Y. 1991. Evidence for increased in vitro recombination with insertion of human hepatitis B virus DNA. *Proceedings of the National Academy of Sciences of the United States of America* 88:9248-52

Hirai H, Roussel MF, Kato JY, Ashmun RA, Sherr CJ. 1995. Novel INK4 proteins, p19 and p18, are specific inhibitors of the cyclin D-dependent kinases CDK4 and CDK6. *Molecular and cellular biology* 15:2672-81

Hsu HC, Jeng YM, Mao TL, Chu JS, Lai PL, Peng SY. 2000. Beta-catenin mutations are associated with a subset of low-stage hepatocellular carcinoma negative for hepatitis B virus and with favorable prognosis. *The American journal of pathology* 157:763-70

Hsu IC, Metcalf RA, Sun T, Welsh JA, Wang NJ, Harris CC. 1991. Mutational hotspot in the p53 gene in human hepatocellular carcinomas. *Nature* 350:427-8

Hsu W, Zeng L, Costantini F. 1999. Identification of a domain of Axin that binds to the serine/threonine protein phosphatase 2A and a self-binding domain. *The Journal of biological chemistry* 274:3439-45

Hung AY, Sheng M. 2002. PDZ domains: structural modules for protein complex assembly. *The Journal of biological chemistry* 277:5699-702

Huo TI, Wang XW, Forgues M, Wu CG, Spillare EA, et al. 2001. Hepatitis B virus X mutants

derived from human hepatocellular carcinoma retain the ability to abrogate p53-induced apoptosis. *Oncogene* 20:3620-8

Hytiroglou P. 2004. Morphological changes of early human hepatocarcinogenesis. *Seminars in liver disease* 24:65-75

Iakova P, Awad SS, Timchenko NA. 2003. Aging reduces proliferative capacities of liver by switching pathways of C/EBPalpha growth arrest. *Cell* 113:495-506

Ilyas M. 2005. Wnt signalling and the mechanistic basis of tumour development. *The Journal of pathology* 205:130-44

Inagawa S, Itabashi M, Adachi S, Kawamoto T, Hori M, et al. 2002. Expression and prognostic roles of beta-catenin in hepatocellular carcinoma: correlation with tumor progression and postoperative survival. *Clin Cancer Res* 8:450-6

Inoue H, Nojima H, Okayama H. 1990. High efficiency transformation of Escherichia coli with plasmids. *Gene* 96:23-8

Ishido S, Hotta H. 1998. Complex formation of the nonstructural protein 3 of hepatitis C virus with the p53 tumor suppressor. *FEBS letters* 438:258-62

Ishitani T, Kishida S, Hyodo-Miura J, Ueno N, Yasuda J, et al. 2003. The TAK1-NLK mitogen-activated protein kinase cascade functions in the Wnt-5a/Ca(2+) pathway to antagonize Wnt/beta-catenin signaling. *Molecular and cellular biology* 23:131-9

Jagadeesh S, Banerjee PP. 2006. Telomerase reverse transcriptase regulates the expression of a key cell cycle regulator, cyclin D1. *Biochemical and biophysical research communications*

Jiang WQ, Zhong ZH, Henson JD, Neumann AA, Chang AC, Reddel RR. 2005. Suppression of alternative lengthening of telomeres by Sp100-mediated sequestration of the MRE11/RAD50/NBS1 complex. *Molecular and cellular biology* 25:2708-21

Johnson PF. 2005. Molecular stop signs: regulation of cell-cycle arrest by C/EBP transcription factors. *Journal of cell science* 118:2545-55

Kaestner KH. 2000. The hepatocyte nuclear factor 3 (HNF3 or FOXA) family in metabolism. *Trends in endocrinology and metabolism: TEM* 11:281-5

Kanazawa A, Tsukada S, Kamiyama M, Yanagimoto T, Nakajima M, Maeda S. 2005. Wnt5b partially inhibits canonical Wnt/beta-catenin signaling pathway and promotes adipogenesis in 3T3-L1 preadipocytes. *Biochemical and biophysical research communications* 330:505-10

Kaneko S, Hallenbeck P, Kotani T, Nakabayashi H, McGarrity G, et al. 1995. Adenovirus-mediated gene therapy of hepatocellular carcinoma using cancer-specific gene expression. *Cancer research* 55:5283-7

Katagiri T, Nakamura Y, Miki Y. 1996. Mutations in the BRCA2 gene in hepatocellular carcinomas. *Cancer research* 56:4575-7

Kawamura N, Nagai H, Bando K, Koyama M, Matsumoto S, et al. 1999. PTEN/MMAC1 mutations in hepatocellular carcinomas: somatic inactivation of both alleles in tumors. *Jpn J Cancer Res* 90:413-8

Kekule AS, Lauer U, Meyer M, Caselmann WH, Hofschneider PH, Koshy R. 1990. The preS2/S region of integrated hepatitis B virus DNA encodes a transcriptional transactivator. *Nature* 343:457-61

Kennell JA, O'Leary EE, Gummow BM, Hammer GD, MacDougald OA. 2003. T-cell factor 4N (TCF-4N), a novel isoform of mouse TCF-4, synergizes with beta-catenin to coactivate C/EBPalpha and steroidogenic factor 1 transcription factors. *Molecular and cellular biology* 23:5366-75

Keydar I, Chen L, Karby S, Weiss FR, Delarea J, et al. 1979. Establishment and characterization of a cell line of human breast carcinoma origin. *Eur J Cancer* 15:659-70

Kicic A, Chua AC, Baker E. 2001. Effect of iron chelators on proliferation and iron uptake in hepatoma cells. *Cancer* 92:3093-110

Kikuchi A, Kishida S, Yamamoto H. 2006. Regulation of Wnt signaling by protein-protein interaction and post-translational modifications. *Experimental & molecular medicine* 38:1-10

Kim SO, Park JG, Lee YI. 1996. Increased expression of the insulin-like growth factor I (IGF-I) receptor gene in hepatocellular carcinoma cell lines: implications of IGF-I receptor gene activation by hepatitis B virus X gene product. *Cancer research* 56:3831-6

Kimura T, Christoffels VM, Chowdhury S, Iwase K, Matsuzaki H, et al. 1998. Hypoglycemia-associated hyperammonemia caused by impaired expression of ornithine cycle enzyme genes in C/EBPalpha knockout mice. *The Journal of biological chemistry* 273:27505-10

Kinzler KW, Nilbert MC, Su LK, Vogelstein B, Bryan TM, et al. 1991. Identification of FAP locus genes from chromosome 5q21. *Science* 253:661-5

Kioussi C, Briata P, Baek SH, Rose DW, Hamblet NS, et al. 2002. Identification of a Wnt/Dvl/beta-Catenin --> Pitx2 pathway mediating cell-type-specific proliferation during development. *Cell* 111:673-85

Kishida M, Hino S, Michiue T, Yamamoto H, Kishida S, et al. 2001. Synergistic activation of the Wnt signaling pathway by Dvl and casein kinase Iepsilon. *The Journal of biological chemistry* 276:33147-55

Kiyono T, Foster SA, Koop JI, McDougall JK, Galloway DA, Klingelhutz AJ. 1998. Both Rb/p16INK4a inactivation and telomerase activity are required to immortalize human epithelial cells. *Nature* 396:84-8

Koch A, Denkhaus D, Albrecht S, Leuschner I, von Schweinitz D, Pietsch T. 1999. Childhood hepatoblastomas frequently carry a mutated degradation targeting box of the beta-catenin gene. *Cancer research* 59:269-73

Kojiro M. 2005. Histopathology of liver cancers. *Best practice & research* 19:39-62

Kondo Y, Kanai Y, Sakamoto M, Mizokami M, Ueda R, Hirohashi S. 1999. Microsatellite instability associated with hepatocarcinogenesis. *Journal of hepatology* 31:529-36

Korinek V, Barker N, Willert K, Molenaar M, Roose J, et al. 1998. Two members of the Tcf family implicated in Wnt/beta-catenin signaling during embryogenesis in the mouse. *Molecular and cellular biology* 18:1248-56

Kovacs KA, Steinmann M, Magistretti PJ, Halfon O, Cardinaux JR. 2003. CCAAT/enhancer-binding protein family members recruit the coactivator CREB-binding protein and trigger its phosphorylation. *The Journal of biological chemistry* 278:36959-65

Kramps T, Peter O, Brunner E, Nellen D, Froesch B, et al. 2002. Wnt/wingless signaling requires BCL9/legless-mediated recruitment of pygopus to the nuclear beta-catenin-TCF complex. *Cell* 109:47-60

Kubicka S, Trautwein C, Niehof M, Manns M. 1997. Target gene modulation in hepatocellular carcinomas by decreased DNA-binding of p53 mutations. *Hepatology (Baltimore, Md* 25:867-73

Kurumiya Y, Nozawa K, Sakaguchi K, Nagino M, Nimura Y, Yoshida S. 2000. Differential suppression of liver-specific genes in regenerating rat liver induced by extended hepatectomy. *Journal of hepatology* 32:636-44

Lammi L, Arte S, Somer M, Jarvinen H, Lahermo P, et al. 2004. Mutations in AXIN2 cause familial tooth agenesis and predispose to colorectal cancer. *American journal of human genetics* 74:1043-50

Landschulz WH, Johnson PF, Adashi EY, Graves BJ, McKnight SL. 1988. Isolation of a recombinant copy of the gene encoding C/EBP. *Genes & development* 2:786-800

Lasfargues EY, Coutinho WG, Redfield ES. 1978. Isolation of two human tumor epithelial cell lines from solid breast carcinomas. *Journal of the National Cancer Institute* 61:967-78

Latres E, Chiaur DS, Pagano M. 1999. The human F box protein beta-Trcp associates with the Cul1/Skp1 complex and regulates the stability of beta-catenin. *Oncogene* 18:849-54

Laurent-Puig P, Legoix P, Bluteau O, Belghiti J, Franco D, et al. 2001. Genetic alterations associated with hepatocellular carcinomas define distinct pathways of hepatocarcinogenesis. *Gastroenterology* 120:1763-73

Lee E, Salic A, Kirschner MW. 2001. Physiological regulation of [beta]-catenin stability by Tcf3 and CK1epsilon. *The Journal of cell biology* 154:983-93

Lee HC, Kim M, Wands JR. 2006. Wnt/Frizzled signaling in hepatocellular carcinoma. *Front Biosci* 11:1901-15

Lee YH, Sauer B, Johnson PF, Gonzalez FJ. 1997. Disruption of the c/ebp alpha gene in adult mouse liver. *Molecular and cellular biology* 17:6014-22

Lee YI, Lee S, Das GC, Park US, Park SM, Lee YI. 2000. Activation of the insulin-like growth

factor II transcription by aflatoxin B1 induced p53 mutant 249 is caused by activation of transcription complexes; implications for a gain-of-function during the formation of hepatocellular carcinoma. *Oncogene* 19:3717-26

Legraverend C, Antonson P, Flodby P, Xanthopoulos KG. 1993. High level activity of the mouse CCAAT/enhancer binding protein (C/EBP alpha) gene promoter involves autoregulation and several ubiquitous transcription factors. *Nucleic acids research* 21:1735-42

Lengauer C, Kinzler KW, Vogelstein B. 1998. Genetic instabilities in human cancers. *Nature* 396:643-9

Libbrecht L, Desmet V, Roskams T. 2005. Preneoplastic lesions in human hepatocarcinogenesis. *Liver Int* 25:16-27

Liew CT, Li HM, Lo KW, Leow CK, Chan JY, et al. 1999. High frequency of p16INK4A gene alterations in hepatocellular carcinoma. *Oncogene* 18:789-95

Lin FT, Lane MD. 1994. CCAAT/enhancer binding protein alpha is sufficient to initiate the 3T3-L1 adipocyte differentiation program. *Proceedings of the National Academy of Sciences of the United States of America* 91:8757-61

Lin FT, MacDougald OA, Diehl AM, Lane MD. 1993. A 30-kDa alternative translation product of the CCAAT/enhancer binding protein alpha message: transcriptional activator lacking antimitotic activity. *Proceedings of the National Academy of Sciences of the United States of America* 90:9606-10

Lin SY, Elledge SJ. 2003. Multiple tumor suppressor pathways negatively regulate telomerase. *Cell* 113:881-9

Little RD, Carulli JP, Del Mastro RG, Dupuis J, Osborne M, et al. 2002. A mutation in the LDL receptor-related protein 5 gene results in the autosomal dominant high-bone-mass trait. *American journal of human genetics* 70:11-9

Liu G, Bafico A, Harris VK, Aaronson SA. 2003. A novel mechanism for Wnt activation of canonical signaling through the LRP6 receptor. *Molecular and cellular biology* 23:5825-35

Liu J, Stevens J, Rote CA, Yost HJ, Hu Y, et al. 2001. Siah-1 mediates a novel beta-catenin degradation pathway linking p53 to the adenomatous polyposis coli protein. *Molecular cell* 7:927-36

Liu P, Wakamiya M, Shea MJ, Albrecht U, Behringer RR, Bradley A. 1999. Requirement for Wnt3 in vertebrate axis formation. *Nature genetics* 22:361-5

Livezey KW, Simon D. 1997. Accumulation of genetic alterations in a human hepatoma cell line transfected with hepatitis B virus. *Mutation research* 377:187-98

Llovet JM, Burroughs A, Bruix J. 2003. Hepatocellular carcinoma. *Lancet* 362:1907-17

Logan CY, Nusse R. 2004. The Wnt signaling pathway in development and disease. *Annual review of cell and developmental biology* 20:781-810

Lucito R, Schneider RJ. 1992. Hepatitis B virus X protein activates transcription factor NF-kappa

B without a requirement for protein kinase C. *Journal of virology* 66:983-91

Lundberg AS, Hahn WC, Gupta P, Weinberg RA. 2000. Genes involved in senescence and immortalization. *Current opinion in cell biology* 12:705-9

Ma DZ, Xu Z, Liang YL, Su JM, Li ZX, et al. 2005. Down-regulation of PTEN expression due to loss of promoter activity in human hepatocellular carcinoma cell lines. *World J Gastroenterol* 11:4472-7

Majumder M, Ghosh AK, Steele R, Ray R, Ray RB. 2001. Hepatitis C virus NS5A physically associates with p53 and regulates p21/waf1 gene expression in a p53-dependent manner. *Journal of virology* 75:1401-7

Mao B, Niehrs C. 2003. Kremen2 modulates Dickkopf2 activity during Wnt/LRP6 signaling. *Gene* 302:179-83

Mao J, Wang J, Liu B, Pan W, Farr GH, 3rd, et al. 2001. Low-density lipoprotein receptor-related protein-5 binds to Axin and regulates the canonical Wnt signaling pathway. *Molecular cell* 7:801-9

Mao TL, Chu JS, Jeng YM, Lai PL, Hsu HC. 2001. Expression of mutant nuclear beta-catenin correlates with non-invasive hepatocellular carcinoma, absence of portal vein spread, and good prognosis. *The Journal of pathology* 193:95-101

Masutomi K, Yu EY, Khurts S, Ben-Porath I, Currier JL, et al. 2003. Telomerase maintains telomere structure in normal human cells. *Cell* 114:241-53

McCrea PD, Turck CW, Gumbiner B. 1991. A homolog of the armadillo protein in Drosophila (plakoglobin) associated with E-cadherin. *Science* 254:1359-61

McKillop IH, Schrum LW. 2005. Alcohol and liver cancer. *Alcohol (Fayetteville, N.Y* 35:195-203

Megason SG, McMahon AP. 2002. A mitogen gradient of dorsal midline Wnts organizes growth in the CNS. *Development (Cambridge, England)* 129:2087-98

Melkonyan HS, Chang WC, Shapiro JP, Mahadevappa M, Fitzpatrick PA, et al. 1997. SARPs: a family of secreted apoptosis-related proteins. *Proceedings of the National Academy of Sciences of the United States of America* 94:13636-41

Mischoulon D, Rana B, Bucher NL, Farmer SR. 1992. Growth-dependent inhibition of CCAAT enhancer-binding protein (C/EBP alpha) gene expression during hepatocyte proliferation in the regenerating liver and in culture. *Molecular and cellular biology* 12:2553-60

Miyoshi Y, Iwao K, Nagasawa Y, Aihara T, Sasaki Y, et al. 1998. Activation of the beta-catenin gene in primary hepatocellular carcinomas by somatic alterations involving exon 3. *Cancer research* 58:2524-7

Molenaar M, van de Wetering M, Oosterwegel M, Peterson-Maduro J, Godsave S, et al. 1996. XTcf-3 transcription factor mediates beta-catenin-induced axis formation in Xenopus embryos. *Cell* 86:391-9

Morali OG, Delmas V, Moore R, Jeanney C, Thiery JP, Larue L. 2001. IGF-II induces rapid beta-

catenin relocation to the nucleus during epithelium to mesenchyme transition. *Oncogene* 20:4942-50

Morin PJ, Sparks AB, Korinek V, Barker N, Clevers H, et al. 1997. Activation of beta-catenin-Tcf signaling in colon cancer by mutations in beta-catenin or APC. *Science* 275:1787-90

Morrison JA, Klingelhutz AJ, Raab-Traub N. 2003. Epstein-Barr virus latent membrane protein 2A activates beta-catenin signaling in epithelial cells. *Journal of virology* 77:12276-84

Mukai F, Ishiguro K, Sano Y, Fujita SC. 2002. Alternative splicing isoform of tau protein kinase I/glycogen synthase kinase 3beta. *Journal of neurochemistry* 81:1073-83

Muller C, Alunni-Fabbroni M, Kowenz-Leutz E, Mo X, Tommasino M, Leutz A. 1999. Separation of C/EBPalpha-mediated proliferation arrest and differentiation pathways. *Proceedings of the National Academy of Sciences of the United States of America* 96:7276-81

Nakabayashi H, Taketa K, Miyano K, Yamane T, Sato J. 1982. Growth of human hepatoma cells lines with differentiated functions in chemically defined medium. *Cancer research* 42:3858-63

Nakagawa H, Murata Y, Koyama K, Fujiyama A, Miyoshi Y, et al. 1998. Identification of a brain-specific APC homologue, APCL, and its interaction with beta-catenin. *Cancer research* 58:5176-81

Nelson WJ, Nusse R. 2004. Convergence of Wnt, beta-catenin, and cadherin pathways. *Science* 303:1483-7

Nerlov C. 2004. C/EBPalpha mutations in acute myeloid leukaemias. *Nature reviews* 4:394-400

Nerlov C, Ziff EB. 1995. CCAAT/enhancer binding protein-alpha amino acid motifs with dual TBP and TFIIB binding ability co-operate to activate transcription in both yeast and mammalian cells. *The EMBO journal* 14:4318-28

Neufeld KL, Nix DA, Bogerd H, Kang Y, Beckerle MC, et al. 2000. Adenomatous polyposis coli protein contains two nuclear export signals and shuttles between the nucleus and cytoplasm. *Proceedings of the National Academy of Sciences of the United States of America* 97:12085-90

Neufeld KL, Zhang F, Cullen BR, White RL. 2000. APC-mediated downregulation of beta-catenin activity involves nuclear sequestration and nuclear export. *EMBO reports* 1:519-23

Niemann S, Zhao C, Pascu F, Stahl U, Aulepp U, et al. 2004. Homozygous WNT3 mutation causes tetra-amelia in a large consanguineous family. *American journal of human genetics* 74:558-63

Noda A, Ning Y, Venable SF, Pereira-Smith OM, Smith JR. 1994. Cloning of senescent cell-derived inhibitors of DNA synthesis using an expression screen. *Experimental cell research* 211:90-8

Novak A, Hsu SC, Leung-Hagesteijn C, Radeva G, Papkoff J, et al. 1998. Cell adhesion and the integrin-linked kinase regulate the LEF-1 and beta-catenin signaling pathways.

Proceedings of the National Academy of Sciences of the United States of America 95:4374-9

Nusse R. 2005. Cell biology: relays at the membrane. *Nature* 438:747-9

Nusse R, Varmus HE. 1982. Many tumors induced by the mouse mammary tumor virus contain a provirus integrated in the same region of the host genome. *Cell* 31:99-109

Oda T, Tsuda H, Scarpa A, Sakamoto M, Hirohashi S. 1992. p53 gene mutation spectrum in hepatocellular carcinoma. *Cancer research* 52:6358-64

Oka Y, Waterland RA, Killian JK, Nolan CM, Jang HS, et al. 2002. M6P/IGF2R tumor suppressor gene mutated in hepatocellular carcinomas in Japan. *Hepatology (Baltimore, Md* 35:1153-63

Osada S, Yamamoto H, Nishihara T, Imagawa M. 1996. DNA binding specificity of the CCAAT/enhancer-binding protein transcription factor family. *The Journal of biological chemistry* 271:3891-6

Ossipow V, Descombes P, Schibler U. 1993. CCAAT/enhancer-binding protein mRNA is translated into multiple proteins with different transcription activation potentials. *Proceedings of the National Academy of Sciences of the United States of America* 90:8219-23

Ozawa M, Baribault H, Kemler R. 1989. The cytoplasmic domain of the cell adhesion molecule uvomorulin associates with three independent proteins structurally related in different species. *The EMBO journal* 8:1711-7

Ozturk M. 1999. Genetic aspects of hepatocellular carcinogenesis. *Seminars in liver disease* 19:235-42

Ozturk N. 2000. *Production of recombinant human beta-catenin protein in E.coli and screening for anti-beta-catenin autoantibodies in cancer sera*. MSc. Thesis. Bilkent University, Ankara

Pabst T, Mueller BU, Harakawa N, Schoch C, Haferlach T, et al. 2001. AML1-ETO downregulates the granulocytic differentiation factor C/EBPalpha in t(8;21) myeloid leukemia. *Nature medicine* 7:444-51

Pantoja C, Serrano M. 1999. Murine fibroblasts lacking p21 undergo senescence and are resistant to transformation by oncogenic Ras. *Oncogene* 18:4974-82

Paradis V, Youssef N, Dargere D, Ba N, Bonvoust F, et al. 2001. Replicative senescence in normal liver, chronic hepatitis C, and hepatocellular carcinomas. *Human pathology* 32:327-32

Park JI, Kim SW, Lyons JP, Ji H, Nguyen TT, et al. 2005. Kaiso/p120-catenin and TCF/beta-catenin complexes coordinately regulate canonical Wnt gene targets. *Developmental cell* 8:843-54

Park YN, Chae KJ, Oh BK, Choi J, Choi KS, Park C. 2004. Expression of Smad7 in hepatocellular carcinoma and dysplastic nodules: resistance mechanism to transforming

growth factor-beta. *Hepato-gastroenterology* 51:396-400

Parker DS, Jemison J, Cadigan KM. 2002. Pygopus, a nuclear PHD-finger protein required for Wingless signaling in Drosophila. *Development (Cambridge, England)* 129:2565-76

Parr BA, McMahon AP. 1994. Wnt genes and vertebrate development. *Current opinion in genetics & development* 4:523-8

Pedersen TA, Kowenz-Leutz E, Leutz A, Nerlov C. 2001. Cooperation between C/EBPalpha TBP/TFIIB and SWI/SNF recruiting domains is required for adipocyte differentiation. *Genes & development* 15:3208-16

Penton A, Wodarz A, Nusse R. 2002. A mutational analysis of dishevelled in Drosophila defines novel domains in the dishevelled protein as well as novel suppressing alleles of axin. *Genetics* 161:747-62

Piao Z, Choi Y, Park C, Lee WJ, Park JH, Kim H. 1997. Deletion of the M6P/IGF2r gene in primary hepatocellular carcinoma. *Cancer letters* 120:39-43

Pinson KI, Brennan J, Monkley S, Avery BJ, Skarnes WC. 2000. An LDL-receptor-related protein mediates Wnt signalling in mice. *Nature* 407:535-8

Playford MP, Bicknell D, Bodmer WF, Macaulay VM. 2000. Insulin-like growth factor 1 regulates the location, stability, and transcriptional activity of beta-catenin. *Proceedings of the National Academy of Sciences of the United States of America* 97:12103-8

Pontisso P, Belluco C, Bertorelle R, De Moliner L, Chieco-Bianchi L, et al. 1998. Hepatitis C virus infection associated with human hepatocellular carcinoma: lack of correlation with p53 abnormalities in Caucasian patients. *Cancer* 83:1489-94

Porse BT, Pedersen TA, Hasemann MS, Schuster MB, Kirstetter P, et al. 2006. The proline-histidine-rich CDK2/CDK4 interaction region of C/EBPalpha is dispensable for C/EBPalpha-mediated growth regulation in vivo. *Molecular and cellular biology* 26:1028-37

Postigo AA, Depp JL, Taylor JJ, Kroll KL. 2003. Regulation of Smad signaling through a differential recruitment of coactivators and corepressors by ZEB proteins. *The EMBO journal* 22:2453-62

Powell SM, Zilz N, Beazer-Barclay Y, Bryan TM, Hamilton SR, et al. 1992. APC mutations occur early during colorectal tumorigenesis. *Nature* 359:235-7

Prange W, Breuhahn K, Fischer F, Zilkens C, Pietsch T, et al. 2003. Beta-catenin accumulation in the progression of human hepatocarcinogenesis correlates with loss of E-cadherin and accumulation of p53, but not with expression of conventional WNT-1 target genes. *The Journal of pathology* 201:250-9

Puisieux A, Lim S, Groopman J, Ozturk M. 1991. Selective targeting of p53 gene mutational hotspots in human cancers by etiologically defined carcinogens. *Cancer research* 51:6185-9

Puisieux A, Ozturk M. 1997. TP53 and hepatocellular carcinoma. *Pathologie-biologie* 45:864-70

Radomska HS, Huettner CS, Zhang P, Cheng T, Scadden DT, Tenen DG. 1998. CCAAT/enhancer binding protein alpha is a regulatory switch sufficient for induction of granulocytic development from bipotential myeloid progenitors. *Molecular and cellular biology* 18:4301-14

Ramji DP, Foka P. 2002. CCAAT/enhancer-binding proteins: structure, function and regulation. *The Biochemical journal* 365:561-75

Ray RB, Ray R. 2001. Hepatitis C virus core protein: intriguing properties and functional relevance. *FEMS microbiology letters* 202:149-56

Ray RB, Steele R, Meyer K, Ray R. 1997. Transcriptional repression of p53 promoter by hepatitis C virus core protein. *The Journal of biological chemistry* 272:10983-6

Regimbeau JM, Colombat M, Mognol P, Durand F, Abdalla E, et al. 2004. Obesity and diabetes as a risk factor for hepatocellular carcinoma. *Liver Transpl* 10:S69-73

Remacle JE, Kraft H, Lerchner W, Wuytens G, Collart C, et al. 1999. New mode of DNA binding of multi-zinc finger transcription factors: deltaEF1 family members bind with two hands to two target sites. *The EMBO journal* 18:5073-84

Reya T, Clevers H. 2005. Wnt signalling in stem cells and cancer. *Nature* 434:843-50

Rocken C, Carl-McGrath S. 2001. Pathology and pathogenesis of hepatocellular carcinoma. *Digestive diseases (Basel, Switzerland)* 19:269-78

Roncalli M, Bianchi P, Bruni B, Laghi L, Destro A, et al. 2002. Methylation framework of cell cycle gene inhibitors in cirrhosis and associated hepatocellular carcinoma. *Hepatology (Baltimore, Md* 36:427-32

Roninson IB. 2003. Tumor cell senescence in cancer treatment. *Cancer research* 63:2705-15

Roose J, Clevers H. 1999. TCF transcription factors: molecular switches in carcinogenesis. *Biochimica et biophysica acta* 1424:M23-37

Roose J, Huls G, van Beest M, Moerer P, van der Horn K, et al. 1999. Synergy between tumor suppressor APC and the beta-catenin-Tcf4 target Tcf1. *Science* 285:1923-6

Roose J, Molenaar M, Peterson J, Hurenkamp J, Brantjes H, et al. 1998. The Xenopus Wnt effector XTcf-3 interacts with Groucho-related transcriptional repressors. *Nature* 395:608-12

Rosen ED, Hsu CH, Wang X, Sakai S, Freeman MW, et al. 2002. C/EBPalpha induces adipogenesis through PPARgamma: a unified pathway. *Genes & development* 16:22-6

Rosin-Arbesfeld R, Townsley F, Bienz M. 2000. The APC tumour suppressor has a nuclear export function. *Nature* 406:1009-12

Ryo A, Nakamura M, Wulf G, Liou YC, Lu KP. 2001. Pin1 regulates turnover and subcellular localization of beta-catenin by inhibiting its interaction with APC. *Nature cell biology* 3:793-801

Salvucci M, Lemoine A, Saffroy R, Azoulay D, Lepere B, et al. 1999. Microsatellite instability in European hepatocellular carcinoma. *Oncogene* 18:181-7

Satoh S, Daigo Y, Furukawa Y, Kato T, Miwa N, et al. 2000. AXIN1 mutations in hepatocellular carcinomas, and growth suppression in cancer cells by virus-mediated transfer of AXIN1. *Nature genetics* 24:245-50

Satyanarayana A, Manns MP, Rudolph KL. 2004. Telomeres and telomerase: a dual role in hepatocarcinogenesis. *Hepatology (Baltimore, Md* 40:276-83

Schnater JM, Kohler SE, Lamers WH, von Schweinitz D, Aronson DC. 2003. Where do we stand with hepatoblastoma? A review. *Cancer* 98:668-78

Schneider S, Steinbeisser H, Warga RM, Hausen P. 1996. Beta-catenin translocation into nuclei demarcates the dorsalizing centers in frog and fish embryos. *Mechanisms of development* 57:191-8

Schrem H, Klempnauer J, Borlak J. 2004. Liver-enriched transcription factors in liver function and development. Part II: the C/EBPs and D site-binding protein in cell cycle control, carcinogenesis, circadian gene regulation, liver regeneration, apoptosis, and liver-specific gene regulation. *Pharmacological reviews* 56:291-330

Scott LM, Civin CI, Rorth P, Friedman AD. 1992. A novel temporal expression pattern of three C/EBP family members in differentiating myelomonocytic cells. *Blood* 80:1725-35

Seeling JM, Miller JR, Gil R, Moon RT, White R, Virshup DM. 1999. Regulation of beta-catenin signaling by the B56 subunit of protein phosphatase 2A. *Science* 283:2089-91

Shafritz DA, Dabeva MD. 2002. Liver stem cells and model systems for liver repopulation. *Journal of hepatology* 36:552-64

Sharma GG, Gupta A, Wang H, Scherthan H, Dhar S, et al. 2003. hTERT associates with human telomeres and enhances genomic stability and DNA repair. *Oncogene* 22:131-46

Shay JW, Bacchetti S. 1997. A survey of telomerase activity in human cancer. *Eur J Cancer* 33:787-91

Shay JW, Roninson IB. 2004. Hallmarks of senescence in carcinogenesis and cancer therapy. *Oncogene* 23:2919-33

Shay JW, Wright WE. 2005. Senescence and immortalization: role of telomeres and telomerase. *Carcinogenesis* 26:867-74

Shen HM, Ong CN. 1996. Mutations of the p53 tumor suppressor gene and ras oncogenes in aflatoxin hepatocarcinogenesis. *Mutation research* 366:23-44

Sherr CJ, McCormick F. 2002. The RB and p53 pathways in cancer. *Cancer cell* 2:103-12

Shimotohno K. 2000. Hepatitis C virus and its pathogenesis. *Seminars in cancer biology* 10:233-40

Shirota Y, Kaneko S, Honda M, Kawai HF, Kobayashi K. 2001. Identification of differentially expressed genes in hepatocellular carcinoma with cDNA microarrays. *Hepatology*

(Baltimore, Md 33:832-40

Simon D, London T, Hann HW, Knowles BB. 1991. Chromosome abnormalities in peripheral blood cells of hepatitis B virus chronic carriers. *Cancer research* 51:6176-9

Sirma H, Giannini C, Poussin K, Paterlini P, Kremsdorf D, Brechot C. 1999. Hepatitis B virus X mutants, present in hepatocellular carcinoma tissue abrogate both the antiproliferative and transactivation effects of HBx. *Oncogene* 18:4848-59

Slagle BL, Zhou YZ, Birchmeier W, Scorsone KA. 1993. Deletion of the E-cadherin gene in hepatitis B virus-positive Chinese hepatocellular carcinomas. *Hepatology (Baltimore, Md* 18:757-62

Smith LT, Hohaus S, Gonzalez DA, Dziennis SE, Tenen DG. 1996. PU.1 (Spi-1) and C/EBP alpha regulate the granulocyte colony-stimulating factor receptor promoter in myeloid cells. *Blood* 88:1234-47

Su LK, Abdalla EK, Law CH, Kohlmann W, Rashid A, Vauthey JN. 2001. Biallelic inactivation of the APC gene is associated with hepatocellular carcinoma in familial adenomatous polyposis coli. *Cancer* 92:332-9

Sugimachi K, Taguchi K, Aishima S, Tanaka S, Shimada M, et al. 2001. Altered expression of beta-catenin without genetic mutation in intrahepatic cholangiocarcinoma. *Mod Pathol* 14:900-5

Sun TQ, Lu B, Feng JJ, Reinhard C, Jan YN, et al. 2001. PAR-1 is a Dishevelled-associated kinase and a positive regulator of Wnt signalling. *Nature cell biology* 3:628-36

Suriawinata A, Xu R. 2004. An update on the molecular genetics of hepatocellular carcinoma. *Seminars in liver disease* 24:77-88

Suzuki T, Yano H, Nakashima Y, Nakashima O, Kojiro M. 2002. Beta-catenin expression in hepatocellular carcinoma: a possible participation of beta-catenin in the dedifferentiation process. *Journal of gastroenterology and hepatology* 17:994-1000

Tago K, Nakamura T, Nishita M, Hyodo J, Nagai S, et al. 2000. Inhibition of Wnt signaling by ICAT, a novel beta-catenin-interacting protein. *Genes & development* 14:1741-9

Takemaru K, Yamaguchi S, Lee YS, Zhang Y, Carthew RW, Moon RT. 2003. Chibby, a nuclear beta-catenin-associated antagonist of the Wnt/Wingless pathway. *Nature* 422:905-9

Takemaru KI, Moon RT. 2000. The transcriptional coactivator CBP interacts with beta-catenin to activate gene expression. *The Journal of cell biology* 149:249-54

Tamai K, Semenov M, Kato Y, Spokony R, Liu C, et al. 2000. LDL-receptor-related proteins in Wnt signal transduction. *Nature* 407:530-5

Tamai K, Zeng X, Liu C, Zhang X, Harada Y, et al. 2004. A mechanism for Wnt coreceptor activation. *Molecular cell* 13:149-56

Tan EH, Hooi SC, Laban M, Wong E, Ponniah S, et al. 2005. CCAAT/enhancer binding protein alpha knock-in mice exhibit early liver glycogen storage and reduced susceptibility to

hepatocellular carcinoma. *Cancer research* 65:10330-7

Taniguchi K, Roberts LR, Aderca IN, Dong X, Qian C, et al. 2002. Mutational spectrum of beta-catenin, AXIN1, and AXIN2 in hepatocellular carcinomas and hepatoblastomas. *Oncogene* 21:4863-71

Tannapfel A, Wittekind C. 2002. Genes involved in hepatocellular carcinoma: deregulation in cell cycling and apoptosis. *Virchows Arch* 440:345-52

Thompson B, Townsley F, Rosin-Arbesfeld R, Musisi H, Bienz M. 2002. A new nuclear component of the Wnt signalling pathway. *Nature cell biology* 4:367-73

Thorgeirsson SS, Grisham JW. 2002. Molecular pathogenesis of human hepatocellular carcinoma. *Nature genetics* 31:339-46

Tien LT, Ito M, Nakao M, Niino D, Serik M, et al. 2005. Expression of beta-catenin in hepatocellular carcinoma. *World J Gastroenterol* 11:2398-401

Timchenko LT, Iakova P, Welm AL, Cai ZJ, Timchenko NA. 2002. Calreticulin interacts with C/EBPalpha and C/EBPbeta mRNAs and represses translation of C/EBP proteins. *Molecular and cellular biology* 22:7242-57

Timchenko N, Wilson DR, Taylor LR, Abdelsayed S, Wilde M, et al. 1995. Autoregulation of the human C/EBP alpha gene by stimulation of upstream stimulatory factor binding. *Molecular and cellular biology* 15:1192-202

Timchenko NA, Harris TE, Wilde M, Bilyeu TA, Burgess-Beusse BL, et al. 1997. CCAAT/enhancer binding protein alpha regulates p21 protein and hepatocyte proliferation in newborn mice. *Molecular and cellular biology* 17:7353-61

Timchenko NA, Wilde M, Iakova P, Albrecht JH, Darlington GJ. 1999. E2F/p107 and E2F/p130 complexes are regulated by C/EBPalpha in 3T3-L1 adipocytes. *Nucleic acids research* 27:3621-30

Timchenko NA, Wilde M, Kosai KI, Heydari A, Bilyeu TA, et al. 1998. Regenerating livers of old rats contain high levels of C/EBPalpha that correlate with altered expression of cell cycle associated proteins. *Nucleic acids research* 26:3293-9

Timchenko NA, Wilde M, Nakanishi M, Smith JR, Darlington GJ. 1996. CCAAT/enhancer-binding protein alpha (C/EBP alpha) inhibits cell proliferation through the p21 (WAF-1/CIP-1/SDI-1) protein. *Genes & development* 10:804-15

Tolwinski NS, Wehrli M, Rives A, Erdeniz N, DiNardo S, Wieschaus E. 2003. Wg/Wnt signal can be transmitted through arrow/LRP5,6 and Axin independently of Zw3/Gsk3beta activity. *Developmental cell* 4:407-18

Topol L, Jiang X, Choi H, Garrett-Beal L, Carolan PJ, Yang Y. 2003. Wnt-5a inhibits the canonical Wnt pathway by promoting GSK-3-independent beta-catenin degradation. *The Journal of cell biology* 162:899-908

Townsley FM, Cliffe A, Bienz M. 2004. Pygopus and Legless target Armadillo/beta-catenin to the

nucleus to enable its transcriptional co-activator function. *Nature cell biology* 6:626-33

Truong BT, Lee YJ, Lodie TA, Park DJ, Perrotti D, et al. 2003. CCAAT/Enhancer binding proteins repress the leukemic phenotype of acute myeloid leukemia. *Blood* 101:1141-8

Tsujiuchi T, Tsutsumi M, Sasaki Y, Takahama M, Konishi Y. 1999. Different frequencies and patterns of beta-catenin mutations in hepatocellular carcinomas induced by N-nitrosodiethylamine and a choline-deficient L-amino acid-defined diet in rats. *Cancer research* 59:3904-7

Twu JS, Schloemer RH. 1987. Transcriptional trans-activating function of hepatitis B virus. *Journal of virology* 61:3448-53

Ueda H, Ullrich SJ, Gangemi JD, Kappel CA, Ngo L, et al. 1995. Functional inactivation but not structural mutation of p53 causes liver cancer. *Nature genetics* 9:41-7

Ueno Y, Moriyama M, Uchida T, Arakawa Y. 2001. Irregular regeneration of hepatocytes is an important factor in the hepatocarcinogenesis of liver disease. *Hepatology (Baltimore, Md* 33:357-62

Umbhauer M, Djiane A, Goisset C, Penzo-Mendez A, Riou JF, et al. 2000. The C-terminal cytoplasmic Lys-thr-X-X-X-Trp motif in frizzled receptors mediates Wnt/beta-catenin signalling. *The EMBO journal* 19:4944-54

van de Wetering M, Cavallo R, Dooijes D, van Beest M, van Es J, et al. 1997. Armadillo coactivates transcription driven by the product of the Drosophila segment polarity gene dTCF. *Cell* 88:789-99

van Es JH, Kirkpatrick C, van de Wetering M, Molenaar M, Miles A, et al. 1999. Identification of APC2, a homologue of the adenomatous polyposis coli tumour suppressor. *Curr Biol* 9:105-8

Veeman MT, Axelrod JD, Moon RT. 2003. A second canon. Functions and mechanisms of beta-catenin-independent Wnt signaling. *Developmental cell* 5:367-77

Verschueren K, Remacle JE, Collart C, Kraft H, Baker BS, et al. 1999. SIP1, a novel zinc finger/homeodomain repressor, interacts with Smad proteins and binds to 5'-CACCT sequences in candidate target genes. *The Journal of biological chemistry* 274:20489-98

Volkmann M, Hofmann WJ, Muller M, Rath U, Otto G, et al. 1994. p53 overexpression is frequent in European hepatocellular carcinoma and largely independent of the codon 249 hot spot mutation. *Oncogene* 9:195-204

Wang GL, Iakova P, Wilde M, Awad S, Timchenko NA. 2004. Liver tumors escape negative control of proliferation via PI3K/Akt-mediated block of C/EBP alpha growth inhibitory activity. *Genes & development* 18:912-25

Wang H, Goode T, Iakova P, Albrecht JH, Timchenko NA. 2002. C/EBPalpha triggers proteasome-dependent degradation of cdk4 during growth arrest. *The EMBO journal* 21:930-41

Wang H, Iakova P, Wilde M, Welm A, Goode T, et al. 2001. C/EBPalpha arrests cell proliferation through direct inhibition of Cdk2 and Cdk4. *Molecular cell* 8:817-28

Wang J, Xie LY, Allan S, Beach D, Hannon GJ. 1998. Myc activates telomerase. *Genes & development* 12:1769-74

Wang ND, Finegold MJ, Bradley A, Ou CN, Abdelsayed SV, et al. 1995. Impaired energy homeostasis in C/EBP alpha knockout mice. *Science* 269:1108-12

Wehrli M, Dougan ST, Caldwell K, O'Keefe L, Schwartz S, et al. 2000. arrow encodes an LDL-receptor-related protein essential for Wingless signalling. *Nature* 407:527-30

Wei W, Sedivy JM. 1999. Differentiation between senescence (M1) and crisis (M2) in human fibroblast cultures. *Experimental cell research* 253:519-22

Wei Y, Fabre M, Branchereau S, Gauthier F, Perilongo G, Buendia MA. 2000. Activation of beta-catenin in epithelial and mesenchymal hepatoblastomas. *Oncogene* 19:498-504

Weidinger G, Moon RT. 2003. When Wnts antagonize Wnts. *The Journal of cell biology* 162:753-5

Weinberg RA. 1995. The retinoblastoma protein and cell cycle control. *Cell* 81:323-30

Wiemann SU, Satyanarayana A, Tsahuridu M, Tillmann HL, Zender L, et al. 2002. Hepatocyte telomere shortening and senescence are general markers of human liver cirrhosis. *Faseb J* 16:935-42

Willert K, Brown JD, Danenberg E, Duncan AW, Weissman IL, et al. 2003. Wnt proteins are lipid-modified and can act as stem cell growth factors. *Nature* 423:448-52

Wong CM, Fan ST, Ng IO. 2001. beta-Catenin mutation and overexpression in hepatocellular carcinoma: clinicopathologic and prognostic significance. *Cancer* 92:136-45

Wong HC, Bourdelas A, Krauss A, Lee HJ, Shao Y, et al. 2003. Direct binding of the PDZ domain of Dishevelled to a conserved internal sequence in the C-terminal region of Frizzled. *Molecular cell* 12:1251-60

Wright WE, Shay JW. 1992. The two-stage mechanism controlling cellular senescence and immortalization. *Experimental gerontology* 27:383-9

Yakicier MC, Irmak MB, Romano A, Kew M, Ozturk M. 1999. Smad2 and Smad4 gene mutations in hepatocellular carcinoma. *Oncogene* 18:4879-83

Yamada T, De Souza AT, Finkelstein S, Jirtle RL. 1997. Loss of the gene encoding mannose 6-phosphate/insulin-like growth factor II receptor is an early event in liver carcinogenesis. *Proceedings of the National Academy of Sciences of the United States of America* 94:10351-5

Yano M, Asahara T, Dohi K, Mizuno T, Iwamoto KS, Seyama T. 1999. Close correlation between a p53 or hMSH2 gene mutation in the tumor and survival of hepatocellular carcinoma patients. *International journal of oncology* 14:447-51

Yildiz-Erdal E. 2003. *Hepatocellular carcinoma viral etiology and molecular mechanisms*. PhD.

Thesis. Bilkent University, Ankara

Young JI, Sedivy JM, Smith JR. 2003. Telomerase expression in normal human fibroblasts stabilizes DNA 5-methylcytosine transferase I. *The Journal of biological chemistry* 278:19904-8

Yu GL, Bradley JD, Attardi LD, Blackburn EH. 1990. In vivo alteration of telomere sequences and senescence caused by mutated Tetrahymena telomerase RNAs. *Nature* 344:126-32

Yuva Y. 2004. *Evaluation of C/EBPα as a candidate tumor suppressor gene in hepatocellular carcinoma.* MSc. Thesis. Bilkent University, Ankara

Zeng L, Fagotto F, Zhang T, Hsu W, Vasicek TJ, et al. 1997. The mouse Fused locus encodes Axin, an inhibitor of the Wnt signaling pathway that regulates embryonic axis formation. *Cell* 90:181-92

Zhang DE, Hohaus S, Voso MT, Chen HM, Smith LT, et al. 1996. Function of PU.1 (Spi-1), C/EBP, and AML1 in early myelopoiesis: regulation of multiple myeloid CSF receptor promoters. *Current topics in microbiology and immunology* 211:137-47

Zhang DE, Zhang P, Wang ND, Hetherington CJ, Darlington GJ, Tenen DG. 1997. Absence of granulocyte colony-stimulating factor signaling and neutrophil development in CCAAT enhancer binding protein alpha-deficient mice. *Proceedings of the National Academy of Sciences of the United States of America* 94:569-74

Zhang X, Xu HJ, Murakami Y, Sachse R, Yashima K, et al. 1994. Deletions of chromosome 13q, mutations in Retinoblastoma 1, and retinoblastoma protein state in human hepatocellular carcinoma. *Cancer research* 54:4177-82

Reprogramming of replicative senescence in hepatocellular carcinoma-derived cells

Nuri Ozturk*, Esra Erdal*†, Mine Mumcuoglu*, Kamil C. Akcali*, Ozden Yalcin*‡, Serif Senturk*, Ayca Arslan-Ergul*, Bala Gur*, Isik Yulug*, Rengul Cetin-Atalay*, Cengiz Yakicier*, Tamer Yagci*, Mesut Tez§, and Mehmet Ozturk*¶‖

*Department of Molecular Biology and Genetics, Bilkent University, Bilkent, Ankara 06800, Turkey; and §Department of 5th Surgery, Numune Training and Research Hospital, Sihhiye, Ankara 06100, Turkey

Communicated by Aziz Sancar, University of North Carolina, Chapel Hill, NC, December 18, 2005 (received for review October 10, 2005)

Tumor cells have the capacity to proliferate indefinitely that is qualified as replicative immortality. This ability contrasts with the intrinsic control of the number of cell divisions in human somatic tissues by a mechanism called replicative senescence. Replicative immortality is acquired by inactivation of p53 and $p16^{INK4a}$ genes and reactivation of hTERT gene expression. It is unknown whether the cancer cell replicative immortality is reversible. Here, we show the spontaneous induction of replicative senescence in p53-and $p16^{INK4a}$-deficient hepatocellular carcinoma cells. This phenomenon is characterized with hTERT repression, telomere shortening, senescence arrest, and tumor suppression. SIP1 gene (*ZFHX1B*) is partly responsible for replicative senescence, because short hairpin RNA-mediated SIP1 inactivation released hTERT repression and rescued clonal hepatocellular carcinoma cells from senescence arrest.

immortality | liver cancer | SIP1 | telomerase | p53

Tumor cells are clonal (1), and tumorigenesis usually requires three to six independent mutations in the progeny of precancerous cells (2). For this to occur, preneoplastic somatic cells would need to breach the replicative senescence barriers. Replicative senescence is a telomere-dependent process that sets a limit to the successive rounds of cell division in human somatic cells (3). Progressive telomere shortening is observed in almost all dividing normal cells. This phenomenon is linked to the lack of efficient *hTERT* expression that is observed in most human somatic cells (3). Replicative senescence (permanent growth arrest also called M_1 stage) is believed to be initiated by a DNA damage-type signal generated by critically shortened telomeres, or by the loss of telomere integrity, leading to the activation of cell cycle checkpoint pathways involving p53, $p16^{INK4a}$, and/or retinoblastoma (pRb) proteins (4, 5). In the absence of functional p53 and $p16^{INK4a}$/pRb pathway responses, telomeres continue to shorten resulting in crisis (also called M2 stage). Cells that bypass the M_2 stage by reactivating *hTERT* expression gain the ability for indefinite cell proliferation, also called immortality (3, 4, 6). There is accumulating evidence that cancer cells undergo a similar process during carcinogenesis to acquire immortality. Telomerase activity associated with *hTERT* reexpression is observed in ≈80% of human tumors (7), and senescence controlling *p53* and $p16^{INK4A}$ genes are commonly inactivated in the majority of human cancers (8). Moreover, experimental transformation of normal human cells to tumor cells requires hTERT-mediated immortalization, as well as inactivation of *p53* and *pRb* genes (9).

Aberrant expression of hTERT, together with the loss of p53 and $p16^{INK4a}$/pRb control mechanisms, suggests that the replicative immortality is a permanent and irreversible characteristic of cancer cells. Although some cancer cells may react to extrinsic factors by a senescence-like stress response, this response is immediate, telomere-independent, and cannot be qualified as replicative senescence (10). Experimental inactivation of telomerase activity in cancer cells mostly results in cell death (11), whereas ectopic expression of p53, $p16^{INK4a}$, or pRb provokes an immediate senescence-like growth arrest or cell death (10). Thus, to date there is no experimental evidence for spontaneous reprogramming of replicative senescence in immortalized cancer cells. Using hepatocellular carcinoma (HCC)-derived Huh7 cells as a model system, here we show that cancer cells with replicative immortality are able to spontaneously generate progeny with replicative senescence. Thus, we provide preliminary evidence for the reversibility of cancer cell immortality. The replicative senescence of cancer cells shares many features with normal cell replicative senescence such as repression of *hTERT* expression, telomere shortening, and permanent growth arrest with morphological hallmarks of senescence. However, the *p53* gene is mutated, whereas $p16^{INK4a}$ promoter is hypermethylated in these cells. Thus, we show that fully malignant and tumorigenic HCC cells that display aberrant hTERT expression and lack functional *p53* and $p16^{INK4a}$ genes are able to revert from replicative immortality to replicative senescence by an intrinsic mechanism. Furthermore, we demonstrate that the *SIP1* gene, encoding a zinc-finger homeodomain transcription factor protein involved in TGF-β signaling (12, 13) and *hTERT* regulation (14), serves as a molecular switch between replicative immortality and replicative senescence fates in HCC cells.

Results

When analyzing clones from established cancer cell lines, we observed that some clones change morphology and cease proliferation at late passages with features reminiscent of cellular senescence (data not shown). We reasoned that this could be an indication for generation of progeny programmed for replicative senescence. We surveyed a panel of HCC and breast carcinoma cell lines and hTERT-immortalized human mammary epithelial cells (hTERT-HME). Plated at low clonogenic density, cells were maintained in culture until they performed 6–10 population doublings (PD), and tested for senescence-associated β-galactosidase (SABG) activity (15). Different cancer cell lines generated progeny with greatly contrasting SABG staining patterns. The first group, represented here by HCC-derived Huh7 and breast cancer-derived T-47D and BT-474 cell lines, generated heterogeneously staining colonies. Cells of some colonies were mostly positive for SABG, but others displayed significantly diminished or complete lack of staining (Fig. 1*A*). The second group, represented by HCC-derived Hep3B and Mahlavu, and hTERT-HME generated only SABG-negative colonies (Fig. 1*B*). Manual counting of randomly selected colonies demonstrated that mean SABG-labeling indexes for Huh7,

Conflict of interest statement: No conflicts declared.

Abbreviations: HCC, hepatocellular carcinoma; PD, population doubling; SABG, senescence-associated β-galactosidase; shRNA, short hairpin RNA.

†Present address: Department of Medical Biology and Genetics, Faculty of Medicine, Dokuz Eylul University, 35210 Izmir, Turkey.

‡Present address: Swiss Institute for Experimental Cancer Research, Ch. des Boveresses 155, CH-1066 Epalinges, Lausanne, Switzerland.

¶To whom correspondence should be addressed. E-mail: ozturk@fen.bilkent.edu.tr.

www.pnas.org/cgi/doi/10.1073/pnas.0510877103

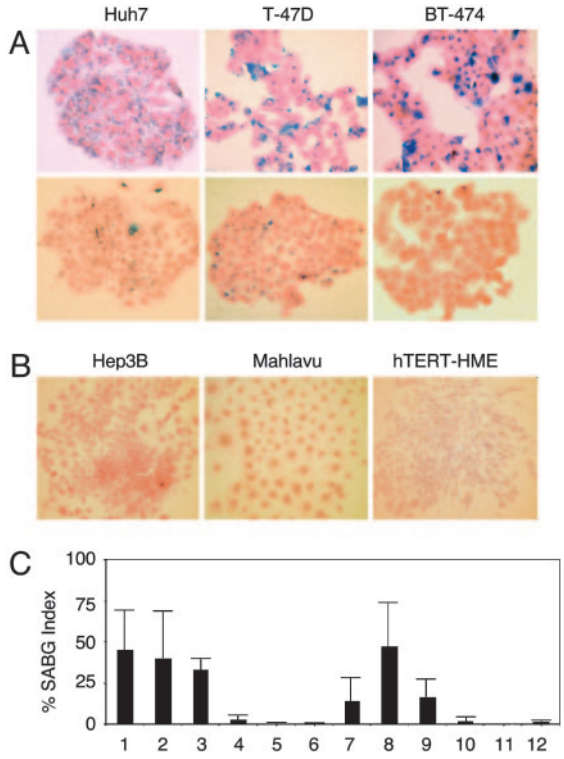

Fig. 1. Established human cancer cell lines generate senescence-associated β-galactosidase (SABG)-expressing progeny. (*A*) Representative pictures of HCC (Huh7) and breast cancer (T-47D and BT-474) cell lines that generate both SABG-positive (*Upper*) and SABG-negative (*Lower*) colonies. (*B*) Representative pictures of HCC (Hep3B and Mahlavu) and telomerase-immortalized mammary epithelial (hTERT-HME) cell lines that generate only SABG-negative colonies. Cells were plated at clonogenic density to generate colonies with 6–10 population doublings, and stained for SABG activity (blue), followed by eosin counterstaining (red). (*C*) Quantification of SABG-positive cells in colonies. Randomly selected colonies ($n \geq 10$) obtained from parental (lanes 1–6) cell lines and expanded clones (lanes 7–12) were counted to calculate the average % SABG positive cells per colony (% SABG index). Lanes 1–6 designate Huh7, T-47D, BT-474, Hep3B, Mahlavu, and hTERT-HME, respectively. Lanes 7–9 are Huh7-derived C1, C3, and C11 clones, and lanes 10–12 are Hep3B-derived 3B-C6, 3B-C11, and 3B-C13 clones. Error bars indicate SD.

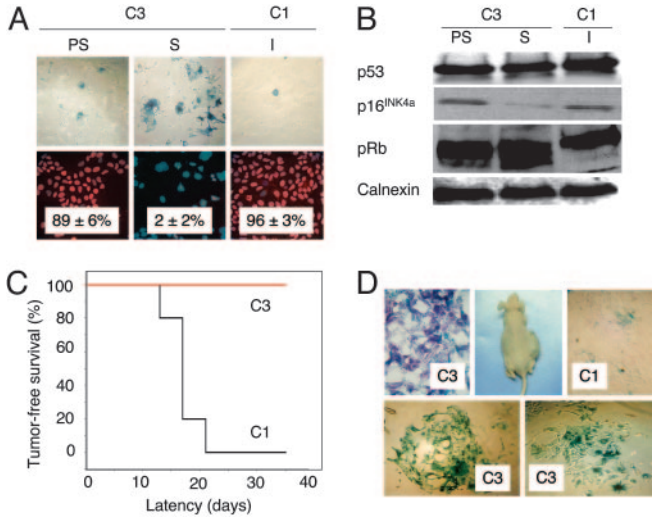

Fig. 2. p53-and p16^{INK4a}-deficient Huh7 cells generate progeny that undergo *in vitro* and *in vivo* replicative senescence resulting in loss of tumorigenicity. (*A*) Huh7-derived clones C3 and C1 were tested for replicative senescence arrest by SABG and BrdUrd staining at different passages. Presenescent C3 and immortal C1 cells display low SABG staining (*Upper*) and high BrdUrd incorporation (*Lower*), whereas senescent C3 cells are fully positive for SABG (*Upper*) and fail to incorporate BrdUrd into DNA after mitogenic stimuli (*Lower*). (*B*) p53 and p16^{INK4a} protein levels show no increase in senescent C3 cells, compared to presenescent C3 and immortal C1 cells, but senescent C3 cells display partial hypophosphorylation of pRb. Calnexin was used as a loading control. Proteins were tested by Western blotting. PS, presenescent (PD 57); S, senescent (PD 80); I, immortal (PD 179). (*C*) C1 cells (black line) were fully tumorigenic, but C3 cells (red line) were not in *nude* mice. (*D*) C1 tumors displayed low SABG staining (*Upper Right*), whereas implanted C3 cells remaining at the injection site are fully positive for SABG *in situ* (*Upper Left*), as well as after short-term *in vitro* selection (*Lower*). Animals were injected with presenescent C3 (PD 59) and immortal C1 (PD 119) cells, and tumors and nontumorigenic cell samples were collected at day 35 and analyzed.

T-47D and BT-474 progenies were 45 ± 23%, 40 ± 29%, and 33 ± 7%, respectively (Fig. 1*C*, lanes 1–3). In contrast, Hep3B, Mahlavu, and hTERT-HME progenies displayed <3 ± 3% mean SABG-labeling indexes (Fig. 1*C*, lanes 4–6). Clones from representative cell lines were expanded and subjected to the same analysis. SABG-staining patterns of all clones tested were closely similar to the patterns of their respective parental cell lines. For example, mean SABG staining indexes of Huh7-derived clones were 14 ± 15%, 47 ± 27%, and 17 ± 11% (Fig. 1*C*, lanes 7–9), whereas Hep3B-derived clones generated <2 ± 3% SABG-positive progenies (Fig. 1*C*, lanes 10–12). We speculated that the first group of cell lines comprised progenies in different stages of replicative senescence process at the time of analysis, whereas the second group of cell lines were composed mostly of immortal cells. The results obtained with the first group were unexpected. These cell lines have been established >20 years ago (16–18) and expanded in culture over many years, with PD well beyond the known senescence barriers for normal human cells (3), but they were still capable of generating presumably senescent progeny.

The study of a potentially active replicative senescence program in the progeny of immortal cancer cell lines requires the long-term follow up of single cell-derived clones. To this end, we chose to focus our investigations on Huh7 cell line. We expanded different Huh7-derived clones in long-term culture and examined their potential to undergo replicative senescence. Some clones performed >100 PD in culture with stable proliferation rates and heterogeneous SABG staining, whereas others sustained a limited number of PD, then entered a growth arrest phase with full SABG staining patterns. For example, C3 clone performed only 80 PD, whereas C1 clone replicated >150 PD. Permanently arrested C3 cells (PD 80) displayed enlarged size, flattened shape, and fully positive SABG staining, whereas early passage C3 (PD 57) and C1 (PD 179) cells displayed normal morphology with heterogeneous SABG staining (Fig. 2*A Upper*). Normal human cells at replicative senescence (M_1) are refractory to mitotic stimulation and display <5% BrdUrd index (19). Growth-arrested C3 cells displayed very low BrdUrd staining (2 ± 2%), in contrast to early passage C3 and late passage C1 cells, which exhibited 89 ± 6%, and 96 ± 3% BrdUrd indexes, respectively (Fig. 2*A Lower*). Senescent C3 cells remained growth arrested, but alive when maintained in culture for at least 3 months, with no emergence of immortal clones (data not shown).

Biological mechanisms of replicative senescence observed here are of particular interest, because senescence-regulatory *p53* is inactivated (20–22) and *p16^{INK4a}* promoter is hypermethylated (23) in Huh7 cells. Accordingly, there was no change in p53 levels, whereas the low level p16^{INK4a} expression did not increase, but decreased in senescent C3 (PD 80) cells, when compared to presenescent C3 (PD 57) or immortal C1 (PD 179) cells. Retinoblastoma protein (pRb) displayed partial hypophos-

phorylation in senescent C3 cells, apparently in a p53- and $p16^{INK4a}$-independent manner (Fig. 2*B*). Cyclin E and A levels were also decreased, but $p21^{cip1}$ levels were elevated in both presenescent and senescent C3 cells (Fig. 5*A*, which is published as supporting information on the PNAS web site). Cyclin D1, CDK4, and CDK2 protein levels (Fig. 5*A*) and $p14^{ARF}$ transcript levels (Fig. 5*B*) did not change.

Cancer cell senescence that we characterized here shared many features with normal cell replicative senescence (3), except that it was not accompanied with wild-type *p53* or *p16*^{INK4a} induction. However, *in vivo* relevance of the replicative senescence observed in cell culture is debated (6). Therefore, we compared *in vivo* replicative potentials of C3 (PD 59) and C1 (PD 119) cells in CD-1 *nude* mice. C3 cells did not form visible tumors, whereas C1 cells were fully tumorigenic in the same set of animals (Fig. 2*C*), like parental Huh7 cells (data not shown; ref. 24). C1 tumors collected at day 35 displayed scattered but low-rate SABG-positive staining, but remnant C3 cell masses collected from their injection sites were fully SABG-positive (Fig. 2*D Upper*). For confirmation, these remnants were removed from two different animals, passaged twice in cell culture for selection, and examined. Nearly all cells displayed senescence features including enlarged size, flattened shape, and highly positive SABG staining (Fig. 2*D Lower*). We concluded that loss of C3 tumorigenicity was due to replicative senescence *in vivo*.

Replicative senescence, also called telomere-dependent senescence is associated with progressive telomere shortening due to inefficient telomerase activity (3). When compared to parental Huh7 cells, presenescent C3 cells at PD 57 had telomeres that have already been shortened to ≈7 kbp from ≈12 kbp. These cells eroded their telomeres to <5 kbp at the onset of senescence. In contrast, immortal C1 clone (PD 179) telomeres did not shorten (Fig. 3*A*). These observations showed a perfect correlation with telomerase activity and *hTERT* expression. Immortal C1 cells displayed robust telomerase activity, whereas both presenescent and senescent C3 cells had no detectable telomerase activity (Fig. 3*B*). Accordingly, the expression of *hTERT* gene was high in C1, but barely detectable in C3 cells (Fig. 3*C*). Thus, senescence observed with C3 cells was characterized with the loss of *hTERT* expression and telomerase activity, associated with telomere shortening.

Mechanisms of *hTERT* expression are presently unclear, but several genes including *SIP1*, *hSIR2*, *c-myc*, *Mad1*, *Menin*, *Rak*, and *Brit1* have been implicated (14, 25). Therefore, we analyzed their expression in C1 and C3 clones. All tested genes, except *SIP1*, were expressed at similar levels in both C1 and C3 clones, independent of *hTERT* expression (Fig. 6, which is published as supporting information on the PNAS web site). SIP1 transcripts were undetectable in C1 cells, but elevated in C3 cells, moderately in presenescent, but strongly in senescent stages (Fig. 3*C*). We verified these findings with another Huh7-derived clone (G12) that displayed replicative senescence resulting in permanent cell proliferation arrest. Like C3, presenescent G12 cells that displayed low SABG staining with high BrdUrd index (98 ± 1%), became fully positive for SABG, and nearly negative for BrdUrd (3 ± 2%) at the onset of senescence (Fig. 7, which is published as supporting information on the PNAS web site). Presenescent G12 cells displayed only a weak *hTERT* repression associated with a slight increase in *SIP1* expression, whereas SIP1 was strongly elevated in hTERT-negative senescent cells (Fig. 3*D*). Thus, there was a close correlation between *SIP1* expression and *hTERT* repression in all Huh7 clones tested. The analysis of *SIP1* and *hTERT* expression in primary HCCs and their corresponding nontumor liver tissues confirmed this relationship. SIP1 transcript levels were high, but *hTERT* expression was low in nontumor liver tissues, whereas respective HCC tumors displayed diminished *SIP1* expression associated with up-regulated *hTERT* expression (Fig. 3*E*).

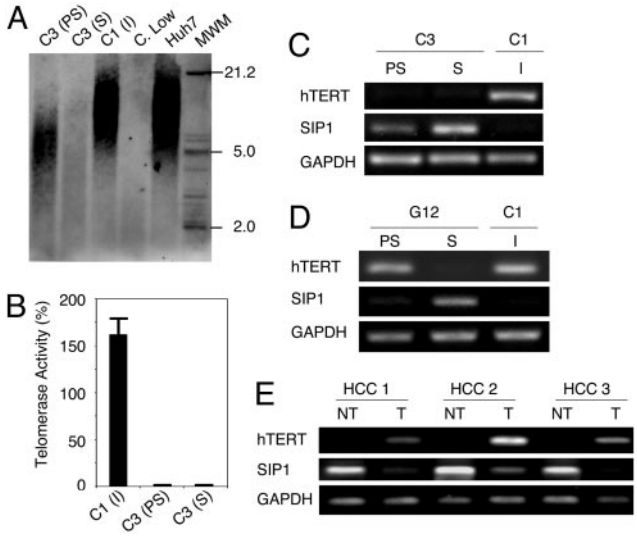

Fig. 3. C3 clonal cells undergo telomere-dependent replicative senescence associated with SIP1 expression and hTERT repression. SIP1 expression is lost, whereas hTERT is induced in primary HCC tumors. (*A*) Genomic DNAs from parental Huh7 and immortal C1 cells display long telomeres, whereas C3 telomeres are progressively shortened in presenescent and senescent stages, respectively. Equal amounts of genomic DNAs were blotted with a telomere repeat probe. C. Low, short telomere control DNA. (*B*) Presenescent and senescent C3 cells have lost telomerase activity, as measured by TRAP assay. Telomerase activity was shown as % value of test samples (± SD) compared to ''high positive'' control sample. (*C*) hTERT expression as tested by RT-PCR was high in immortal C1, but decreased to weakly detectable levels in C3 cells. Inversely, SIP1 expression tested by RT-PCR was undetectable in C1 cells, but showed a progressive increase in presenescent and senescent C3 cells. (*D*) Inverse relationship between SIP1 and hTERT expression was confirmed with another senescence-programmed Huh7 clone named G12 (for SABG and BrdUrd assays, see Fig. 7). hTERT expression in G12 showed a slight decrease in presenescent stage, followed by a loss at the onset of senescence. Inversely, the expression of SIP1 gene was weakly positive in presenescent G12, but highly positive in senescent G12 cells. C1 was used as control. PS, presenescent; S, senescent; I, immortal. (*E*) Negative correlation between hTERT and SIP1 expression in primary tumors (T) and nontumor liver tissues (NT).

The *SIP1* gene (Zinc finger homeobox 1B; *ZFHX1B*) encodes a transcriptional repressor protein that interacts with SMAD proteins of the TGF-β signaling pathway and CtBP corepressor (12, 13). This gene has recently been implicated in TGF-β-dependent regulation of *hTERT* expression in breast cancer cells (14). Our observations implicated *SIP1* gene as a candidate regulator of replicative senescence in HCC cells. To investigate whether *SIP1* expression constitutes a protective barrier against hTERT expression and senescence bypass, we constructed SIP1 short hairpin RNA (shRNA)-expressing plasmids, based on a reported effective SIP1 siRNA sequence (14). SIP1 shRNA was expressed by using either G-418-resistance plasmid pSuper.retro.neo+GFP or puromycin-resistance plasmid pSUPER.puro (see *shRNA* in *Methods*). Presenescent C3 cells at PD 75 were used for transfections, 3–4 weeks before expected senescence arrest stage. pSuper.retro.neo+GFP-based SIP1 shRNA suppressed the accumulation in SIP1 when expressed transiently (Fig. 4*A*, day 5). This resulted in a weak increase in *hTERT* expression. Transfected cells were maintained in culture in the presence of 500 μg/ml G-418 and observed for 30 days. At this period, C3 cells transfected with a control plasmid reached senescence-arrested stage with further up-regulation of *SIP1* expression (Fig. 4*A*, day 30) and resistance to BrdUrd incorporation after mitogenic stimuli (BrdUrd index = 3 ± 1%; Fig. 4*B Upper Left*). In sharp contrast, SIP1 shRNA-transfected cells lost

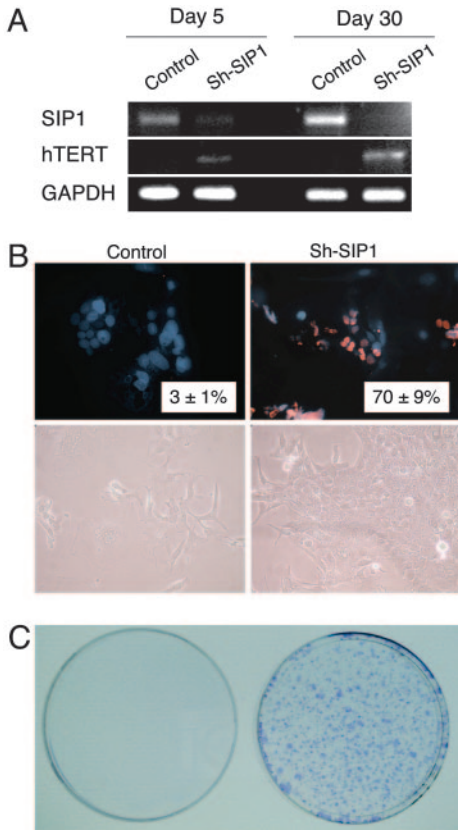

Fig. 4. ShRNA-mediated down-regulation of endogeneous SIP1 transcripts releases hTERT repression and rescues C3 cells from senescence arrest. (*A*) At day 5 after transfection, SIP1 shRNA-transfected cells (Sh-SIP1) show decreased expression of SIP1 and weak up-regulation of hTERT expression. At day 30, the expression of SIP1 is lost completely, and hTERT expression is stronger. (*B*) Cells transfected with empty vector (Control) are senescence-arrested as evidenced by resistance to BrdUrd incorporation (*Upper Left*) and morphological changes (*Lower Left*), but cells transfected with SIP1 shRNA vector (Sh-SIP1) escaped senescence arrest as indicated by high BrdUrd index (*Upper Right*) and proliferating cell clusters (*Lower Right*). (*C*) Colony-forming assay shows that C3 cells formed large number of colonies following puromycin selection after transfection with a puromycin-resistant SIP1-shRNA-expressing plasmid (*Right*), whereas cells transfected with empty vector did not survive (*Left*). SIP1 shRNA was expressed by using either G-418-resistance plasmid pSuper.retro.neo+GFP (*A* and *B*) or puromycin-resistance plasmid pSUPER. puro (*C*). Presenescent C3 cells at PD 75 were transfected with either SIP1 shRNA-expressing or empty plasmid vectors, maintained in culture in the presence of appropriate selection media and tested at days 5 (*A*) and 30 (*A–C*).

SIP1 expression and up-regulated *hTERT* transcripts (Fig. 4*A*, day 30). Furthermore, *SIP1*-inactivated cells escaped senescence, as evidenced with 70 ± 9% BrdUrd index (Fig. 4*B Upper Right*). Morphologically, SIP1 shRNA-transfected cells formed proliferating clusters, whereas cells transfected with control plasmid displayed hallmarks of senescence such as scattering, enlargement, and multiple nuclei (Fig. 4*B Lower*). Twelve independent clones were selected from SIP1 shRNA-transfected C3 cells. All but one of these clones have performed so far >15 PD beyond the expected senescence barrier (data not shown). As an additional confirmatory assay, C3 cells were transfected with the puromycin-selectable *pSUPER.puro-based* SIP1 shRNA vector and subjected to puromycin selection. SIP1 shRNA-transfected cells survived and formed large number of colonies after 30 days of puromycin selection. In contrast, no surviving colony was obtained from cells transfected with the control plasmid, as expected (Fig. 4*C*).

Discussion

Our observations provide experimental evidence for the generation of senescence-arrested clones from immortal HCC and breast cancer cell lines. Detailed analysis of clones from HCC-derived Huh7 cell line further indicates that what we observe is a replicative senescence, but not a stress-induced premature senescence-like arrest. Clonal C3 cells displayed telomerase repression, progressive telomere shortening, and permanent growth arrest after ≈80 PD with senescence-associated morphological changes and positive SABG staining. Similar changes have also been observed with G12, another independently derived clone. Thus, we demonstrate that immortal cancer cells have the intrinsic ability to reprogram the replicative senescence. As expected, this shift in cell fate results in a complete loss of tumorigenicity. The replicative senescence arrest that we identified with clonal C3 cells was not accompanied with the induction of the *p53*, $p16^{INK4a}$, $p14^{ARF}$, or $p21^{Cip1}$ gene. The nonparticipation of *p53* and $p16^{INK4a}$ to the senescence arrest described here was expected, in the light of published observations showing that Huh7 cells express a mutant p53 protein (20–22) and they are deficient in $p16^{INK4a}$ expression (23). Although the levels of $p21^{Cip1}$ protein displayed a slight increase in C3 cells, this was not related to senescence arrest, as early passage proliferating C3 cells also displayed this slight increase (Fig. 5). The early loss of *hTERT* expression in this clone could contribute to early $p21^{Cip1}$ up-regulation, because hTERT is known to down-regulate $p21^{Cip1}$ promoter activity (26). *p53*, $p16^{INK4a}$, $p14^{ARF}$, and $p21^{Cip1}$ form a group of replicative senescence-related cell cycle checkpoint genes. The lack of induction of these genes in senescence-arrested C3 cells clearly indicates that there are additional genes involved in senescence arrest in these tumor-derived cells.

The loss of *hTERT* expression in senescence programmed clones prompted us to analyze the expression of genes that have been implicated in *hTERT* regulation. Among seven candidate genes studied, only one, the *SIP1* gene, displayed a differential expression between immortal and senescence-programmed clones. This gene has been identified as a mediator of TGF-β-regulated repression of *hTERT* expression in a breast cancer cell line, although it was not effective in an osteosarcoma cell line (14). In our studies, SIP1 was not expressed in immortal hTERT-expressing C1 clone, but expressed in senescence-programmed hTERT-repressed C3 and G12 clones (Fig. 3 *B* and *C*). Furthermore, experimental depletion of SIP1 transcripts resulted in hTERT up-regulation in C3 clonal cells (Fig. 4*A*). This effect has been confirmed by using SKHep1, another HCC cell line (data not shown). Thus, we demonstrate that the *SIP1* gene acts as an hTERT repressor in HCC cells. More importantly, we also showed the bypass of senescence arrest after functional inactivation of SIP expression by shRNA in senescence-programmed C3 clonal cells. In contrast to C3 cells transfected with a control plasmid, SIP1 shRNA-treated cells displayed continued proliferation beyond PD ≈80 as evidenced by 70% BrdUrd incorporation index, and formation of large number of colonies. Selected shRNA-transfected clones from these experiments have already performed >15 PD beyond the senescence barrier. Thus, our findings indicate that the functional inactivation of *SIP1* in senescence-programmed cancer cells is sufficient to bypass senescent arrest.

SIP1 is a zinc finger and homeodomain containing transcription factor that exerts a repressive activity by binding to CACCT sequences in regulatory elements of target genes (12, 27). The *SIP1* gene is expressed at high levels in almost all human somatic tissues tested, including liver (28). Therefore, we also performed comparative analysis of hTERT and *SIP1* expression in nontumor liver and primary HCC tissues. *SIP1*

was strongly positive in nontumor liver samples, but its expression was significantly decreased in corresponding HCC samples. Inversely, *hTERT* expression was negative or low in nontumor liver samples, but highly positive in HCC tumors (Fig. 3*E*). We also detected complete loss of *SIP1* expression in 5 of 14 (36%) of HCC cell lines (data not shown). Taken together with *in vitro* studies, these observations strongly suggest that *SIP1* acts as a tumor suppressor gene in HCC. Although SIP1, as a repressor of *E-cadherin* promoter, has been suggested to be a promoter of invasion in malignant epithelial tumors (29), a tumor suppressive activity by the repression of *hTERT* and inhibition of senescence arrest is not precluded.

Hepatocellular carcinoma is one of the most common cancers worldwide. Liver cirrhosis is the major etiology of this tumor with limited therapeutic options (30, 31). Telomere shortening and senescence play a major role in liver cirrhosis, from which the neoplastic HCC cells emerge with high rates of telomerase reactivation (32). Furthermore, *p53* and $p16^{INK4a}$ are the most frequently inactivated genes in these tumors. This fact enhances the importance of our findings for potential therapeutic applications of replicative senescence programming in HCC.

Methods

Tissues, Cells, and Clones. Snap-frozen HCC and nontumor liver tissues were used. HCC and breast cancer cell lines T-47D (ATCC) and BT-474 (ATCC) were cultivated as described (33). hTERT-HME cells (Clontech) were cultivated in DMEM/Ham's F-12 (Biochrom) containing insulin (3.5 μg/ml), EGF (0.1 ng/ml), hydrocortison (0.5 μg/ml), and 10% FBS (Biochrom). Huh7- and Hep3B-derived isogenic clones were obtained by either G-418 selection after transfection with neomycin-resistance pcDNA3.1 (Invitrogen) or pEGFP-N2 (Clontech) plasmids, or by low-density cloning. Huh7-derived isogenic clones C1 and C3 were obtained with pCDNA3.1, and G12 with pEGFP-N2. Huh7-derived C11, and Hep3B-derived 3B-C6, 3B-C11 and 3B-C13 were obtained by low-density cloning. Cells transfected with calcium phosphate/DNA-precipitation method were cultivated in the presence of geneticin G-418 sulfate (500 μg/ml; GIBCO), and isolated single cell-derived colonies were picked up by using cloning cylinders and expanded in the presence of 200 μg/ml geneticin G-418 sulfate. For low-density cloning, cells were plated at 30 cells per cm^2 and single-cell derived colonies were expanded. Initial cell stocks were prepared when total number of cells became 1–3 $\times$ 10^7, and the number of accumulated population doubling (PD) at this stage was estimated to be 24, assuming that the progeny of the initial colony-forming cells performed at least 24 successive cell divisions until that step. Subsequent passages were performed every 4–7 days, and the number of additional PD was determined by using a described protocol (34).

Low-Density Clonogenic Assay. Cells (30–50 per cm^2) were plated in six-well plates and grown 1–3 weeks to obtain isolated colonies formed with 100–1,000 cells. The medium was changed every 4 days, and colonies were subjected to SABG staining (see below).

***In Vivo* Studies.** Cells were injected s.c. into CD-1 *nude* mice (Charles River Breeding Laboratory). Tumors and nontumorigenic cells at the injection sites were collected at day 35 and analyzed directly or after *in vitro* culture by SABG assay (see below). These experiments have been approved by the Bilkent University Animal Ethics Committee.

SABG Assay. SABG activity was detected by using a described protocol (15). After DAPI or eosin counterstaining, SABG-positive and negative cells were identified and counted.

BrdUrd Incorporation Assay. Subconfluent cells were labeled with BrdUrd for 24 h in freshly added culture medium and tested as described (33), using anti-BrdUrd antibody (Dako) followed by tetramethylrhodamine B isothiocyanate-labeled secondary antibody (Sigma). DAPI (Sigma) was used for counterstaining.

Immunoblotting. Antibodies against cyclin D1, CDK4, CDK2, $p21^{Cip1}$, pRb (all from Santa Cruz Biotechnology), cyclin E (Transduction), cyclin A (Abcam), $p16^{INK4a}$ (Abcam), p53 (clone 6B10; ref. 35), and calnexin (Sigma) were used for immunoblotting as described (33).

RT-PCR. RT-PCR expression analysis was performed as described (33), using primers listed in Table 1, which is published as supporting information on the PNAS web site.

TRAP and Telomere Length Assays. Telomerase activity and telomere length assays were performed by using Telo*TAGGG* Telomerase PCR $ELISA^{PLUS}$ and Telo*TAGGG* Telomere Length Assay (Roche Diagnostics), following kit instructions.

shRNA. SIP1-directed shRNA was designed according to a previously described effective siRNA sequence (14) using the pSUPER RNAi system instructions (Oligoengine) and cloned into pSuper.retro.neo+GFP and pSUPER.puro (Oligoengine), respectively. SIP1 shRNA-encoding sequence was inserted by using 5′-GATCCCCCTGCCATCTGATCCGCTCTTTCAAGAGAAGAGCGGATCAGATGGCAGTTTTTA-3′ (sense) and 5′-AGCTTAAAAACTGCCATCTGATCCGCTCTTCTCTTGAAAG AGCGGATCAG ATGGCAGGGG-3′ (antisense) oligonucleotides.

The integrity of the inserted shRNA-coding sequence has been confirmed by nucleic acid sequencing of recombinant plasmids. Clone C3 cells were transfected with calcium phosphate precipitation method, using either pSuper.retro.neo+GFP-based or pSUPER.puro-based SIP1 shRNA expression plasmid, and cells were maintained in the presence of 500 μg/ml geneticin G-418 sulfate and 2 μg/ml puromycin (Sigma), respectively. Empty vectors were used as control. Media changed every 3 days, and cells were tested at days 5 and 30.

We thank E. Galun, G. Hotamisligil, F. Saatcioglu, and A. Sancar for reading the manuscript and helpful suggestions. This work was supported by Grant SBAG-2774/104S045 from the Scientific and Technological Research Council of Turkey (TUBITAK) and funds from Bilkent University and Turkish Academy of Sciences (TUBA).

1. Nowell, P. C. (1976) *Science* **194,** 23–28.
2. Vogelstein, B. & Kinzler, K. W. (1993) *Trends. Genet.* **9,** 138–141.
3. Shay, J. W. & Wright, W. E. (2005) *Carcinogenesis* **26,** 867–874.
4. Campisi, J. (2005) *Cell* **120,** 513–522.
5. Dimri, G. P. (2005) *Cancer Cell* **7,** 505–512.
6. Ben-Porath, I. & Weinberg, R. A. (2004) *J. Clin. Invest.* **113,** 8–13.
7. Shay, J. W. & Bacchetti, S. (1997) *Eur. J. Cancer* **33,** 787–791.
8. Sherr, C. J. & McCormick, F. (2002) *Cancer Cell* **2,** 103–112.
9. Boehm, J. S. & Hahn, W. C. (2005) *Curr. Opin. Genet. Dev.* **15,** 13–17.
10. Roninson, I. B. (2003) *Cancer Res.* **63,** 2705–2715.
11. Shay, J. W. & Roninson, I. B. (2004) *Oncogene* **23,** 2919–2933.
12. Verschueren, K., Remacle, J. E., Collart, C., Kraft, H., Baker, B. S., Tylzanowski, P., Nelles, L., Wuytens, G., Su, M. T., Bodmer, R., *et al.* (1999) *J. Biol. Chem.* **274,** 20489–20498.
13. Postigo, A. A., Depp, J. L., Taylor, J. J. & Kroll, K. L. (2003) *EMBO J.* **22,** 2453–2462.
14. Lin, S. Y. & Elledge, S. J. (2003) *Cell* **113,** 881–889.
15. Dimri, G. P., Lee, X., Basile, G., Acosta, M., Scott, G., Roskelley, C., Medrano, E. E., Linskens, M., Rubelj, I., Pereira-Smith, O., *et al.* (1995) *Proc. Natl. Acad. Sci. USA* **92,** 9363–9367.
16. Lasfargues, E. Y., Coutinho, W. G. & Redfield, E. S. (1978) *J. Natl. Cancer Inst.* **61,** 967–978.

17. Keydar, I., Chen, L., Karby, S., Weiss, F. R., Delarea, J., Radu, M., Chaitcik, S. & Brenner, H. J. (1979) *Eur. J. Cancer* **15,** 659–670.
18. Nakabayashi, H., Taketa, K., Miyano, K., Yamane, T. & Sato, J. (1982) *Cancer Res.* **42,** 3858–3863.
19. Wei, W. & Sedivy, J. M. (1999) *Exp. Cell Res.* **253,** 519–522.
20. Bressac, B., Galvin, K. M., Liang, T. J., Isselbacher, K. J., Wands, J. R. & Ozturk, M. (1990) *Proc. Natl. Acad. Sci. USA* **87,** 1973–1977.
21. Volkmann, M., Hofmann, W. J., Muller, M., Rath, U., Otto, G., Zentgraf, H. & Galle, P. R. (1994) *Oncogene* **9,** 195–204.
22. Kubica, S., Trauwein, C., Niehof, M. & Manns, M. (1997) *Hepatology* **25,** 867–873.
23. Roncalli, M., Bianchi, P., Bruni, B., Laghi, L., Destro, A., Di Gioia, S., Gennari, L., Tommasini, M., Malesci, A. & Coggi, G. (2002) *Hepatology* **36,** 427–432.
24. Kaneko, S., Hallenbeck, P., Kotani, T., Nakabayashi, H., McGarrity, G., Tamaoki, T., Anderson, W. F. & Chiang, Y. L. (1995) *Cancer Res.* **55,** 5283–5287.
25. Wang, J., Xie, L. Y., Allan, S., Beach, D. & Hannon, G. J. (1998) *Genes Dev.* **12,** 1769–1774.
26. Young, J. I., Sedivy, J. M. & Smith, J. R. (2003) *J. Biol. Chem.* **278,** 19904–19908.
27. Remacle, J. E., Kraft, H., Lerchner, W., Wuytens, G., Collart, C., Verschueren, K., Smith, J. C. & Huylebroeck, D. (1999) *EMBO J.* **18,** 5073–5084.
28. Cacheux, V., Dastot-Le Moal, F., Kaariainen, H., Bondurand, N., Rintala, R., Boissier, B., Wilson, M., Mowat, D. & Goossens, M. (2001) *Hum. Mol. Genet.* **10,** 1503–1510.
29. Comijn, J., Berx, G., Vermassen, P., Verschueren, K., van Grunsven, L., Bruyneel, E., Mareel, M., Huylebroeck, D. & van Roy, F. (2001) *Mol. Cell* **7,** 1267–1278.
30. Thorgeirsson, S. S. & Grisham, J. W. (2002) *Nat. Genet.* **31,** 339–346.
31. Bruix, J., Boix, L., Sala, M. & Llovet, J. M. (2004) *Cancer Cell* **5,** 215–219.
32. Satyanarayana, A., Manns, M. P. & Rudolph, K. L. (2004) *Hepatology* **40,** 276–283.
33. Erdal, E., Ozturk, N., Cagatay, T., Eksioglu-Demiralp, E. & Ozturk, M. (2005) *Int. J. Cancer* **115,** 903–910.
34. Masutomi, K., Yu, E. Y., Khurts, S., Ben-Porath, I., Currier, J. L., Metz, G. B., Brooks, M. W., Kaneko, S., Murakami, S., DeCaprio, J. A., *et al.* (2003) *Cell* **114,** 241–253.
35. Yolcu, E., Sayan, B. S., Yagci, T., Cetin-Atalay, R., Soussi, T., Yurdusev, N. & Ozturk, M. (2001) *Oncogene* **15,** 1398–1401.